1. p 11, para 3, line 5: should read "……development, follistatin……"
2. p 23, para 2, the last line: add "Recently, TNF-induced protein 6 (Tnfip6) and pentraxin 3 (Ptx3) have been identified as novel factors induced by GDF-9 in granulosa cells of preovulatory follicles (Varani, *et al.*, 2002). Disruption of Ptx3 gene leads to subfertility in females because of defects in the integrity of the cumulus cell-oocyte complex, whereas Ptx3 null males are fertile."
3. p25, para 1, the last line: add "Of note, BMP-6 knockout mice are fertile (data provided by M. Matzuk)."
4. p27, para 2, line 2: should read "…, the roles of follistatins in the ovary…."
5. p30, line 25: should read "Unfortunately, no data are……", also in the last line, add "Additionally, the high levels of follistatin in the testis may also block BMPs and/or other TGF-β superfamily proteins, resulting in the disruption of spermatogenesis (refer to the next section)."
6. p 43, para 2, line 10: should read "…cause competitive effects."
7. p 44, para 2, line 9: should read "….members of TGF-β superfamily to modulate their functions……."
8. p 69, 2.2.11.3: Heading should read "……fetal testes into the outer ears….."
9. p 73, para 2, line 10: should read "……activin/inhibin βA subunit minigene…"
10. p 75, para 1, line 1: should read "C57/129 ……"
11. p 80, para 1, line 2: should read "…..Thus, 6 follistatin null……" and para 3, line 6: should read "…..in many of seminiferous tubules, there….."
12. p 82, para 1, line 3: should read "……follistatin homozygous mutant mice….."
13. p 83, para 1, line 3: should read "seminiferous tubules, there was……."
14. p 86, para 3, line 4: should read "…..PAC-FS was firstly obtained by screening…."
15. p 87, para 3, line 1: should read "First, the PAC-FS……."
16. p 88, para 1, line 1: should read "First, the human……"
17. p 92, para 2, line 1: should read "……..were transformed with the……"
18. p 96, para 1, line 3: should read "……95 kb and 25 kb of human follistatin genomic sequences….."
19. p 104, the last line: should read "timed mating" for "plug mating"
20. Figure 5.10 title: remove "" before "The"
21. p 111, para 1, line 4: should read "……appear to be compatible with the gross…." and para 3, line 9: "mRNA expression" not "mRNA expressions"
22. Figure 5.15 legend: add "In the figure, the follistatin mRNA expression in the rescued mice is from the human follistatin transgenes, and that in wild type mice is from endogenous mouse follistatin gene"
23. p 112, last line: should read "…..for each organ of each line, the sample…."
24. p 115, para 2, line 3: should read "is significantly decreased……." and para 2, line 4: should read "of fs-ko, it was rare to……."
25. pages 116-117: supplement with the argument that "The view that follistatin/activin system may be involved in the development of genital tubercle is supported by the phenotypes of activin βB knockin mice (Brown, *et al.*, 2000), displaying increased penis size in male. Too much local activin βA without the antagonism of follistatin in fs-ko mice may lead to decreased genital tubercle size, whereas no activin βA in the activin βB knockin mice generates the opposite phenotype in this aspect. Alternatively, local activin βB alone in the activin βB knockin mice may induce the enlargement of penis or clitoris. Unfortunately, this report did not include the data about the early development of genital tubercle in the activin βB knockin mice to understand whether the changes of genital tubercle size arise from the first or second mechanism. Further studies are required to elucidate these hypotheses."

26. p 120, para 2, the last 2 lines: should read "in this chapter, we chose to compare the mouse follistatin genomic sequences with the human follistatin genomic sequences."
27. p 122, para 1, line 2: should read "Sequences were retrieved that contained……."
28. p 124, para 2, line 7: should read "For clear recognition of CNS……"
29. p 125, para 2, the reference for the second sentence: (Strachan and Read, *Human Molecular Genetics 2nd ed, chapter 8*).
30. p 129, para 1, the last line: should read "…….only one follistatin isoform."
31. p 130, para 3, line 9 & 10: should read "however, the efficiency……*Escherichia coli*……."
32. p 136, para 3, line 6: should read "…….as pNEB-S3. The…"
33. p 155, para 1, line 7: should read "……..the tips of the tails of FS^{95}-315-ko.1…."
34. p 156, para 2, the second last line: should read "…….*in vitro* showed the reverse."
35. p 157, para 1, line 1: should read "…….levels; however, no published….."
36. p 164, the second line: should read "However, the myostatin transgenic mice…."
37. p 164, para 2: supplement with the argument that "Another explanation for the phenotype of the eyes of FS^{95}-315-ko mice can be based on the potential interaction between follistatin and activin during the development of eyes, since activin A was shown to be able to promote progenitor differentiation into photoreceptors in the retina (Davis, *et al.*, 2000) as well as the activin βB knockin mice seem to have small eyes (Brown, *et al.*, 2000)."

Genetically Engineered Mouse Models for the Study of Follistatin Biology

A thesis submitted for the degree of
DOCTOR OF PHILOSOPHY

by

Shyr-Yeu Lin
MD

Monash Institute of Reproduction and Development
Monash University
AUSTRALIA

10 September 2003

- Table of contents -

Materials and Methods Section:

- Chapter 2 -

Result Section 1: Transplantation of Fetal Follistatin Null Testes

- Chapter 3 -

Development of fetal follistatin null testes transplanted into the ears of RAG mice 72

Result Section 3: Development of Human Follistatin Isoform-specific Mouse Models

- Chapter 7 -

Conclusion Section:

Appendices and References:

- Abbreviations -

wt	wild-type mice
fs-ko	follistatin knockout mice
FS^{25}-wt	mice carrying 25 kb human follistatin transgene in the mouse wild-type background
FS^{95}-wt	mice carrying 95 kb human follistatin transgene in the mouse wild-type background
FS^{25}-ko	mice carrying 25 kb human follistatin transgene in the mouse follistatin knockout background
FS^{95}-ko	mice carrying 95 kb human follistatin transgene in the mouse follistatin knockout background
FS^{95}-288-wt	mice carrying 95 kb human follistatin transgenes which specifically express human follistatin-288 in the mouse wild-type background
FS^{95}-315-wt	mice carrying 95 kb human follistatin transgenes which specifically express human follistatin-315 in the mouse wild-type background
FS^{95}-288-ko	mice carrying 95 kb human follistatin transgenes which specifically express human follistatin-288 in the mouse follistatin knockout background
FS^{95}-315-ko	mice carrying 95 kb human follistatin transgenes which specifically express human follistatin-315 in the mouse follistatin knockout background
TGF-β	transforming growth factor-β
BMP	bone morphogenetic protein
GDF	growth differentiation factor

SMAD	a fusion of the names of two genes, the *Drosophila* gene *Mad (mothers against dpp)* and the *C. elegans* gene *sma (small body size)*
bp	base pairs
cDNA	complementary deoxyribonucleic acid
DNA	deoxyribonucleic acid
kb	kilobase pairs
kD	kilodalton
mRNA	messenger ribonucleic acid
PCR	polymerase chain reaction
OD	optical density
RNA	ribonucleic acid

- Summary -

Follistatin is a protein that binds and inactivates a growth factor termed activin that has multiples functions. Attempts to understand the role of follistatin by targeted gene inactivation to produce follistatin knock-out mice (fs-ko) resulted in the death of these mice within 12hrs of birth due to developmental defects preventing the use of this model in understanding the postnatal functions of follistatin. To further explore the functions of follistatin, several *in vivo* models were created and studied.

First, to understand the role of locally produced follistatin in testicular development, the follistatin null testes were transplanted into the ears of the castrated adult RAG male mice (Chapter 3), resulting in a model in which the local production of follistatin in testes is absent but circulating follistatin is available from the host. Histological analysis of the testicular grafts 7~8 weeks after transplantation displayed full development of spermatogenesis both in the follistatin null the wild-type grafted testes, suggesting that the local produced follistatin may not be essential for normal spermatogenesis.

Secondly, to define the human follistatin locus and identify some regulatory elements in it, an attempt was to rescue the fs-ko mice by inserting 25 kb and 95 kb human genomic sequences of the follistatin locus into the mouse follistatin null background (Chapter 4 ~ 6). Two transgenic models were generated that carry 25 kb (FS^{25}-ko) or 95 kb (FS^{95}-ko) genomic constructs, but have no mouse endogenous follistatin gene. Both the FS^{25}-ko and FS^{95}-ko mice did survive for 24 hrs and their phenotypes in various systems were between those of the wild-type (wt) and fs-ko mice and closer to those of fs-ko. These data suggest that while the information contained in both genomic constructs may be similar, it is not sufficient to rescue the phenotypes of the fs-ko. During these studies developmental abnormalities in the fs-ko mice were further defined in the lung, liver and the development of the ovary and genital tubercle.

In view of the distinct biochemical characteristics of follistatin isoforms, two isoform specific genetic models were created to determine whether the follistatin isoforms have distinct physiological functions (Chapter 7 ~ 8). The isoform specific transgenes were

constructed using the 95 kb human genomic sequence of the follistatin locus as a basis to do DNA engineering. The resultant transgenic mice were then crossed onto the mouse follistatin knockout background, leading to the follistatin-288 specific (FS^{95}-288-ko) and follistatin-315 specific (FS^{95}-315-ko) models. Strikingly, FS^{95}-315-ko mice survived in contrast to FS^{95}-288-ko, indicating the distinct functions of follistatin isoforms. The phenotypes of FS^{95}-315-ko indicated that follistatin may be involved in the development of the eye and vasculogenesis and/or angiogenesis as shown by abnormal tail development.

These observations together with the evidence of the failure of the FS^{95}-ko (expressing follistatin-288 and follistatin-315) to survive, raise the possibility that follistatin-288 may counter-act the effects of follistatin-315 in some aspects of development. To further confirm this hypothesis, the doubly "rescued" mice are being generated by crossing the FS^{95}-288-ko and FS^{95}-315-ko lines.

- Declaration -

I hereby certify that this thesis comprises only my original work, except where due acknowledgement is made to the work of others. This thesis is less than 100,000 words in length, excluding tables, figures, references, and appendices. The work presented in this thesis contains no material, which has been accepted for the award of any other degree or diploma in any university or other institution, and, to the best of my knowledge and belief, contains no material published or written by another person, except where due reference is made in the text.

[redacted]

Shyr-Yeu Lin

- Acknowledgements -

It had been my dream to do a PhD in life science since I was qualified as a specialist in OB/GYN, as in my view the current medicine is so limited that many diseases can only be treated conservatively without a way to cure. However, I did not dare to imagine that I could finish my PhD program because many obstacles were in front of me for my experiments, and especially for writing up my thesis. There are many people to whom I should express my sincere gratitude. Without them I could not have achieved this thesis.

First, I would like to express my gratitude to my supervisor, Prof. David de Kretser, for his teaching, for many things he has done for me and many opportunities he has given to me. My thanks should start with a welcome letter from David that encouraged me to come to MIRD. During these years in MIRD, he was patient to listening to me when I needed to talk to him, encouraged me when I felt frustrated, and gave me his support when I needed help. I have learned a lot from his logical thinking, especially when I was writing a review article and my thesis. In addition, special thanks should have to go to him for supporting me in learning the culture technique of human embryonic stem cells when he realized that stem cell biology will be one of the areas I want to develop in the future. In my view, a good teacher can teach students not only by language, but also by his behavior. Many times when I left the lab, he was the only one who was still working in the building. He could teach me histology until 9 pm. Those things touched me so much. I often think of why such a knowledgeable person can be still so curious about science, why an academic giant can be so modest to respect and encourage young scientists. I felt very lucky to have David as my supervisor and I have learned this of philosophy during my PhD. Prof. de Kretser will be a model I would like to follow if I could lead a research group in the future.

My sincere gratitude should also go to my co-supervisor, Dr. John Morrison, for his teaching and support during my PhD. In fact, John is my first teacher in the molecular biology technique. Most of time when I encountered problems in my experiments, I went to him directly and he always left what he was doing and discussed my problems with me. John was very responsible for me. Without his pushing me, this thesis could be

finished much later. I also felt lucky to have this opportunity of working with John for my PhD project. As he is an excellent geneticist, I learned a lot of concepts of genetics during my PhD, which has definitely influenced my academic career.

I also would like to thank many people in MIRD, from whom I have learned, who talked with me and who always smiled to me. The Ingenko team should also be thanked for carrying out the pronuclear microinjection for transgenic mice. Special thanks should go to Rebecca Craythorn for continuing my work when I was writing up my thesis. I also thank Lynda Foulds for proof-reading my draft.

My sincere thanks also go to Dr. Sen-Lin Tang and Dr. Jessie Chen for their friendship with me and my family during my stay in Melbourne. I would like to express my sincere gratitude to Mrs. Judy Huang for her helping us in settling down in Melbourne. Of course, my parents should be thanked for educating me to try to be a person who is useful for the human communities and never forgets the help from others.

I want to thank my lovely daughters, Donna and Joyce, for accompanying me during my PhD. Th ɔugh observations of their growth, I have been feeling that life is amazing, miraculous and precious. This feeling continues pushing me to decipher the secrets in it. And finally, I want to thank my wife, Jean, who never complains of scarcity of time I have given to her, instead, usually reminds me of whether I persevere with my ideals. I should thank her as the supervisor of my life.

Chapter 1

Introduction

Chapter Outline:

1.1 Introduction

Inhibin and activin were isolated and characterized from gonads on the basis of their ability to act as nonsteroidal feedback modulators of pituitary follicle-stimulating hormone (FSH) secretion. The secretion of FSH is enhanced by activin while inhibin is inhibitory (Ling, *et al.*, 1985; Robertson, *et al.*, 1985; Ling, *et al.*, 1986; Vale, *et al.*, 1986). The inhibins and activins are classified as members of the transforming growth factor-β (TGF-β) superfamily and are now known to play pivotal roles in developmental and reproductive processes. Follistatin, a glycosylated single-chain protein with no structural similarity to but functionally linked to members of TGF-β superfamily, was originally isolated from ovarian follicular fluid on the basis of suppression of FSH secretion by pituitary cells (Esch, *et al.*, 1987; Robertson, *et al.*, 1987; Ueno, *et al.*, 1987). Subsequently, follistatin was shown to be an activin-binding protein with the capacity to neutralize the majority of the actions of the activins (Nakamura, *et al.*, 1990). Since their isolation, physiological studies have shown that the inhibins function principally as reproductive hormones (DePaolo, 1997; Mather, *et al.*, 1997), while the activins have predominantly paracrine or autocrine functions in many systems (DePaolo, 1997; Mather, *et al.*, 1997). Since follistatin can inhibit the majority of the actions of activins, its biology had been considered as an integral part of the physiology of the activins. Moreover, recent compelling evidence suggests that follistatin binds and regulates the function of other members of TGF-β superfamily (Iemura, *et al.*, 1998), thereby complicating and further highlighting the study of follistatin biology. The chapter presents the background for this thesis and provides the rationale for follistatin biology. It will first focus on the biochemical characteristics of follistatin, and then introduce the biology of this protein in different systems, especially comprehensively discussing the role of follistatins in the ovary, as this is the area that has been most abundantly studied. The chapter concludes by discussing an emerging concept that follistatins are functioning in a complex network system.

1.1.1 TGF-β superfamily

Our current knowledge suggests that follistatin functions mostly through its ability to bind and neutralize the actions of some members of the TGF-β superfamily. The TGF-β superfamily of growth factors includes more than 30 structurally related proteins in mammals that have diverse functions during embryonic development and adult tissue homeostasis. These proteins can be grouped into four families: the TGF-β family, the activin family, the bone morphogenetic protein (BMP) family, and the growth differentiation factor (GDF) family, although some of TGF-β superfamily members may fall outside these three groupings.

1.1.1.1 Structure of TGF-β superfamily members

Members of the TGF-β superfamily are synthesized as large precursor proteins that are composed of an amino-terminal signal sequence, a pro-domain and a mature domain (carboxyl-terminal domain) (Figure 1.1a). The amino-terminal signal may direct the precursor to a secretory pathway. The variable pro-domain may facilitate folding, dimerization and regulation of TGF-β superfamily members (Kingsley, 1994). The actual signaling molecule is made up of hetero- or homodimers of the highly conserved carboxyl-terminal domain. Within this carboxyl-terminal domain, the presence of seven cysteine residues is a virtually consistent feature of the members of this superfamily. Six of these cysteines, forming three disulfide bonds within each monomer subunit, interact to build a structure termed a cystine knot (Figure 1.1b). This knot consists of an eight-member ring constructed from two disulfide bonds, while a third disulfide bond is threaded through the central area of the ring (Daopin, *et al.*, 1992; Schlunegger and Grutter, 1992; Böttner, *et al.*, 2000). Moreover, this knot locks the base of several β-sheet strands together, apparently contributing to the stabilization of TGF-β superfamily members in various conformations. The remaining cysteine residue in each monomer forms an additional disulfide bond that links two monomers into a dimer (Figure 1.1b). This cysteine is missing in some members, for example, GDF-3 and GDF-9, however many hydrophobic contacts also exist between the two monomer subunits that may promote dimerization even in the absence of a disulfide bond (Kingsley, 1994).

Figure 1.1. The structure of TGF-β superfamily members.

a) A precursor protein of monomers of TGF-β superfamily members consists of a signal sequence, pro-domain and a mature domain (carboxyl-terminal domain). Cleavage at a dibasic site (RXXR motifs) releases a mature domain that contains seven highly conserved cysteine residues, forming three intra-monomeric disulfide bonds (C_I-C_{IV}, C_{II}-C_V and C_{III}-C_{VI}).

b) The cystine knot motif arises from these three intra-monomeric disulfide bonds by two (C_{II}-C_V and C_{III}-C_{VI}) of them building an eight-membered ring structure, through which the third one (C_I-C_{IV}) passes. The remaining cysteine (labeled with *) forms an inter-monomeric disulfide bond with that of the other monomer into a dimer. (Based on Böttner *et al.* 2000)

Figure 1.1a

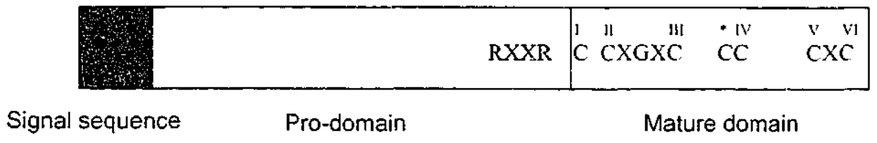

Figure 1.1b

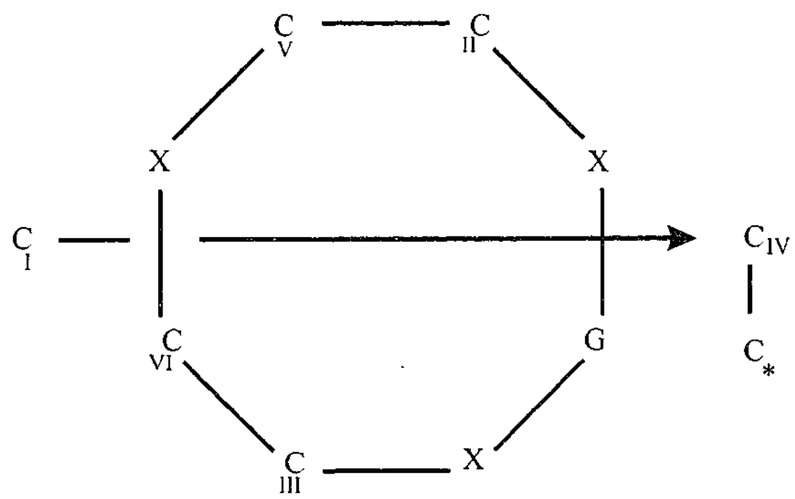

1.1.1.2 Activins and inhibins

Historically the inhibin/activin-related proteins are the members of the family to which follistatin is functionally linked. Inhibins are dimers of a unique α-subunit dimerized to either βA or βB subunit giving inhibin A (α-βA) or inhibin B (α-βB). Homo-dimerization or hetero-dimerization of either βA or βB subunits generates three activins, named activin A (βA-βA), activin B (βB-βB) and activin AB ((βA-βB). Three additional β subunits (mammalian βC and βE, and *Xenopus* βD) have also been cloned (Oda, *et al.*, 1995; Fang, *et al.*, 1996; Schmitt, *et al.*, 1996). Although their functions are yet to be determined, a recent study demonstrated that the liver is the major organ for production of βC and βE subunits and potential dimerization exists between βA and βC subunits, βA and βE subunits, and βC and βE subunits (Mellor, *et al.*, 2000; Vejda, *et al.*, 2002). Moreover, cotransfection studies suggest that the βC subunit is unable to form a dimer with the inhibin α subunit (Mellor, *et al.*, 2000).

1.1.1.3 Other members of TGF-β superfamily

In addition to the inhibins and activins, to date myostatin (also called GDF-8), BMP-4, BMP-7 and BMP-15 (also called GDF-9B) have all been identified as potential binding partners of follistatin (Shimasaki, *et al.*, 1999; Lee and McPherron, 2001; Otsuka, *et al.*, 2001c). It is very likely that other members of TGF-β superfamily that interact with follistatin will be reported in the future. The functions of the members that are binding partners or potential binding partners of follistatin are discussed in the following sections.

1.1.2 Signaling pathways of the TGF-β superfamily

Members of the TGF-β superfamily use a common mechanism to signal to the nucleus. They bind to membrane receptors on the cell surface of target cells, which have an intracytoplasmic serine/threonine kinase domain, leading to the assembly of a receptor complex that phosphorylates proteins of the SMAD family. The SMADs then move into the nucleus, where they bind DNA and recruit the required transcriptional co-activators or co-repressors to control gene expression (Massagué, 1998; Massagué and Wotton,

2000) (Figure 1.2). The specific pairs of receptors to which the ligands of the TGF-β superfamily bind, fall into two groups designated as the type I and type II receptors. Generally, each ligand has its own specific receptors; however some may be shared by different TGF-β ligands. When the ligand binds to the receptors, it brings together two type I receptors and two type II receptors to form an activated receptor complex. In this complex, the type I receptor becomes phosphorylated by the type II receptor and in turn phosphorylates the SMAD proteins that transmit the signal (Attisano, *et al.*, 1993; Ebner, *et al.*, 1993; Liu, *et al.*, 1995; Nohno, *et al.*, 1995; Rosenzweig, *et al.*, 1995; Nishitoh, *et al.*, 1996; Massagué, 1998).

SMAD is a fusion of the names of two genes, the *Drosophila* gene *Mad (mothers against dpp)* and the *C. elegans* gene *sma (small body size)*. They are classified into three groups based on their roles in the signaling pathways: the receptor-regulated SMADs (R-SMADs), the common mediator SMADs (co-SMADs), and the inhibitory SMADs (I-SMADs). In vertebrates, the type I receptors signal through SMAD2 and SMAD3 for activin, TGF-β and nodal, whereas those for the BMPs, GDFs and anti-Müllerian hormone/Müllerian inhibiting substance (AMH/MIS) do so through SMAD1, SMAD5 and SMAD8. These SMADs are collectively called R-SMADs. The co-SMAD, SMAD4, is required to form a complex with the R-SMAD before moving into the nucleus. However, increased expression of the I-SMADs, SMAD6 or SMAD7, inhibits TGF-β, activin and BMP signaling (Figure 1.2). In addition, the signaling network of the TGF-β superfamily has been complicated by recent studies revealing that the SMAD signaling system is also modulated by cross-talk with other kinase signaling cascades (Heldin, *et al.*, 1997; Attisano and Wrana, 1998; Derynck, *et al.*, 1998; Whitman, 1998; Massagué and Wotton, 2000; Zimmerman and Padgett, 2000). Also, intriguingly, a recent paper showed that TGF-β can signal through SMAD 2/3 or SMAD 1/5 depending on which type I receptor (activin receptor-like kinase ALK 1 or ALK 5) is recruited, thereby regulating the activation state of endothelium via a fine balance between ALK 1 and ALK 5 signaling (Goumans, *et al.*, 2002).

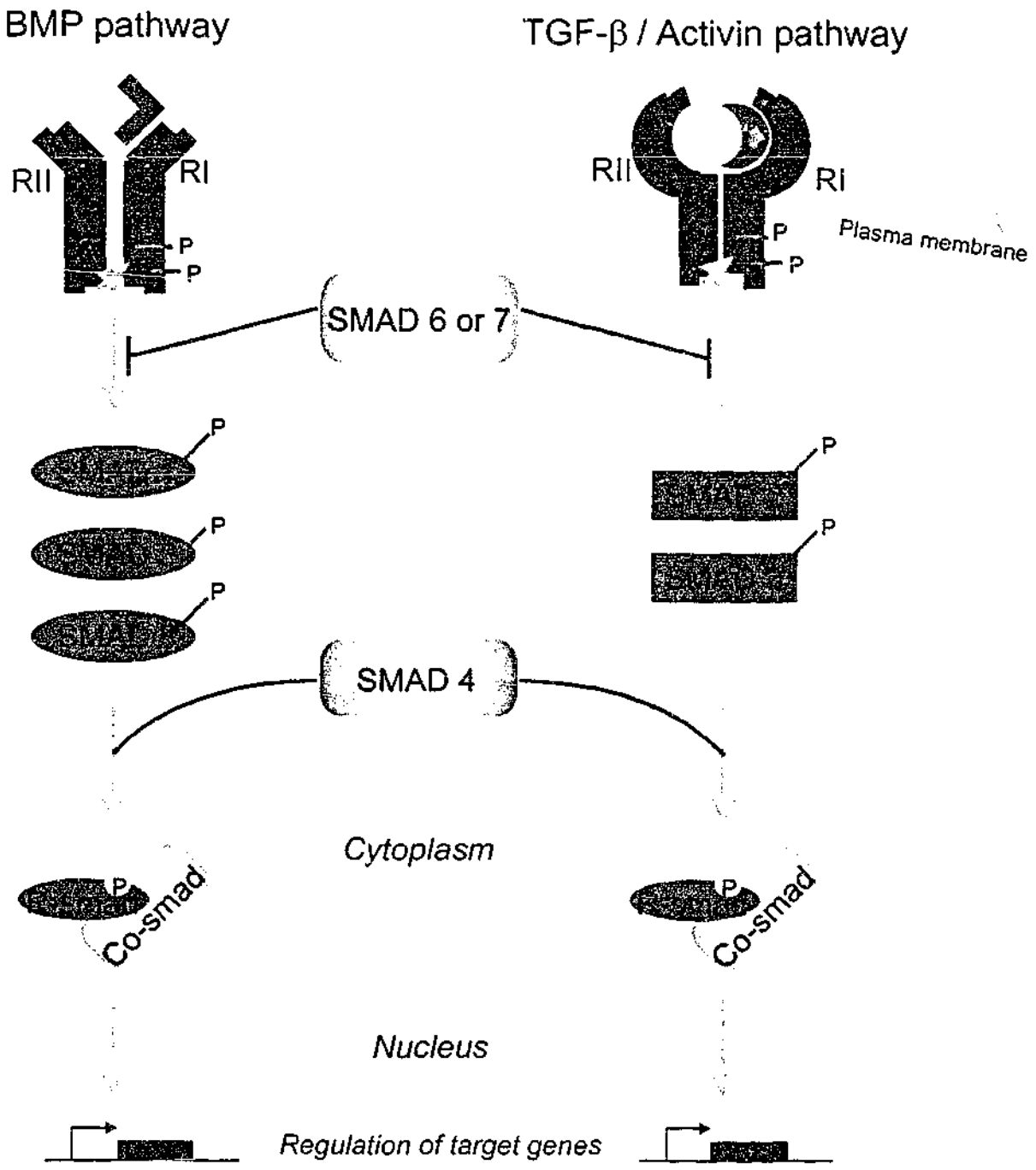

Figure 1.2. The basic TGF-β superfamily members-SMAD pathway.

After forming a ligand-receptor complex, the receptor I (RI), phosphorylated by the receptor II (RII), in turn phosphorylates R-SMAD (SMAD 2, 3 for TGF-β/activin; SMAD 1, 5, 8 for BMPs). The further assembly of R-SMAD and Co-SMAD (SMAD 4) makes the resulting SMAD complex free to move into the nucleus and regulate the target genes of TGF-β superfamily members with some transcriptional co-activators or co-repressors. In addition, I-SMADs (SMAD 6 or 7) can inhibit TGF-β, activin and BMP signaling.

1.2 Structural characterization of follistatins

1.2.1 The follistatin gene

Follistatin is a highly conserved protein among species with 97% amino acid homology between the human and mouse (http://www.ncbi.nlm.nih.gov/cgi-bin/UniGene/). The human follistatin gene localizes to chromosome 5q11.2 (http://www.ncbi.nlm.nih.gov/Locus Link/) and consists of 6 exons (Fig. 1.3). The first exon encodes for the putative signal sequence, followed by four exons which encode four domains with the last three domains being highly similar to each other, and the sixth exon encodes for the 27 extra amino acids at the carboxyl terminal of the 344-residue precursor (Shimasaki, *et al.*, 1988b).

Follistatin expression is tightly regulated during development (Feijen, *et al.*, 1994; Merino, *et al.*, 1999; Patel, *et al.*, 1999). To further understand the regulation of follistatin expression, several research groups studied the follistatin gene promoter. Characterization of the rat follistatin gene promoter identified three transcription start sites located at about 30 bp downstream of three distinct TATA-like sequences. The promoter region revealed several DNA motifs for transcription factors, including Sp1, Ap-2, Ap-1, and a CRE-like sequence. These elements are consistent with the evidence that the follistatin gene is regulated through both the protein kinase A and protein kinase C pathways in many studies (Miyanaga and Shimasaki, 1993). Moreover, a recent study demonstrated that the murine follistatin promoter region has at least three distinct transcription initiation sites, each preceded by a TATA box and located within the 500 bp upstream of the translational start site, and several consensus binding sites for transcription factors including Ap-1, Brachyury-T, CREB, SP1, Ap-2 and Tcf (de Groot, *et al.*, 2000).

1.2.2 Follistatin isoforms from alternative pre-mRNA splicing

Molecular analysis of the various isoforms showed that follistatin is encoded by a single gene and the variety of molecular weights (31-39 kDa) arise from alternative splicing, glycosylation and proteolytic cleavage (Robertson, *et al.*, 1987; Ueno, *et al.*, 1987;

Figure 1.3. Schematic representation of follistatin (FS) gene, alternative mRNA splicing and protein processing

Human or mouse follistatin gene has 6 exons that are transcribed into pre FS-317 mRNA and pre FS-344 mRNA via alternative mRNA splicing. Both mRNA are then translated into pre FS-317 and pre FS-344, which subsequently become FS-288 and FS-315 by cleavage of signal peptide. FS-288 and FS-315 both have a N domain and FS domains I, II and III with an additional C domain in FS-315.

pre FS-317 mRNA: the precursor follistatin-317 mRNA; pre FS-344 mRNA: the precursor follistatin-344 mRNA; pre FS-317: a precursor of 317 amino acids of follistatin; pre FS-344: a precursor of 344 amino acids of follistatin; FS-288: follistatin-288; FS-315: follistatin-315.

Figure 1.3

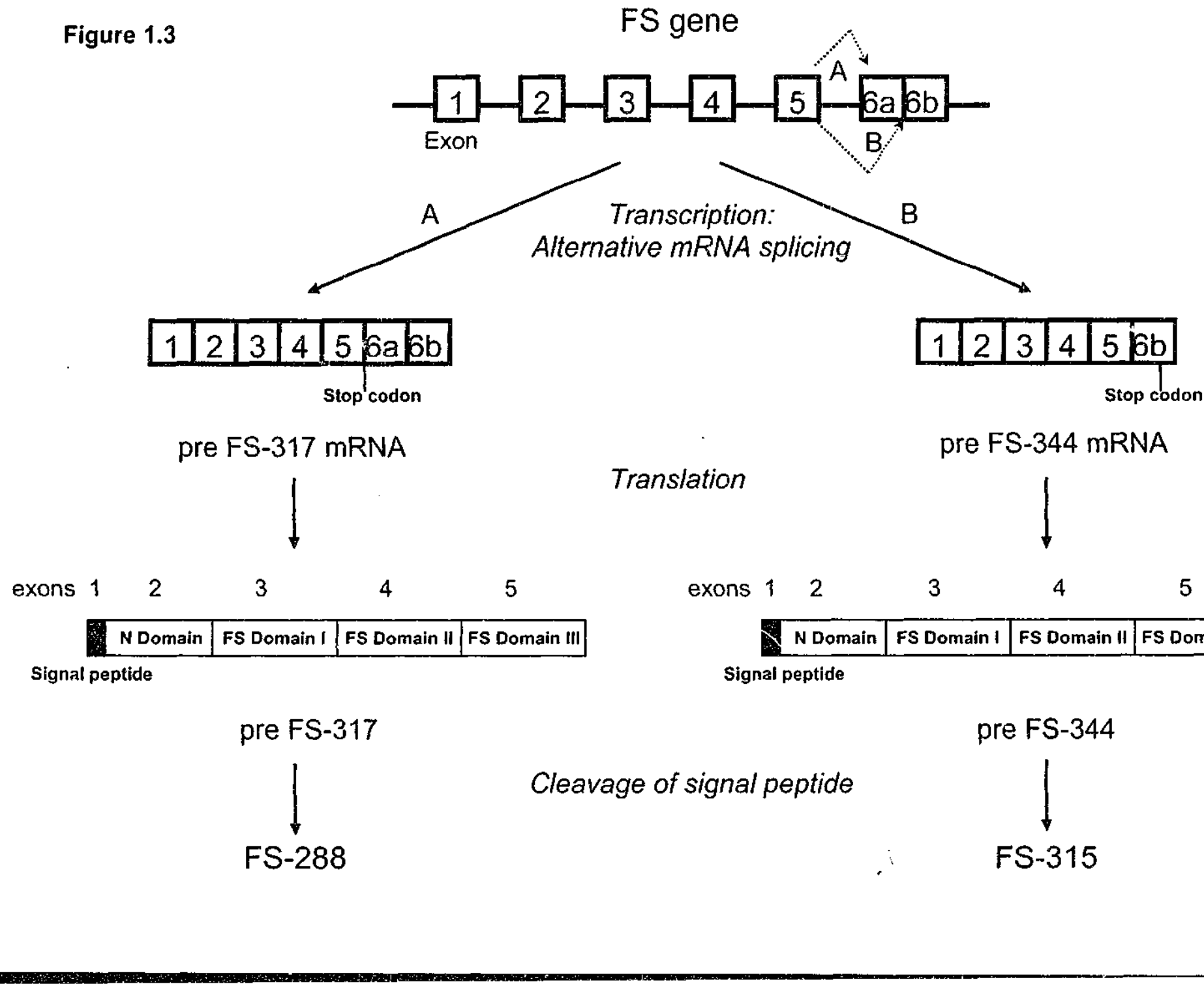

Shimasaki, *et al.*, 1988b). Alternative splicing occurs at the 3'-terminal of the gene between exon 5 and exon 6 (Fig. 1.3). The splicing out of intron 5, generating a stop codon immediately following the last amino acid of exon 5, leads to the termination of the coding sequence for a precursor of 317 amino acids (pre-follistatin 317), the COOH-terminal truncated form. On the other hand, exon 6a is spliced out together with intron 5 to generate a precursor of 344 amino acids (pre-follistatin 344) (Shimasaki, *et al.*, 1988b; Shimasaki, *et al.*, 1988a). Cleavage of the signal peptide (29 amino acids) generates the mature follistatin isoforms of 288 and 315 amino acids (follistatin-288 and follistatin-315). In addition, the majority of follistatin isolated from porcine ovary was follistatin-303 which appears to be derived from follistatin-315 by proteolytic cleavage of the 12 C-terminal amino acids (Sugino, *et al.*, 1993).

1.2.3 Protein structure: domains and related members

1.2.3.1 Domains of follistatin

The most notable structural characteristic of follistatin is the large number of cysteine residues (n = 36) contained in this small protein with forms that range in mass from 31 to 39 kDa. After removal of a 29-amino acid leader sequence, the mature protein contains 5 domains (Fig. 1.3): an N-terminal domain of 63 amino acids (a.a.), three domains of 73- to 75-a.a. (domain I, II and III), and a highly acidic C-terminal domain of 27 a.a. only in follistatin-315 (Shimasaki, *et al.*, 1988b; Shimasaki, *et al.*, 1988a). The N-terminal domain contains 6 cysteine residues, while domains I, II and III all have 10 cysteine residues. A study using site-directed mutagenesis revealed that the N-terminal domain of follistatin is critical for its binding activity to activin (Inouye, *et al.*, 1991a). Furthermore, it was suggested that a highly basic amino acid region (a.a. 72-86) of the first follistatin domain is associated with the capacity of follistatin to bind to heparan sulfate and also is involved in its interaction with activin. Moreover, this highly basic amino acid region of follistatin-315 is masked by the C-terminal 27 amino acid extension (an acidic a.a.-rich region) (Inouye, *et al.*, 1992; Sumitomo, *et al.*, 1995) which has been proposed to inhibit the ability of follistatin-315 to associate with the extra-cellular matrix (Sumitomo, *et al.*, 1995). Two recent reports have further defined the role of the N-terminal domain of follistatin (Wang, *et al.*, 2000; Sidis, *et al.*, 2001).

Deletion of the total N-terminal domain, disruption of N-terminal disulfides, and deletion of the first two residues all lead to a significant decrease in activin-binding ability and abolish the ability of follistatin to suppress activin bioactivity (Sidis, *et al.*, 2001). In addition, two discontinuous sequences (a.a. 3-26 and a.a. 46-59) in the N-terminal domain were identified as the regions capable of binding ^{125}I labeled activin A (Wang, *et al.*, 2000). Moreover, all of the cysteine residues in follistatin are involved in disulfide bonds and native follistatin can bind activin only if the follistatin disulfide bonding is intact (Wang, *et al.*, 2000). Of note, the use of specific monoclonal antibodies to probe the structural effects of activin binding on the other domains of follistatin revealed no effects on follistatin domains I or II. However, changes in the recognition of domain III and C-domain were found, suggesting a modification of the antigenic structures of these regions after activin binding to follistatin (Wang, *et al.*, 2000).

1.2.3.2 Related members of follistatin family

Recently, other proteins have been identified and distinguished by their conserved alignments of 10 cysteine residues that are similar to follistatin domains, probably via the process of exon shuffling (Patthy and Nikolics, 1993; Schneyer, *et al.*, 2001). These proteins, including agrin, testican and SPARC (secreted protein acidic and rich in cysteines), are collectively referred to as follistatin-related genes (Schneyer, *et al.*, 2001). However, these proteins do not appear to share the action of follistatin. Importantly, a new member of the follistatin-related gene family, termed FSRP (follistatin-related protein), is also able to bind activin-A and BMPs in a fashion similar to follistatin (Tortoriello, *et al.*, 2001). FSRP contains an N-domain and two follistatin domains, but lacks a heparin binding domain. The activin-binding site in FSRP is in the second domain including the COOH-terminal acidic region. By contrast, the NH_2-terminal region and the first domain in follistatin are more likely to be involved in the activin-binding ability (Tsuchida, *et al.*, 2000; Sidis, *et al.*, 2002). Moreover, FSRP was identified primarily in the nucleus (Tortoriello, *et al.*, 2001), whereas follistatin immunoreactivity was found in the nucleus and cytoplasm of spermatogenic cells (Ogawa, *et al.*, 1997; Meinhardt, *et al.*, 1998). Clearly, further studies of the biology of

these related proteins would enhance our knowledge of the structure-function relationships of follistatin.

1.2.4 Functions as a binding protein

1.2.4.1 As a binding protein of activin

The actions of follistatin appear to be associated with its ability to bind and neutralize various members of the TGF-β superfamily. The activin–follistatin binding complex is generally considered to be composed of one activin and two follistatin molecules, whereas inhibin, containing one β-subunit, has only one binding site for follistatin, implying that follistatin binds to activin and inhibin through the common β subunits (Shimonaka, *et al.*, 1991; de Winter, *et al.*, 1996). However, it is unclear whether follistatin can prevent inhibin binding to the activin receptor. It is important to compare the affinity of follistatin for activin to that of activin for the activin receptors (type I and II) to better understand the role follistatin plays in a physiological sense. The published estimates for the affinity (Kd) of follistatin for activin ranges from 50 to 900 pM, which is similar to that of activin for its receptors (from 100 to 400 pM) (Phillips and de Kretser, 1998). This fact explains why follistatin can function as a potent modulator of the actions of activin.

1.2.4.2 As a binding protein of other TGF-β superfamily members

In addition, follistatin can antagonize the actions of BMP-4 in *Xenopus* embryos and mouse teratocarcinoma cells, and can interact directly with BMP-4 *in vitro* (Fainsod, *et al.*, 1997). Follistatin was also found to inhibit the effects of OP-1 (also known as BMP-7), if added at a 10-fold excess (Yamashita, *et al.*, 1995). Interestingly, during chick limb development follistatin promotes the ability of BMP-7 to induce muscle growth but inhibits the ability of BMP-7 to induce apoptosis and muscle loss by flexible and reversible binding to BMP-7 (Amthor, *et al.*, 2002). A recent study in the early *Xenopus* embryo has demonstrated that follistatin can inhibit the effects of BMP-2, -4 and -7 by direct binding to a complex of BMP and its receptor (Iemura, *et al.*, 1998). Follistatin has also been shown to have the capacity to inhibit myostatin, another TGF-β family

member that acts as a negative regulator of skeletal muscle mass, from binding to receptors (Lee and McPherron, 2001). A recent report has also demonstrated that follistatin can bind to BMP-15 to form an inactive complex and suppress the bioactivities of BMP-15 (Otsuka, *et al.*, 2001c). Taken together, growing evidence indicates that not only does follistatin function as an activin binding protein, but also interacts with other TGF-β family members, presumably through a similar binding mechanism.

1.2.4.3 Association with heparan sulfate proteoglycans

Another important binding characteristic of follistatin is its association with heparan sulfate proteoglycans on cell surfaces. The C-terminal amino acid sequence appears to have a critical role for follistatin binding to heparan sulfate proteoglycans, since the C-terminal truncated form, follistatin-288, showed much higher affinity for the rat granulosa cell surface (a Kd of 2 nM) than follistatin-303, while follistatin-315 had no affinity (Sugino, *et al.*, 1993). Considering the strong interaction of activin with follistatin, the membranes of cells containing heparan sulfate proteoglycans are potentially major stores of both activin and follistatin. This concept is further supported by the evidence that the administration of heparin is able to induce a rapid and robust release of activin A and follistatin in the circulation of patients undergoing cardiovascular procedures (Phillips, *et al.*, 2000). Moreover, the association with cell surfaces promotes endocytotic degradation of the activin-follistatin complex in rat pituitary cells (Hashimoto, *et al.*, 1997).

1.2.4.4 Interaction with α_2-macroglobulin and BMP binding protein Ep45

Follistatin can also bind to α_2-macroglobulin (Phillips, *et al.*, 1997), but the significance of this property is still unclear. Also interestingly, a newly recognized BMP binding protein, Ep45, is able to modulate the suppressive action of follistatin on BMP in *Xenopus* embryos system. Microinjection of Ep45 mRNA into *Xenopus* embryos blocked the ability of follistatin to suppress BMP activity, whereas it had no effect on the other BMP antagonists, chordin and noggin (Iemura, *et al.*, 1999).

1.2.5 Difference between follistatin isoforms

The only difference in structure between follistatin-288 and follistatin-315 is that follistatin-315 has an additional 27 amino acids at the carboxyl terminal. Does this distinguish the functions of the isoforms in some important way? Why is this alternative mRNA splicing event for follistatin conserved in mammals (Shimasaki, *et al.*, 1988b; Shimasaki, *et al.*, 1988a; Michel, *et al.*, 1990)? Are they just redundant products from evolution, or are both follistatin isoforms essential for normal development and homeostasis? To answer these questions the first step would be to understand the difference between the follistatin isoforms, although our current knowledge on their function is far from complete.

1.2.5.1 Are both follistatin isoforms distributed in similar amounts and at identical locations in tissues

To determine the relative expression levels of pre-follistatin 344 mRNA and pre-follistatin 317 mRNA, S1-Nuclease analysis of total RNA from rat tissues, including kidney, pancreas, uterus, muscle, lung, testis, cortex, thymus, pituitary, adrenal, heart and ovary, has demonstrated that pre-follistatin 317 mRNA was expressed at less than 5% of pre-follistatin 344 mRNA (Michel, *et al.*, 1990). The reasons why pre-follistatin 344 mRNA is more abundant than pre-follistatin 317 mRNA are not known. Similarly it is unclear whether the relative ratio between the amounts of follistatin-288 and follistatin-315 is delicately regulated and crucial to normal function in diverse systems. Interestingly, the use of enhanced resolution gel filtration, immunoprecipitation and sulfated carbohydrate binding confirmed that follistatin-288 is the predominant form present in human follicular fluid, whereas the main form in serum is follistatin-315 (Schneyer, *et al.*, 1996). Together with the fact that the cell surface and the extra-cellular matrix are rich in heparan sulfate proteoglycans to which follistatin-288 has much higher affinity to bind than follistatin-315 (Sugino, *et al.*, 1993), suggests that follistatin-288 is primarily a membrane bound form of follistatin while follistatin-315 is a circulating form. The distinct difference between the amounts of follistatin-288 and follistatin-315 in different locations implies different biological roles of the follistatin isoforms.

1.2.5.2 Do both follistatin isoforms have similar affinity for activins and/or neutralizing ability for activins

Follistatin-288 is approximately 10-fold more potent than follistatin-315 in suppressing FSH secretion from the rat pituitary cells *in vitro* (Inouye, *et al.*, 1991b). Further, all six molecular species of follistatin purified from porcine ovaries had almost the same activin binding activity (Kd = 540-680 pM). However, the COOH-terminal truncated form, follistatin-288, showed much higher affinity for the rat granulosa cell surface than follistatin-303, and follistatin-315 had no affinity. When administered to cultures of rat anterior pituitary cells, follistatin-288 was more potent in suppressing FSH release than follistatin-303 and follistatin-315 (Sugino, *et al.*, 1993). Another study using heparan sulfate purified from *Xenopus* embryos is consistent with a report by Sugino and colleagues in that the affinity of FS288 for heparan sulfate is much higher than that of FS315 (Yamane, *et al.*, 1998). Furthermore, a novel role for follistatin was shown by an *in vitro* study where, using ^{125}I-activin A, the cell surface-associated follistatin, follistatin-288, was able to accelerate the endocytotic internalization of activin into pituitary cells resulting in its degradation by lysosomal enzymes (Hashimoto, *et al.*, 1997). In contrast, follistatin-315 did not show this action. Putting these observations together led to the hypothesis that the difference between follistatin-288 and follistatin-315 in suppressing FSH secretion by pituitary gonadotrophs may be due to their different capacities to neutralize activin. Since the previous studies have shown that follistatin isoforms have the same activin binding activity (Sugino, *et al.*, 1993), the difference may be explained by the greater cell surface association of follistatin-288 through heparan sulfate side chains of proteoglycan on the pituitary cells. However, a recent study using surface plasmon resonance and affinity cross-linking suggested an alternate explanation (Hashimoto, *et al.*, 2000). Firstly, the inhibitory effect of follistatin-288 on activin-induced transcriptional responses is more potent than that of follistatin-315 in the presence or absence of heparan sulfates. Secondly, follistatin-288 prevented activin from binding to its type II receptor more completely than did follistatin-315. Furthermore, there was a 10-fold difference in the Kd of follistatin-288 and follistatin-315 for activin A. These observations lead to a conclusion that the activin-neutralizing activity of follistatin isoforms is dependent on their affinity for activin. It is unclear why the studies using polyethylene glycol precipitation or surface

plasmon resonance biosensor analysis to determine the affinity of two follistatin isoforms for activin have different results. However, since the inhibitory effect of follistatin isoforms on activin-induced transcriptional responses was not altered by the presence or absence of heparan sulfates, the explanation that the activin-neutralizing activity of follistatin isoforms is dependent on their affinity for activin is more convincing.

1.2.5.3 Do both follistatin isoforms exert similar functions and effects in diverse tissues

Comprehensive studies addressing this particular question are lacking in the literature. While in rat pituitary cells *in vitro*, follistatin-288 promoted proteolytic degradation, activin-follistatin-315 complexes seemed to avoid the endocytotic and proteolytic degradation and were found to be relatively more stable (Hashimoto, *et al.*, 1997). Together with the different distribution and binding affinities of follistatin-288 and follistatin-315 (Michel, *et al.*, 1990; Schneyer, *et al.*, 1996; Hashimoto, *et al.*, 2000), one of the roles of follistatin-315 may be as a reservoir for activin, to prevent activin from proteolysis locally and to help regulate the distribution, function and activity of activin in various tissues and bodily fluids (Delbaere, *et al.*, 1999; McPherson, *et al.*, 1999). Alternatively, follistatin-315 may bind and neutralize the actions of activin resulting from "over production" at local sites. It remains unclear whether mechanisms exist to permit the dissociation of activin from follistatin-315 to exert its biological effects as Schneyer *et al.* (1996) claim that the binding of activins to follistatin is almost irreversible.

1.2.6 Distribution of follistatins

As follistatin has been localized to a diverse set of tissues, it is clear that the function of this protein is related to these tissues in the body. A summary of the follistatin distribution is given in Table 1.1.

Table 1.1 Distribution of follistatin

Tissue	mRNA	Protein
Reproductive system		
Testis	Germ cells, Sertoli cells	Germ cells, Sertoli cells, Leydig cells
Ovary	Granulosa cells, early corpus luteum	Granulosa cells, early corpus luteum
Uterus	Detected	Myometrium
Pregnancy membranes	Decidua, placenta	Placenta, decidua, amnion, chorion
Urogenital system		
Kidney	Collecting tubules	Proximal and distal tubules
Prostate	Basal epithelial cells, fibroblastic stroma	Epithelial cells, stroma
Endocrine system		
Pituitary	Folliculostellate cells, somatotropes, gonadotropes	Somatotropes
Adrenal	Detected	Cortex
Thyroid	Not known	Follicular cells
Pancreas	Epithelium	Islets (β cells)
Neural system		
Forebrain	Neocortex, olfactory region, thalamus, hypothalamus	Neurons
Cerebellum	Detected	Not known
Spinal cord	Detected	Not known
Digestive system		
Salivary gland	Detected	Not known
Liver	Detected	Hepatocytes
Stomach	Smooth muscle, epithelium	Not known
Hematopoietic system		
Bone	Osteoblasts, osteocytes	Chondrocytes, osteoblasts
Spleen	Not detected	White pulp
Thymus	Detected	Not known
Heart	Detected	Not known
Blood vessels	Smooth muscle cells, endothelial cells	Smooth muscle cells, endothelial cells
Lung	Epithelium	Not known
Muscle	Detected	Detected
Skin	Epithelium	Not known
Eye	Detected	Not known

Based on Phillips and de Kretser (1998).

The following sections discuss the function of follistatin in different organs and the role of follistatin in the ovary is used as an example since there are numerous papers on this topic in comparison to other tissues.

1.3 Follistatins in ovary

1.3.1 Location and secretion of follistatins

Within the ovary the granulosa cells in antral follicles and luteinized granulosa cells are the main sites of follistatin mRNA expression. Other structures, such as the theca cells, stroma and oocytes, appear to be devoid of follistatin mRNA (Shimasaki, *et al.*, 1989; Nakatani, *et al.*, 1991; Fleming, *et al.*, 1992; Tisdall, *et al.*, 1992; Roberts, *et al.*, 1993; Woodruff, *et al.*, 1993; Braw-Tal, 1994; Braw-Tal, *et al.*, 1994; Tisdall, *et al.*, 1994), although follistatin mRNA has been observed in human oocytes (Sidis, *et al.*, 1998). The localization of follistatin protein displays a similar pattern to that of follistatin mRNA. However, follistatin protein was also detected in the theca cell layers of human small antral follicles in the absence of follistatin mRNA expression, and then became undetectable with the development of a dominant follicle (Roberts, *et al.*, 1993). Thus, the granulosa cells are the cell type in the ovary that is responsible for producing and secreting follistatin in most species.

It is important to note that the level of follistatin mRNA expression within the ovary depends on the developmental stages of follicles. Follistatin mRNA expression within the antral follicles increases as follicular maturation progresses and declines during the atretic process (Nakatani, *et al.*, 1991; Roberts, *et al.*, 1993; Lindsell, *et al.*, 1994). Moreover, the follistatin protein appears to be present in only the selected dominant follicles (Nakatani, *et al.*, 1991). At the same time, primordial through to primary follicles do not express follistatin mRNA (Kogawa, *et al.*, 1991b; Nakatani, *et al.*, 1991; Braw-Tal, 1994; Braw-Tal, *et al.*, 1994; Tisdall, *et al.*, 1994), implying that follistatin may not be involved in the initial stage of recruitment of follicles. Species differences occur, as the expression of follistatin is maintained in the primate corpus luteum, whereas in other species, expression drops dramatically after ovulation in the

developing corpus luteum (Kogawa, *et al.*, 1991b; Nakatani, *et al.*, 1991; Roberts, *et al.*, 1993; Ogawa, *et al.*, 1994; Wada, *et al.*, 1996).

The follistatin expression in granulosa cells can be regulated through both cyclic AMP-dependent / protein kinase A (PKA) and protein kinase C (PKC) pathways (Klein, *et al.*, 1991; Lindsell, *et al.*, 1993; Miyanaga, *et al.*, 1993; Lindsell, *et al.*, 1994; Shukovski, *et al.*, 1995; Tano, *et al.*, 1995; Tuuri, *et al.*, 1996; Shintani, *et al.*, 1997). Interestingly, FSH, an activator of the PKA pathway, stimulates inhibin but not activin production, whereas GnRH, an activator of the PKC pathway, stimulates activin, and to a lesser degree, inhibin production. Both FSH and GnRH enhance follistatin protein production in an additive manner (Miyanaga, *et al.*, 1993).

In addition, the degree of differentiation of granulosa cells may influence follistatin production in response to FSH, LH and activin A. FSH *in vitro* enhanced follistatin production by undifferentiated and partially differentiated granulosa cells, but not by fully differentiated granulosa cells. In contrast, the only detectable effect of LH on follistatin production was on partially differentiated granulosa cells. Activin A promoted follistatin production by undifferentiated and partially differentiated granulosa cells, but suppressed follistatin production by fully differentiated granulosa cells (Shintani, *et al.*, 1997). Moreover, an *in vivo* study in rats suggested that the expression of follistatin in preovulatory follicles might be suppressed by the primary gonadotropin surge during proestrus (Ogawa, *et al.*, 1994). Hence, the decrease of follistatin production in preovulatory follicles may occur before ovulation, possibly due to the primary gonadotropin surge. Nevertheless, whether this phenomenon is crucial to the ovulation process needs further research.

Other stimulators of ovarian follistatin *in vitro* include activin, epidermal growth factor (EGF) and prostaglandin E2 (Michel, *et al.*, 1992; Lindsell, *et al.*, 1993; Tano, *et al.*, 1995; Tuuri and Ritovs, 1995; Shintani, *et al.*, 1997). In addition, the stimulation of follistatin production by FSH can be suppressed by EGF but enhanced by activin (Michel, *et al.*, 1992). Follistatin also antagonized the action of activin on the follistatin mRNA production (Tano, *et al.*, 1995), suggesting that a local regulatory loop may be present in the granulosa cells.

1.3.2 Effects of overexpression of follistatin on ovarian function

Follistatin deficient mutants died soon after birth, making it difficult to study ovarian function in that model (Matzuk, *et al.*, 1995a). However, overexpression of mouse follistatin results in reproductive defects in transgenic mice (Guo, *et al.*, 1998). In this report, a mouse metallothionein-I promoter was fused to a 5.1-kb genomic fragment, resulting in overexpression of mouse follistatin transgene in many tissues of several lines. In line 4, a highly expressing line, the FSH levels were significantly suppressed and histological analysis showed small ovaries with a block in folliculogenesis. It seems likely that the decreased FSH results from the blocking of FSH stimulation by activin. It is unclear whether this phenotype represents purely the effects of FSH deficiency or whether there is a direct effect of the increased follistatin expression. Nevertheless, in lines 9 and 5, in which follistatin was moderately overexpressed and in which the FSH level was not suppressed, there was still some disruption in folliculogenesis. The phenotypes ranged from subfertility, a block at the stage of the early antral follicle, to a block at the stage of the early primary follicle. Hence, the results also underline the importance of follistatin in ovarian function.

1.3.3 Interaction with activins

1.3.3.1 Location of inhibin/activin subunits

The functions of follistatin in the ovary have been related to those of activins (Table 1.2), particularly following the identification that follistatin was an activin binding protein. Hence, it is necessary to understand the actions of activins in the ovary before trying to understand follistatin biology in the ovary. Several studies have assessed the location of inhibin/activin α, βA and βB subunits in the ovary (Roberts, *et al.*, 1993; Eramaa, *et al.*, 1995; Mather, *et al.*, 1997; Sidis, *et al.*, 1998). Neither βA nor βB mRNA was detectable in oocytes, but α subunit mRNA was weakly detectable in some human oocytes (Sidis, *et al.*, 1998). The α subunit is present in granulosa cells and theca cells of antral follicles, luteinized granulosa cells, but not in luteinized theca cells. The βA subunit mRNA and protein was observed in granulosa cells of all stages and theca cells of developing dominant follicles, whereas the βB subunit was only found in granulosa

Table 1.2 The antagonism between activin and follistatin in the ovary

	Granulosa cells	The numbers of FSH and LH receptors in granulosa cells	Steroidogenesis	Oocytes
Activin	↑ differentiation ↓ premature luteinization	↑	↑ E_2 ↑ P_4 in undifferentiated granulosa cells ↓ P_4 in differentiated granulosa cells ↓ androgen	↑ meiotic & cytoplasmic maturation ↑ developmental competence to form blastocysts
Follistatin	↑ luteinization or atresia	↓	↓ E_2 ↓ P_4 in undifferentiated granulosa cells ↑ P_4 in differentiated granulosa cells ↑ androgen	↓ meiotic & cytoplasmic maturation ↓ developmental competence to form blastocysts

E_2 : estrogen; P_4 : progesterone; ↑: increase or promote; ↓: decrease or inhibit. (See text for details)

cells of small antral follicles. Additionally, the transcripts for all four activin receptor subtypes (ActRIA, ActRIB, ActRIIA, and ActRIIB) were detectable in oocytes, granulosa cells and theca cells. Thus, generally inhibins and activins appear to be produced by granulosa cells and exert both autocrine and paracrine actions. Since granulosa cells are also the main cells that produce follistatin in the ovary, they may be the primary and foremost sites where the homeostasis of the follistatin/activin/inhibin system is maintained in the ovary. Collectively, the location of follistatin and inhibin/activin subunits suggests that follistatin and inhibin may play a role at the later stages of follicular development, while activin exerts its effects primarily at the early stages of follicular development (Nakatani, *et al.*, 1991; Roberts, *et al.*, 1993; Lindsell, *et al.*, 1994; Eramaa, *et al.*, 1995; Mather, *et al.*, 1997; Sidis, *et al.*, 1998). These studies also lead to the hypothesis that the orderly transition from an activin-dominant to an inhibin / follistatin-dominant microenvironment is critical for dominant follicle development (Knight and Glister, 2001).

1.3.3.2 Effects on granulosa cells and follicles

It is a generally accepted concept that activin, either alone or with FSH, exerts an autocrine effect on granulosa cells, promoting differentiation during the preantral and early antral stages of folliculogenesis and inhibiting premature luteinization at the later stages of antral follicle development. Follistatin, on the other hand, modulates granulosa cell function in favor of luteinization or atresia by neutralizing the actions of activin and may also directly modulate progesterone metabolism by granulosa cells (Findlay, 1993; Li, *et al.*, 1995; Miro and Hillier, 1996). However, recent studies have demonstrated that the stimulatory action of activin on the proliferation of granulosa cells may not occur at all stages of the granulosa cells (Woodruff, *et al.*, 1990; Yokota, *et al.*, 1997; Liu, X, *et al.*, 1998; Mizunuma, *et al.*, 1999). A study on preantral follicles revealed that activin A had no effect on preantral follicles from adult mice and blocked FSH-stimulated follicular growth, although activin A enhanced the growth of preantral follicles from immature mice (Yokota, *et al.*, 1997). Intriguingly, the same investigation demonstrated *in vitro* that activin secreted by secondary follicles caused primary follicles to become dormant at the resting stage, an action reversed by follistatin (Mizunuma, *et al.*, 1999). Taken together, the findings suggest that activin and

follistatin have a role in regulating the initiation of folliculogenesis and in determining the size of the cohort of growing follicles during ovarian follicle recruitment.

1.3.3.3 Effects on FSH and LH receptors in granulosa cells

Follistatin antagonizes the stimulatory effects of activin on the expansion of FSH receptors and LH receptors in granulosa cells (Xiao, *et al.*, 1992; Tsuchiya, *et al.*, 1999). Activin alone (3-100 ng/ml) caused a 4-fold increase in FSH receptor number in cultured granulosa cells from diethylstilbestrol-treated immature rats. This effect was suppressed 31% by follistatin (100 ng/ml) treatment, which alone, had no effect on FSH receptor number. Activin at a higher dose (100 ng/ml) prevented FSH-induced down-regulation of FSH receptor number, whereas at lower concentrations (3-30 ng/ml) it enhanced down-regulation of FSH receptor number by 20%. Further, it is noteworthy that follistatin alone prevented FSH-induced down-regulation by increasing FSH receptor number up to 40-50% (Xiao, *et al.*, 1992). In rat granulosa cells, activin in the presence of FSH also induced LH receptor expansion significantly, and follistatin inhibited this effect in a dose-dependent manner (Tsuchiya, *et al.*, 1999). Jointly, activin may play a pivotal role in the acquisition of responsiveness to FSH by granulosa cells of preantral follicles, an essential step for their further development. The low level of follistatin expression in early stages of follicles may facilitate this process.

1.3.3.4 Effects on steroidogenesis

The actions of activin and follistatin on steroidogenesis in granulosa cells appear to vary according to the degree of maturity of granulosa cells. *In vitro* studies involving undifferentiated or partially differentiated granulosa cells have shown that activin enhances gonadotropin-stimulated P450 aromatase activity and estradiol production regardless of the developmental stage. However, activin promotes the gonadotropin-stimulated progesterone production in undifferentiated granulosa cells whereas it suppresses this effect in partially differentiated granulosa cells (Hutchinson, *et al.*, 1987; Miro, *et al.*, 1991; Shukovski, *et al.*, 1991; Hillier and Miro, 1993). Further, studies using fully differentiated granulosa cells revealed that activin suppresses gonadotropin-stimulated P450 side chain cleavage enzyme (P450scc) expression and progesterone

production (Miro, *et al.*, 1991; Cataldo, *et al.*, 1994): these effects can be antagonized by follistatin, presumably through its capacity to bind activin (Xiao, *et al.*, 1992; Cataldo, *et al.*, 1994). These findings suggest that activin may stimulate the early differentiation of granulosa cells, while retarding the late differentiation and luteinization. Presumably follistatin plays a role of modulator, suppressing activin at early stages, and potentiating luteinization at later stages.

1.3.3.5 Effects on theca cells

The main role of theca cells is to synthesize androgen that will be used as a substrate for the production of estrogen by granulosa cells. Studies on human, rat and bovine theca cells revealed that activin attenuates LH-induced androgen production and suppresses the increase of androgen production stimulated by estradiol, and that follistatin can reverse the inhibitory effects of activin (Hsueh, *et al.*, 1987; Hillier, 1991; Wrathall and Knight, 1995). In contrast, activin is capable of inducing the proliferation of theca cells, whereas follistatin antagonizes this effect (Duleba, *et al.* 2001).

1.3.3.6 Effects on oocytes

Activin *in vitro* has been shown to promote meiotic and cytoplasmic maturation of the oocytes, an effect that can be inhibited by follistatin (Sadatsuki, *et al.*, 1993; Alak, *et al.*, 1996; Alak, *et al.*, 1998). Furthermore, a study on denuded or cumulus-enclosed bovine oocytes revealed that activin potentiates their developmental competence to form blastocysts, whereas follistatin reverses or neutralizes the effect of activin (Silva and Knight, 1998). Together, these findings suggest that activin and follistatin may contribute to the regulation of oocyte maturation and competence.

1.3.4 Interaction with other members of TGF-β superfamily in the ovary

Recent compelling evidence indicates that follistatin can exert effects by binding to other members of TGF-β superfamily, especially BMPs, in the ovary (Yamashita, *et al.*, 1995; Iemura, *et al.*, 1998; Otsuka, *et al.*, 2001c). These findings open another window to follistatin biology and also make it more intriguing. The functions of GDF-9, BMP-

15 (also known as GDF-9b), BMP-6, BMP-4 and BMP-7 in the ovary and their potential interactions with follistatin will be discussed here (Table 1.3).

1.3.4.1 Location of GDF-9 and BMP-15 in ovary

Within the mouse ovary GDF-9 and BMP-15 mRNA are detected specifically in the oocytes of small primary follicles, but not in the primordial follicles. Additionally, BMP-6 transcripts are expressed in oocytes at high levels and at lower levels in follicular cells (Elvin, *et al.*, 2000). However, in cows and pigs, a low level GDF-9 expression has been detected in oocytes of primordial follicles, suggesting species variation in GDF-9 expression at the earliest stages of follicular development (Bodensteiner, *et al.*, 1999). Moreover, the transcripts of both BMP-15 and GDF-9 are present persistently in the oocyte in all subsequent stages of folliculogenesis and in ovulated oocytes (Elvin, *et al.*, 2000). Further, in humans, the mRNA and protein for GDF-9 and BMP-15 were detected in the oocytes of primary follicles by *in situ* hybridization and immunohistochemical analysis. The expression of GDF-9 mRNA begins slightly earlier than that of BMP-15 in human oocytes during follicular development (Aaltonen, *et al.*, 1999). Presumably the interactions between follistatin and GDF-9 and BMP-15 would not occur in small follicles as follistatin is only expressed in the granulosa cells of larger follicles.

1.3.4.2 GDF-9

Folliculogenesis in the ovaries of GDF-9-deficient mice is blocked at the type 3b (primary) follicle (Dong, *et al.*, 1996). The ovaries are hypoplastic despite elevated serum FSH and LH levels. In addition, immunohistochemical staining with proliferating cell nuclear antigen and TUNEL labeling verified that granulosa cells of GDF-9-deficient type 3b primary follicles lose competence to proliferate and undergo apoptosis. The GDF-9-deficient follicle is also unable to recruit theca cell precursors to form a theca layer surrounding the follicle (Elvin, *et al.*, 1999a). Further characterization of GDF-9-deficient oocytes (Carabatsos, *et al.*, 1998) revealed that, based on germinal vesicle chromatin patterns, fully grown oocytes isolated from GDF-9-deficient mice progress to advanced stages of differentiation equivalent to those found in antral

Table 1.3 The actions of other TGF-β superfamily members that follistatin potentially binds to in the ovary

	Folliculogenesis	Granulosa cell	Theca cell	Steroidogenesis	Interaction with follistatin
GDF-9	Deficiency in mouse: homozygous mutants→ blocked at the stage of primary follicles; abnormal ultrastructural features of oocytes Induce *in vitro* cumulus expansion	↑ proliferation (FSH-independent) ↓ FSH-induced differentiation	Deficiency in mouse: unable to recruit the theca cell precursors	↑ FSH-independent P_4 and E_2 production ↓ FSH-induced P_4 and E_2 production ↓ FSH-induced LH receptor production	?
BMP-15	Deficiency in sheep: homozygous mutants→ blocked at the stage of primary follicles; heterozygous mutants→ increased ovulation Deficiency in mouse: homozygous mutants→ subfertile, decreased ovulation	↑ proliferation (FSH-independent)	?	↓ FSH receptor production ↓ FSH-induced FSH and LH receptor production ↓ FSH-induced P_4 production ↔ FSH-induced E_2 production	↓ the effects of BMP-15 on the proliferation, FSH receptor and steroidogenesis
BMP-6	?	↔ proliferation	?	↓ FSH-induced P_4 production ↔ FSH-induced E_2 production	?
BMP-4	?	?	?	↑ FSH-induced E_2 production ↓ FSH-induced P_4 production	?
BMP-7	↑ follicular growth ↓ ovulation and luteinization	↑ proliferation	?	↑ FSH-induced E_2 production ↓ FSH-induced P_4 production	?

E_2: estrogen; P_4: progesterone; ↑: enhance or promote; ↓: suppress or inhibit; ↔: no effect; ?: no available mammalian data. (See text for details)

follicles of control (heterozygous) mice. Abnormal ultrastructural features of GDF-9-deficient oocytes were found, including perinuclear organelle aggregation, unusual peripheral Golgi complexes, and a failure to form cortical granules. Modified interconnections between granulosa cells and oocytes were also observed by ultrastructural (EM) and fluorescence microscopic analysis of follicles from GDF-9-deficient mice. These findings point to abnormal cytoplasmic maturation of GDF-9-deficient oocytes and the granulosa cell to oocyte aberrations. Interestingly, when compared to gene expression in control ovaries by Northern blot analysis, an increase in kit ligand expression, and a decrease in inhibin/activin βB and follistatin expression, were observed in GDF-9-deficient ovaries (Elvin, *et al.*, 1999a).

The mechanisms by which GDF-9 deficiency causes the changes of expression levels of these growth factors need to be further defined. To validate the functions of GDF-9 in the follicles at later stages, recombinant mouse GDF-9 was produced (Elvin, *et al.*, 1999b) and can induce hyaluronan synthase 2 (HAS2), cyclooxygenase 2 (COX-2), and steroidogenic acute regulator protein (StAR) mRNA synthesis but suppresses urokinase plasminogen activator (uPA) and LHR mRNA synthesis in cultured mouse granulosa cells. Consistent with the induction of StAR mRNA by GDF-9, recombinant GDF-9 enhances progesterone synthesis by granulosa cells in the absence of FSH. Importantly, recombinant GDF-9 *in vitro* induces cumulus expansion of oocytectomized cumulus cell-oocyte complexes. This phenomenon is also consistent with the fact that GDF-9 can cause induction of HAS2 and suppression of the protease uPA in granulosa cells, both being critical events in the production of the hyaluronic acid-rich extracellular matrix during cumulus expansion. Further, treatment with recombinant GDF-9, but not FSH, can stimulate proliferation of cultured rat granulosa cells from both early antral and preovulatory follicles (Vitt, *et al.*, 2000). Although GDF-9 treatment alone stimulates basal steroidogenesis in granulosa cells, co-treatment with GDF-9 attenuates FSH-stimulated progesterone and estradiol production as well as FSH-induced LH receptor formation. Additionally, the suppressive effects of GDF-9 on FSH-induced granulosa cell differentiation may be associated with decreases in the FSH-induced cAMP production (Vitt, *et al.*, 2000).

1.3.4.3 BMP-15

BMP-15 is a potent stimulator of granulosa cell proliferation and this mitogenic effect is FSH-independent (Otsuka, *et al.*, 2000). In addition, although BMP-15 alone has no effect on steroidogenesis, it suppresses FSH-induced progesterone production, but has no effect on FSH-induced estradiol production (Otsuka, *et al.*, 2000). This is consistent with the evidence that BMP-15 decreases the steady levels of transcripts induced by FSH, including StAR, P450scc, 3β-hydroxysteroid dehydrogenase (3β-HSD), LH receptor, inhibin/activin subunits (α, βA and βB) and the FSH receptor. Importantly, BMP-15 markedly suppresses both the basal and FSH-induced increases in the FSH receptor mRNA levels. Taken with the finding that BMP-15 suppresses steroidogenesis induced by FSH, but not by forskolin, the down regulation of FSH receptor expression may be the primary effect of BMP-15 in suppressing FSH action (Otsuka, *et al.*, 2001b).

Moreover, genetic studies on BMP-15 further point to its importance in folliculogenesis. In BMP-15 homozygous mutants in sheep, folliculogenesis is blocked at the stage of primary follicles that mimics the phenotype of GDF-9 deficiency (Galloway, *et al.*, 2000). In contrast, BMP-15 heterozygous mutants of sheep have increased ovulation and multiple pregnancies. However, mutation of BMP-15 in mice did not cause the same phenotype as that in sheep (Yan, *et al.*, 2001). In mice, BMP-15 knockout (BMP-$15^{-/-}$) ovaries were grossly indistinguishable from either BMP-15 heterozygous (BMP-$15^{+/-}$) or wild-type ovaries. Additionally, BMP-$15^{+/-}$ females did not have increased ovulation. Nonetheless, BMP-$15^{-/-}$ females were subfertile and had decreased ovulation and fertilization rates. Also, the fertility of BMP-$15^{-/-}$,GDF-$9^{+/-}$ double mutant females was reduced compared with that of BMP-$15^{-/-}$, BMP-$15^{+/-}$, or GDF-$9^{+/-}$ female mice. These findings indicate that the dosage of intact BMP-15 and GDF-9 alleles influences the destiny of oocytes and subsequent fertility (Yan, *et al.*, 2001).

1.3.4.4 BMP-6

Unlike BMP-15 and GDF-9, BMP-6, which is another oocyte-derived growth factor, has no effect on the mitogenic activity of rat granulosa cells (Otsuka, *et al.*, 2001a). BMP-6 activity on steroidogenesis resembles BMP-15 but differs from GDF-9

activities. In other words, BMP-6 suppresses FSH-induced progesterone production but not estradiol production. BMP-6 also exerts a similar action to BMP-15 by suppressing the steady state mRNA levels of FSH-induced StAR and P450scc, without affecting P450 aromatase mRNA level, supporting its differential function on FSH-regulated progesterone and estradiol production. However, the mechanism of inhibition of FSH action by BMP-6 is different from that by BMP-15. BMP-6 inhibits FSH action most likely through the down-regulation of adenylate cyclase activity, whereas BMP-15 suppresses the basal FSH receptor expression without affecting adenylate cyclase activity (Otsuka, *et al.*, 2001a).

1.3.4.5 Structural homology among GDF-9, BMP-15 and BMP-6

GDF-9 and BMP-15 are more homologous to each other than to any other members of TGF-β superfamily (Dube, *et al.*, 1998). In the carboxyl terminal domain, GDF-9 and BMP-15 are 52.9% identical, whereas BMP-6 shares 28.4% and 37.3% protein sequence identity with GDF-9 and BMP-15, respectively. Of interest, the monomer subunits of GDF-9 and BMP-15 have an even number of cysteines (6 for GDF-9, and 6 for human BMP-15 or 8 for mouse BMP-15). In contrast, most of the monomer subunits of the other TGF-β superfamily members have 7 or 9 cysteines. The odd cysteine is used to link two monomer subunits by forming an inter-molecular disulfide bond leading to a covalently-linked dimer. Accordingly, GDF-9 and BMP-15 are proposed to form non-covalently associated dimers.

1.3.4.6 Interactions of follistatin with BMP-15, GDF-9 and BMP-6

Although there are no reports describing the interaction between follistatin and GDF-9 or BMP-6, a recent publication has demonstrated that follistatin inhibits the function of BMP-15 (Otsuka, *et al.*, 2001c). Follistatin-288 *in vitro* inhibited BMP-15-induced thymidine uptake by rat granulosa cells in a dose dependent manner, whereas follistatin-288 alone exerted no effect on the mitosis of granulosa cells. Regarding FSH receptor expression, follistatin also caused a reversal of the suppressive effect of BMP-15 and the consequent level of FSH receptor mRNA was similar to that seen when follistatin-288 was added alone. In addition, follistatin-288 has been shown to be able to reverse

the inhibitory effect of BMP-15 on FSH-induced progesterone production. Further, the use of surface plasmon resonance has demonstrated direct binding of follistatin to BMP-15 (Otsuka, *et al.*, 2001c). This observation clearly broadens the roles of follistatin in the ovary. Moreover, given the high identity between GDF-9 and BMP-15 in structure, it is very likely that follistatin also binds to GDF-9 and modulates its function.

1.3.4.7 BMP-4 and BMP-7

In contrast to GDF-9, BMP-15 and BMP-6, which are expressed by oocytes, the transcripts of BMP-4 and BMP-7 have been detected prominently in theca cells (Shimasaki, *et al.*, 1999). *In situ* hybridization histochemistry identified strong mRNA expression of BMP-4 and -7 in the theca cells and BMP receptor types IA, IB, and II in the granulosa cells and oocytes of most follicles in ovaries of normal cycling rats, indicating potential paracrine mechanisms. Further *in vitro* studies showed that BMP-4 and -7 differentially modulated FSH actions in rat granulosa cells. Specifically, physiological concentrations of BMP-4 and -7 enhanced and suppressed FSH-induced estradiol and progesterone production, respectively (Shimasaki, *et al.*, 1999). Furthermore, the capability of BMP-7 to stimulate FSH induced estradiol production is enhanced by its potentiation of P450 aromatase although it did inhibit FSH-induced StAR mRNA expression. However, BMP-7 did not influence expression of mRNA for P450-scc and 3β-HSD (Lee, *et al.*, 2001).

To further define the functions of BMP-7, *in vivo* injection of BMP-7 into the ovarian bursa of rats led to decreased numbers of primordial follicles but increased numbers of primary, preantral, and antral follicles, suggesting that BMP-7 may potentiate the transition of follicles from the primordial stage to the pool of primary, preantral, and antral follicles. This effect is consistent with the finding that BMP-7 stimulated DNA synthesis and proliferation of granulosa cells from small antral follicles *in vitro*. On the other hand, in the same *in vivo* experiment BMP-7 decreased the ovulation rate. Hence, in general, BMP-7 appears to promote follicular growth and development, while simultaneously suppressing ovulation and luteinization (Lee, *et al.*, 2001).

Moreover, it is noteworthy that follistatin has been reported to be able to bind BMP-2, -4, -7, and BMP-4/7 heterodimers and to inhibit the biological activities of these proteins in *Xenopus* embryos (Yamashita, *et al.*, 1995; Iemura, *et al.*, 1998). However, further studies are required to clarify the interactions between follistatin and BMP-4 and -7 and their physiological relevance within the mammalian ovary.

1.3.5 Brief summary

In light of the recent studies on the functions of follistatins and members of TGF-β superfamily, the role of follistatins in ovary cannot be explained properly by their modulation of only the ultra-short feedback loop of the actions of activins. Follistatins may behave like a buffer that can adjust the multiple actions of TGF-β superfamily members to an appropriate physiological combination that facilitates the normal functions of ovaries. This hypothesis requires further study. Furthermore, if it is true, do the mechanisms, which regulate follistatin expression, act upstream or downstream of the actions of TGF-β superfamily members?

1.4 Follistatins in testis

1.4.1 Distribution

In the adult rat testis, follistatin mRNA has been located in many germ cells, Sertoli cells at all stages of the seminiferous cycle and endothelial cells of blood vessels, but not in Leydig cells and macrophages (Meinhardt, *et al.*, 1998). Among germ cells, follistatin mRNA could not be detected in type A and intermediate spermatogonia, whereas small amounts were observed in type B spermatogonia. Similar amounts could be seen in preleptotene and leptotene primary spermatocytes. However, mRNA expression was low in late leptotene and early zygotene primary spermatocytes and increased in pachytene and diplotene primary spermatocytes. Follistatin mRNA expression subsequently declined but remained evident in spermatids from steps 1 to 10 and declined thereafter to the undetectable levels from steps 16 to 19 (Meinhardt, *et al.*, 1998). Using immunohistochemistry with two different antisera to follistatin, follistatin protein was found in spermatogonia, primary spermatocytes at all stages except the

zygotene stage, spermatids at all stages and in endothelial cells, Sertoli cells and Leydig cells (Meinhardt, *et al.*, 1998). Moreover, follistatin immunoreactivity has been also observed in both Leydig and Sertoli cells of the human testis (Anderson, *et al.*, 1998).

In a recent study on the perinatal rat testis, follistatin mRNA was detected in Sertoli cells from day 21.5 postcoitum. Further, follistatin mRNA was absent from gonocytes at day 21.5 postcoitum and at birth but it was observed in germ cells at day 3 and 9 after birth. Follistatin protein appeared to be present in germ cells at day 3 after birth and Sertoli cells, but not Leydig cells by immunostaining (Meehan, *et al.*, 2000), implying age-specific expression and actions during the early post-natal development of the rat testis.

1.4.2 Regulation of secretion

There is a paucity of studies on regulation of follistatin production and secretion in the testis. Michel *et al.* (1993), using Sertoli cell-enriched cultures from testes of immature rats to study the regulation of follistatin mRNA expression in Sertoli cells, have shown that the expression of follistatin mRNA can be enhanced by the protein kinase C-dependent pathway and epidermal growth factor (EGF), but not regulated by FSH and the protein kinase A-dependent pathway. No effects on follistatin mRNA level were exerted by prostaglandin E_2, all-trans-retinoic acid, extracellular adenosine triphosphate, testosterone and activin on immature Sertoli cell-enriched cultures (Michel, *et al.*, 1993). The latter contrast with recently published data which demonstrates that activin A induces follistatin secretion by immature Sertoli cells *in vitro* (Buzzard, *et al.*, 2003).

1.4.3 Interaction with activins

The α-subunit mRNA and protein have been demonstrated in Sertoli cells and Leydig cells but not in germ cells of the immature and adult testis (Cuevas, *et al.*, 1987; Shaha, *et al.*, 1989; Majdic, *et al.*, 1997; Noguchi, *et al.*, 1997). The mRNA and protein for the βA and βB subunits are present in Sertoli cells of the rat and human testis (Kaipia, *et al.*, 1992; Majdic, *et al.*, 1997; Anderson, *et al.*, 1998; Andersson, *et al.*, 1998). Further, there are data revealing that Leydig cells and peritubular cells can produce activin A *in*

vitro (Lee, W. *et al.*, 1989; de Winter, *et al.*, 1994). Additionally, immunohistochemical studies in human testis have identified the protein for βB subunit in spermatogonial, primary spermatocytes and round spermatids (Andersson, *et al.*, 1998). In terms of activin receptors, expression of mRNA for ActRIIA was detected in primary spermatocytes, early round spermatids, Sertoli cells and Leydig cells, whereas spermatogonia express ActRIIB mRNA (de Winter, *et al.*, 1992; Kaipia, *et al.*, 1992; Kaipia, *et al.*, 1993). In addition, ActRIA mRNA was identified in Sertoli cells and Leydig cells but not in germ cells, whereas the mRNA for ActRIB was detected in germ cells, especially in round spermatids (de Jong, 1997).

Most of studies concerning the interactions of follistatin and activins are limited to *in vitro* experiments and the usual parameter measured in rodents is mRNA since measurements of follistatin protein secretion have not been possible due to the absence of a suitable assay. In germ-Sertoli cell cocultures prepared from 21-day old rats, follistatin has been shown to antagonize the ability of activin A to stimulate reaggregation of Sertoli cell monolayers, but has no effect on the ability of activin A to enhance [3H]-thymidine incorporation (Mather, *et al.*, 1993). A study using fragment cultures of rat testis has revealed age specific actions of activin A and follistatin on testicular development. In fragment cultures from day 9, but not from day 3 or day 18, activin A, synergizing with FSH, stimulates Sertoli cell proliferation, which follistatin was able to abolish (Boitani, *et al.*, 1995). Another study using rat testis fragment cultures has demonstrated that the combination of FSH and follistatin may function as mediators of early postnatal testis development to enhance progression of gonocytes into spermatogonia (Meehan, *et al.*, 2000). Additionally, both activin and follistatin alone suppressed Sertoli cell proliferation and their effect could be reversed while adding activin and follistatin together, implying the existence of a third system regulating postnatal testis development (Meehan, *et al.*, 2000).

1.4.4 Effects of overexpression of follistatin on testis function

A mouse model of the overexpression of follistatin has demonstrated some defects of reproductive function (Guo, *et al.*, 1998). The female part of this study has been discussed in section 1.3.2. This section will focus on the male part. Five transgenic lines

were created. Two parameters that we should know before interpreting the phenotypes are the local expression levels of the follistatin transgene in testes and the serum levels of FSH in the transgenic mice. Compared to the wild type, the mRNA expression of follistatin in testes in lines 7 and 10 were slightly increased; in contrast, those in lines 4, 5 and 9 were significantly augmented. With regard to the serum FSH levels, among these 5 lines only line 4 had significant low levels compared to the wild type. As a result, males from lines 7 and 10 were fertile. In contrast, males from lines 4, 5 and 9 were infertile. Further, the weights of the testes from lines 4, 5 and 9 were significantly decreased whereas those from lines 7 and 10 were slightly smaller compared to the wild type, implying that there were effects of follistatin on testicular function. Histological analyses showed that sections of testes from lines 7 and 10 had normal spermatogenesis; in remarkable contrast, those from lines 5 and 9 with significantly measured follistatin expression showed Sertoli cells only in the seminiferous tubules, Leydig cell hyperplasia and partial or total tubule degeneration. Surprisingly, despite the small size of the testes and infertility, sections of testes from line 4 displayed fairly normal spermatogenesis. Lines 5 and 9 may be good models to elucidate the local effects of follistatin on testis since their serum FSH levels were normal and their mRNA expression levels of follistatin in testes were high. Their phenotypes of testes indicate that overexpression of follistatin would be harmful to the process of spermatogenesis. Nevertheless, the low serum levels of FSH in line 4 complicated the interpretation of the testicular phenotypes since the testes showed normal spermatogenesis. The low FSH may cause a reduction in Sertoli cell numbers and hence the decreased testicular size. It is not clear whether the overexpression of follistatin is the direct cause of the seminiferous tubule failure in lines 5 and 9 or whether it acts indirectly by neutralizing the action of endogenously produced activin. Unfortunately no data are available on testicular morphology in the βA null mice as they die at birth (Matzuk, *et al.*, 1995b). Further, overexpression of βA in mice resulted in spermatogenic disruption suggesting that high levels of activin are indeed detrimental to spermatogenesis (Tanimoto, *et al.*, 1999). Links between the phenotypes of this model and the follistatin overexpression model could arise if the high follistatin expression induced an increase in βA expression locally in the testis causing spermatogenic damage.

1.4.5 Interaction with BMPs

While to date no studies have been reported showing the direct interactions of follistatin with BMPs in the testis, some data have already pointed to this possibility in view of the discussion about the binding of follistatins BMPs in section 1.2.4.2. Other indirect evidence can be supported by two mouse transgenic models that are the βA subunit overexpressed mice (Tanimoto, *et al.*, 1999) and the follistatin overexpressed mice (Guo, *et al.*, 1998). Both models displayed spermatogenic disruption. At first glance, it may not be easy to explain why the overexpression of βA subunit and follistatin both revealed a similar phenotype in testes, since activin and follistatin have been regarded as being antagonists in many aspects of biology. It is possible that this disruption of spermatogenesis is the effect of factors which can be modulated by follistatin, acting upstream or downstream of activin A. As a result, the overexpression of both follistatin and activin A are, in fact, on the same track leading to spermatogenic disruption. The possible candidates may be BMP 8A and BMP 8B since both BMP 8A and BMP 8B transcripts are localized to the germ cells in the testes by *in situ* hybridization during specific stages of spermatogenesis, with highest levels of mRNA in round spermatids steps 6 ~ 8 after 3 weeks of age (Zhao and Hogan, 1996). Subsequent studies have demonstrated that BMP 8B is essential for the initiation and maintenance of spermatogenesis (Zhao, *et al.*, 1996) whereas BMP 8A is involved in the maintenance of spermatogenesis and the integrity of the epididymis (Zhao, *et al.*, 1998)

1.5 Follistatins in pituitary

1.5.1 Location

Inhibin, activin and follistatin have been recognized as important growth factors regulating FSH secretion by pituitary cells for more than 10 years. There is a consensus that inhibin, produced principally in the gonads, exerts its endocrine action at the pituitary. By contrast, activin and follistatin exert their autocrine or paracrine effects at the pituitary (de Kretser, *et al.*, 2002). In other words, the follistatin protein that is produced by pituitary cells, not from systemic circulation, plays a role at the pituitary. A study, by microsequencing of fractions derived from conditioned medium by bovine

pituitary-derived folliculostellate cells, showed that these cells are capable of producing and secreting follistatin (Gospodarowicz and Lau, 1989). Follistatin was also isolated from bovine pituitary (Kogawa, *et al.*, 1991a). Further, both activin and follistatin have been demonstrated to be produced in gonadotrophs and other cell types of adult female rat pituitary (Roberts, *et al.*, 1989; Lee, *et al.*, 1993). Additionally, follistatin mRNA was detected in 70% of LH-β cells, 44% of FSH-β cells, and 35% of folliculostellate cells in the pituitary of diestrous rats (Kaiser, *et al.*, 1992). However, in the human pituitary, follistatin protein has been found only in somatotrophs (Wada, *et al.*, 1996). These data provide the basis of autocrine and paracrine roles of follistatins at the pituitary, which were demonstrated by the studies of Kogawa *et al* (Kogawa, *et al.*, 1991a).

1.5.2 Regulation of secretion

There are many factors, including gonadotrophin-releasing hormone (GnRH), LH, activin, inhibin, progesterone, estrogen, testosterone, corticosterone, interleukin-1β (IL-1β), and even follistatin itself, which are involved in regulating the secretion of follistatin in the pituitary.

Gonadectomy resulted in an increase in follistatin mRNA levels in the pituitary of female and male rats, which may be due to the stimulus of GnRH (Kaiser, UB and Chin, 1993; Dalkin, *et al.*, 1998). Of note, different modes of administration of GnRH have different effects on follistatin secretion. Treatment of male rat pituitary cells with pulses of GnRH (5 min; 10 nM) applied every 60 min stimulated a 14.0-fold increase in FSH-β mRNA with no change in follistatin mRNA (Besecke, *et al.*, 1996). In contrast, pulses of GnRH applied every 30 and 15 min led to stepwise increased levels in follistatin mRNA and decreased levels in FSH-β mRNA, and continuous infusion of GnRH elicited a 4.1-fold increase in follistatin mRNA, with no significant increase in FSH-β mRNA (Besecke, *et al.*, 1996).

Activin (Bilezikjian, *et al.*, 1993; DePaolo, *et al.*, 1993; Bilezikjian, *et al.*, 1996; Dalkin, *et al.*, 1996) and estradiol (Kaiser and Chin, 1993) up-regulate follistatin mRNA expression; nevertheless, testosterone (Bilezikjian, *et al.*, 1996) inhibin (Bilezikjian, *et*

al., 1996; Dalkin, *et al.*, 1998) and follistatin itself (Dalkin, *et al.*, 1996) seem to down-regulate follistatin mRNA expression. IL-1β is also a stimulator of follistatin expression (Bilezikjian, *et al.*, 1998). In addition, LH, progesterone, and corticosterone appear to suppress follistatin mRNA expression in the rat pituitary at early estrus (Tebar, *et al.*, 2000).

1.5.3 Functional roles

The pivotal role of activin, inhibin, and follistatin in regulating FSH synthesis and secretion is well established (DePaolo, *et al.*, 1991b; DePaolo, 1997). The activin/inhibin/follistatin system, interacting with hypothalamic factors, gonadal steroids, corticosterone, and cytokines, may control pituitary function in endocrine, paracrine, and autocrine ways.

The main role of follistatin in the pituitary is generally considered to be through neutralization of the effects of activin, although it may have some other potential pathways to regulate FSH synthesis and secretion (Bilezikjian, *et al.*, 1996; Dalkin, *et al.*, 1996). There is considerable evidence that follistatin exerts its effects by blockade of the effects of activin, resulting in a decrease in both FSH synthesis (Carroll, *et al.*, 1989; DePaolo, *et al.*, 1993; Dalkin, *et al.*, 1996; Besecke, *et al.*, 1997) and secretion (Robertson, *et al.*, 1990; Wang, QF, *et al.*, 1990a; Wang, *et al.*, 1990b; DePaolo, *et al.*, 1991a; Depaolo, *et al.*, 1992; DePaolo, *et al.*, 1993; Meriggiola, *et al.*, 1994; Tilbrook, *et al.*, 1995; Besecke, *et al.*, 1997). Furthermore, using primary cultured rat pituitary cells, Hashimoto's group suggested that cell-associated follistatin-288 accelerates the uptake of activin A into pituitary cells, and thus has a role in the degradation of activin (Hashimoto, *et al.*, 1997).

A recent study using the ovariectomized / phenoxybenzamine-treated / testosterone-replaced adult female rat showed that the mRNA expression levels of follistatin and FSH-β in pituitary were inversely related with high follistatin expression at high-amplitude GnRH doses; instead, low amplitude GnRH selectively increased the mRNA expression of FSH-β and activin/inhibin βB. Moreover, GnRH-driven increases in follistatin mRNA continue for 6-12 h before a reduction of FSH-β mRNA was noted,

implying that GnRH may regulate the production of FSH in part through the activin / follistatin system (Dalkin, *et al.*, 1999).

The gonadal steroids, progesterone and testosterone, and the adrenal steroid corticosterone enhance FSH-β subunit mRNA and FSH secretion *in vivo* and *in vitro* (Gharib, *et al.*, 1990; Krey, *et al.*, 1993; Miyake, *et al.*, 1993; McAndrews, *et al.*, 1994; Tebar, *et al.*, 2000). Studies on rat anterior pituitary cell cultures revealed that follistatin can suppress the FSH release induced by activin A, progesterone, testosterone, and corticosterone (Bohnsack, *et al.*, 2000). Moreover, increasing progesterone concentrations up to 1000 nM could not abolish the suppressive effect of follistatin on FSH release; in contrast, activin A was able to neutralize the follistatin effect on FSH at a concentration of 100 ng/ml. In the same study by Bohnsack *et al*, both corticosterone and progesterone could not influence the levels of follistatin mRNA in the absence or presence of estrogen. However, activin A increased follistatin mRNA amounts in the absence of estrogen, although no effect by activin A was shown in the presence of estrogen. Taken together, it raised the possibility that activin may be able to affect steroid-mediated pathways by modulating the effects of follistatin as well as the expression of follistatin mRNA (Bohnsack, *et al.*, 2000) In addition, follistatin may have a synergistic effect with estradiol on suppressing FSH secretion (Depaolo, *et al.*, 1992).

Interleukin-1β in cultured rat anterior pituitary cells was observed to attenuate FSH secretion in response to activin A, while at the same time, stimulating follistatin and activin/inhibin βB mRNA, suggesting that IL-1β may regulate gonadotrope responses to activin through modulating the local balance of follistatin and activin B within the pituitary (Bilezikjian, *et al.*, 1998). Furthermore, the role of follistatin in the control of FSH secretion in the pituitary may differ in different species, since no post-castration increase in the pituitary follistatin gene expression was observed in the male monkey, in contrast to studies in the rat (Winters, *et al.*, 2001).

Of note, a recent report may change some previous concepts (Huang, *et al.*, 2001). In primary pituitary cell cultures derived from transgenic mice that carry the ovine FSH-β promoter linked to a luciferase reporter gene (oFSH β Luc), BMP-7 or BMP-6 was able

to stimulate oFSH β Luc expression by 6-fold. At the same time, BMP-7 and BMP-6 promoted endogenous FSH secretion by 10- and 14-fold, and were also able to induce transient expression of the oFSH β Luc in a transformed gonadotrope cell line, LbetaT2. It is noteworthy that two bioneutralizing antibodies to BMP-7, which cross-react with BMP-6, but not with activin A, significantly decreased basal oFSH β Luc expression and FSH secretion from transgenic mouse pituitary cultures similarly to follistatin, whereas neither of the bioneutralizing antibodies to activin A or activin B had an effect. Based on these data, Huang *et al* (2001) suggested that the down regulation of basal FSH secretion by follistatin is more likely through its binding and antagonizing effect on BMP-7, rather than that for activin A or activin B, in primary mouse pituitary cell cultures.

1.6 Follistatins in pregnancy

1.6.1 Amniotic and circulatory levels during gestation

The data from early pregnancy have revealed that follistatin was present in highest concentrations in the extra-embryonic coelomic fluid, with less in maternal serum and lowest amounts in amniotic fluid (Riley, *et al.*, 1998). The amniotic fluid concentrations of follistatin are similar between weeks 15 and 20 of pregnancy, although those of inhibin A, inhibin B and activin A gradually increase with gestation (Muttukrishna, *et al.*, 1999). Studies on serum levels during pregnancy showed that the concentrations of follistatin increased progressively to a peak in week 36 (or week 38-39 in some studies). At the same time, the activin A: follistatin ratio in serum levels increased from 0.5 in week 5 to 1.8 in week 36 (Wakatsuki, *et al.*, 1996; Woodruff, *et al.*, 1997; Fowler, *et al.*, 1998; O'Connor, *et al.*, 1999). The parallel increase in the secretion of these two proteins throughout pregnancy probably reflects feto-placental secretion and suggests a significant role in gestational physiology. Moreover, it is noteworthy that follistatin levels were not different between women undergoing a normal or abnormal pregnancy, while activin A levels were remarkably increased in patients with pregnancy-induced hypertension, pre-eclampsia, and pre-eclampsia accompanied by intra-uterine growth retardation (D'Antona, *et al.*, 2000).

1.6.2 Tissue source / localization

Follistatin mRNA was observed at the implantation site at days 6, 8 and 10 of gestation, but not in the placenta at later stages of gestation in rats (Kaiser, M, *et al.*, 1990). Subsequent studies also showed that follistatin is present at the sites of implantation (sheep) (Wongprasartsuk, *et al.*, 1994) and in the placenta itself (human) (de Kretser, *et al.*, 1994; Petraglia, *et al.*, 1994; Yokoyama, *et al.*, 1995), largely in the syncitial cells of the placental villi (Petraglia, *et al.*, 1994).

1.6.3 Functional role

Most of what is known about the function of follistatins in implantation and the placenta is mainly on the role of follistatin as an antagonist to activin. Activin A can promote cytotrophoblast cell differentiation (Caniggia, *et al.*, 1997) and enhance endometrial stromal cell decidualization (Jones, *et al.*, 2002). These actions can be eliminated by follistatin. At the same time, follistatin can reverse the inhibitory effect of activin A on the production of the prolactin receptor mRNA in decidual cells (Gu, *et al.*, 1996). Within the placenta, follistatin also antagonizes the effects of activin in stimulating the production of GnRH, human chorionic gonadotropin, and progesterone (Petraglia, *et al.*, 1989; 1990; Petraglia, *et al.*, 1994; Shi, *et al.*, 1994). Taken together, activin A appears to facilitate the process of implantation and the formation of the placenta, whereas follistatin tends to antagonize the actions of activin A. It is important to note that these concepts are based only on *in vitro* experiments.

1.7 Follistatins in development

1.7.1 The expression of follistatin at the embryonic stage

Follistatin transcripts could be observed in both the decidua and the embryo at the early postimplantation stages of mouse development. Furthermore, the primitive streak region, specific rhombomeres in hindbrain, somites, paraxial mesoderm and parietal endoderm cells attached to the Reichert's membrane displayed strong expression of follistatin (Albano, *et al.*, 1994; Feijen, *et al.*, 1994). Additionally, *in vitro* systems

modeling early murine embryonic development have demonstrated that expression of follistatin can be changed by the induction of differentiation of P19 embryonal carcinoma and embryonic stem cells by retinoic acid (van den Eijnden-van Raaij, *et al.*, 1992). The expression of follistatin in pig embryo development was observed predominantly in the trophoblast (days 8 ~ 9), then shifted to the epiblast (day 10), and the node and primitive streak (streak stages) (van de Pavert, *et al.*, 2001). Regarding the mid-gestational human fetus, follistatin has been shown to be expressed in spinal cord, cerebrum, cerebellum, heart, skeletal muscle, kidney, salivary gland, liver, adrenal and gonads (Tuuri, *et al.*, 1994).

1.7.2 Follistatin in pattern formation

As the embryo develops, not only do cells increase in number and undergo differentiation, but they must also be well arranged spatially within an organized body plan, a process termed 'pattern formation'. From studies in *Xenopus*, activin, Vg-1 and the *Xenopus* nodal-related molecules (Xnrs) can induce dorsal types of mesoderm such as muscle and notochord (Slack, 1994; Harland and Gerhart, 1997), whereas, bone morphogenetic proteins (BMPs) 2, 4 and 7 can induce ventral types of mesoderm such as blood (Graff, 1997). BMPs 2, 4 and 7 also promote epidermal differentiation and prevent the formation of neural tissue (Wilson and Hemmati-Brivanlou, 1995). As a BMP antagonist, follistatin can dorsalize ventral mesoderm (Sasai, *et al.*, 1995) and induce neural tissue (Hemmati-Brivanlou, *et al.*, 1994) consistent with the evidence that follistatin can inhibit the activity of BMPs 2, 4 and 7 by forming a complex with BMP and its receptor (Iemura, *et al.*, 1998). Moreover, follistatin can block the effect of the anti-dorsalizing morphogenetic protein (ADMP) that represses head formation during gastrulation in Xenopus (Dosch and Niehrs, 2000). Hence, follistatin appears to play an important role in regulating pattern formation during development.

1.7.3 Follistatin in organogenesis

In the aspect of digit formation, follistatin expression can be found peripheral to the digit chondrogenic aggregates marking the prospective tendinous blastemas. At the same time, exogenous application of follistatin was able to block physiological and

activin-induced digit formation (Merino, *et al.*, 1999). During endochondral bone development the reduction of follistatin expression may be required for the conversion of cartilage to bone (Funaba, *et al.*, 1996). Moreover, by interacting with activin and BMP signaling, follistatin may participate in tooth development (Heikinheimo, *et al.*, 1998). Besides, follistatin seems to potentiate skeletal muscle development, which activin, conversely, represses (Link and Nishi, 1997). There is also evidence indicating that follistatin could inhibit avian cardiac myogenesis at a specific stage (Ladd, *et al.*, 1998). Moreover, follistatin is able to inhibit the dendrite-promoting activity of BMP-5 in cultured sympathetic neurons, suggesting the role of follistatin in neuron development (Beck, *et al.*, 2001). Concerning the development of the avian iris and ciliary body which undertakes a transition from smooth to striated muscle, follistatin stimulated the emergence of striated muscle, but repressed smooth muscle differentiation. In contrast, activin displayed opposing effects (Link and Nishi, 1998). Additionally, follistatin appears to be one of the mesenchymal factors essential for the development of the exocrine tissue of the pancreas while repressing the differentiation of the endocrine cells of the pancreas (Miralles, *et al.*, 1998). In kidney, follistatin induces branching tubulogenesis and antagonizes activin A that inhibits this process (Kojima, *et al.*, 2001). Similarly, follistatin seems to increase branching morphogenesis in ventral prostate development in the absence of testosterone (Cancilla, *et al.*, 2001). Finally, the evidence of defects in the gonads of follistatin overexpressed mice points to the involvement of follistatin in gonadal development (Guo, *et al.*, 1998). Overall, there is growing evidence showing that follistatin has widespread effects in development. However, given the complexity of follistatin biology, considerable effort is still required to understand how this molecule can regulate such diverse developmental pathways.

1.7.4 Developmental defects in follistatin knockout mice

Follistatin-deficient mice were reported with retardation in their growth, decreased mass of the diaphragm and intercostal muscles, shiny taut skin, skeletal defects of the hard palate and the thirteenth pair of ribs, abnormal development of whiskers and teeth. They failed to breathe well, and died soon after birth (Matzuk, *et al.*, 1995a). This mouse model did elicit some roles of follistatin in development. However, early postnatal

lethality limits the information available on the role of follistatin in postnatal development.

1.8 Follistatins in muscle

The phenotypes of the follistatin-null mice, which presented muscle defects, suggest that follistatin is required for muscle development and growth (Matzuk, *et al.*, 1995a). In developing skeletal muscle, activin has been shown to inhibit muscle development, whereas follistatin potentiates muscle development (Link and Nishi, 1997). The mechanisms of how follistatin functions in muscle are still being explored. Myostatin (also termed GDF-8) is a TGF-β superfamily member that is a negative regulator of skeletal muscle. Mice carrying a targeted deletion of the myostatin gene have a dramatic increase in skeletal muscle mass (McPherron, *et al.*, 1997). Furthermore, transgenic mice with the human follistatin-288 gene and a skeletal muscle specific promoter, leading to specific expression of transgenes in skeletal muscle, showed increased muscling resulting from a combination of hyperplasia and hypertrophy of muscle cells (Lee and McPherron, 2001). In addition, overexpression of a dominant negative form of ActRIIB in skeletal muscle also resulted in the same phenotype. *In vitro* studies (Lee and McPherron, 2001) have further demonstrated that the purified C-terminal myostatin dimer is able to bind to ActRIIB and, to a lesser extent, ActRIIA and follistatin is able to prevent this action of myostatin. Additionally, the increase in muscle mass observed in mice with human follistatin constructs were much greater than those seen in myostatin null mice, indicating that at least part of the effect of follistatin may be due to the inhibition of other ligands besides myostatin.

A recent excellent study has further defined the mechanism whereby follistatin acts to increase muscle mass (Amthor, *et al.*, 2002). BMP-7 has been shown to have the capacity to both stimulate and restrict muscle growth. The opposing activities are concentration-dependent because BMP-7 stimulates muscle growth by up-regulating Pax-3 expression when applied at a low concentration, whereas it restricts muscle growth by inducing apoptosis when applied at a high concentration (Amthor, *et al.*, 1998). When follistatin was applied together with a high concentration of BMP-7, it potentiated the stimulatory effect of BMP-7 on Pax-3 expression, suppressed BMP-7-

induced apoptosis, and resulted in excessive muscle growth (Amthor, *et al.*, 2002). Since the association and dissociation kinetics of BMP-7 and follistatin demonstrated that follistatin binds BMP-7 rapidly and is also able to dissociate, follistatin appears to act to store and present BMP-7 at a sub-apoptosis concentration, which enhances muscle growth. This concept also provides the potential model to explain the diverse role of follistatin in various tissues.

1.9 Follistatins in kidney

In transgenic mice expressing the dominant-negative type II activin receptor (ActRII), the number of glomeruli in the kidneys was about 180% of that found in wild type mice (Maeshima, *et al.*, 2000). This phenotype suggests that activin would inhibit branching of the ureteric bud during kidney development. Studies using an *in vitro* system of Madin-Darby Canine Kidney (MDCK) cells showed that hepatocyte growth factor (HGF) could induce tubulogenesis, an effect that could be blocked by activin A. Importantly, follistatin promotes branching tubulogenesis, potentially through binding and neutralizing the action of activin A. During renal regeneration, follistatin is also able to reduce tissue damage and accelerate regeneration of tubular cells. Thus, follistatin may be useful to facilitate regeneration of the renal tubules by antagonizing the actions of endogenous activin A (Maeshima, *et al.*, 2001). Interestingly, a recent study using a rat model of unilateral ureteral obstruction has revealed that BMP-7 blunted the progression of renal fibrosis and facilitated the return of normal renal function (Morrissey, *et al.*, 2002). To date, while the details of the interactions between follistatin and BMP-7 in kidney are yet unclear, they both appear to promote the regenerative process after renal damage.

1.10 Follistatins in liver

There is an emerging role of follistatin in liver regeneration. Data from studies on rat liver showed that activin can induce apoptosis of hepatocytes *in vivo* and *in vitro*, whereas follistatin blocked the response to activin. Conversely, inhibin, which antagonizes the actions of activin in many systems, had little effect on the response to activin (Schwall, *et al.*, 1993). Subsequently, some reports further demonstrated that a

single administration of follistatin promoted DNA synthesis after partial hepatectomy in rats. Also activin A produced in the remnant liver may exert a tonic inhibitory effect on liver regeneration. Hence follistatin may be useful as a potential therapeutic agent to help liver regeneration (Kogure, *et al.*, 1995). This evidence has been further supported by results indicating that follistatin is quite effective in promoting liver regeneration by inducing immediate onset of DNA synthesis in 90% hepatectomized rats (Kogure, *et al.*, 1998).

1.11 Follistatins in skin

The importance of follistatin in skin can be revealed as follistatin null mice have a special phenotype in skin: shiny taut skin. Histological analysis of skin of the follistatin knockout mice demonstrated that keratin-6 was expressed abnormally in the interfollicular epidermis, which was normally only expressed in the outer root sheath of hair follicles (Matzuk, *et al.*, 1995a). Furthermore, overexpression of follistatin-315 in the epidermis of transgenic mice led to a mild dermal and epidermal atrophy. To characterize the role of follistatin overexpression in skin, an experimental injury demonstrated a severe delay in wound healing. In addition, formation of granulation tissue was significantly decreased, causing a decrease in wound breaking strength (Wankell, *et al.*, 2001). These findings appears to be associated with the activin antagonizing actions of follistatin, since activin A has been shown to be a potent stimulator of the wound healing process (Munz, *et al.*, 2001). However, on the other hand, although there was delay in wound healing in follistatin overexpressed mice, the injury healed and the resulting scar area was smaller than in control animals (Wankell, *et al.*, 2001). These observations may make follistatin a potential agent to reduce scar formation in some clinical situations.

1.12 Follistatins in brain

An emerging role of follistatin in brain was also noted because of its antagonism to activin A that has been shown to have neuroprotective effects after brain injury. In a hypoxic-ischemic brain injury model of infant rats, the intracerebroventrical administration of recombinant human activin A has been demonstrated to reduce

neuronal loss in several regions of brain. At the same time, the down-regulation of follistatin expression post injury was observed. That may allow activin A to become more accessible to neurons after injury (Wu, *et al.*, 1999). More interestingly and importantly, basic fibroblast growth factor, which is a well documented neuroprotective and neurotrophic growth factor, strongly promoted lesion-associated induction of activin A. Further, in the presence of follistatin, basic fibroblast growth factor cannot rescue neurons from death (Tretter, *et al.*, 2000). Together, these data imply that a strategy to down-regulate follistatin and up-regulate activin A expression may provide a way to prevent or decrease neuronal loss in ischemic or traumatic brain injury.

1.13 Summary of phenotypes of transgenic mouse models

The importance of the inhibin/activin/follistatin system is evident by the phenotypes generated by the transgenic mouse models resulting in targeted disruption of the production of these proteins, most of which have been described in the previous sections. Here, the summary of these phenotypes is presented in Table 1.4. In view of these phenotypes, follistatin null mutants and mice deficient in βA or βA/ βB subunits have some similar phenotypes, suggesting that some actions of follistatin may be to modulate the factors that act upstream or downstream of some activin pathways. Moreover, to date no models can show that the phenotypes resulting from the overexpression of follistatin are similar to those from the knockout of activins, or that the phenotypes arising from the overexpression of activins are similar to those arising from the knockout of the follistatin gene, implying that some of the actions of activins cannot be antagonized by follistatin, and/or follistatin also modulates other factors rather than activins. Further, the phenotypes generated by deletions of ligands of activin are different from those generated by deletions of their receptors, raising the possibility that other ligands may signal through the activin receptors. Thus, these transgenic models highlight not only the importance of the inhibin/activin/follistatin system, but also pose some questions that have not been considered previously and require further study.

Table 1.4 Summary of phenotypes of transgenic mouse models of inhibin/activin/follistatin system

Mutation(s)	Phenotypes
Deletion of follistatin gene (Matzuk, *et al.*, 1995c)	Neonatal lethality; growth retardation, decreased mass of breathing muscles, shiny taut skin, cleft palate, absence of the thirteenth pair of ribs, short of one lumbar vertebra, abnormal development of whiskers and teeth.
Overexpression of follistatin (Guo, *et al.*, 1998)	Shiny, irregular fur; infertility depending on transgene expression; variable degrees of Leydig cell hyperplasia, tubular degeneration, disruption of spermatogenesis, small testes; thin uteri, small ovaries, a block in folliculogenesis at various stages.
Deletion of α subunit gene (Matzuk, *et al.*, 1994; Matzuk, *et al.*, 1992; Matzuk, *et al.*, 1996)	Granulosa/Sertoli cell and adrenal tumours; cancer cachexia-like syndrome; infertility in females; secondary infertility in males.
Deletion of βA subunit (Matzuk, *et al.*, 1995b)	Neonatal lethality: cleft palate; lack of whiskers; tooth defects.
Overexpression of βA subunit in testes (Tanimoto, *et al.*, 1999)	Sterility in males; disruption of spermatogenesis, testicular degeneration.
Deletion of βB subunit (Schrewe, *et al.*, 1994; Vassalli, *et al.*, 1994)	Large litters; extended gestation period; nursing defects; eyelid closure defects at birth.
Deletion of βA and βB subunits (Matzuk, *et al.*, 1995a)	Additive defects of βA and βB subunit null mutations.
Deletion of ActRIB (Gu, *et al.*, 1998)	Embryonic lethality; development blocked at pre-gastrulation stage.
Deletion of ActRIIA (Matzuk, *et al.*, 1995a)	Partial neonatal lethality with cranio-facial deformities; viable males display delayed fertility, females are infertile.
Deletion of ActRIIB (Oh and Li, 1997)	Neonatal lethality; severe cardiovascular defect; loss of lateral asymmetry; axial skeletal defects.

1.14 Molecular context

Although convincing evidence that follistatin could interact with multiple members of the TGF-β superfamily leads to a increasing complexity of follistatin biology, it is also important to note that there may be interplays between these growth factors in the molecular context of follistatin. These interplays could occur at three levels. Firstly, they may occur at the receptor level. Since there is a high degree of homology between the structures of TGF-β superfamily members, it is likely that different members bind to the same receptor, resulting in competitive effects. For example, activin and BMP-7 bind to the same type II receptors, ActRII and ActRIIB (Macias-Silva, *et al.*, 1998).

Secondly, these interplays may occur from crosstalk between the signaling pathways of TGF-β superfamily members. For example, signaling by activin and BMP-2/4 has been shown to interact antagonistically. In *Xenopus* ectodermic explants, activin induces dorsal-type mesoderm, whereas BMP-2/4 induces ventral mesoderm and blocks the dorsal mesoderm-inducing activity of activin. Investigation of the mechanisms underlying this phenomenon has revealed that this antagonism between activin and BMP-2/4 may be explained by intracellular competition for a limited pool of SMAD4, under certain physiological situations (Candia, *et al.*, 1997). It has been proposed that SMAD4 is limiting in cells, hence the simultaneous activation of two signaling pathways could cause competitive affects. The outcome of this competition may dictate the ultimate signals. Another example is BAMBI (BMP and Activin membrane-bound inhibitor) (Onichtchouk, *et al.*, 1999), which is induced by BMP signaling and inhibits not only BMP signaling, but also activin and TGF-β signaling.

Finally, these interplays may occur indirectly via the interactions of factors whose concentrations are regulated by TGF-β superfamily members. In other words, some of the TGF-β superfamily members may not only interplay with each other directly, but also regulate the same factors, *e.g.* sex steroids (Miro, *et al.*, 1991; Shukovski, *et al.*, 1993; Alak, *et al.*, 1998; Shimasaki, *et al.*, 1999; Dooley, *et al.*, 2000; Otsuka, *et al.*, 2001a). Thus, the physiological activities of these TGF-β superfamily members arise from the net stimulatory or inhibitory inputs that impinge upon downstream targets,

such as sex steroids. Based on the concepts mentioned here, follistatin functions in a multidimensional network, not just a simple linear system.

1.15 Conclusion

It has been well known that follistatin can bind to activin and neutralize its activity (Nakamura, *et al.*, 1990). Given that activin is an important factor regulating cellular homeostasis (divide or die), differentiation (at fetal and adult stages) and hormonal homeostasis (the balance among hormones), follistatin has been shown to play a significant role in diverse areas of biology. In the area of reproduction, a wealth of evidence suggests that follistatin plays a significant role in pituitary, ovary and testis in an autocrine / paracrine fashion, and that most of follistatin biology may be explained by its antagonism with activin. However, recent compelling findings suggest that follistatin binds to other members of TGF-β superfamily modulating their functions in a manner analogous to activin. Hence, follistatin has been shown to be able to bind to BMPs and antagonize their effects in Xenopus embryos (Yamashita, *et al.*, 1995; Fainsod, *et al.*, 1997; Iemura, *et al.*, 1998). Follistatin has also been shown to have the capacity to inhibit the action of myostatin, which is another TGF-β superfamily member and acts as a negative regulator of skeletal muscle mass (Lee and McPherron, 2001). In addition, follistatin is able to bind and suppress the activities of BMP-15 in the ovary (Otsuka, *et al.*, 2001c). These findings open a new window of opportunity to assess the role of follistatin. The functions of follistatin arise not only from its interaction with activin, but also potentially from its interactions with other TGF-β superfamily members.

Activin and BMP-2, -4 are considered to function as morphogens during *Xenopus* development (Gurdon and Bourillot, 2001). Morphogens are defined as secreted signaling molecules that form a gradient of concentration from the localized source and induce different cell fates of surrounding cells according to the local concentration of a morphogen perceived by the cells. Thus morphogens can organize a field of surrounding cells into patterns. However, these gradient-dependent activities of morphogens may be produced in another way (Dale and Wardle, 1999). The morphogens may be secreted locally in the entire field and a gradient of activity of

morphogens can be formed from the modulation of the morphogen activity by the inhibitor of a morphogen due to the long-range diffusion of the inhibitor from a localized source. Rethinking the role of follistatin in development, follistatin may play a role as an inhibitor of morphogens that are members of the TGF-β superfamily. Moreover, it is worthy to further study whether the inhibitory actions of follistatins on members of the TGF-β superfamily do form a local gradient of concentrations of these proteins, as well as whether this phenomenon is important if it does exist.

Interestingly, a recent paper in chick limb development showed that follistatin not only binds to BMP-7 in muscle, but also appears to be able to monitor and refine the concentration of BMP-7 in a way that promotes muscle growth (Amthor, *et al.*, 2002). This finding also implicates some potential roles of follistatin in maintaining homeostasis in the body. Moreover, members of the TGF-β superfamily may antagonistically or synergistically act with each other. For example, BMP-3 is a negative regulator of bone density, opposing osteogenic activity displayed by other BMPs (Daluiski, *et al.*, 2001); antagonistic actions of activin and BMP-2/4 exist during early embryogenesis of Xenopus (Kaufmann, *et al.*, 1996; Candia, *et al.*, 1997); GDF-9 and BMP-15 exert their activities synergistically in the ovary (Yan, *et al.*, 2001). Collectively, the findings suggesting that follistatin could bind to other TGF-β superfamily ligands besides activin and the interplays that exist among these ligands, lead to the idea that the role of follistatin in biology may be much more complex than initially predicted. We may imagine that follistatin functions as a spring between TGF-β superfamily ligands which are like the balls connected to the springs (Figure 1.4). When the interactions between the balls occur the springs will try to pull or push back the balls to the original sites, suggesting that follistatin may respond to the changes of ligands and endeavor to restore homeostasis. What is less clear is whether the role of follistatin in regulating the biology of ligands is simply dictated by the local concentration of follistatin. This appears unlikely given the complexity of the systems that have been described. However, to date few regulators of follistatin function have been reported (Iemura, *et al.*, 1999). In conclusion, in view of the data and discussion presented above, the biology of follistatin is not just an integral part of the physiology of activin.

Figure 1.4 The schematic model depicts a complex system in follistatin biology.

Follistatin functions as a spring between TGF-β superfamily members which are like balls connected to the springs (follistatin). When the activities of the TGF-β superfamily members change due to interactions with each other, follistatin would try to pull or push these balls back to the original sites to maintain homeostasis. The whole system may also recruit some co-factors that regulate the expression of follistatin or help follistatin in keeping homeostasis.

Figure 1.4

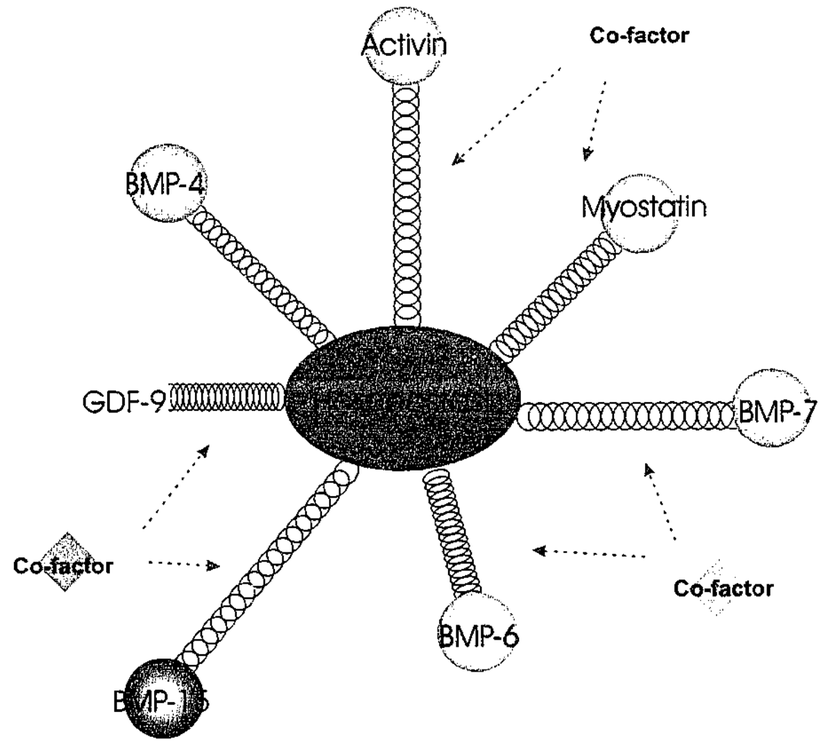

1.16 The scope of the thesis

The introduction to this thesis clearly demonstrates that the biology of follistatin is complex and involves its interactions with a number of TGF-β superfamily members in the control of a diversity of systems. This view is supported by the observations of mice with targeted disruption of the follistatin gene (fs -/-) (Matzuk, *et al.*, 1995a) which showed perturbations of a multitude of systems even though the mice died at birth.

With the generous cooperation of Dr. Marty Matzuk, this thesis explores the use of the fs -/- mouse to further expand our understanding of the biology of follistatin. These studies used several techniques to augment our knowledge.

First, this thesis describes experiments designed to understand the importance of follistatin in postnatal testicular development. We were curious about the development of follistatin deficient testes. Thus, the fetal follistatin null testes were transplanted into the outer ears of immunocompromised adult male mice. This design created an *in vivo* model where these follistatin null testes were grown in an environment with systemic follistatin supply but without the local production of follistatin. The result will be presented in the **Result Section 1 (Chapter 3)**.

Considering the importance of follistatin and the complexity of its molecular context, studying the regulatory elements of the follistatin locus of the human genome is an important step to help decipher the secrets of follistatin biology. In the thesis, the first step to elucidate these issues *in vivo* has been made through generation of mice carrying different lengths of human genomic sequences of the follistatin locus in the mouse follistatin knockout background. This part of the research provided some insights into the human follistatin locus as well as the phenotype analyses of follistatin knockout mice. The results will be presented in the **Result Section 2 (Chapter 4 ~ 6)**.

While both follistatin isoforms (follistatin-288 and follistatin-315) are different from each other only in the C-terminal ends of the protein, that, however, causes distinct biochemical characteristics. Therefore, it was hypothesized that the different roles both

follistatin isoforms are playing are the essential parts of follistatin biology. To test this hypothesis, it was planned to create two kinds of mouse models. Each of them will carry one of the follistatin isoform-specific transgenes but no mouse follistatin gene. Firstly, two kinds of constructs were made from the human genomic sequences of the follistatin locus with about 95 kb in length, owing to the intention of using the natural promoters and regulatory elements to drive the expression of transgenes. The resulting constructs were then used to create two kinds of transgenic mice. This part of the work will be presented in the **Result Section 3 (Chapter 7 ~ 8)**. Because of the limitation of the duration of the PhD program, the thesis describes the making of the constructs but only a brief analysis of the outcome of insertion of these constructs.

Chapter 2

Materials and methods

Chapter Outline:

2.1 Materials

The solutions used in the following experiments can be referred to in Appendix Ia and the manufacturers of reagents in Appendix Ib. Sequences of PCR primers can be referred to in Appendix II.

2.1.1 DNA size standards

The following size standards were purchased from New England Biolabs (Beverly, MA, USA):

100 bp DNA ladder: 1517 bp, 1200 bp, 1000 bp, 900 bp, 800 bp, 700 bp, 600 bp, 500/517 bp, 400 bp, 300 bp, 200 bp, 100 bp.

1 kb DNA ladder: 10 kb, 8 kb, 6 kb, 5 kb, 4 kb, 3 kb, 2 kb, 1.5 kb, 1.0 kb, 0.5 kb.

MidRange I PFG marker: 291 kb, 276 kb, 257.5 kb, 242.5 kb, 227.5 kb, 209 kb, 194 kb, 179 kb, 160.5 kb, 145.5 kb, 130.5 kb, 112 kb, 97 kb, 82 kb, 63.5 kb, 48.5 kb, 33.5 kb, 15 kb.

The following size standards were purchased from GibcoBRL (Ontario, Canada):

High molecular weight DNA marker: 48502 bp, 38416 bp, 33498 bp, 29942 bp, 24776 bp, 22621 bp, 19399 bp, 17057 bp, 15004 bp, 12220 bp, 10086 bp, 8612 bp, 8271 bp.

High DNA mass ladder: 200 ng (10 kb), 120 ng (6 kb), 80 ng (4 kb), 60 ng (3 kb), 40 ng (2 kb), 20 ng (1 kb).

Low DNA mass ladder: 200 ng (2000 bp), 120 ng (1200 bp), 80 ng (800 bp), 40 ng (400 bp), 20 ng (200 bp), 10 ng (100 bp).

2.1.2 Oligonucleotides

Oligonucleotides were designed using primer3 software (http://www.genome.wi.mit.edu /cgi-bin/primer/primer3.cgi) and purchased from Sigma Genosys (Sigma Aldrich, Castle Hill, NSW, Australia) or Geneset Pacific Pty. Ltd (Lismore, Australia).

2.1.3 Vectors

A number of phagemid vectors were used in the assembly of the transgenic constructs. These were:

pNEB193 (New England Biolabs, Beverly, MA, USA): referred to as pNEB (Genbank accession #: L09137).

pSL1180 (Pharmacia, Uppsala, Sweden): referred to as pSL (Genbank accession #: U13865).

pCRII (Invitrogen): referred to as pCR, a TA cloning vector.

PAC-FS: this PAC vector was obtained from the human PAC DNA library of the Murdoch Institute, Melbourne, and contains the genomic sequence of the human follistatin locus used in the thesis. This vector was a generous gift of Dr. Panos.

2.1.4 Restriction endonucleases

The restriction endonucleases used in the thesis for DNA engineering were purchased from New England Biolabs (Beverly, MA, USA). The digestion conditions were set up by following the instructions provided with the products.

2.1.5 Chemicals

All chemicals used in the following experiments were of analytical grade, except where noted. The solutions and buffers used in the experiments can be referred to in Appendix I.

2.2 Methods

2.2.1 Preparation of DNA

2.2.1.1 Small-scale preparation of plasmid DNA from bacterial cells

Plasmid DNA was prepared on a small-scale from 10 ml overnight culture using an alkaline lysis method (Sambrook, *et al.*, 2001). A single bacterial colony was grown overnight at 37°C in a shaking incubator in 10 ml LB medium containing ampicillin (50 µg/ml). The overnight culture was pelleted and the cells were then lysed using a modified alkaline lysis protocol and the cell debris precipitated in the presence of sodium acetate. A phenol/chloroform extraction (Section 2.2.1.5) was performed to remove remaining cell debris and protein.

2.2.1.2 Large-scale preparation of plasmid DNA from bacterial cells

Large-scale purification of plasmid DNA was prepared by the Qiagen (Hilden, Germany) Maxi Kit protocol. Briefly, a single colony was grown overnight at 37°C in a shaking incubator in 250 ml LB medium containing ampicillin (50 µg/ml). Cells were pelleted, resuspended, treated with RNase A and lysed using alkaline lysis. This was followed by neutralization and precipitation of cell debris. The remaining solution was then passed through a Qiagen 500 column and washed. The DNA was eluted and then precipitated with isopropanol. Pellets were resuspended in TE buffer (Appendix Ia) after being washed with 70% ethanol.

2.2.1.3 Large-scale preparation of PAC DNA from bacterial cells

Purification of high-molecular weight circular DNA can be performed by chromatography on Qiagen resin (Sambrook, *et al.*, 2001). However, this protocol will not work for linear high-molecular-weight DNA, which binds irreversibly to the column. An overnight culture of bacteria carrying PAC DNA was grown in 500 ml ~ 1 L of LB medium containing 25 µg/ml kanamycin. The cells were pelleted by centrifugation of 5000 g and then digested by lysozyme at a final concentration of 1

mg/ml and the modified alkaline procedure described in the Qiagen literature. The lysate was centrifuged at 15,000 g for 30 min at 4°C, following the addition of chilled P3 buffer and incubation on ice for 20 min. The supernatant was then promptly transferred to a fresh tube and filtered through several layers of cheesecloth. The filtered lysate was passed through a Qiagen-tip column equilibrated with QBT buffer (Appendix Ia). The column was washed with 30 ml of wash buffer. The PAC DNA was then eluted with 15 ml of elution buffer. The eluted DNA was precipitated with 0.7 volume of isopropanol and washed with 70% ethanol. The DNA was then resuspended in TE buffer for the further experiments.

2.2.1.4 Preparation of glycerol stocks

Glycerol stocks were routinely made by mixing well 500 µl of overnight bacterial culture in LB medium (Appendix Ia) containing appropriate antibiotics, with 500 µl of sterile glycerol. They can then be stored in -70°C for extended periods of time.

2.2.1.5 Phenol/chloroform extraction

An equal volume of Tris buffered phenol (pH>7.8) was added to the DNA solution and the mixture quickly vortexed. Phases were separated by a centrifugation at 20,000 g for 5 min, and the aqueous phase transferred to a clean microcentrifuge tube. An equal mixture of Tris buffered phenol (pH>7.8) and chloroform (1:1) was then added to the DNA solution and again mixed by vortexing. Phases were separated and the aqueous phase was transferred to a clean microcentrifuge tube. This process was repeated until no protein was visible at the interface of the aqueous and organic phases. Finally an equal volume of chloroform was added to the DNA solution, the mixture quickly vortexed, and the phases separated by centrifugation. The aqueous phase was transferred to a fresh microcentrifuge tube and DNA precipitated as described in A8.12 of *Molecular Cloning* (Sambrook, *et al.*, 2001).

2.2.1.6 Preparation of genomic DNA from mouse ear-clips for PCR

DNA was isolated from mouse ear clips for the purpose of genotyping. Ear clips were placed in lysis solution (Appendix Ia) and incubated at 55°C for 90 min. The proteinase

K was then inactivated by heating to 98°C for 10 min. Samples could then be stored at –20°C or used immediately for genotyping (2~3 µl per PCR reaction).

2.2.1.7 Isolation of DNA from mouse tails without extraction by organic solvents

1cm of mouse tail was placed in 0.5 ml of mouse-tail lysis buffer 1 (Appendix 1a) in a microfuge tube, and then incubated at 55°C for 3~4 hrs in a horizontal position on a rocking platform or with agitation in a shaking incubator. The digested sample was centrifuged at maximum speed for 10 minutes at room temperature. The supernatant was then transferred to a fresh microfuge tube containing 0.5 ml of isopropanol at room temperature. The contents of the tube were mixed by inversion. The stringy precipitate of DNA was fished out with a clean disposable sealed capillary tube. The precipitate was briefly touched to a Kimwipe to remove excess alcohol and then the DNA was transferred to a fresh microfuge tube. The DNA was dried at room temperature and then dissolved in 200 µl of TE (pH 8.0), by rocking it gently overnight at 4°C. The DNA can be used for PCR screening or Southern blotting (Laird, *et al.*, 1991).

2.2.1.8 Preparation of DNA for microinjection

DNA, smaller than 30 kb, was further cleaned by ethidium bromide extraction (Stemmer, 1991). Briefly, DNA was mixed with ethidium bromide (10 mg/ml), which is thought to displace any bound proteins, before a phenol/chloroform extraction was completed (section 2.2.1.5). Water-saturated butanol was subsequently used to extract any remaining ethidium bromide; DNA was then precipitated and resuspended in 0.1 x TE. Samples were then drop dialysed as described in A8.11 of *Molecular Cloning* (Sambrook, *et al.*, 2001).

As it was possible that cleaning of PAC DNA with ethidium bromide may form an un-dissolved precipitate after ethidium bromide extraction, PAC DNA was further cleaned with chromatography by Qiagen resin described in section 4.45 of *Molecular Cloning* (Sambrook, *et al.*, 2001). Subsequently, the sample was further purified by drop dialysis.

2.2.2 DNA cloning

2.2.2.1 Restriction endonuclease digestion

DNA digestions were performed according to manufacturers' protocols for a minimum of one hour. All restriction endonucleases were purchased from New England Biolabs (Beverly, MA, USA).

2.2.2.2 Agarose gel electrophoresis

DNA underwent electrophoresis on 1x TAE (Appendix I) agarose (Progen Industries Limited, Darra Qld, Australia) gels of appropriate concentration and with 0.5 μg/ml ethidium bromide.

2.2.2.3 Pulsed field gel electrophoresis (PFGE)

In practical terms, DNA greater than ~20 kb in length cannot be easily separated by applying a constant electrical field to horizontal agarose gels (Sambrook, *et al.*, 2001). To do DNA engineering in PAC-FS, ~110 kb in length, pulsed field gel electrophoresis (PFGE) was required to resolve this problem. PFGE was applied on a CHEF Mapper®XA Pulse Field Electrophoresis System (Bio-Rad Laboratories, California, USA). The routine conditions were set up with 0.5x TBE (Appendix Ia), 1% molecular agarose (Progen Industries Limited, Darra Qld, Australia), and at 14°C. The detailed conditions, including switch time, run time duration, voltage gradient and electric directions, were individualized for every single run of PFGE and set up by the CHEF Mapper Interactive Algorithm, the software provided by the manufacture.

2.2.2.4 Recovery of DNA fragments from agarose gel

When DNA fragments in the gel were less than 10 kb in length, DNA was extracted from agarose gels using the Qiagen Gel Extraction Kit, as per the supplier's instructions.

When DNA fragments in the gel were greater than 10 kb in length, DNA was recovered from agarose gels with β-agarase I. β-agarase I was purchased from New England Biolabs. DNA was excised in 0.8% low-melting-temperature agarose (SeaPlaque GTG agarose), and isolated as per supplier's instructions. Briefly, agarose was melted at 65°C for 10 min, then diluted in an appropriate volume of 10x β-agarase buffer (10mM Tris-HCl (pH 6.5), 1mM Na_2EDTA). β-agarase was then added to this mixture at 10 U/100 µl, and the reaction incubated at 40°C for at least one hour. Reactions were then incubated on ice for 20 min, and centrifuged at 15,000 x g for 15 minutes. Supernatant was then removed to a clean microcentrifuge tube, and DNA precipitated (Sambrook, *et al.*, 2001).

2.2.2.5 DNA ligation

DNA ligation was carried out as described in Sambrook, *et al.* (2001). T4 DNA ligase was purchased from New England Biolabs. Briefly, 50 ng of vector was incubated with an appropriate amount of insert DNA (a molar ratio of insert to vector of 1-3:1), ligation buffer, 200 Weiss U of T4 DNA ligase and an appropriate volume of dH_2O. Reactions were incubated at room temperature, or 16°C overnight, or cyclic temperature (Section 2.2.2.7) before being transformed.

2.2.2.6 In-gel ligation

Sometimes, in-gel ligation can decrease the handling of DNA to prevent shearing of the DNA during handling as well as to save time. The insert DNA was first excised in 0.6% low-melting-temperature agarose (SeaPlaque GTG). The agarose slice of the insert DNA was then remelted by heating to 68°C for 5 minutes, and cooled to 37°C. A final reaction mixture of 50 µl comprises an appropriate amount of T4 DNA ligase, dH_2O, ligation buffer, vector and the remelted agarose gel slice of insert DNA. However, a final concentration of gel should not exceed 0.5% SeaPlaque GTG in the reaction mixture. The components were gently mixed with a pipette and incubated at room temperature overnight.

2.2.2.7 Cyclic temperature ligation

Since low temperature (around 10°C) favors DNA strand annealing and high temperature (around 30°C) favors enzymatic joining, cycling through the steps given below offers a good balance between reaction conditions for DNA annealing and ligation, and increases cloning efficiency (Pusch, *et al.*, 1997). The steps of temperature setting were as follows:

Step	Temp.(°C)	Time	Cycles
0	22	10 min	
1	16	10 min	5 x
2	4	30 s	
3	27	30 s	50 x
4	13	30 s	
5	4	30 s	
6	16	1 h	2 x
7	22	1 h	
8	18	3 h	
9	4	indefinite	

2.2.2.8 TA cloning

TA cloning kits (Invitrogen) were used to clone PCR products by following the manufacturer's instructions. Briefly, vectors were pre-prepared containing 5′ thymidine overhangs to take advantage of 3′ endotransferase activity of Taq DNA polymerase, which causes a single 3′ deoxyadenosine to be added to the 3′ end of the PCR product. Thus, through ligation and transformation, PCR products could be cloned.

2.2.2.9 Transformation of E. coli

2.2.2.9.1 Chemical transformation

DH5α cells and INVαF′ cells:

DH5α chemically competent cells were prepared and transformed as described in Biolabs' instructions. INVαF′ cells were the component of TA Cloning Kit purchased from Invitrogen.

For transformation, competent cells were thawed on ice, then 5-10 ng plasmid DNA was added to the cells, gently mixed and incubated, on ice, for 30 minutes. Cells were then heat shocked by placing them at 42°C for 30 seconds, and returned to ice for 2 minutes. Following heat shock, cells were added to 900 µl SOC media (Appendix Ia) and incubated at 37°C for 60 minutes shaking at 225 rpm, to allow expression of antibiotic resistant gene. The cells were then plated on LB agar (Appendix Ia) with ampicillin (50 µg/ml) and incubated at 37°C overnight.

2.2.2.9.2 Electroporation

DH10B cells:

DH10B electrocompetent cells were purchased from (Life Technologies). The ligation reaction mixture or plasmid DNA was pre-prepared in H_2O or low salt solution. DH10B cells were removed from the -70°C freezer and thawed on ice. 1~3 µl of ligation reaction was added to an aliquot of 25 µl of competent cells, followed by gently mixing and incubating on ice for 1~2 minutes. The cells were then placed in a pre-chilled cuvette (Biorad 0.1). The conditions of electroporation were set up in a Biorad Gene Pulsar with 1.8 kV, 200 Ohms and 25 µFD. Following electroporation, 1 ml of SOC (Appendix Ia) at room temperature was added to the cells immediately. The cells were then incubated at 37°C for 60 minutes shaking at 225 rpm. The cells were then plated on LB agar with appropriate antibiotics and incubated at 37°C overnight.

2.2.3 Preparation of RNA from tissues

2.2.3.1 Total RNA extraction

Total RNA extraction from mouse tissues was performed by the method of Chomczynski and Sacchi (1987). All solutions used were made with 0.1% diethyl pyrocarbonate-treated water (DEPC-dH_2O) to prevent RNase activity. Organs were homogenized using an Ultra-Turrax T25 homogenizer in solution D (Appendix Ia) at 10 ml per gram of tissue. To this was added, sequentially, 0.1 volumes of 2M NaOAc (pH 4.0), 0.1 volumes water-saturated phenol, and 0.2 volumes chloroform-isoamyl alcohol (49:1). Tubes were mixed by inversion between each step with a final vigorous mix. Tubes were placed on ice for 15 minutes followed by centrifugation at 10,000 rpm for 20 minutes at 4°C. The aqueous phase was transferred to a fresh tube containing 1 volume of isopropanol and placed at -20°C for a minimum of 1 hour. RNA was pelleted by centrifugation at 10,000 rpm for 20 minutes at 4°C, resuspended in 0.3 volumes of solution D and reprecipitated with an equal volume of isopropanol at -20°C for 1 hour. RNA was again pelleted by centrifugation and resuspended in 75% ethanol. This step was repeated then the RNA pellet was air dried and resuspended in dH_2O (DEPC). RNA concentration was measured by spectrophotometry at 260 nm (1 OD_{260} = 40 µg of RNA /ml) and 280 nm (protein) for quality control. High RNA purity was determined as having an OD_{260}/OD_{280} value of around 2.0.

An alternative method is using RNeasy Mini Kit of Qiagen as per manufacturer's instructions.

2.2.3.2 mRNA isolation

mRNA isolation from tissues used Dynabeads Oligo $(dT)_{25}$ of DYNAL BIOTECH ASA (OSLO Norway) as per manufacturer's instructions.

2.2.4 Reverse transcription

Superscript II (Invitrogen) was used for reverse transcription according to manufacturer's instructions. Briefly, 1ng - 5 µg of total RNA or 1ng – 500ng of mRNA

was incubated with anchored oligo-dT primers at 95°C for 10 minutes, to denature both oligonucleotides and the RNA. This mixture was then cooled and added to buffers supplied by the manufacturer, 0.01 M dithiothreitol (DTT), and Superscript II reverse transcriptase. Reactions were incubated at 42°C for 1 hour, before being inactivated at 65°C for 10 minutes. 1-2 µl of this reaction was then used in PCR reactions.

2.2.5 Polymerase chain reaction (PCR)

2.2.5.1 General protocol

In all PCR reactions the enzyme Taq DNA polymerase (Pharmacia) was used, unless otherwise stated. The reaction conditions, unless otherwise stated, were:

DNA[1]		
dNTPs	2 mM	3 µl
10x Buffer[2]		3 µl
Forward primer	50 µM	final 1 µM
Reverse primer	50 µM	final 1 µM
Tag DNA polymerase	5 U/ µl	final 1 U
dH_2O		to 30 µl

[1]DNA concentration was dependent on the template used, genomic DNA (10-100 ng), plasmid DNA (0.1-10 ng).

[2]The buffer as supplied contained 500 mM KCl, 15 mM $MgCl_2$, 100 mM Tris-HCl (pH 9.0 at room temperature).

PCR reactions were performed in a GeneAmp PCR 2400, 2700 or 9600 thermal cycler (Perkin Elmer Corporation, Foster City, CA, USA) and, unless otherwise stated, cycled as follows:

Initial denaturation	94°C	5 min	
Amplification: denaturation	94°C	30 sec	35 cycles
annealing	58°C	30 sec	
extension	72°C	1 min/kb	
Final extension	72°C	1 or 5 min	
Holding temperature	15°C	Hold	

2.2.5.2 PCR primers

All the PCR primers used in the following studies can be referred to in Appendix II.

2.2.5.3 Automated sequencing

Automated sequencing was performed by the MIRD/PHIMR joint sequencing facility (Monash Medical Centre, Clayton, Australia). All reactions were completed using the ABI Prism BigDye Terminator Cycle Sequencing Kit (Perkin Elmer Corporation), according to the manufacturer's instructions.

2.2.6 Southern hybridization analysis

2.2.6.1 Transfer of DNA

After electrophoresis the gel was incubated in denaturation buffer (Appendix Ia) for 30 minutes, gently rocking, at room temperature. The gel was then washed in dH_2O and the DNA transferred to a pre-moistened Hybond XL membrane (Amersham Pharmacia, Buckinghamshire, England) by capillary action in the denaturation buffer. After transfer, membranes were washed in 2x SSC, 5 mM Tris (pH 7.5), and air dried at 80°C for 2 hours.

2.2.6.2 ^{32}P labeling of probes

Specific PCR products were electrophoresed and isolated from the agarose gels and labeled using Rediprime II labeling Kit (Amersham Pharmacia) as per manufacturer's instructions.

2.2.6.3 Hybridization and membrane washing

Membranes were prehybridized in Church's buffer (Appendix Ia) containing 0.1 µg/µl denatured herring sperm DNA (Promega Corp.) for 1 hour at 65°C. Approximately $2x10^6$ cpm/ml of probe was added to the prehybridization solution and allowed to hybridize overnight at 65°C.

The membranes were then washed for 15 minutes at 65°C in 2x SSC, 0.1% SDS. They were then washed for 15 minutes in 0.1x SSC, 0.1% SDS at 65°C. This was repeated until the background level of cpm was minimal; the membranes were then sealed in plastic and exposed to Kodak X-ray films at room temperature or with intensifying screens at -70°C.

2.2.7 Quantification of gene expression with real-time PCR

2.2.7.1 Principle

Real-time PCR in the following studies was performed using a LightCycler™ (Roche Diagnostic Co, Mannheim, Germany).

There are two methods for online detection and evaluation of fluorimetric PCR reactions in glass capillaries. The PCR products formed may be detected via fluorophores that bind to all double-stranded DNA molecules regardless of sequence (Sequence-Independent Detection with SYBR Green I). The other way is with fluorophores coupled to sequence-specific oligonucleotide hybridization probes that only detect certain PCR products (Sequence-Specific Detection with Hybridization Probes). The former method was used in the following studies.

DNA Detection with SYBR Green I Dye:

The fluorescent dye SYBR Green I binds to the minor groove of the DNA double helix. In solution, the unbound dye exhibits very little fluorescence, however, fluorescence is greatly enhanced upon DNA-binding. Thus, when the LightCycler instrument's optical filter is set to match the wavelengths of excitation and emission, the amount of total DNA can be measured. The principle is outlined in the following figures (from the manufacturer's instructions).

Figure 2.1a

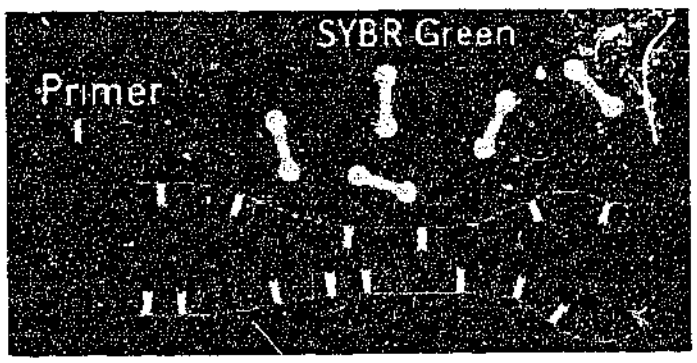

Figure 2.1a: At the beginning of amplification, the reaction mixture contains the denatured DNA, the primers, and the dye. The unbound dye molecules weakly fluoresce, producing a minimal background fluorescence signal which is subtracted during computer analysis.

Figure 2.1b

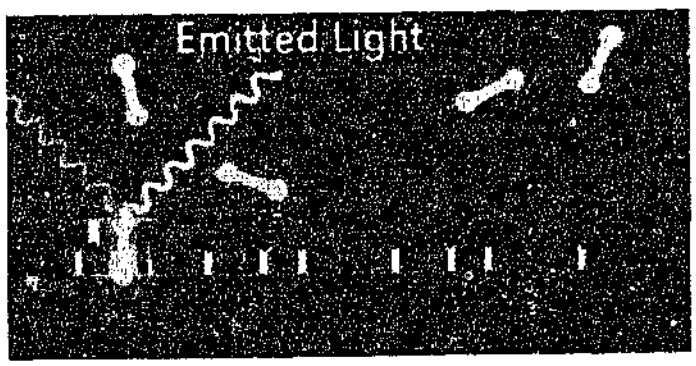

Figure 2.1b: After annealing of the primers, a few dye molecules can bind to the double strand. DNA binding results in a dramatic increase of the SYBR Green I molecules to emit light upon excitation.

Figure 2.1c

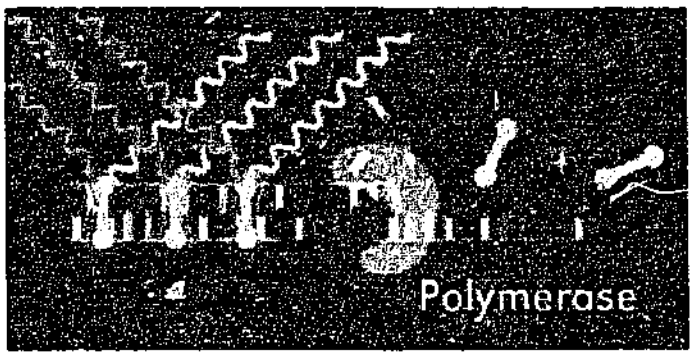

Figure 2.1c: During elongation, more and more dye molecules bind to the newly synthesized DNA. If the reaction is monitored continuously, an increase in fluorescence is viewed in real-time. Upon denaturation of the DNA for the next heating cycle, the dye molecules are released and the fluorescence signal falls. Fluorescence measurement is set at the end of the elongation step of every PCR cycle to monitor and record the increasing amount of amplified DNA.

2.2.7.2 Set up PCR conditions

Real-time PCR conditions were set up as per the LightCycler Operator's Manual (Roche Molecular Biochemicals). $MgCl_2$ concentration was adjusted to between 2 and [illegible]M. The amount of cDNA for each single reaction was 2 µl of original reverse transcription product, 1:10 dilution, or 1:100 dilutions of the original to try to allow the crossing point (Cp) to be located between 10 and 30. For initial experiments, a standard concentration of 0.5 µM for each primer was used. The concentration of primers may be adjusted between 0.3 and 1.0 µM. In amplification, denaturing phase was set up at 95°C for 0 second (the duration was increased up to 5 seconds if the template was GC rich). Annealing phase was usually set up for 5 seconds at annealing temperature, depending on primers. Elongation phase was set up at 72°C for an elongation time, which was usually calculated by amplicon length (bp) divided by 25.

2.2.7.3 Quantification

The amount of cDNA was quantified as per the LightCycler Operator's Manual (Roche Molecular Biochemicals). Using the software of the LightCycler, the amplification of

target cDNA in an unknown sample was compared against a standard curve prepared with known concentrations of the same target. The standard samples were amplified in separate capillaries but within the same LightCycler run (external standards). Typically, a standard curve was prepared from 5 samples, which were prepared by serial dilution.

2.2.8 Animal ethics

The production, care and analysis of the animals used in the following studies was in accordance with the guidelines set out in the animal ethics applications MMCA 1999/18, MMCA 2000/43 and MMCA 2001/03.

2.2.9 Histological analysis

2.2.9.1 Tissue preparation for paraffin sections

Tissues were immersed in 70% ethanol for several hours, following Bouin's fixation. Tissues were then kept in fresh 70% ethanol before tissue processing. Using an automatic tissue processor (Histokinette 2000, Reichert Jung, Germany), tissues were dehydrated in graded concentrations of ethanol (70%, 95% and 100%), histolene (Fronine, Riverstone, NSW, Australia) and melted paraplast (Oxford labware, St Louis, MO, USA). Tissues were placed in melted paraffin, set in moulds and allowed to cool. Horizontal sections of 5 µm thickness were cut using a microtome (Leitz, Hawthorn, Victoria, Australia), floated on diethyl pyrocarbonate (DEPC)-treated water, and mounted on Superfrost Plus slides (Selby-Biolab, Melbourne, Australia).

2.2.9.2 Histochemical staining

2.2.9.2.1 Haemotoxylin and eosin (H&E) staining

Paraffin tissues were H&E stained using standard techniques. Briefly, paraffin sections were rehydrated using descending concentrations of ethanol, before being placed in water for 5 minutes. The sections were then immersed in Harris' Haemotoxylin for 5 minutes, running tap water for 5 minutes, dipped in acid ethanol, water for 5 minutes, Scotts tap water for 1 minute, then water for 5 minutes. Staining was checked for

intensity, and if too intense, slides were placed back in acid ethanol, and the successive steps repeated. Subsequently, slides were placed in aqueous eosin for 3 minutes, dipped in water, dehydrated, cleared and mounted with DPX (BDH, Dorset, England).

2.2.9.2.2 Periodic acid-Schiff (PAS) reaction staining

Sections were brought to water gradually as for H&E staining. Then sections were immersed in 0.5% periodic acid (Histolabs, Riverstone, NSW, Australia) for 10 minutes, followed by rinsing in distilled water for 10 minutes. Sections were then immersed in Schiff's reagent (Appendix 1) for 20 minutes, in 1% Harris' haematoxylin for 1 minute, in running tap water for 5 minutes, dipped in acid ethanol, washed in running water for 5 minutes, immersed in Scott's blue for 5 minutes, and then washed in running water for 5 minutes. Sections were then dehydrated, coverslipped, and mounted in DPX.

2.2.9.3 Immunohistochemistry

Briefly, sections were dewaxed, rehydrated, treated with 50 mM glycine, pH 3.5 at 90°C for 10 minutes, and then 3% hydrogen peroxide for 5 minutes. The slides were washed in running tap water (5 minutes), in distilled water briefly, and then in TBS (Appendix 1) (2 X 5 minutes). Primary antibody in TBS/0.1% BSA was added to sections after incubation with blocking agent (5% of normal serum in TBS/0.1% BSA) for 20 minutes at room temperature in a humid chamber. The sections were then incubated overnight at room temperature. Following that, sections were washed in TBS (3 X 5 minutes), incubated with secondary antibody in TBS/0.1% BSA for 1 hour at room temperature, washed in TBS (3 X 5 minutes), and then incubated with streptavidin-HRP (1:500 dilution) for 30 minutes at room temperature. At the end of the incubation, sections were washed three times in TBS. The sections were then incubated with DAB-H_2O_2 solution (Appendix 1) for 10 minutes, washed in distilled water, counterstained with Harris' haemotoxylin, washed in running tap water for 5 minutes, dehydrated (graded ethanol and histosol) and mounted under glass coverslips with DPX.

2.2.10 Generation of transgenic mice

2.2.10.1 Mice

FVB mice were obtained from Animal Resources Centre, Western Australia (ARC – WA).

2.2.10.2 Hormonal stimulation and mating

Mature (6 ~ 8 week old) females were induced to superovulate by intra-peritoneal (i.p.) injections of 5 IU pregnant mare's serum gonadotropin (PMSG) at 4pm followed 44 ~ 48 hr later by 5 IU hCG. At the time of the hCG injection each female was placed with one male. On the following morning the females were checked for vaginal plugs.

2.2.10.3 Culture media

The medium used for the mouse embryo culture was KSOM (Appendix I). The medium used for embryo collection, microinjection and transfer was M2 (Appendix I).

2.2.10.4 Embryo collection

Mated females were killed by cervical dislocation between 21-23 hr after the hCG injection. The eggs enclosed in cumulus cells were collected from oviducts. The cumulus cells were removed by incubation in M2 supplemented with hyaluronidase (300 IU/ml). The cumulus-free eggs containing pronuclei were placed in KSOM culture medium and incubated at 37°C under 5% CO_2/95% air.

2.2.10.5 DNA microinjection

For microinjection, 20 to 30 eggs were transferred into a drop of M2 medium in the injection chamber. The microinjection procedure was performed under 200x magnification. About 1 to 2 pl of DNA solution (1 ~ 2ng/μL) was injected into a male pronucleus of each egg. The injected group of eggs was cultured in KSOM at 37°C under 5% CO_2/95% air. When all available eggs had been injected, they were examined

under the microscope and those which survived injection, were transferred into the oviducts of pseudopregnant female mice.

2.2.10.6 Embryo transfer

Injected eggs were surgically transferred into oviducts of pseudopregnant female mice. On average, 20-25 eggs were transterred into each female. Pups were born 20 days following the transfer and weaned at 3 weeks of age.

2.2.10.7 Detection of transgenic mice

Genomic DNA from mouse ear clips (section 2.2.1.6) or from mouse tails (section 2.2.1.7) were used for genotyping by PCR. At least three pairs of primers targeting different locations were used for detecting founders.

2.2.11 Surgical techniques

2.2.11.1 Anaesthesia

Before the surgical procedures of testis transplantation, the experimental mice were given an i.p. injection of the anaesthetic mixture as follows:

Rompun (Xylazil 20), 20 mg/ml	0.5 ml
Ketamine, 100 mg/ml	0.5 ml
PBS (GibcoBRL, Ontario, Canada)	9.0 ml
Total Volume	10 ml

The single dosage was usually 0.3 ml ~ 0.45 ml of the anaesthetic mixture depending on the response of mice.

2.2.11.2 Castration procedure

Sterile technique was applied throughout. After undergoing appropriate anaesthesia, 8 ~ 10 week old male mice were put in a supine position. A 5 mm median scrotal incision

was made. The membranes surrounding the right testis were grasped and ruptured, enabling the right testis to be pushed out of the scrotum. The vascular pedicle of the testis was then ligated with 4-0 Catgut sutures, followed by the removal of the testis. The same procedures were performed for the opposite testis. The scrotal skin was then approximated by two interrupted sutures with No. 3 silk suture material.

2.2.11.3 Transplant of the fetal testes onto the outer ears of adult male mice

A 1.5 mm opening was made on the dorsal surface of the ear at a point about two-thirds from the ear tip. Through it a channel under the skin was formed toward the ear tip by blunt dissection with scissors. The tip of the channel was then pierced by a fine needle. Subsequently, the fetal testicular graft was placed through the new opening in the skin of the outer ear and into the subcutaneous channel. The graft was pushed gently as far toward the tip of the channel as possible. The wound in the ear is self-sealing and no sutures were necessary.

2.2.11.4 Bouin's fixation of day 0 mouse pups

Firstly, 50 ml of Bouin's fixative (Appendix Ia) was prepared for the fixation of tissue from each single pup. The day 0 pup was decapitated and the head was immersed in Bouin's fixative immediately. After the tail was cut for genotyping, 1 ml of Bouin's fixative was injected into subcutaneous space on the whole body area. Subsequently, the treated body was immersed in Bouin's fixative. After 20 ~ 24 hours of immersion fixation, the bodies of pups were dissected for histological analysis and to identify any grossly anatomical abnormalities.

2.2.11.5 Dissection of day 0 mouse pups after fixation

Dissection of the "fixed" day 0 mouse pups was performed under the dissecting microscope. Firstly, the body was put in a supine position and fixed on the wax plate through 4 extremities by 4 fine pins. Several pieces of skin tissue were then excised for histological analysis. Thyroid glands were removed and collected. Then the peritoneal and thoracic cavities were opened by scissors. The thymus was subsequently removed and collected. The diaphragm was gently pulled down. The heart was separated and

collected by sharp dissection of the surrounding tissues and great arteries. Then the esophagus was cut and the lungs were removed from the thoracic cavity and collected. The whole gastrointestinal (GI) system, as well as the liver, spleen, and pancreas, was removed from the peritoneal cavity by cutting the descending colon. The livers and the spleens were separated from the GI system and collected. The remaining GI system with pancreas was collected *en masse*. Then the gonads were identified and collected by sharp dissection. Usually the ovaries were located below the kidneys and the testes could be found beside the urinary bladder. Following that, the kidneys were collected by cutting the supplying vessels and the ureters. Then an urogenital mass was removed and collected that included the genital tubercle, the orifices of urinary and GI tracts, urethra, urinary bladder, prostates (in male), seminal vesicle and part of the vas deferens (in male), vagina (in female), uterus and the partial oviducts (in female), the partial descending colon, and part of the ureters. To remove the urogenital mass, the skin of the external genitalia was incised carefully, and then the muscles of the pelvic floor and the pelvic bones were sharply dissected. The space between the descending colon and the lower vertebrae was entered smoothly. Finally, an intact urogenital mass could be removed. The vertebrae and the extremities were then also collected. For further histological analysis, the collected organs were put in 70% ethanol.

2.2.12 Steps of cross breeding to generate mice carrying human transgenes in mouse follistatin knockout background

To validate the function of the human follistatin transgenes, a two-step cross-breeding was applied to get the mice carrying the transgenes on to the mouse follistatin knockout background. Firstly, the transgenic mice, generated by microinjection of transgenic DNA, were crossed with mice heterozygous for the deletion of the mouse follistatin gene. From the first step, the mice were produced that carried the transgenes and had only one allele of the mouse follistatin gene. In the second step of cross-breeding, these mice were then crossed with similar mice or mice heterozygous for the deletion of the mouse follistatin gene. From the second step, the target mice were produced that carried the transgenes and had no mouse follistatin genes. Thus, the human follistatin genes could be assessed in these target mice. The whole procedure is simplified in Figure 2.2.

Figure 2.2 The two-step cross-breeding

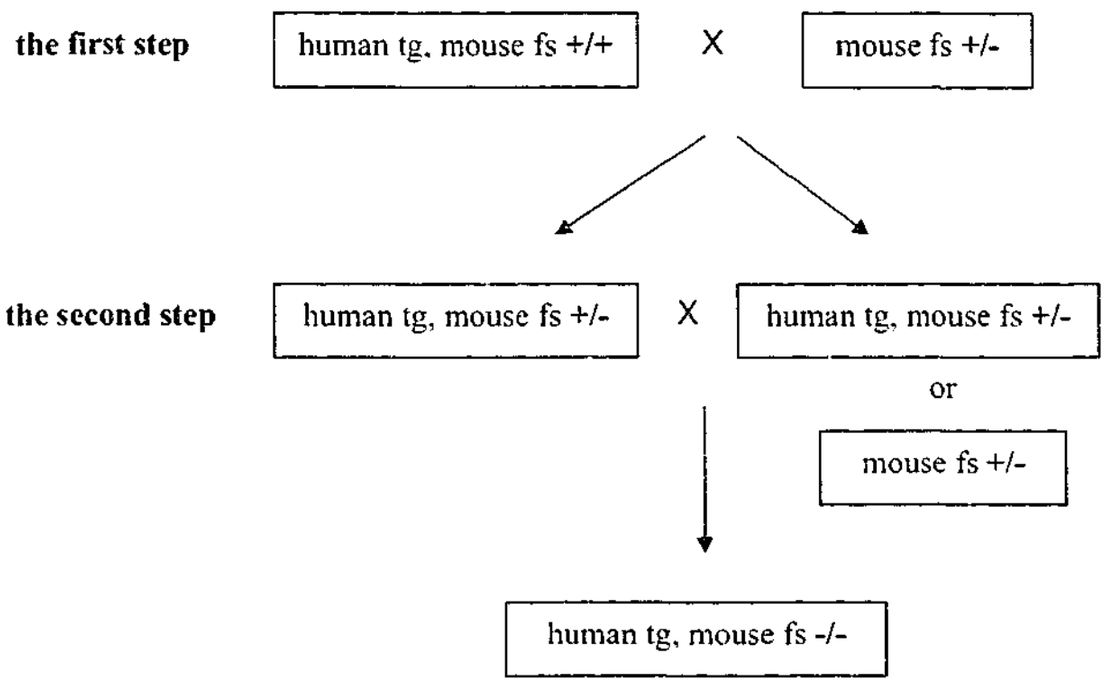

human tg: human follistatin transgene
mouse fs: mouse endogenous follistatin gene

Chapter 3

Development of fetal follistatin null testes transplanted into the ears of RAG mice

Chapter Outline:

3.1 Introduction

Activins and inhibins have been suggested to function as local modulators of spermatogenesis (de Kretser, *et al.*, 2001). Activin A *in vitro* enhanced spermatogonial proliferation (Mather, *et al.*, 1990; Hakovirta, *et al.*, 1993) and also promoted reaggregation of Sertoli cells and germ cells in the absence of basement membrane and peritubular cells (Mather, *et al.*, 1990). In contrast, inhibins were shown to suppress spermatogonial proliferation when injected locally into the adult hamster testis (van Dissel-Emiliani, *et al.*, 1989). Nevertheless, follistatin antagonized the action of activin A to stimulate reaggregation of Sertoli cell monolayers but did not modulate the activin induced stimulation of [3H]-thymidine incorporation into these same germ-Sertoli cell cocultures (Mather, *et al.*, 1993).

Attempts to study the role of follistatin on the diverse actions of activins by targeted disruption of the follistatin gene were complicated by the death of follistatin null mice at birth (Matzuk, *et al.*, 1995). These follistatin null mice had multiple defects, including growth retardation, decreased mass of the diaphragm and intercostal muscles, shiny taut skin, skeletal defects, and abnormal development of whiskers and teeth. The effects of the absence of follistatin on spermatogenesis could not be evaluated due to the neonatal death of these mice. Evidence of a role of follistatin and activin on spermatogenesis emerged from the overexpression of follistatin in male mice which resulted in decreased testis size, spermatogenic disruption and Leydig cell hyperplasia (Guo, *et al.*, 1998). Further preferential overexpression of the human activin/inhibin βA subunit mini gene in mouse testes leads to spermatogenic disruption (Tanimoto, *et al.*, 1999).

Another potential role of follistatin in spermatogenesis is to be a modulator of BMPs. BMP-4 has been shown to be required for the generation of primordial germ cells in the mouse embryo (Lawson, *et al.*, 1999). Further, the targeted disruptions of the genes encoding BMP-8B and BMP-8A have demonstrated that BMP-8B is essential for the initiation and maintenance of spermatogenesis, as well as the generation of primordial germ cells (Zhao, *et al.*, 1996; Ying, *et al.*, 2000), whereas the role of BMP-8A is involved in the maintenance of spermatogenesis and the integrity of the epididymis

(Zhao, *et al.*, 1998). Since follistatin has already been shown to be able to bind and modulate some members of BMPs, e.g. BMP-2, BMP-4, BMP-7, or BMP-15, (Chapter 1), it is likely that follistatin is also able to modulate the actions of BMP-4, BMP-8A and BMP-8B on spermatogenesis based on the structural similarity between BMP members.

To further understand the role of locally produced follistatin in testis development, the fetal follistatin null testes were transplanted into the outer ears of the castrated adult immunocompromised male mice, in order to establish a model where the local follistatin of the testes was depleted, whereas the circulatory follistatin was still maintained. Thus, in this chapter the surgical technique was developed that was subsequently applied in establishing a mouse model of testis-specific follistatin deficiency.

3.2 Experimental design & procedures

3.2.1 Experimental animals

C 57/129 hybrid mice heterozygous for the deleted follistatin allele were used to produce follistatin null fetuses (Matzuk, *et al.*, 1995). Testes were collected from fetuses that were delivered by Cesarean section at day 18 of gestation. Graft recipients were 8 ~ 9 week-old RAG male mice. RAG (recombination activating gene 1) mice are immunodeficient and produce no mature T cells or B cells. All mice were obtained from the Central Animal House at Monash University, Australia, and were housed under a 12-hour light/dark regime at 22°C. This study was approved by Animal Ethics Committee of Monash University (MMCA 2000/43) and conforms to the conditions laid down by the NH&MRC/CSIRO/AAC Australian Code of Practice for the Care and Use of Animals for Scientific Purposes (1997).

3.2.2 Collection of fetal testes for transplantation

Following the decapitation of the fetus, the abdomen was opened and the testes associated with the surrounding tissues were dissected free and transferred to Dulbecco's phosphate-buffered saline (GIBCO BRL, Life Technologies) at room temperature before transplantation. The testes were then transplanted into the host's outer ears, using a technique similar to that previously reported in the rat (Johnson, *et al.*, 1996).

3.2.3 Transplantation and castration procedures

Sterile technique was applied throughout in an SPF (specific pathogen free) room. The anaesthetic method applied to the host of fetal testes (RAG male mice) is described in Section 2.2.11.1. The castration procedure and the procedures for transplanting the fetal testes into the outer ears of adult male mice are described in Section 2.2.11.2 and Section 2.2.11.3, respectively.

3.2.4 Genotyping

A tail biopsy from each mouse of 1.5 mm length was digested in 100 µL lysis buffer (10 mM Tris-HCl pH 8.3, 50 mM NaCl, 0.2% Tween 20) plus 1 µL proteinase K (19 mg/ml) at 55°C for 65 min, then at 98°C for 12 min, and kept on ice to perform a polymerase chain reaction (PCR) later. Two pairs of PCR primers, which were the pair of hHPRT.3F and hHPRT.3R and the pair of Foldel.F and Foldel.R (see sequences in Appendix III), were used for differentiating homozygous and heterozygous for the deleted follistatin allele, and wild type. The PCR conditions can be referred to in Section 2.2.5.1. hHPRT.3F and hHPRT.3R were used for targeting the replacement cassette of the deleted mouse follistatin gene. The PCR products from the primer pair of hHPRT.3F and hHPRT.3R were 208 bp in size. Therefore, when there was a band of 208 bp, the genotype of the pup should be a heterozygote or a homozygote of the follistatin knockout. Foldel.F and Foldel.R were used for targeting the mouse follistatin gene. The PCR products from the primer pair of Foldel.F and Foldel.R were 157 base pairs in size. Therefore, when there was a band of 157 bp, the genotype of the pup should be a wild type or a heterozygous follistatin mutant. Thus, the combination of these two pairs of primers could detect the genetic status of the pups. The possible results from PCR genotyping were tabulated in Table 3.1 and a gel picture is shown in Figure 3.1.

3.2.5 Histological analysis of grafted testes

Periodic acid-Schiff (PAS) reaction staining:

Testes were fixed in Bouin's fixative for 3 ~ 5 hours, then rinsed in 70% ethanol, embedded in paraffin wax, serial sectioned at 5 µm thickness, and stained with PAS staining (Section 2.2.9.1 & Section 2.2.9.2.2).

Immunohistochemistry:

The method for immunohistochemistry can be referred to in Section 2.2.9.3. The antiserum, JM19, was raised against human recombinant follistatin 288 in rabbits (Meinhardt, *et al.*, 1998).

Table 3.1 The PCR primers for screening follistatin mutant homozygotes, heterozygotes and wild-type mice

Primer	Sequence (5'→3')	Tm (°C)	Targeting site	Product size	fs –/–	fs –/+	wt
hHPRT.3F	F: TGCTGACCTGCTGGATTACA	60.4	the sequence in the replacement cassette in follistatin knockout mice	208 bp	+	+	–
hHPRT.3R	R: CTGCATTGTTTTGCCAGTGT	59.7					
Foldel.F	F:: CGCTGCCAGGTCCTGTATAA	60.9	the mouse follistatin gene	157 bp	–	+	+
Foldel.R	R:: CTTTACAAGGGATGCAGTTGG	59.4					

(fs –/–: follistatin mutant homozygotes, fs –/+: follistatin mutant heterozygotes, wt: wild-type mice)

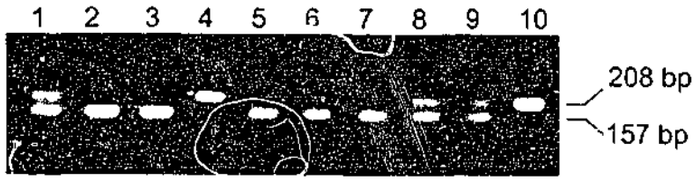

Figure 3.1 PCR for genotyping the pups

This gel picture is an example of genotyping results. The PCR reactions were run with two pairs of primers: hHPRT.3F and hHPRT.3R; Foldel.F and Foldel.R. The PCR products from the primer pair of hHPRT.3F and hHPRT.3R were 208 bp in length, targeting the replacement cassette of the sequences in the knocked-out follistatin gene. The PCR products from the primer pair of Foldel.F and Foldel.R were 157 bp in length, targeting the sequences of the mouse follistatin gene. Thus, lanes 2, 3 and 7 represent wild type pups, lanes 1, 5, 6, 8 and 9 represent the follistatin deleted heterozygotes. Lanes 4 and 10 represent the follistatin knockout pups.

3.2.6 Experimental design

Three ways of preparation of testicular grafts:

The surgical techniques were first developed with the fetal testes of the wild type. Three kinds of pre-treatments of fetal testes have been tried. The first trial was that the testis with its accessory tissues (the attached efferent ducts and head of the epididymis) was transplanted into the ears of mouse hosts. The second trial was that the tunica of the fetal testis was punctured to allow ease of entry of tissue fluids before transplantation with its accessory tissues. The third trial was that only fetal testes were transplanted without puncture into the ears of mouse hosts, and their accessory tissues were cut off before transplantation. After collecting and preparing fetal testes, surgery for testis transplantation was performed as soon as possible. At the same time, the recipient mice were castrated after transplantation of fetal testes. Seven to eight weeks after transplantation, the recipient mice were killed and the testicular grafts in the outer ears of the hosts were then collected for histological analysis. Because at the very early stage of transplantation, when there was no direct blood supply, the survival of grafted testes may depend on the diffusion of nutrition from the host, these 3 different ways of preparation of testicular grafts were tested to determine which one would be best to use for the further experiments.

Experimental procedures:

Testicular grafts without their accessory tissues were used for the further experiments for reasons described in the results section. Once fetal testes were prepared for transplantation and fetal tails were collected for genotyping, surgery for testicular transplantation was performed as soon as possible. One male recipient received only one pair of testes from a single male fetus. Following the operation, genotyping of fetal tails was done. The mice receiving heterozygous follistatin knockout testicular grafts were killed on the next day. Only the mice receiving homozygous follistatin knockout or wild type testicular grafts were left until 7 ~ 8 weeks after surgery. At that time, the recipient mice were killed and the testes in the outer ears were collected for histological analysis. The percentages of the seminiferous tubules in which there were germ cells

and the percentages of the seminiferous tubules in which there was full development of spermatogenesis were recorded. Independent samples t-test was used for statistical analysis.

3.3 Results

3.3.1 Assessing three alternate methods of preparing testicular grafts

The first trial (fetal testes + their accessory tissues) was applied on 50 fetal testes, the second trial (punctured fetal testes + their accessory tissues) on 60 fetal testes, and the third trial (fetal testes cut off from their accessory tissues) on 42 fetal testes. The survival rates of testicular grafts for these three groups were all 100%. The grafted testes did increase in size in the outer ears of recipient mice (Figure 3.2). The increased volumes of grafted testes varied from 50 fold to about 100 fold. There were no differences in the survival rates and the increased volumes of grafted testes after transplantation among these three trials.

However, only the third trial led to the full development of spermatogenesis. Almost all sections of the grafted testes from the first trial showed Sertoli cells only in the seminiferous tubules. Most sections from the second trial also displayed Sertoli cells only in the seminiferous tubules although in some areas, germ cells could be found. In contrast, the sections of the grafted testes from the third trial revealed complete spermatogenesis occupying about 15 ~ 25% of the area of the sections. About 60 ~ 80% of the area of the sections showed the germ cells. Some areas of the sections still displayed Sertoli cells only and dilated seminiferous tubules. In the further experiments, the third method of preparing fetal testicular grafts was used for the experimental and control groups (follistatin null fetal testes and wild type fetal testes).

3.3.2 Genotyping results

In total, 22 male fetuses were collected for this study, among which 7 were follistatin mutant homozygous, 4 were wild type, and 11 were follistatin mutant heterozygous. Each pair of testes was transplanted into an individual castrated RAG male mouse. 11 mice receiving follistatin mutant heterozygous testes were killed once the genotypes of testicular grafts were known. Four of 7 mice receiving follistatin mutant homozygous testes died some days after surgery for no apparent reason. Finally, only 3 RAG mice

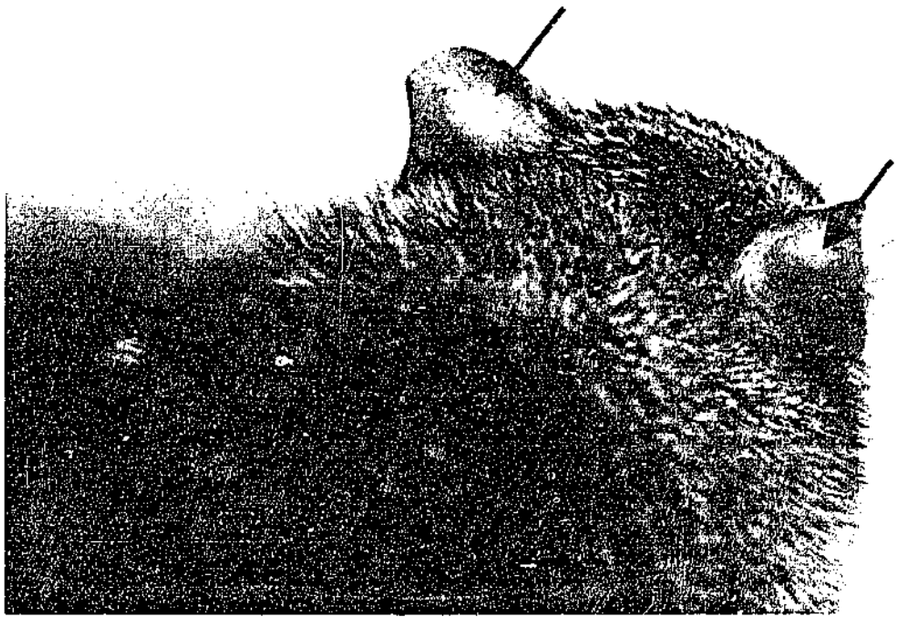

Figure 3.2

Fetal testes that have enlarged in the external ears of the adult castrated RAG male mouse are shown (indicated by arrows).

receiving follistatin mutant homozygous testes and 4 receiving wild type testes were alive until 7 ~ 8 weeks after transplantation. Thus 6 follistatin null and 8 wild type grafted testes were used for histological analyses.

3.3.3 Full development of spermatogenesis in both grafted fetal follistatin null and wild type testes

Histological assessment of the morphology of the follistatin null and wild type fetal testes showed no differences (Figure 3.3a & d) at day 18 of gestation. The sections of fetal testes with or without the follistatin gene both exhibited a similar pattern. There were many primitive seminiferous cords where Sertoli cells formed the walls of tubules with peritubular cells surrounding them and gonocytes located in the center of the cords (Figure 3.3a & d). Leydig cells could also be found within the interstitial tissue of the testes between the seminiferous tubules and characterized as round or ovoid cells with a large round centrally located nucleus.

Interestingly, histological analyses revealed that there was full development of spermatogenesis both in follistatin null and wild type testis grafts (Figure 3.3b & e) 7 ~ 8 weeks after transplantation. In some of the seminiferous tubules, spermatogonia, spermatocytes, round spermatids and elongating spermatids could be identified. There seemed to be no distinction between these testes with different genetic backgrounds based on their histology. However, in many of seminiferous tubules there was luminal dilation (Figure 3.3c & f) with disorganization of seminiferous epithelium, as well as premature sloughing of postmeiotic germ cells. In some cross sections of seminiferous tubules, only Sertoli cells could be found without any germ cells. The percentages of seminiferous tubules with germ cells showed no statistical difference between the follistatin null and wild type testes (85.9 ± 3.7% vs 83.7 ± 5.1%). Similarly, the percentages of seminiferous tubules with complete spermatogenesis were not statistically different between follistatin null and wild type testes (18.6 ± 1.3% vs 19.8 ± 1.7%).

Figure 3.3 Spermatogenesis in testes transplanted into the outer ears of RAG mice

(a): follistatin knockout fetal testis; (d): wild type fetal testis; (b) & (c): follistatin knockout grafted testes after 7 ~ 8 weeks of transplantation; (e) & (f): wild type knockout grafted testes after 7 ~ 8 weeks of transplantation. The pictures of (a), (b), (d) and (e) are 40x magnification and those of (c) and (f) are 10x magnification. Before transplantation, follistatin knockout and wild type fetal testes exhibited a similar pattern of histology (a & d). There were many seminiferous cords with Sertoli cells and peritubular cells forming the walls, gonocytes located in the center of cords and some Leydig cells located within the interstitial tissue. 7 ~ 8 weeks after being transplanted into the outer ears of RAG mice, the grafted testes have grown showing seminiferous tubules with a lumen and full spermatogenesis (b & e). Germ cells present included spermatogonia, spermatocytes, round spermatids and elongating spermatids. However, probably as a result of a blockage of fluid flow, some seminiferous tubules displayed a dilation of lumen with disorganization of epithelia and premature sloughing of postmeiotic germ cells (c & f).

Figure 3.3

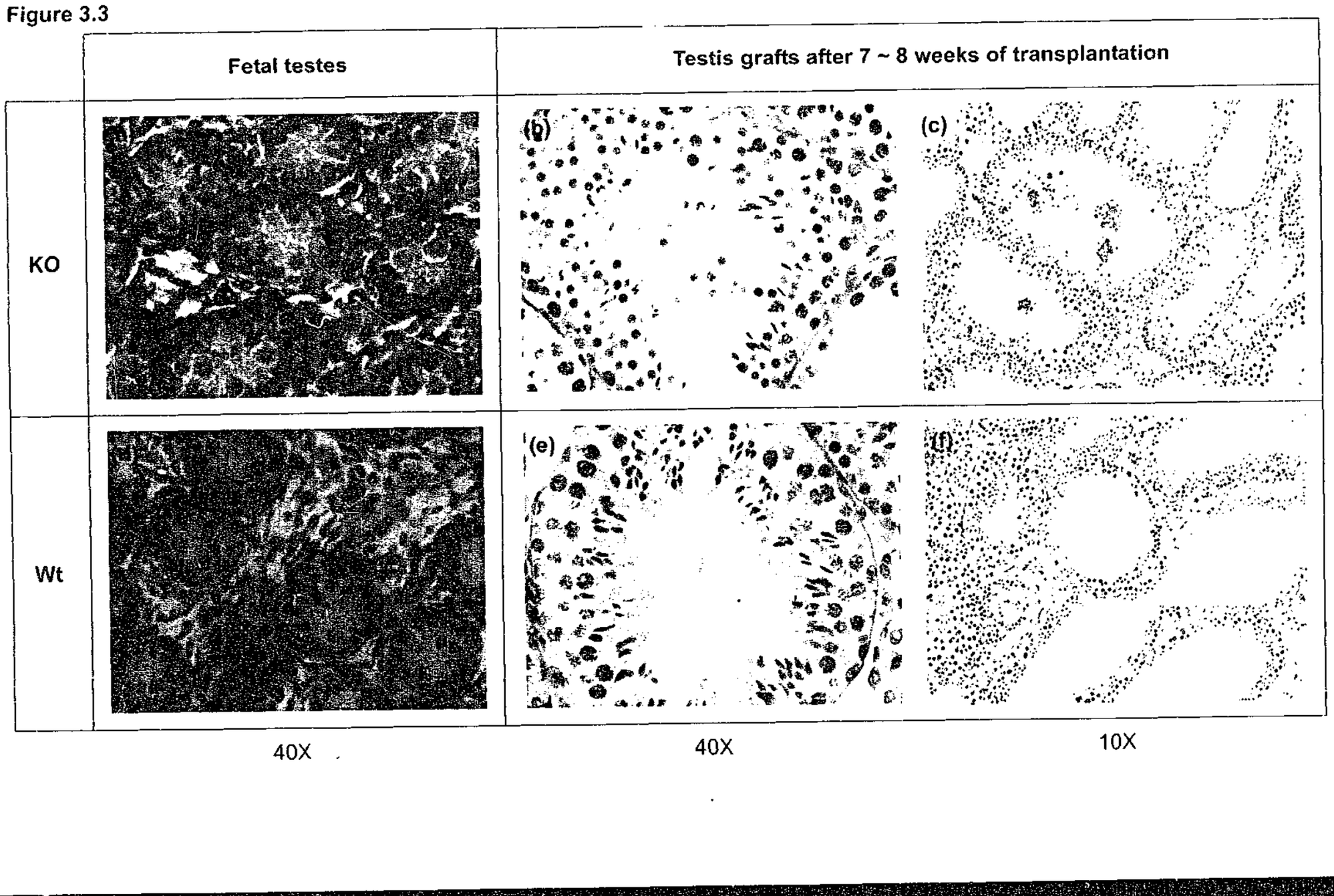

3.3.4 Follistatin protein was detected in both grafted fetal follistatin null and wild type testes

In view of the possibility of follistatin from the host being provided to the follistatin null testes, immunohistochemistry for follistatin protein was performed (Figure 3.4). Again, the sections from follistatin null and wild type testis grafts showed a similar pattern of follistatin protein location. Follistatin protein was most evident in Leydig cells. Follistatin was also found in Sertoli cells, spermatogonia, some of spermatocytes, spermatids and peritubular myoid cells. In addition, the skin of the outer ears of hosts and endothelial cells lining blood vessels showed a marked immunoreaction for follistatin.

Figure 3.4 Follistatin protein was detected in both grafted follistatin knockout and wild type testes

The pictures show the immunohistochemical analysis for follistatin in the grafted testes and are 20x magnification. (a) & (c) are the negative controls for the follistatin knockout testis and the wild type testis, respectively. (b) & (d) are the experimental groups for the follistatin knockout testis and the wild type testis, respectively. In the sections from both the follistatin knockout testes and the wild type testes, Leydig cells were the cell types that were stained most obviously (b & d). In addition, Sertoli cells, peritubular myoid cells, spermatogonia, some of spermatocytes and spermatids were all stained positively. The skin of the outer ears and the endothelial cells of blood vessels of connective tissue also showed positive stains. In conclusion, the grafted follistatin knockout and wild type testes exhibited a similar pattern of distribution of follistatin proteins.

Figure 3.4

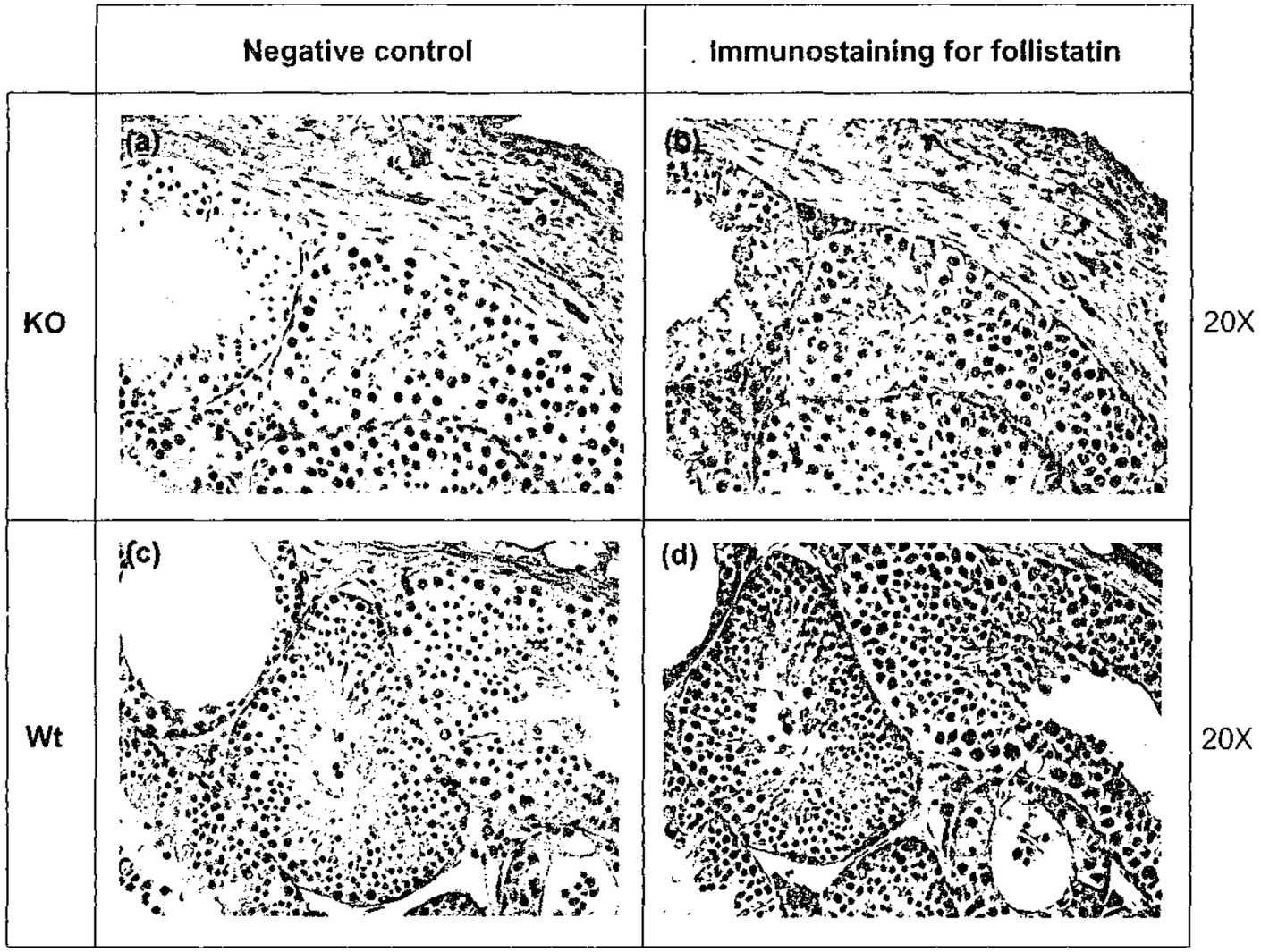
Negative control
Immunostaining for follistatin
KO
Wt
(a)
(b)
(c)
(d)
20X
20X

3.4 Discussion

3.4.1 Technique development of transplanting fetal testes into the ears of adult male mice

As far as I know, this is the first trial of this technique in mice although it has been applied in rats with satisfactory results (Johnson, *et al.*, 1996). The main reason for transplanting fetal testes is that follistatin homologous mutant mice die soon after birth (Matzuk, *et al.*, 1995) and further assessment of testis function in this model was not feasible. This model of testis transplantation can be considered as an *in vivo* organ culture system of fetal testes whose original owners cannot survive due to some severe genetic defects. Moreover, it may be used as a general tool to produce sperm from fetal testes of genetic models that die at birth allowing further applications of IVF (*in vitro* fertilization) or ICSI (intra-cytoplasm sperm injection) in order to maintain the genetic manipulated mouse lines.

Fetal follistatin null testes were transplanted in the outer ears of castrated RAG male mice, leading to the availability of follistatin-315 to the transplanted testes via the blood supply, but these testes could not produce follistatin locally. The reason for choosing the outer ear as the grafting site is because the local temperature of the outer ears is similar to that of scrotum (Johnson, *et al.*, 1996). Moreover, because the fetal mouse testis is around 1.5 mm to 2 mm in diameter, the nutrition required for maintaining the testes initially after transplantation can be provided by diffusion until new vessels, developed by angiogenesis, establish a vascular supply to the testicular graft. As a result, these phenomena are the likely reasons why the fetal testicular grafts can survive after surgery. The importance of the efficiency of nutrition diffusion from hosts may explain why the third method of preparation of fetal testes achieved the best results, since fetal testes were cut off from their accessory tissues before grafting, resulting in a decreased total volume of the graft and an increased ratio of the surface area to the volume of the graft to allow maximal diffusion from the hosts to the grafted testes during the initial critical period.

3.4.2 Spermatogenesis in grafted testes

Fetal mouse grafted testes were able to grow in the outer ears of RAG castrated male mice and displayed full development of spermatogenesis. However, in some of the seminiferous tubules there was luminal dilation, probably owing to the block of fluid flow. Further, some of seminiferous tubules showed Sertoli cells only, probably as a result of poor nutrition supply that damaged the spermatogonia at the initial critical stage before the completion of vasculogenesis and angiogenesis.

In this study, the most interesting point may be that the fetal follistatin null and wild type testes after transplantation both showed full differentiation in spermatogenesis (Figure 3.3). Are the results demonstrating that follistatin is not important for testis development? In the over-expressed follistatin models generated by Matzuk and colleagues (Guo, *et al.*, 1998), lines 5 and 9 did not have suppressed FSH levels, but still showed spermatogenic disruption, indicating that follistatin is not irrelevant to testis development. Further, testis-restricted expression of human βA subunit in mice also caused testicular degeneration (Tanimoto, *et al.*, 1999). Since follistatin can antagonize the action of activin, this phenotype can relatively and indirectly reflect the effect of follistatin under-expression in testis development. These reports suggested that follistatin plays a role in testis development and function.

The results presented in this chapter strongly suggest that locally produced follistatin may not be necessary for full testicular development since spermatogenesis proceeds to completion in the absence of local production. These data, supported by the immunohistochemistry showing that the transplanted knockout testis contains immunoreactive follistatin, support the conclusion that circulating follistatin from the host is sufficient to allow testicular development.

3.4.3 Summary and future directions

In summary, the work in this chapter presented a model of testis transplantation that may be also applicable to the study of other regulatory agents involved in testicular

development. Further, this model suggested that the effects of intra-testicular production of follistatin can be substituted by the systemic supply of follistatin from the host.

Whilst histological analyses showed that the follistatin knockout fetal testis grafts attained full spermatogenesis as demonstrated histologically, it did not provide direct evidence of the normal function of spermatozoa from the follistatin knockout testis grafts. *In vitro* fertilization experiments using these sperm may help in further elucidating the capacity of these sperm from grafted testes.

Chapter 4

Characterization and assembly of the genomic constructs of the human follistatin gene

Chapter Outline:

4.1 Introduction

The role of follistatin in regulating reproductive function has been recognized for more than 10 years. Recently a broader context for follistatin biology has emerged. Follistatin can bind to a number of other members of the TGF-β superfamily in addition to modulating their activities. Taken together, studies of the regulation of follistatin expression would be a vital area of follistatin biology since follistatin may affect the balance of actions of the TGF-β superfamily members. In this thesis, transgenesis studies were initiated in an attempt to define the regulatory sequences of the human follistatin gene.

Transgenic mice are frequently used to study the control of gene expression. To define the DNA sequence that confers the specific pattern of expression, different lengths of genomic sequences can be transferred into the germ line by gene transfer. The gene transfer method most popularly used is the microinjection of DNA directly into the pronuclei of fertilized mouse eggs (Gordon, *et al.*, 1980). Consequently genomic elements essential for gene regulation may be identified.

The first aim of this chapter is to characterize the PAC-FS vector. PAC-FS is the vector of P1 artificial chromosome (PAC) harboring a human follistatin genomic sequence that includes the follistatin gene and approximately 45 kb upstream and downstream sequences around the gene. PAC-FS was firstly obtained from screening the human DNA PAC library of the Murdoch Institute (Melbourne, Australia), which was a generous gift of Dr. Panos. Then, PAC-FS was characterized by mapping the restriction sites that are useful for assembling the construct, pNEB-FS, described in this Chapter.

The second aim of this chapter is to construct pNEB-FS, which carries the human follistatin gene and its approximately 16 kb upstream and 3 kb downstream sequences in a 2.7 kb vector, pNEB 193 (*New England Biolabs, Inc.*).

4.2 Experimental design & procedures

4.2.1 Mapping restriction sites

Restriction endonuclease digestion (Section 2.2.2.1), agarose gel electrophoresis (Section 2.2.2.2) and Southern hybridization analysis (Section 2.2.6) were performed to map restriction sites of PAC-FS.

4.2.2 DNA cloning

The techniques of DNA cloning for assembling pNEB-FS can be referred to in Section 2.2.2.

4.2.3 Experimental procedures

Firstly, the PAC-FS vector was characterized and the useful restriction sites in it were identified. Then a fragment of DNA, including the human follistatin gene cut from PAC-FS, was cloned into the pNEB 193 vector by several steps of DNA cloning, leading to pNEB-FS. pNEB-FS was further validated by restriction digestion. Following that, the DNA of PAC-FS and pNEB-FS was prepared for microinjection.

4.3 Results

4.3.1 Characterization of PAC-FS

Firstly, the human PAC DNA library of the Murdoch Institute was screened for the PAC vector harboring the human follistatin gene by PCR using the primer pair of fol.1F and fol.1R (Appendix III), which targeted exon 1 of human follistatin gene. Clone 210 and clone 22 were found to carry the human follistatin gene (Figure 4.1). Clone 22 was used for the subsequent DNA engineering, since it contained the appropriate flanking regions of the human follistatin gene, spanning about 45 kb upstream and downstream sequences. Afterwards, the PAC vector of Clone 22 harboring the human follistatin gene was designated as 'PAC-FS'.

4.3.1.1 Mapping the restriction sites

When I started my PhD, the human genomic sequences had not been released. However, at that time, the sequence of human follistatin gene (about 6 kb) was published (Shimasaki, *et al.*, 1988), although its upstream and downstream sequences were not yet available. To map the restriction sites of the upstream and downstream sequences of the PAC-FS, several restriction endonucleases were used to cut the PAC-FS, then the DNA digests were electrophoresed in the agarose gel. The DNA in the gel was subsequently transferred onto two positively charged nylon membranes, which covered both sides of the gel via capillary transfer (Figure 4.2a). Two different probes were separately used for Southern hybridization (Section 2.2.6) on the two positively charged nylon membranes. The two probes were made to sequences of exon 1 and exon 5 of the human follistatin gene, so they could detect the fragments which included exon 1 and exon 5, respectively. After autoradiography, the fragments containing exon 1 or exon 5 could be identified (Figure 4.2b).

Based on results from using different combinations of restriction endonucleases, the location of specific restriction sites of the PAC-FS could be deduced (Figure 4.2c). An example is shown in the Figure 4.2. 'A' is a known site within the follistatin gene. The

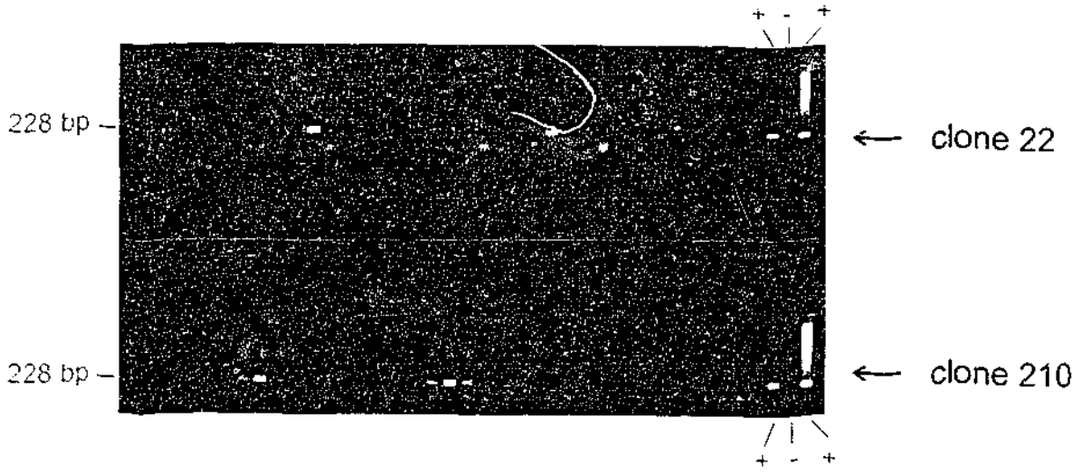

Figure 4.1 Screen PAC human DNA Library for the follistatin gene using a PCR based screening

The gel picture shows several positive colonies from clone 22 and clone 210 while using the pair of primers, fol.1.F and fol.1.R, to do PCR. The positive colonies should have a 228 bp band of PCR products. Lanes labeled "*" contain PCR-positive products. Lanes labeled "+" represent positive controls and lanes labeled "-" represent negative controls.

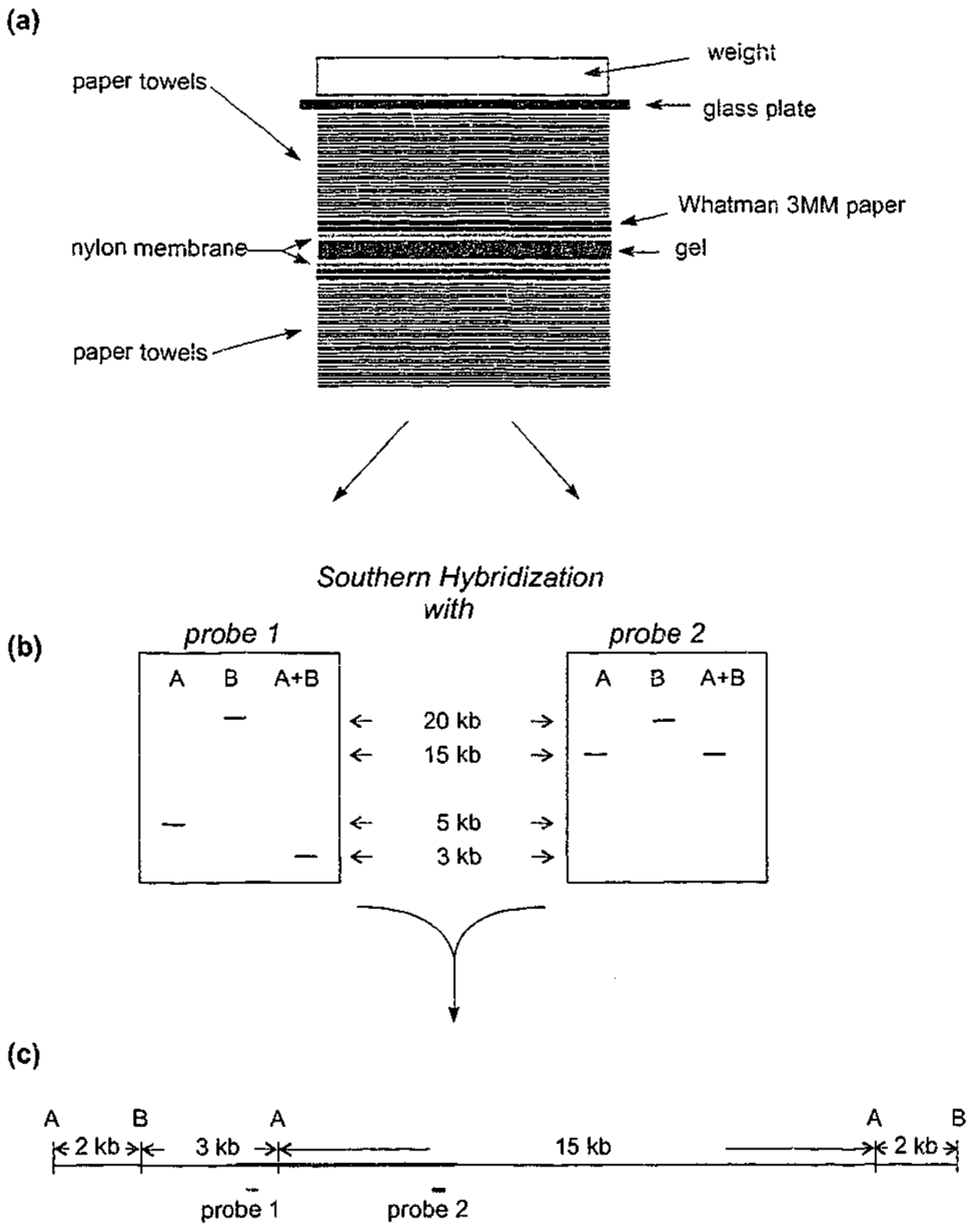

Figure 4.2 Mapping restriction sites

An example describing the method for mapping the restriction sites: (a) Capillary transfer of DNA after treatments of restriction endonucleases A, B, or A+B from agarose gels to two nylon membranes with solid supports simultaneously. (b) Southern hybridization was then performed with probe 1 and probe 2 for the two membranes, respectively. Probe 1 was made of exon 1 of the follistatin gene, and probe 2 was made of exon 5 of the follistatin gene. (c) Since site A is a known site within the follistatin gene, the sites of A in upstream and downstream areas, and the initially unknown sites B can be deduced from the sizes of the bands in the two membranes.

fragment of DNA, containing exon 1, after treatment with the restriction endonucleases 'A', showed 5 kb in size. However, after the double digestion of 'A+B', the size of the band is 3 kb, deducing that 'B' cuts through the original fragment digested with 'A'. Moreover, the size of the fragment AB, containing exon 1, should be 3 kb. Similarly, while using probe 2, which was made of exon 5, the bands containing exon 5 after the treatments of 'A' or 'A+B' are both the same size, 15 kb. This implies that the site 'B' is located beyond the fragment AA containing exon 5 and indicates that the fragment AA should be 15 kb in size. Further, the fragment, containing exon 5, after the digestion of 'B' is 20 kb in size, leading to the conclusion that the portion within the fragment BB, and at the same time beyond the fragment AA which contains exon 5, should be 5 kb (20 kb -15 kb = 5 kb) in size. Taken together with the size of the fragment AB (3 kb) that contains exon 1, the 3′ site 'B' should be 2 kb (5 kb – 3 kb = 2 kb) far away from the 3′ site 'A' (Figure 4.2c).

4.3.1.2 The useful restriction sites

Many restriction endonucleases, including NotI, EcoRI, SalI, Sse 8387I, SwaI, FseI, PacI, SfiI, AscI, XhoI, PvuII, KpnI, SpeI, NcoI, RsrII, ScaI, XmaI, AflII, NheI, NaeI, SacI. SacII, HindIII, AhdI, EcoRV, PmeI, XbaI, were used to characterize PAC-FS. Based on the data of seven Southern blotting experiments from various combinations of the restriction endonucleases mentioned above, the sites SacI and PacI were chosen for use in constr' cting the shorter genomic construct, pNEB-FS. The experimental evidence for the sites SacI and PacI was shown here (Figure 4.3).

In Figure 4.3, the lanes 1, 5 and 12 were the DNA digests from the treatments of SacI, PacI and SacI + PacI, respectively. Figure 4.3a shows the electrophoresed gel picture, whereas Figures 4.3b and 4.3c show the pictures of Southern hybridization of the two positively charged nylon membranes to which the DNA in the gel was transferred. Figure 4.3b represents the autoradiographic picture of the membrane hybridized by the probe of exon 1. Since there is one known SacI site within the follistatin gene, just about 250 bp away from the beginning of the follistatin gene, the sizes of the bands in the lanes 1 and 12 indicate that another SacI site locates about 16 kb upstream and there are no more SacI and PacI sites between this SacI site and the SacI site within the follistatin

Figure 4.3 The experimental evidence of the SacI and PacI sites useful in the assembly of the pNEB-FS vector

In (a), (b) and (c), lanes 1, 5 and 12 represent the DNA digests of PAC-FS with SacI, PacI and SacI + PacI, respectively. (a) The DNA digests were electrophoresed in 0.4% agarose gel. High molecular weight (HMW) DNA makers (*Life Technologies*) were used to estimate the DNA size. The DNA in the gel was then transferred onto the two positively charged nylon membranes. (b) represents the autoradiographic picture of the membrane hybridized with the probe of exon 1 of the human follistatin gene. The bands from the digestion of SacI and SacI + PacI were the same in size (16 kb), and the band from the digestion of PacI is much bigger in size. It was deduced that the upstream DNA sequence between the two SacI sites was 16 kb, and there was no SacI or PacI sites within it. (C) represents the autoradiographic picture of the membrane hybridized with the probe of exon 5 of the human follistatin gene. The band from the double digestion of SacI + PacI was 9 kb in size, indicating that the PacI site is located about 3 kb downstream of the gene, since the size of the gene is about 6 kb. Thus, the map (d) can be deduced.

Figure 4.3

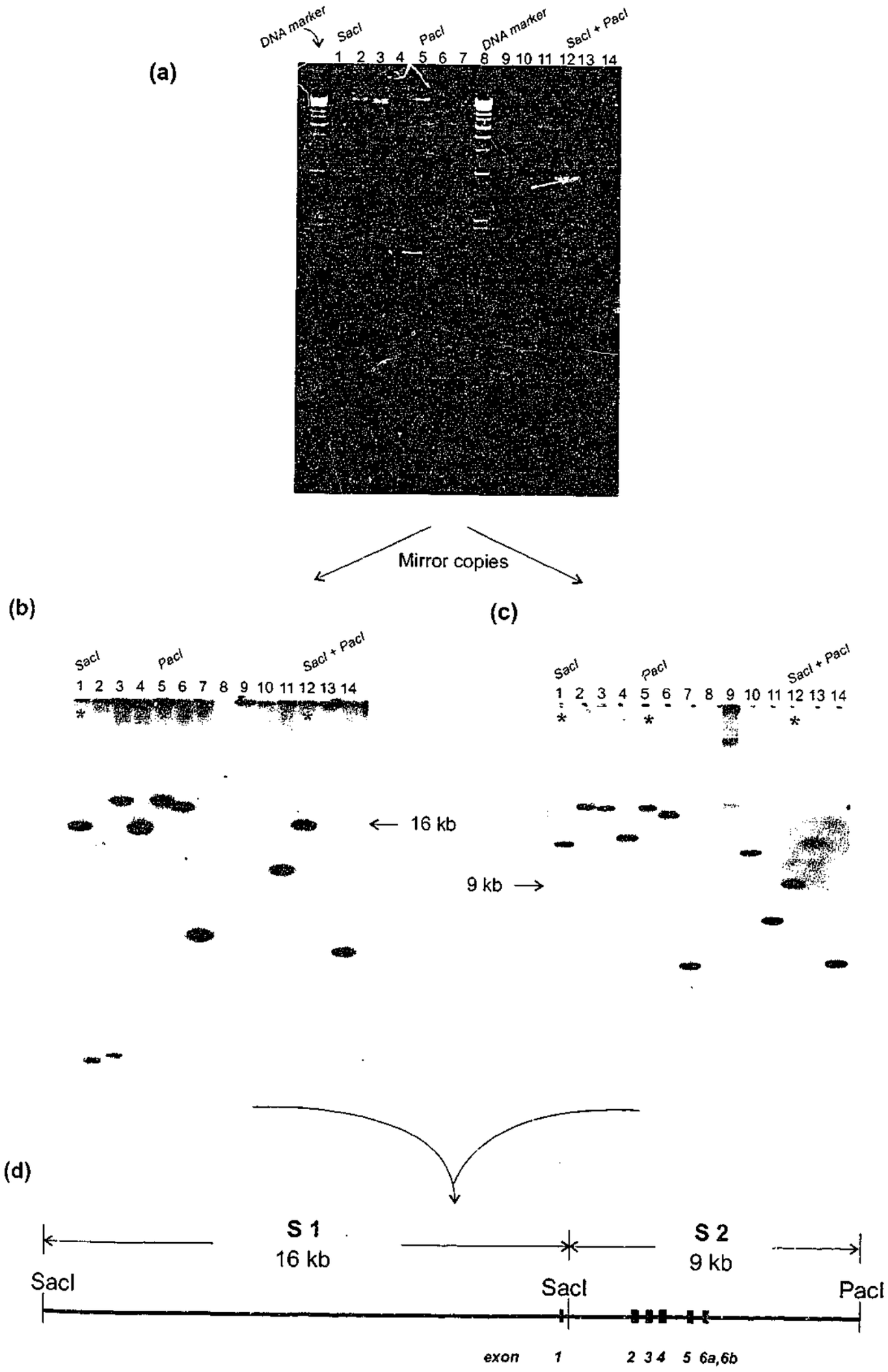
(a)
DNA marker
SacI
PacI
DNA marker
SacI + PacI
1 2 3 4 5 6 7 8 9 10 11 12 13 14
Mirror copies
(b)
(c)
SacI
PacI
SacI + PacI
1 2 3 4 5 6 7 8 9 10 11 12 13 14
16 kb
9 kb
(d)
S 1
16 kb
S 2
9 kb
SacI
SacI
PacI
exon 1 2 3 4 5 6a,6b

gene. Figure 4.3c represents the autoradiographic picture of the membrane hybridized by the probe of exon 5. The sizes of the bands in the lanes 5 and 12 indicate that there is a single PacI site located about 3 kb downstream of the last follistatin exon. Figure 4.3d illustrates the SacI and PacI sites mapped within the PAC-FS genomic clone. These sites were subsequently used to assemble the pNEB-FS construct.

4.3.2 Assembly of pNEB-FS

4.3.2.1 Strategy

Because the sites SacI and PacI are unique within pNEB 193 (Figure 4.4b), this vector was chosen for the assembly of a shorter transgene that includes the follistatin gene and its approximately 16 kb upstream and 3 kb downstream flanking sequences. For the convenience of description, S1 (Figure 4.3d) represents the fragment that contains the 16 kb upstream and exon 1, and is cut from the PAC-FS with the restriction endonuclease SacI. S2 (Figure 4.3d) represents the fragment that contains the rest of the follistatin gene and its 3 kb downstream sequence, and has the sites of SacI and PacI on both edges. Thus S1 plus S2 represents the DNA fragment cloned in the pNEB-FS.

PAC-FS and pNEB 193 were cut with the double digestion of SacI plus PacI (Figure 4.4b & c). This released S2 from PAC-FS which was then cloned into pNEB 193, designated as pNEB-S2. Similarly, PAC-FS and pNEB 193 were digested with SacI (Figure 4.4a & b). The released S1 from PAC-FS was then cloned into pNEB 193, designated as pNEB-S1. Subsequently, pNEB-S1 and pNEB-S2 were digested with SacI (Figure 4.4d & e). The released S1 from pNEB-S1 was cloned into the linearized pNEB-S2 to form pNEB-FS (Figure 4.4f). This last cloning step generated two possible outcomes, as S1 may be inserted in either direction. A PCR screen, designed to identify clones in the desired orientation, was used as a final screening step (Figure 4.4f).

4.3.2.2 Generation of the pNEB-S2 vector

PAC-FS and pNEB 193 were double digested with the restriction endonucleases SacI and PacI (Figure 4.4b & c). The DNA digests were then electrophoresed in a 0.4 % agarose gel (Figure 4.5a & d). The target bands, which were 9 kb for S2 (Figure 4.5c)

Figure 4.4 Strategy of assembling pNEB-FS

On the left side of the figure, PAC-FS (a) and pNEB 193 (b) were digested with SacI to release S1 from PAC-FS and form the vector 1 from pNEB 193. Ligation of S1 with vector 1 led to pNEB-S1 (d). On the right side of the figure, PAC-FS (c) and pNEB 193 (b) were double digested with SacI and PacI to release S2 from PAC-FS and form vector 2 from pNEB 193. Subsequent ligation of S2 and vector 2 resulted in pNEB-S2 (e). pNEB-S1 (d) and pNEB-S2 (e) were then digested with SacI to release S1 from pNEB-S1 and linearize pNEB-S2, both of which were then ligated together to form pNEB-FS (f).

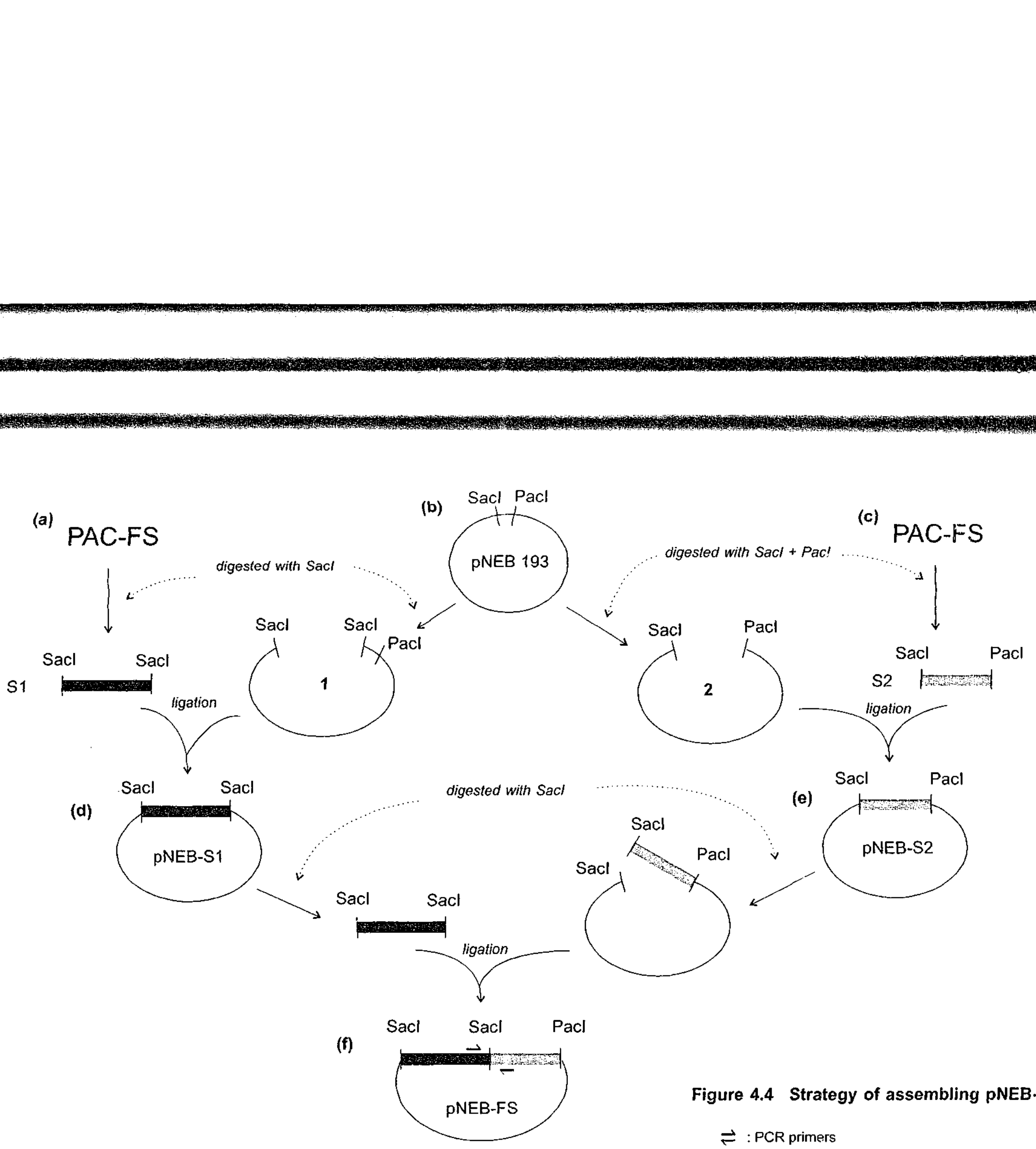

Figure 4.4 Strategy of assembling pNEB-FS

⇄ : PCR primers

and 2.7 kb for the resulting pNEB 193 (Figure 4.5b), were trapped in low melting temperature (LMT) agarose gel, which was then excised. After heating the LMT gel containing the target bands to 68°C for 10 min, it was kept at 37°C. The ligation reaction was set up with T_4 DNA ligase and with a molar ratio of 3:1 of the insert to the vector. The in-gel ligation reaction mixture was left at room temperature overnight. The ligation reaction mixture (Figure 4.5e) was then to be used to transform the $INV_{\alpha}F'$ cells (Invitrogen, CA, USA). The cells were plated out on LB agar plates containing ampicillin 75 μg/ml, and incubated at 37°C overnight. Sixteen colonies were screened by PCR using the primers of 'pNEB193-F' and 'fs-sac-R'. One positive colony was identified (Figure 4.5f).

4.3.2.3 Generation of the pNEB-S1 vector

To clone S1 into pNEB 193, PAC-FS and pNEB 193 were digested with the restriction endonuclease SacI (Figure 4.4a & b). The DNA digests were then electrophoresed in 0.4% agarose gel (Figure 4.6a & b). The target bands were excised from the LMT gel. The size of the band in the gel for S1 (Figure 4.6d) is about 16 kb, and for the resultant linearized pNEB 193 (Figure 4.6c) about 2.7 kb. After cutting the LMT gel in which the target bands were located, the DNA was extracted from the LMT gel with β-agarase (Section 2.2.2.4), precipitated and then dissolved in 1x TE. The ligation reaction was set up with T_4 DNA ligase with a 3:1 molar ratio of the insert to the vector. Cyclic temperature variations were used for the ligation reaction (Section 2.2.2.7).

The DH 5α cells were chemically transformed with the resulting ligation reaction mixture. The procedure was as usual, except the culture temperature was set at 30°C because instability of the insert was experienced during growing *E coli* harboring pNEB-S1 (Figure 4.6e). The lower temperature resulted in a decrease in growth velocity, but was thought to promote the stability of the insert. The pair of the primers fol.1.F and pNEB193-F was used for PCR screening the colonies. Three positive colonies were obtained (Figure 4.6f).

Figure 4.5 Generation of pNEB-S2 vector

After pNEB 193 and PAC-FS were cut with double restriction endonucleases, SacI + PacI, the target bands, which were 2.7 kb and 9 kb for the linearized pNEB 193 (b) and the S2 (c), respectively, were obtained in the LMT gel (a &d) following electrophoresis. The ligation reaction (e) was set up for these two target bands. The chemically competent cells were then transformed with the ligation reaction mixture. After growing the competent cells on LB agar containing ampicillin overnight, 16 colonies were screened for the correct construct. One of them (*) was positive for the pNEB-S2 vector by PCR screening with the primers pNEB193-F and fs-sac-R (f). The positive colony should have a 271 bp band of PCR products.

Figure 4.5

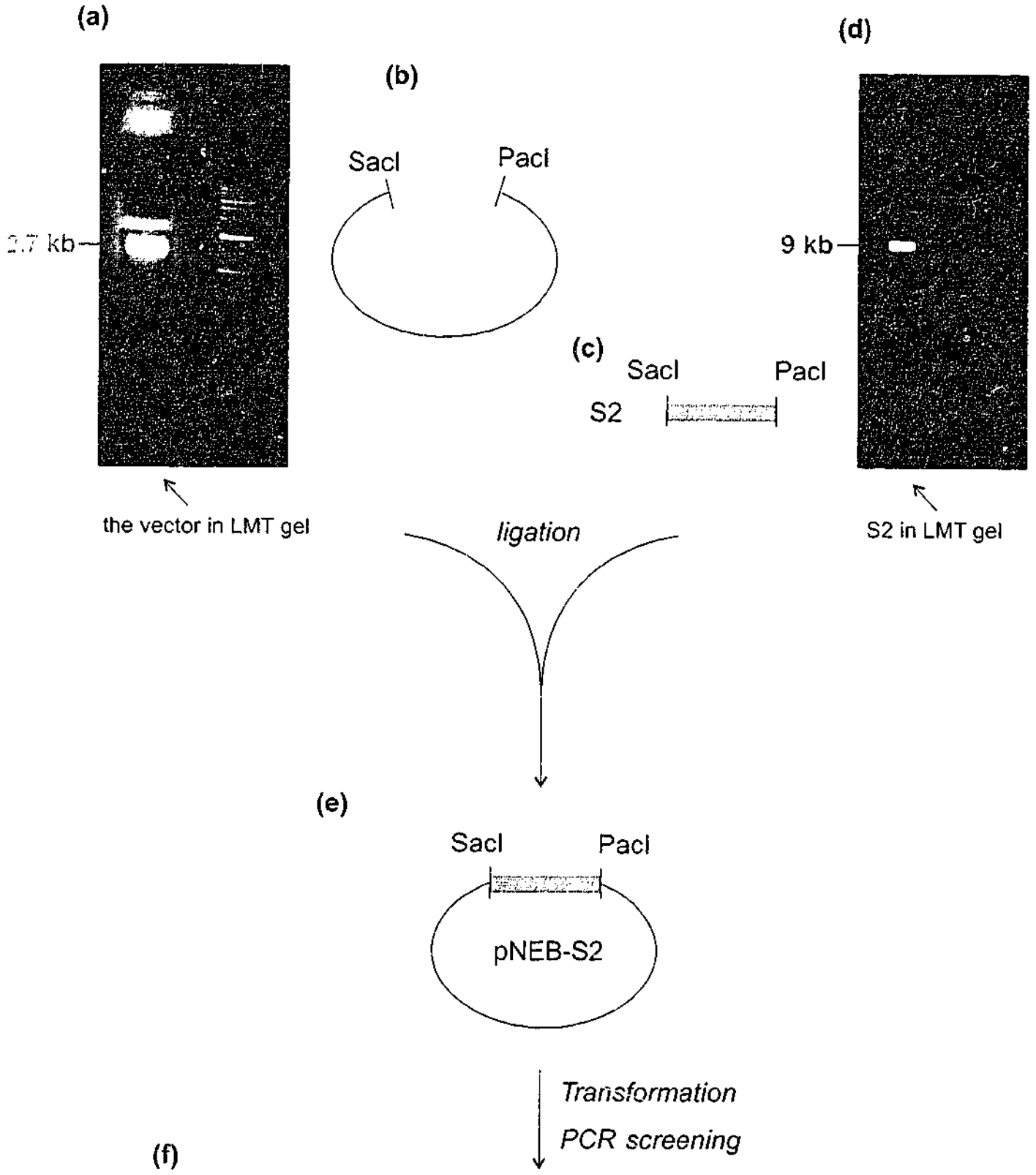
(a)
2.7 kb
the vector in LMT gel
(b)
SacI
PacI
(c)
SacI
PacI
S2
(d)
9 kb
S2 in LMT gel
ligation
(e)
SacI
PacI
pNEB-S2
Transformation
PCR screening
(f)

Figure 4.6 Generation of the pNEB-S1 vector

The pNEB 193 vector and PAC-FS were digested with the restriction endonuclease SacI. The target bands, which were 16 kb and 2.7 kb for S1 (d) and the linearized pNEB 193 (c), respectively, were obtained in LMT gel (a & b) following electrophoresis of the DNA digests. The colonies of the competent cells, following transformation with the ligation reaction mixture (e) of the two target bands and grown on LB agar containing ampicillin, were screened for the pNEB-S1 (e) vector using PCR with the primers fol.1.F and pNEB193-F. Three positive colonies (*) were obtained (f) that had a 251 bp band of PCR products.

Figure 4.6

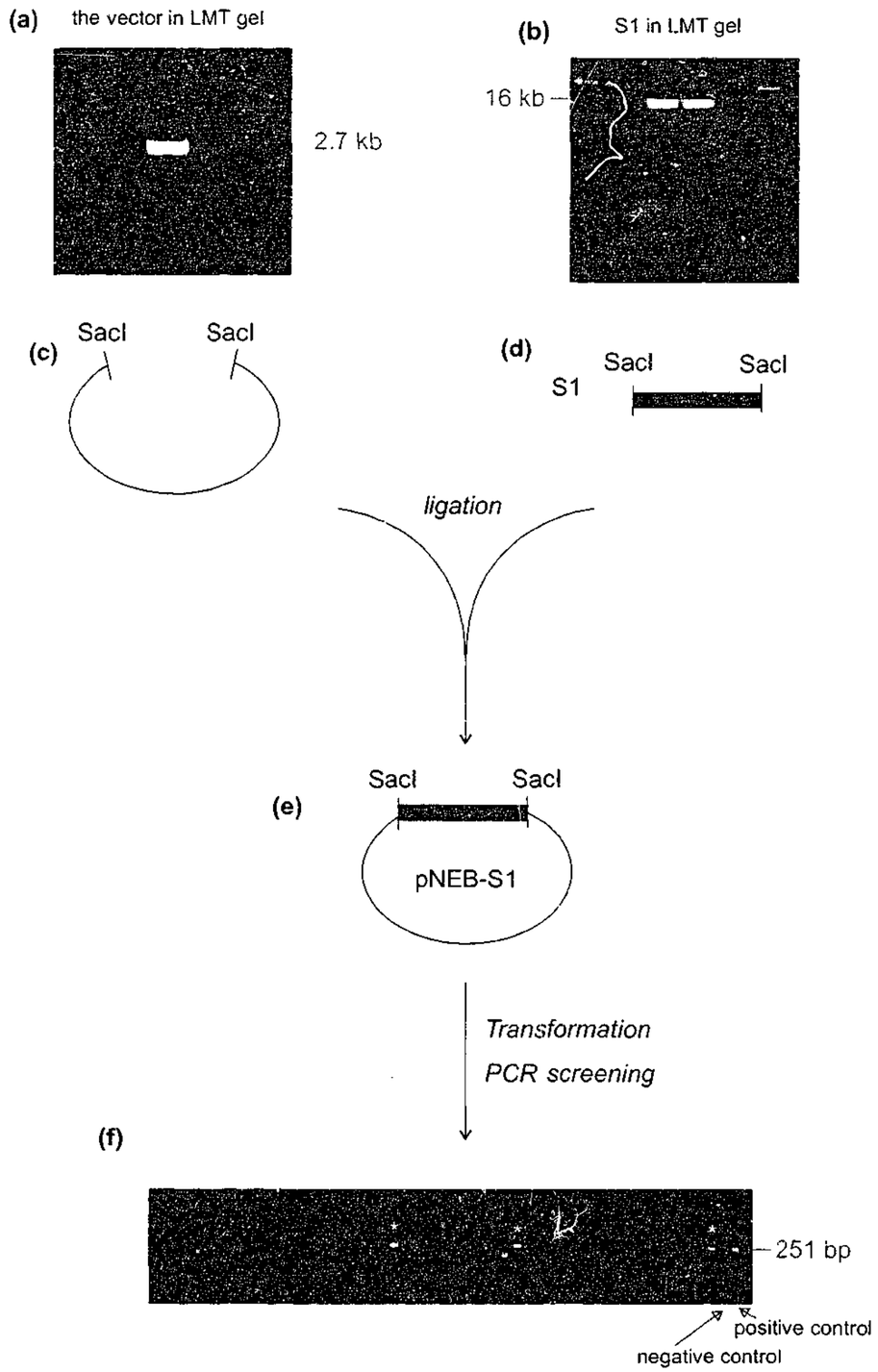

4.3.2.4 Generation of the pNEB-FS vector

pNEB-S1 and pNEB-S2 were digested with SacI, releasing S1 from pNEB-S1 and linearizing pNEB-S2 (Figure 4.4d & e). The DNA digested was electrophoresed and the target bands, S1 (about 16 kb) (Figure 4.7c) and the linearized pNEB-S2 (about 12 kb) (Figure 4.7d), were entrapped and excised from the LMT agarose gel (Figure 4.7a & b). The DNA was then extracted from the gel by β-agarase (Section 2.2.2.4). A high concentration T_4 DNA ligase was used for ligation reaction. The molar ratio of S1 to pNEB-S2 was set at 1:1. The ligation temperature was set up by the cyclic temperature ligation protocol (Section 2.2.2.7).

The electrocompetent DH 10B cells (Invitrogen, CA, USA) were transformed by the ligation reaction mixture (Figure 4.7e). The resulting cells were plated on the LB agar containing 100 μg/ml ampicillin and cultured at 30°C overnight. The pair of primers, fol.1.F and fs-sac-R, was used for PCR screening. More than 15 colonies were positive (Figure 4.7f).

Fourteen colonies were chosen to be further cultured in 5 ml LB medium at 37°C overnight. PCR was then performed for these 14 clones again. The bands in the gel became faint (Figure 4.8a). Instability of the insert was suspected. Glycerol stocks were made for 6 of the clones. Four clones were further grown in 100 ml TB medium at 30°C overnight, and then the DNA preparation was made. The DNA was electrophoresed after digestion with SacI (Figure 4.8b). The bands appeared to be correct in size, however the amount of DNA was of low yield (Figure 4.8b).

4.3.3 Preparation of constructs for microinjection

4.3.3.1 Purification

Purification of pNEB-FS:

Considering the low DNA abundance and the possible instability of the insert, large scale preparation of the clone was attempted. The clone of pNEB-FS was grown in 2 liters of LB medium at 37°C overnight, and then a maxi-prep of DNA (Section 2.2.1.2)

Figure 4.7 Generation of the pNEB-FS vector

After the restriction digestion of SacI for pNEB-S1 and pNEB-S2, the DNA digests were electrophoresed (a). As shown here, the lane of pNEB-S1 contained not only S1 (16 kb) and the vector (2.7 kb), but also the band (labeled with **) which arose from the instability of the insert. However, the correct bands, which were 16 kb for S1 (c) and 12 kb for the linearized pNEB-S2 (d), could be targeted and entrapped in LMT gel (b). Following the ligation and the transformation for pNEB-FS (e), several positive clones (*) were detected by PCR screening (f) with the primers fol.1.F and fs-sac-R, showing a 470 bp band for a positive result.

Figure 4.7

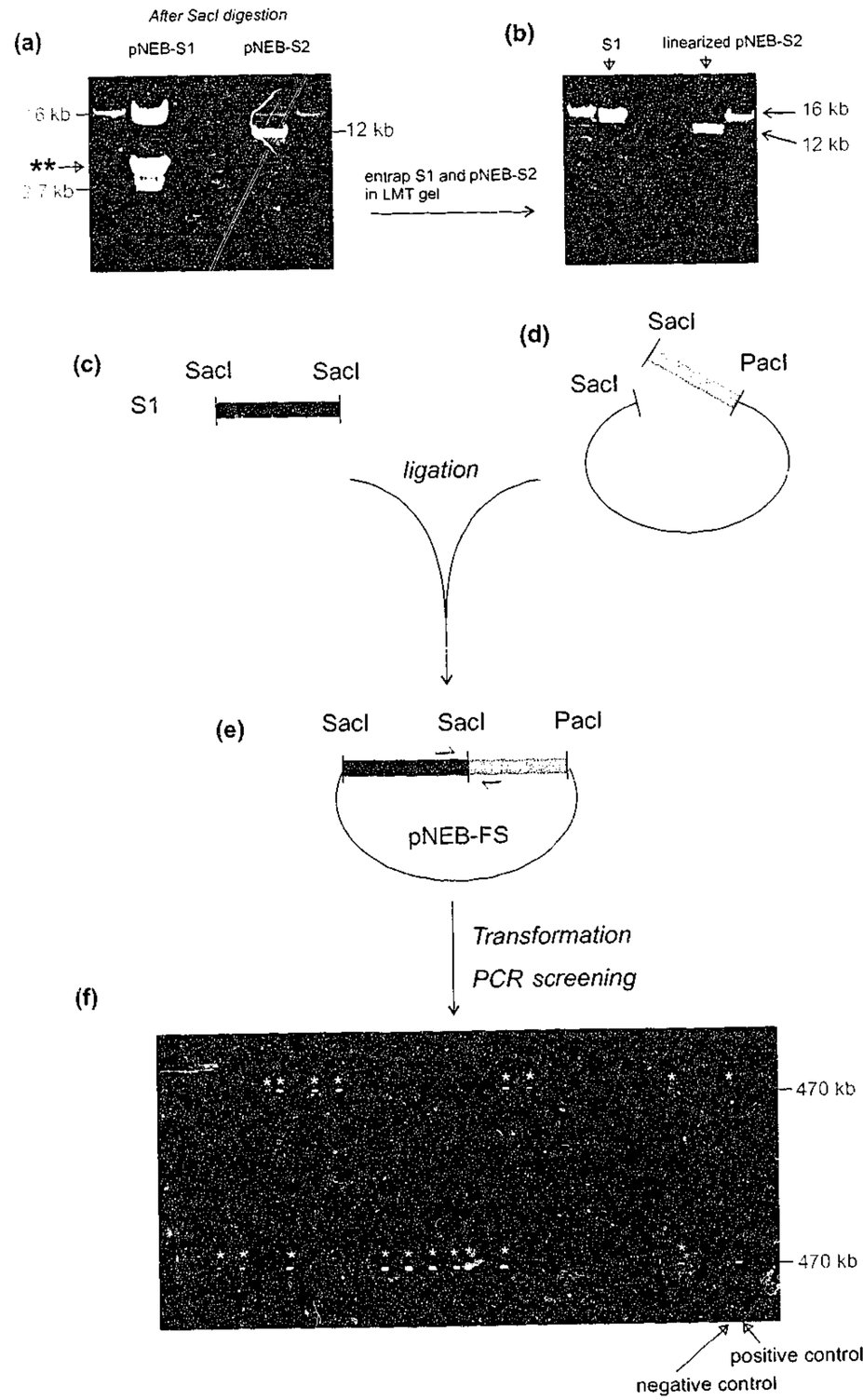

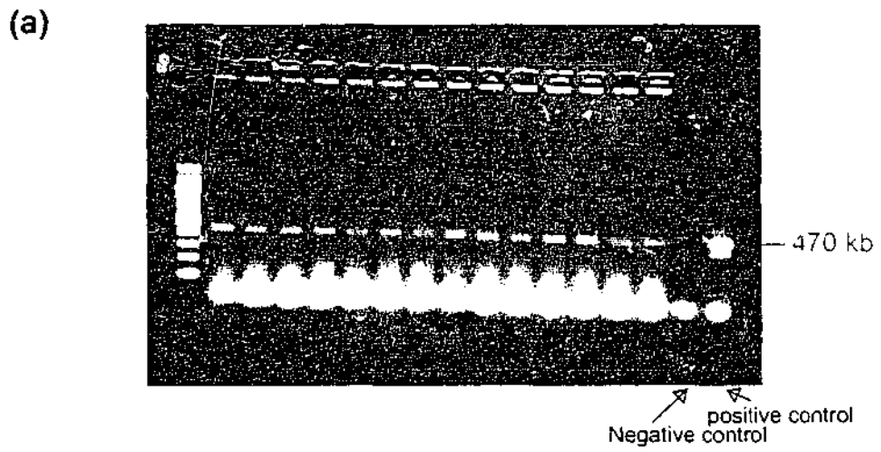

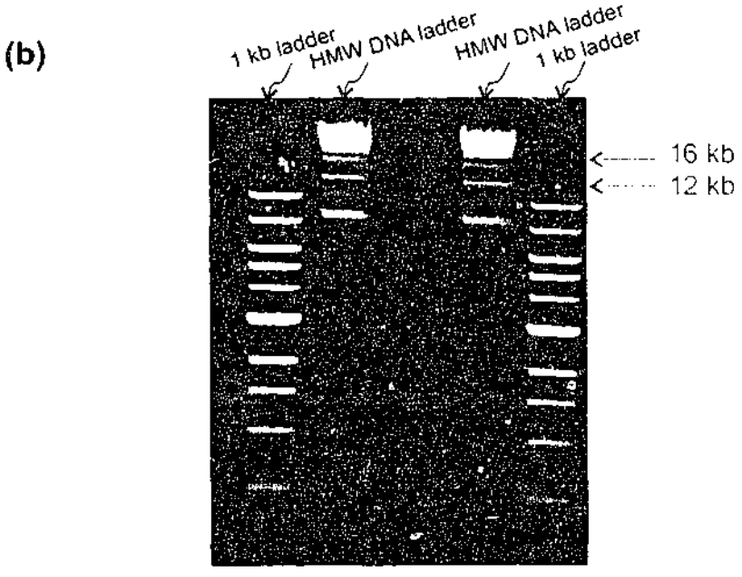

Figure 4.8 The instability of the inserts of pNEB-FS during the growth of the host cells

(a) After growing the positive clones of pNEB-FS in LB containing ampicillin overnight, the same PCR reaction was run again. The positive bands became faint, implying that some of inserts may have been lost during the growth of the host cells. (b) However, the SacI digestion for the DNA extracted from the cells showed the correct band sizes (16 kb and 12 kb).

was made. 50 µg of the DNA was digested with PacI and then electrophoresed. As shown in Figure 4.9a, it is apparent that multiple clones were present, further suggesting instability of the clone. Fortunately, I was able to obtain enough of the correct sized fragment for consequent applications (Figure 4.9b).

To prepare the DNA of pNEB-FS, DNA of the correct size was entrapped in LMT gel and excised following electrophoresis as mentioned above. The DNA was then recovered from the gel with β-agarase (Section 2.2.2.4). An ethidium bromide extraction was followed to further purify the DNA (Section 2.2.1.8). This extraction uses ethidium bromide to displace proteins bound to the DNA, which was then removed by phenol and chloroform. As a final step, drop dialysis was used to remove excess salts and to then replace the solution with the buffer solution that was used during microinjection (Section 2.2.1.8).

Purification of PAC-FS:

For purifying the DNA of PAC-FS, an ethidium bromide extraction was not suitable for high-molecular-weight DNA. An alternative protocol using chromatography on Qiagen resin was used (Section 2.2.1.8). Then drop dialysis was performed to allow the DNA to dissolve in the appropriate buffer solution for microinjection.

4.3.3.2 Quantification and validation

Spectrophotometry was used to quantify the amounts of prepared DNA. The optical density (OD) reading at 260 nm allows calculation of the concentration of DNA. An OD of 1 corresponds to ~ 50 µg/ml for double-strand DNA. The ratio between the readings at 260 nm and 280 nm (OD_{260} : OD_{280}) was also specially noticed since pure preparations of DNA have OD_{260} : OD_{280} values of 1.8.

There was no need to validate PAC-FS since it was originally from the human PAC library. After purification, pNEB-FS was further validated by restriction digestions (Figure 4.10). They displayed all the correct sized bands in the electrophoresis gel.

(a)

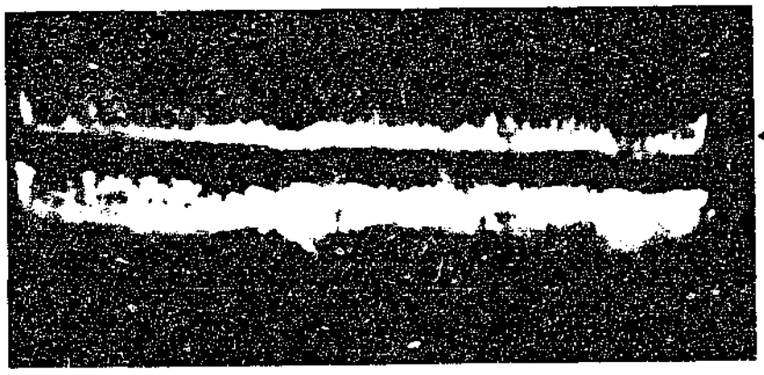

(b)

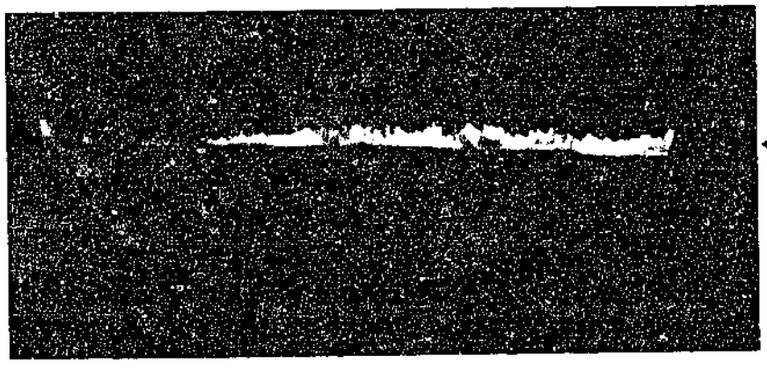

Figure 4.9 Purification of pNEB-FS for microinjection

To resolve the problem that the instability of the inserts of pNEB-FS was induced during the growth of the host cells, 50 μg of the pNEB-FS DNA was digested with the restriction endonuclease PacI and then electrophoresed in the 10 cm well of the agarose gel. (a) It is apparent that there were bands other than the correct bands (28 kb). (b) Despite these limitations there were still significant amounts of the desired DNA after excising the other wrong bands.

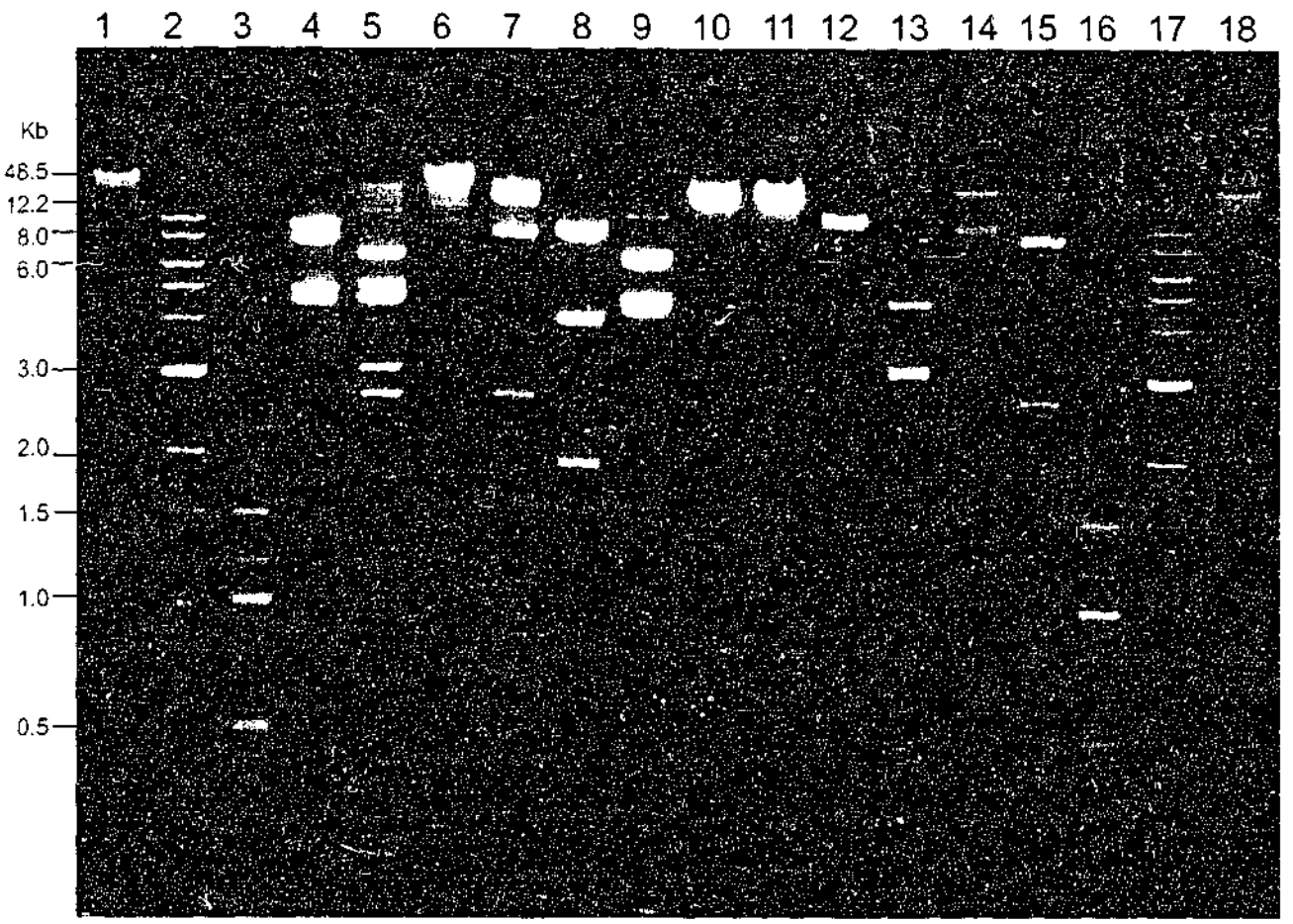

Figure 4.10 Validation of pNEB-FS

The linearized pNEB-FS by PacI, after purification (Figure 4.9), was further validated by restriction digestions to check if there was occurrence of rearrangement of DNA during the procedures of DNA cloning. The electrophoresis gel showed all the correct sized bands. Lanes 1 & 18: high molecular weight DNA marker. Lanes 2 & 17: 1 kb DNA ladder. Lanes 3 & 16: 100 bp DNA ladder. Lanes 4 ~ 15 representing the digestion mixtures of 3 vectors were tabulated as follows:

	Restriction endonuclease digestion			
	EcoRV	HindIII	XhoI	SacI + PacI
Linearized pNEB-FS	Lane 4	5	6	7
pNEB-S1	Lane 8	9	10	11
pNEB-S2	Lane 12	13	14	15

4.4 Discussion

4.4.1 Application of genomic DNA in transgenic studies

From recent studies on genomics a concept has emerged that inter-species sequence comparisons can identify non-coding sequences having gene regulation properties, originating from the hypothesis that sequences regulating gene expression tend to be conserved between species. This concept has been further supported by numerous transgenic studies demonstrating that genomic transgenes from various mammals, when introduced into the mouse genome, can have a similar expression pattern to that in the natural host (Lacy, *et al.*, 2000). More intriguingly, some transgenic studies showed that even a gene, for which the mouse lacks an orthologue, can be expressed in mice in a manner that mimics its expression in its natural host (Frazer, *et al.*, 1995). These concepts and evidence together formed the background of the work described in the Result Section 2 (chapter 4 ~ 6) of the thesis, focusing on the functional analysis of 95 kb and 25 kb human follistatin genomic transgenes in follistatin knockout mice as well as computational analysis of the human follistatin locus through the human-mouse sequence comparison.

4.4.2 Summary and further directions

The work presented in this chapter was the characterization of PAC-FS, assembly of pNEB-FS and preparation of DNA of PAC-FS and pNEB-FS. PAC-FS includes the human follistatin gene and its 45 kb upstream and 45 kb downstream flanking sequences in addition to the 15 kb sequence of the backbone vector PAC. However, pNEB-FS contains the human follistatin gene and its 16 kb upstream and 3 kb downstream flanking sequences in addition to the 3 kb sequence of the backbone vector pNEB 193. PAC-FS and pNEB-FS, which contain different lengths of genomic sequences of human follistatin locus, were both further used to generate transgenic lines (Chapter 5).

Chapter 5

Functional analysis of 25 kb and 95 kb genomic sequences of the human follistatin locus in the follistatin knockout mice

Chapter Outline:

5.1 Introduction

In an attempt to define the human follistatin locus, the genomic constructs of the human follistatin gene, PAC-FS and pNEB-FS (Sections 4.3.1 & 4.3.2) that contained 95 kb and 25 kb of genomic sequences, respectively, were used to create two transgenic mouse models. The aim was to drive the human follistatin gene within the constructs by the natural regulatory elements located within the genomic sequences of the human follistatin locus. The transgenic mice were then crossed with follistatin mutant heterozygotes (fs +/-) to assess whether the transgenes would be sufficiently active in the follistatin knockout background to rescue the follistatin knockout (fs -/-).

The germ-line transmission of transgenes is required to establish a transgenic line. Because differentiation between soma and germ line occurs early in mammals, experiments involving genetic manipulation have to be performed as early as possible during ontogenesis. There are four different methods that are currently used to generate transgenic mice: i) pronuclear microinjection of DNA into a zygote; ii) transfection of preimplantation embryos with recombinant retroviruses carrying the gene of interest; iii) gene transfer into embryonic stem cells by using calcium phosphate-mediated DNA transformation, electroporation, retroviral infection or lipofection (Gossler, *et al.*, 1986; Robertson, *et al.*, 1986; Strauss and Jaenisch, 1992); iv) intracytoplasmic coinjection of unfertilized mouse oocytes with exogenous DNA and sperm heads whose membranes had been disrupted (Perry, *et al.*, 1999). Pronuclear microinjection was adopted for these experiments primarily because the technique was readily available within the Institute.

After the pronuclear microinjection was performed and before chromosomal integration occurs, the microinjected DNA molecules usually recombine into a large tandemly arranged concatemer. This head-to-tail array suggests a process of homologous recombination between multiple copies of the microinjected DNA (Bishop and Smith, 1989). The subsequent integration of pronuclear microinjected DNA has been demonstrated by *in situ* hybridization in diverse regions of the mouse genome (Michalova, *et al.*, 1988; Dobie, *et al.*, 1996; Festenstein, *et al.*, 1996). Moreover, in

most cases, the integration of transgenes will take place at only one site although occasionally separate integration sites can occur (Lacy, *et al.*, 1983). These findings further support the concept that integration sites of transgenes are randomly distributed at unpredictable chromosomal sites. Hence, to avoid the wrong inference from the phenotypes due to the integration effects, at least two independent transgenic lines for each transgene are required to get an objective assessment of transgene function.

To acquire an unbiased deduction from assessing these two transgenes with different lengths of flanking regions, it is important to validate them in mouse follistatin knockout background. There are three main reasons why the biological functions of both genomic sequences should be analyzed in the knockout background. First, because it is the natural regulatory elements within the genomic sequence that drive the human transgene expression, and since many of the essential regulatory elements are likely to have been conserved during evolution, it is probable that human genomic transgenes and mouse endogenous genes may compete or synergize with each other to control the total expression levels of follistatin. Hence, the real expression levels of human genomic transgenes cannot be assessed properly in the presence of mouse endogenous genes. Secondly, follistatin expression is developmental and tissue related. Since the natural regulatory elements of follistatin genes may have been conserved between mouse and human, the regulatory elements within the follistatin human transgenes of genomic sequences may only be able to regulate the follistatin expression in a natural manner when they function in the mouse follistatin knockout background. Finally, since the fs-ko mice die at birth, assessing the ability of the transgenes to rescue this phenotype is a powerful assay to assess the true function of the transgenes.

5.2 Experimental design & procedures

5.2.1 Experimental animals

FVB mice used for microinjection were obtained from Animal Resources Centre, Western Australia. The production, care and analysis of the mice were in accordance with the guidelines set out in the animal ethics applications MMCA 1999/18 and MMCA 2001/03.

FVB transgenic mice carrying the construct PAC-FS or pNEB-FS (Chapter 4) were crossed with the C57/129 hybrid mice heterozygous for the deleted follistatin allele (Matzuk, *et al.*, 1995) in an attempt to obtain the human follistatin transgenic mice in the mouse follistatin knockout background. This study was approved by the Animal Ethics Committee of Monash University (MMCA 1999/18 and MMCA 2001/03) and conforms to the conditions laid down by the NH&MRC/CSIRO/AAC Australian Code of Practice for the Care and Use of Animals for Scientific Purposes (1997).

5.2.2 Pronuclear microinjection of transgenic DNA

The preparation of the DNA of transgenes, *i.e.* pNEB-FS and PAC-FS, for microinjection was described in Section 4.3.3. The methods associated with microinjection, *i.e.* hormonal stimulation and mating, embryo collection, DNA microinjection and embryo transfer, were described in Sections 2.2.10.2 ~ 2.2.10.6.

5.2.3 Procedures for genotyping

Genomic DNA was prepared from mouse ear-clips (Section 2.2.1.6), and then was used for genotyping. Genotyping to detect founders generated by pronuclear microinjection of zygotes was performed by PCR using four pairs of primers that target four different sites of transgenes. PCR primers were designed using primer3 (http://www-genome.wi.mit.edu/cgi-bin/primer/primer3_www.cgi) based on the human genomic sequence of the follistatin locus (source: NCBI, NT_023081 contigs). The genotype of the transgenic mice born from the founders was determined by PCR reactions using one

of these four pairs of primers. These sequences of these four pairs of primers, '10kb-UP.AF & R', '5kb-UP.AF & R', 'Southern.AF & R', and '1.5kb-DOWN.AF & R' are found in Table 5.1. The conditions for each PCR reaction were set up as described in Section 2.2.5.1.

To genotype the offspring from the cross-breeding program, genomic DNA was isolated from mouse tails (refer to Section 2.2.1.7). Three pairs of primers, human.FS.2F & R, mouse.FS.2F & R and hHPRT.3F & R, were used to identify pups with different genetic backgrounds via PCR reactions. The details of these primers are found in Table 5.2. The conditions of PCR reactions for these three pairs of primers were summarized as follows:

Reaction 1: using double pairs of primers (human.FS.2F & R and hHPRT.3F & R)

DNA [1]		
dNTPs	2 mM	3 µl
10x Buffer [2]		3 µl
human.FS.2F	50 µM	0.4 µl
human.FS.2R	50 µM	0.4 µl
hHPRT.3F	50 µM	0.4 µl
hHPRT.3R	50 µM	0.4 µl
Tag DNA polymerase	5 U/ µl	0.2 µl
dH_2O		to 30 µl

Reaction 2: using one pair of primers (mouse.FS.2F & R)

DNA [1]		
dNTPs	2 mM	3 µl
10x Buffer [2]		3 µl
mouse.FS.2F	50 µM	0.4 µl
mouse.FS.2R	50 µM	0.4 µl
Tag DNA polymerase	5 U/ µl	0.2 µl
dH_2O		to 30 µl

[1]10-100 ng genomic DNA was used. [2]The buffer as supplied contained 500 mM KCl, 15 mM $MgCl_2$, 100 mM Tris-HCl (pH 9.0 at room temperature).

Table 5.1 PCR primers for detecting transgenic founders

Primer	Sequence (5'→3')	Tm (°C)	Targeting site	Product size
10kb-UP-A.F	F: GTGGCCTTCTGGAGACTGAG	60	10kb upstream of human follistatin gene	236 bp
10kb-UP-A.R	R: CATGATGGCACGAACCTGTA	60.5		
5kb-UP-A.F	F: AACATCCCCATTCTAAGGCA	59.3	5kb upstream of human follistatin gene	174 bp
5kb-UP-A.R	R: GCCTTGCTTTCCCCTTTAAT	59.5		
Southern-F	F: CTGGGTCACTGGTAACTGACATT	60.3	intron 1 of human follistatin gene	506 bp
Southern-R	R: GAGTCCTACCTTTACAGGGGATG	60.2		
1.5kb-DOWN-A.F	F: TTTCAAACACCATGACCCAA	59.7	1.5kb downstream of human follistatin gene	297 bp
1.5kb-DOWN-A.R	R: ACCGGAGAAGTTACGACCCT	60		

Table 5.2 PCR primers for genotyping pups from the second step of cross-breeding

Primer	Sequence (5'→3')	Tm (°C)	Targeting site	Product size
hHPRT.3F	F: TGCTGACCTGCTGGATTACA	60.4	the sequence in the replacement cassette in follistatin knockout mice	208 bp
hHPRT.3R	R: CTGCATTGTTTTGCCAGTGT	59.7		
human.FS.2F	F: ACTGCTCACTCACCCACCTC	60.3	the human follistatin gene	260 bp
human.FS.2R	R: CTGCAAGTTGGGAAGAAGGA	60.3		
mouse.FS.2F	F: TGTGCCTCTTTCCAACTCCT	59.8	the mouse follistatin gene	305 bp
mouse.FS.2R	R: ATCTATCGCCCTTGGGTCTT	59.9		

PCR conditions for both reactions 1 and 2 were set up as follows:

Initial denaturation	94°C	5 min	
Amplification: denaturation	94°C	30 sec	30 cycles
annealing	58°C	30 sec	
extension	72°C	30 sec	
Final extension	72°C	1 min	
Holding temperature	15°C	Hold	

5.2.4 Establishment and gross examination of independent transgenic lines

To maintain the transgenic lines and to further use the transgenic lines to cross with the follistatin knockout heterozygotes, the mating of founders with wild type mice was set up. Weights at birth and weaning times were recorded for 3 litters of each line. Gross examination was performed including appearance, movement and feeding. Fertility was also checked, based on whether there were offspring from the mating of transgenic mice with wild-type mice.

5.2.5 Two step cross-breeding program to obtain "rescued mice"

The transgenic mice carrying the human follistatin transgenes were crossed with the follistatin knockout heterozygotes via two steps of cross-breeding (refer to Section 2.2.12), to generate "**rescued**" mice since the follistatin null mutants die soon after birth: rescued mice represent the mice that expressed the human follistatin transgenes, in the absence of the endogenous mouse gene.

5.2.6 General characterization of day 0 pups from the second step of cross-breeding

Newborn pups were generally characterized by their appearance, weight, crown-rump length (CRL), breathing ability and survival rates. CRL was a length measured from the top of the head to the base of the tail.

5.2.7 Dissection of day 0 mouse pups

The surgical techniques for dissection of day 0 mouse pups were described in Section 2.2.11.5.

5.2.8 Histological analysis

The methodology for histological analysis can be referred to in Section 2.2.9.

5.2.9 Quantification of human follistatin mRNA expression in rescued mice

Preparation of total RNA and mRNA from tissues is described in Sections 2.2.3.1 and 2.2.3.2.

In order to determine the mRNA expression levels of the human follistatin transgenes and the mouse follistatin endogenous gene in day 0 pups, reverse transcription (refer to in Section 2.2.4) was performed using Superscript II (Invitrogen) using mRNA from different organs (heart, lung, liver, kidney, muscle and skin).

Quantitative PCR for cDNA was then carried out with a real-time fluorimetric capillary based thermocycler (LightCycler™, Roche Diagnostic Co, Mannheim, Germany). The principle of quantification is described in Section 2.2.7. The three pairs of PCR primers are described in Table 5.3, among which human.screen.2F & R was specific for human follistatin cDNA, mouse.screen.2F & R was specific for mouse follistatin cDNA, and b-actin.F & R was specific for mouse housekeeping gene β actin cDNA. They were designed to the human follistatin mRNA sequence (GENBANK: NM_013409), the mouse follistatin mRNA sequence (GENBANK: NM_008046) and the mouse β actin mRNA sequence (Ensembl Gene Report: ENSMUST00000031564), respectively. The real-time PCR conditions for these three pairs of primers were described in Table 5.4.

5.2.10 Statistics

SPSS® 11.0 (SPSS Inc., Chicago, USA) was the statistical software used to undertake the statistical analyses. Comparisons between multiple numeric data sets were

Table 5.3 Primers of the real-time PCR assays for human and mouse follistatin cDNA, and mouse β actin cDNA

Primer	Sequence (5'→3')	Tm (°C)	Targeting site	Product size
Human.screen.2F	F: TGTGGTGGACCAGACCAATA	59.8	Human follistatin cDNA	101 bp
Human.screen.2R	R: TGACTCCATCATTCCCACAG	59.5		
Mouse.screen.2F	F: CCAGACTGTTCCAACATCACC	60.4	Mouse follistatin cDNA	112 bp
Mouse.screen.2R	R: CTAGTTCCGGCTGCTCTTTG	60.2		
b-actin F	F: GCTACAGCTTCACCACCACA	59.9	Mouse β actin cDNA	208 bp
b-actin.R	R: AAGGAAGGCTGGAAAAGAGC	60.0		

Table 5.4 Conditions of the real-time PCR using the LightCycler™ for the primers "human.screen.2", "mouse.screen.2" and "b-actin"

	PCR primers:		
	human.screen.2	mouse.screen.2	b-actin
Reaction volume	20 µl	20 µl	20 µl
PCR Master Mix:			
Primers	0.5 µM	0.5 µM	0.5 µM
$MgCl_2$	4 mM	4 mM	4 mM
SYBR green I	2 µl	2 µl	2 µl
PCR protocol:			
heating/cooling rate	20°C/sec	20°C/sec	20°C/sec
1. pre-incubation:	95°C/10 min	95°C/10 min	95°C/10 min
number of cycles	1	1	1
2. amplification:			
denaturation	95°C/10 sec	95°C/10 sec	95°C/10 sec
anealing	59°C/3 sec	63°C/2 sec	58°C/3 sec
extension	72°C/5 sec	72°C/5 sec	72°C/9 sec
acquisition mode	single	single	single
number of cycles	45	45	45
3. melting:			
melting temperature	65°C/15 sec	65°C/15 sec	65°C/15 sec
acquisition mode	continuous	continuous	continuous
melting	95°C with 0.1°C/sec	95°C with 0.1°C/sec	95°C with 0.1°C/sec
4. cooling	40°C/30 sec	40°C/30 sec	40°C/30 sec

performed using one-way ANOVA followed by Tukey's HSD post-hoc test. Mann-Whitney test was used for two independent nonparametric samples. Differences between groups were deemed significant where $p < 0.05$.

5.2.11 Experimental design

The vectors pNEB-FS and PAC-FS that harbor the 25 kb and 95 kb genomic sequences, respectively, were injected into the male pronuclei of mouse zygotes to generate transgenic mice. Subsequently, independent transgenic lines were established that were further crossed onto the mouse follistatin knockout background via the two-step cross-breeding with follistatin knockout heterozygotes. Consequently, from the second step of cross-breeding the rescued mice, knockout mice and wild-type mice can be obtained and phenotyped. The analyses included: functional analysis to see if the rescued mice were able to survive; morphological analysis including gross anatomical and histological examinations; quantification of follistatin mRNA expression in the rescued mice.

To simplify the following description, various labelings were used to designate the different mouse lines:

- wt: wild-type mice
- fs-ko: follistatin knockout mice
- FS^{25}-wt: mice carrying 25 kb human follistatin transgene in the mouse wild-type background.
- FS^{95}-wt: mice carrying 95 kb human follistatin transgene in the mouse wild-type background.
- FS^{25}-ko: mice carrying 25 kb human follistatin transgene in the mouse follistatin knockout background.
- FS^{95}-ko: mice carrying 95 kb human follistatin transgene in the mouse follistatin knockout background.

5.3 Results

5.3.1 Pronuclear microinjection data

For the pNEB-FS vector that was linearized and contained a 25 kb genomic sequence of the human follistatin locus, 323 fertilized oocytes with two pronuclei were collected for microinjection. Following microinjection, 208 embryos that looked morphologically normal at the one-cell stage were transferred into the oviducts of the foster mice, resulting in the birth of 36 pups (Table 5.5).

Likewise, for the PAC-FS vector that was circular (Camper and Saunders, 2000) and contained a 95 kb genomic sequence of the human follistatin locus, 1353 zygotes with two pronuclei were collected for microinjection. Subsequently, 810 embryos at the one-cell stage that looked morphologically normal were transferred into the oviducts of the foster mice, resulting in the birth of 89 pups (Table 5.5).

5.3.2 Transgenic founders and gross examination of transgenic lines

Three transgenic founders (1 female, 2 males), designated as **FS^{25}-wt.1**, **FS^{25}-wt.2** and **FS^{25}-wt.3**, were obtained from pronuclear microinjection of the pNEB-FS vector; for the PAC-FS vector, two transgenic founders were obtained (2 females), designated as **FS^{95}-wt.1** and **FS^{95}-wt.2** (Figure 5.1).

Independent transgenic lines were generated by crossing founders with wild-type FVB mice. Offspring from each line and wild-type showed no difference in appearance (normal whiskers, fur, tails, eyes *etc.*) and normal daily activities. They were all also fertile. Weights at birth and at weaning times were not statistically different between each line and wild-type, based on the data of 3 litters from each line (Table 5.6). Thus, transgenic mice of the lines FS^{95}-wt.1, FS^{95}-wt.2, FS^{25}-wt.1, FS^{25}-wt.2 and FS^{25}-wt.3 were grossly normal.

The lines FS^{95}-wt.1, FS^{95}-wt.2, FS^{25}-wt.1 and FS^{25}-wt.2 were further analyzed for the mRNA expression of transgenes. PCR targeting human follistatin cDNA and mouse

Table 5.5 Pronuclear microinjection data for pNEB-FS and PAC-FS vectors

	No. of zygotes with two pronuclei	No. of 1-cell embryos transferred	No. of fosters used	Pups born
pNEB-FS	323	208	13	36
PAC-FS	1353	810	37	89

Figure 5.1 Genotyping evidence for detecting transgenic founders

This figure shows the genotyping evidence used to detect transgenic founders. (-) indicates the negative control. (+) indicates the positive control. Four pairs of PCR primers, 10kb-UP-AF & R, 5kb-UP-AF & R, Southern.F & R and 1.5 kb-DOWN-AF & R, are characterized in Table 5.1. (a) ~ (d) are the gel pictures for screening the transgenic founders carrying the pNEB-FS vector. (e) ~ (h) are the gel pictures for screeing the transgenic founders carrying the PAC-FS vector. (a) & (e) used the primer pair of 10kb-UP-AF & R; (b) & (f) used the primer pair of 5kb-UP-AF & R; (c) & (g) used the primer pair of Southern.F & R; (d) & (h) used the primer pair of 1.5 kb-DOWN-AF & R. Thus, there are three founders from the pNEB-FS vector and two founders from the PAC-FS vector.

Figure 5.1

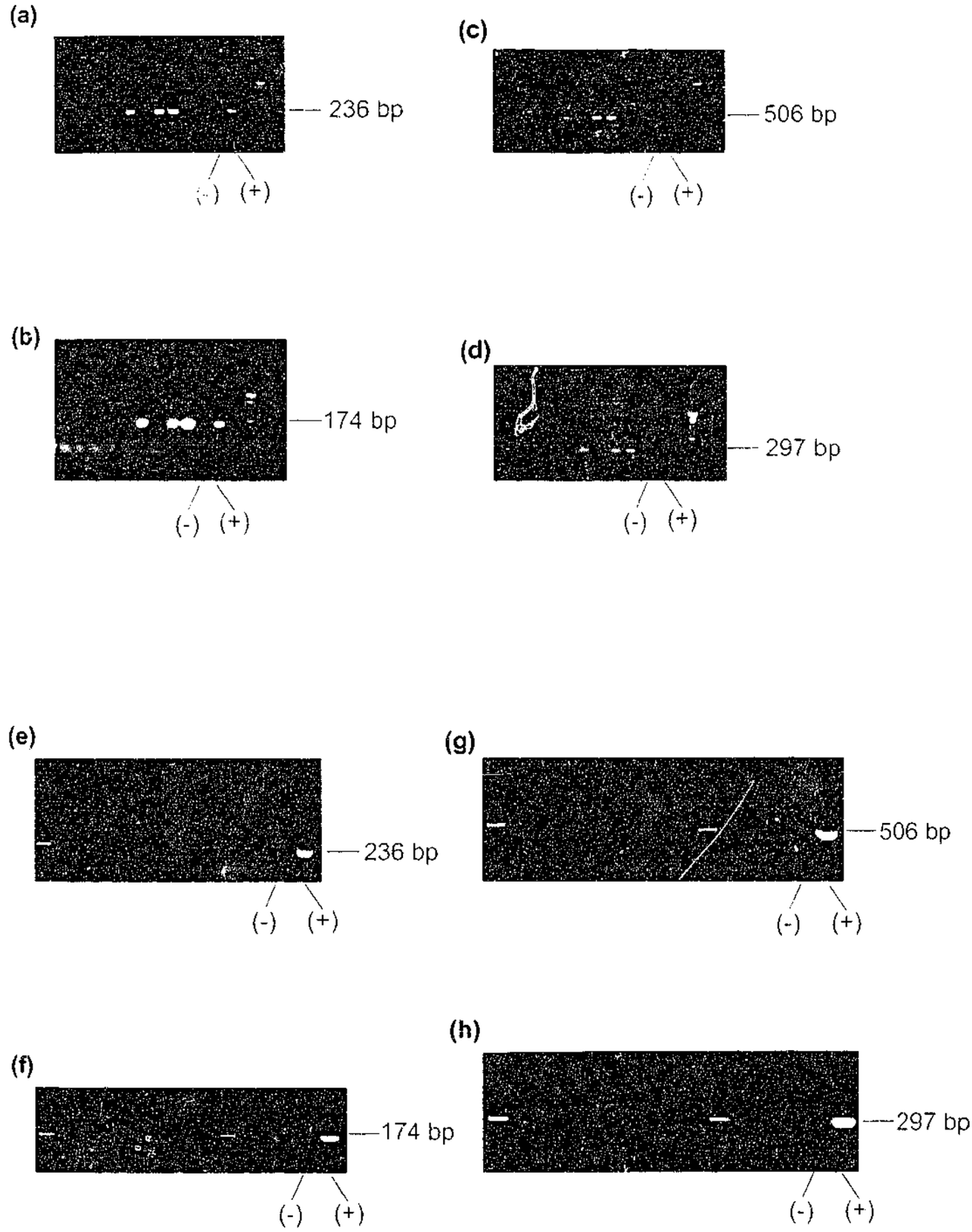

Table 5.6 Weights at birth and at weaning time of transgenic mice and their wild-type littermates

	Number	Mean ± standard deviation (at birth) (gm)	Mean ± standard deviation (at weaning) (gm)
FS^{25}-wt.1	11	1.30 ± 0.09	9.33 ± 0.34
FS^{25}-wt.2	11	1.31 ± 0.04	9.31 ± 0.31
FS^{25}-wt.3	10	1.33 ± 0.06	9.38 ± 0.33
FS^{95}-wt.1	10	1.32 ± 0.08	9.33 ± 0.34
FS^{95}-wt.2	9	1.30 ± 0.10	9.42 ± 0.30
Wild-type	39	1.31 ± 0.08	9.40 ± 0.35

follistatin cDNA was performed separately in the LightCycler™. The data was then managed by the software of the LightCycler™. Subsequently, the ratios of expression levels of follistatin transgenes to the endogenous gene were obtained through the division of the transgene expression levels by endogenous gene expression levels (Table 5.7). The ratios in ovary, testis, muscle, kidney, liver and brain were approximately in the range of 0.05 to 0.0001 (Table 5.7).

5.3.3 Survival rates of mice at weaning ages from the second step of cross-breeding

Two independent transgenic lines arising from each construct were chosen to be further bred into the mouse follistatin knockout background, depending on their availability at that time. As such, only the lines FS^{95}-wt.1, FS^{95}-wt.2, FS^{25}-wt.1 and FS^{25}-wt.2 were used for the two-step cross-breeding.

The **rescued mice** were designated **FS^{25}-ko.1** and **FS^{25}-ko.2** that stemmed from the lines FS^{25}-wt.1 and FS^{25}-wt.2, respectively, as well as **FS^{95}-ko.1** and **FS^{95}-ko.2** that originated from the lines FS^{95}-wt.1 and FS^{95}-wt.2, respectively.

Initially, I attempted to cross the transgenic lines FS^{95}-wt.1, FS^{25}-wt.1 and FS^{25}-wt.2 onto the mouse follistatin knockout background using "normal mating". Normal mating means that the mating was set up by putting males and females together until the females delivered pups, and vaginal plugs after mating were not routinely checked. From the second step of cross-breeding, at weaning time (3~4 weeks old) 252 pups were collected and genotyped for the line FS^{95}-wt.1, 219 pups for the line FS^{25}-wt.1 and 231 pups for the line FS^{25}-wt.2. Unfortunately, no rescued mice were found in contrast to our original prediction. The details of the genetic background of these mice are described in Table 5.8.

5.3.4 General characterizations of day 0 pups from the second step of cross-breeding

Because of the results described in the previous section, normal mating was shifted to "plug mating" for the second step of cross-breeding. Plug mating means that the mating

Table 5.7 The ratios of mRNA expression levels of human follistatin transgenes to mouse endogenous gene (human follistatin mRNA / mouse follistatin mRNA) in different tissues of independent transgenic lines

	ovary	testis	muscle	kidney	liver	brain
FS^{95}-wt.1	8.9E-05	3.8E-02	1.8E+00	6.2E-03	1.4E 02	8.3E-02
FS^{95}-wt.2	5.5E-04	1.7E-02	1.3E-01	2.2E-01	1.7E-02	4.0E-02
FS^{25}-wt.1	6.9E-04	3.4E-02	8.5E-02	2.7E-02	4.8E-02	2.1E-02
FS^{25}-wt.2	9.3E-05	4.4E-02	5.2E-01	6.5E-03	8.0E-02	1.1E-02

(The data was presented as computer scientific notation. For example, "4.0E-0.2" means "4.0×10^{-2}". For each line, the data of testis, muscle, kidney, liver and brain was from the same male mouse of each line, whereas the datum of ovary was from another female mouse of each line.)

Table 5.8 The genetic backgrounds of mice from the second step of crossing the lines FS^{95}-wt.1, FS^{25}-wt.1 and FS^{25}-wt.2 onto the mouse follistatin knockout background.

Transgenic line	tg+, fs-/- (rescued mice)	tg+, fs+/-	tg+, fs+/+	tg-, fs-/- (fs-ko mice)	tg-, fs+/-	tg-, fs+/+ (wt mice)	Total
FS^{95}-wt.1	0	81	46	0	87	38	252
FS^{25}-wt.1	0	75	37	0	70	37	219
FS^{25}-wt.2	0	80	35	0	77	39	231

(tg+ means transgene positive; tg- means transgene negative; fs-/- means the deletion of both alleles of the mouse follistatin gene; fs+/- means the deletion of one allele of the mouse follistatin gene; fs+/+ means the intact mouse follistatin gene.)

was set up by putting males and females together and checking if there were vaginal plugs every day. Once vaginal plugs were found, the male and the female were then separated, and the due dates of delivery could be predicted (usually on day 18 ~ day 20 after mating). The pregnant females near the due dates were checked four times a day in order that rescued mice could be observed shortly after birth. The other transgenic line carrying 95 kb genomic transgene, FS^{95}-wt.2, was also used in these experiments. Thus, there were two independent lines for each genomic construct that were further crossed onto the mouse follistatin background.

Genotyping data:

An example of the gel pictures from genotypic assays are presented in Figure 5.2. Totally, 11 FS^{25}-ko.1, 10 FS^{25}-ko.2, 10 FS^{95}-ko.1, 9 FS^{95}-ko.2, 19 fs-ko and 19 wt were collected for further analysis. The pups with other genetic backgrounds were excluded from the analysis.

Appearance of pups:

In general, the rescued mice FS^{25}-ko.1, FS^{25}-ko.2, FS^{95}-ko.1 and FS^{95}-ko.2 looked similar to fs-ko, except that the rescued mice appeared to be able to move more actively and breathe better at the initial stage after birth (Figure 5.3a~c). However, the rescued mice may not have been fed properly since milk-color could not be observed in their stomach in contrast to the fs-ko mice. The rescued mice were able to move their extremities freely and change a supine position to a prone position easily, but were unable to crawl like wild-type mice, suggesting that they were physically weaker than their wild-type littermates.

Weights and crown-rump lengths (CRLs):

The details of the birth weights of the rescued mice FS^{25}-ko.1, FS^{25}-ko.2, FS^{95}-ko.1 and FS^{95}-ko.2, as well as wt and fs-ko are shown in Table IV.1 of Appendix IV. Comparing the weights of the different lines (Appendix IV, Table IV.2) revealed that wt was significantly heavier at birth than all the other lines. fs-ko was lighter than FS^{95}-ko.1 and

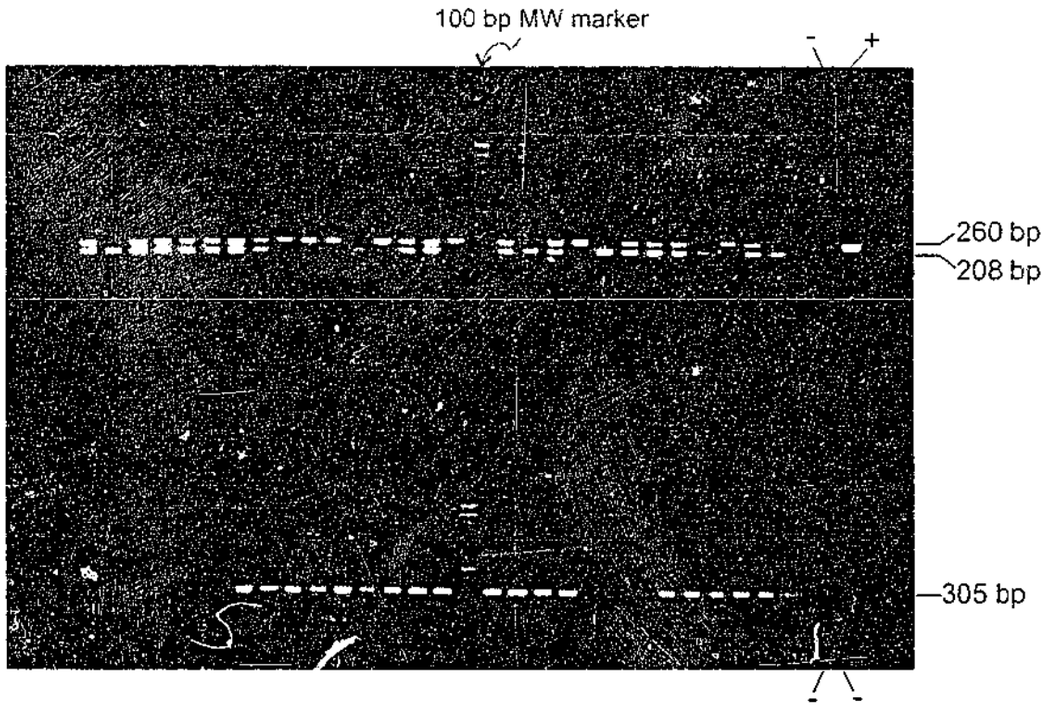

Figure 5.2 An example of genotyping pups from the second step of cross-breeding to identify "rescued mice".

The three pairs of PCR primers used here were "hHPRT.3F & R", "human.FS.2F & R" and "mouse.FS.2F". Their characteristics were described in Table 5.2. The size of PCR products for hHPRT.3F & R was 208 bp; for human.FS.2F & R, 260 bp; for mouse.FS.2F & R, 305 bp. The upper panel is the gel picture for PCR with double pairs of primers (human.FS.2F & R and hHPRT.3F & R); the lower panel is for PCR with single pair of primers (mouse.FS.2F & R). The lanes 1~29 were for the experimental samples, the lane 30 was for water, and the lane 31 was for the PAC-FS vector. Therefore, the wild-type mice should have 260 bp (-), 208 bp (-) and 305 bp (+). The follistatin knockout mice should have 260 bp (-), 208 bp (+) and 305 bp (-). The rescued mice should have 260 bp (+), 208 bp (+) and 305 bp (-). As such, the lanes 2 and 21 ( ) represented the follistatin knockout mice; the lanes 1, 3, 4, 5, 6, 7, 22 and 23 (*) represented the rescued mice.

Figure 5.3 The comparisons of appearances of fs-ko, wt, FS^{25}-ko.1, FS^{25}-ko.2, FS^{95}-ko.1 and FS^{95}-ko.2

All pictures shown here were day 0 pups. (a) These four pups were the rescued mice. From left to right were FS^{25}-ko.1, FS^{25}-ko.2, FS^{95}-ko.1 and FS^{95}-ko.2. All actively moved and breathed well, and their skin was pink. (b) The left one was fs-ko that was dying. The right one was FS^{95}-ko.1 that was active and breathing well. (c) This picture shows the size comparison. The left two were FS^{25}-ko.1 and the right one was wt. (d) ~ (i) show the whisker characteristics. (d): fs-ko. (e): wt. (f): FS^{25}-ko.1. (g): FS^{25}-ko.2. (h): FS^{95}-ko.1. (i): FS^{95}-ko.2. Only wt showed straight whiskers, all the others had disoriented whiskers.

Figure 5.3

(a)

(b)

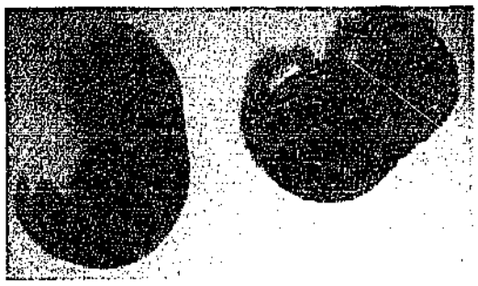

(c)

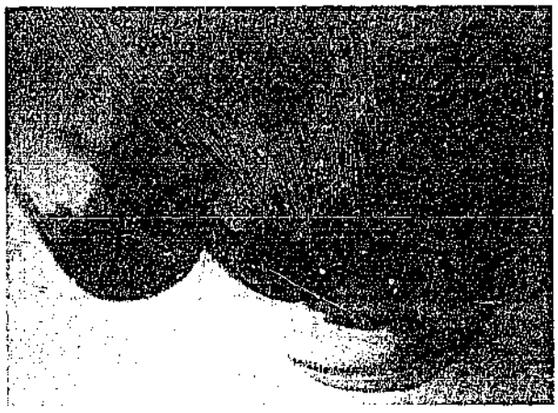

(d)

(f)

(h)

(e)

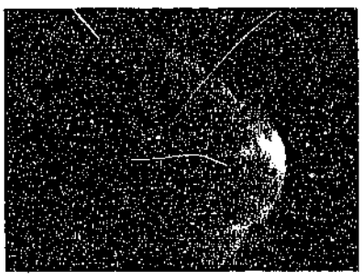

(g)

(i)

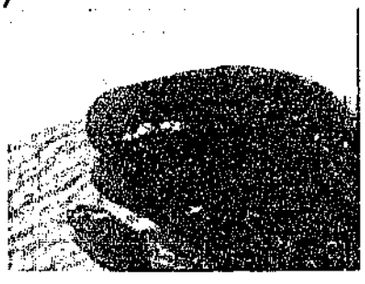

wt mice ($p < 0.05$) at birth. Further, comparisons between the four rescued lines did not show significant differences in their weights (Figure 5.4).

The CRL data of these mice at birth is described in Table IV.3 of Appendix IV. The CRLs of wt were significantly longer than that of all other lines ($p < 0.05$). When compared to the four lines of rescued mice, CRL of fs-ko was shorter than that of the two FS^{95}-ko lines ($p < 0.05$) but not different from that of two FS^{25}-ko lines. In addition, there was no consistent difference in the CRLs between FS^{25}-ko and FS^{95}-ko lines although FS^{95}-ko.1 had a significantly longer CRL than FS^{25}-ko.2 ($p < 0.05$) (Figure 5.5, details see Table IV.4 of Appendix IV).

Survival rates and breathing activities:

Although there was no obvious difference in appearance between the four lines of the rescued mice and fs-ko, there were distinctive survival rates and breathing activities for the rescued mice and fs-ko within one day after birth. In the first observation after birth, the survival rates for fs-ko, FS^{25}-ko.1, FS^{25}-ko.2, FS^{95}-ko.1, FS^{95}-ko.2 and wt were 57.9%, 100%, 90%, 100%, 100% and 100%, respectively. Further, the second observation after birth, the survival rates for fs-ko, FS^{25}-ko.1, FS^{25}-ko.2, FS^{95}-ko.1, FS^{95}-ko.2 and wt were 10.5%, 90.9%, 80%, 90%, 88.9% and 100%, respectively (Table 5.9). Both sets of data for fs-ko were significantly lower compared to either the four lines of the rescued mice or wt. However, on the second day after birth, neither the rescued mice nor fs-ko survived.

In order to grade the breathing activities at birth, the breathing ability was designated "bad" if the mice displayed very slow respiratory rates with purple skin color; it was recorded as "fair" if the mice displayed respiratory distress without movement, but still had a pink skin color; it was considered as "good" if the mice breathed easily and energetically with pink skin color. Based on this grading system, 15.8% of fs-ko revealed good breathing, 36.8% of them were fair and 47.4% of them were bad at birth. In contrast, most of the rescued mice and wt displayed good breathing activities at birth (Table 5.10).

Figure 5.4

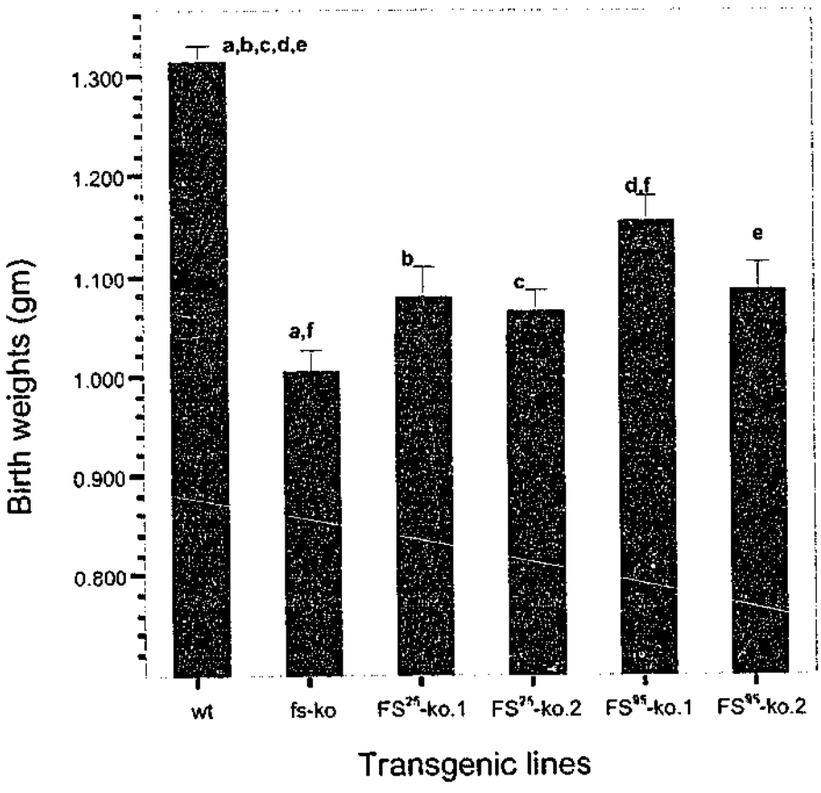

Figure 5.4 The birth weights of the lines wt, fs-ko and the rescued mice

At birth, the wt mice were heavier than all mice of the other lines. The fs-ko mice were lighter than FS^{95}-ko.1 and wt mice. All four lines of rescued mice were not significantly different in their birth weights. (a, b, c, d, e, and f mean $p < 0.05$ between groups).

Figure 5.5

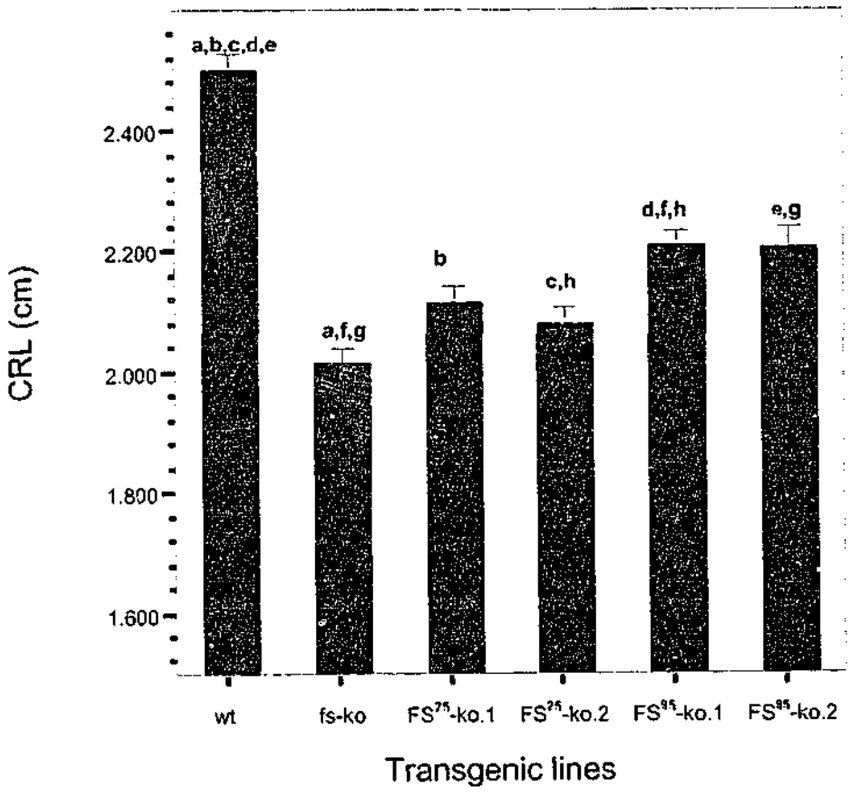

Figure 5.5 The crown-rump lengths (CRL) of the lines wt, fs-ko and the rescued mice at birth

At birth, the CRL of wt mice were longer than those of other lines. The CRL of fs-ko mice were shorter than those of FS^{95}-ko.1 and FS^{95}-ko.2 mice. In addition, the CRL of FS^{95}-ko.1 were longer than those of FS^{25}-ko.2. (a, b, c, d, e, f, g and h mean $p < 0.05$ between groups).

Table 5.9 The survival rates of the rescued mice, knockout mice and wild-type mice

			Transgenic line					
			fs-ko	FS-25.1	FS-25.2	FS-95.1	FS-95.2	wt
*First observation after birth	alive	Count	11	11	9	10	9	19
		% within the group	57.9%	100.0%	90.0%	100.0%	100.0%	100.0%
	dead	Count	8		1			
		% within the group	42.1%		10.0%			
*Second observation after birth	alive	Count	2	10	8	9	8	19
		% within the group	10.5%	90.9%	80.0%	90.0%	88.9%	100.0%
	dead	Count	17	1	2	1	1	
		% within the group	89.5%	9.1%	20.0%	10.0%	11.1%	
Total		Count	19	11	10	10	9	19
		% within the group	100.0%	100.0%	100.0%	100.0%	100.0%	100.0%

(* The observations were based on a frequency of four times a day from day 18 postcoitus. The events of intercourse were recognized by vaginal plugs.)

Table 5.10 The breathing activities of the rescued mice, knockout mice and wild-type mice at birth

		Transgenic line					
		fs-ko	FS^{25}-ko.1	FS^{25}-ko.2	FS^{95}-ko.1	FS^{95}-ko.2	wt
good	Count	3	11	8	9	9	19
	% within the group	15.8%	100.0%	80.0%	90.0%	100.0%	100.0%
fair	Count	7		1	1		
	% within the group	36.8%		10.0%	10.0%		
bad	Count	9		1			
	% within the group	47.4%		10.0%			
Total	Count	19	11	10	10	9	19
	% within the group	100.0%	100.0%	100.0%	100.0%	100.0%	100.0%

(The breathing ability was designated "bad" if the mice displayed very slow respiratory rates with purple skin color; it was recorded as "fair" if the mice displayed respiratory distress without movement, but still had a pink skin color; it was considered as "good" if the mice breathed easily and energetically with pink skin color.)

Skin and whisker characteristics:

The skin of all four lines of the rescued mice looked taut and shiny, similar to that of fs-ko. The skin of some of the rescued mice appeared looser and less shiny when compared to fs-ko. There appeared to be no difference in whiskers between the rescued mice and fs-ko, which assumed a disoriented pattern (Figure 5.3d~i).

Characteristics of external genitalia:

In normal wt mice at birth, there is an obvious protrusion, called the genital tubercle, on the external genitalia. In contrast, the area where the external genitalia should form was completely flat in fs-ko. Most of the pups from all four lines of the rescued mice had a similar phenotype although some of them displayed a slight swelling in the external genital area. (Figure 5.6a~f). Obstruction of the lower urinary system was ruled out, since drops of urine could be pushed out with gentle pressure on the urinary bladders of the pups.

Gross anatomy of urogenital organs:

Since the genital tubercles of fs-ko and the rescued mice were aplastic or under-developed, the question raised was whether the urogenital organs also had developmental defects. However, under a dissecting microscope, there were no gross abnormalities of the urogenital organs (Figure 5.6g~i).

5.3.5 Histological analysis of day 0 pups from the second step of cross-breeding

In preparation for histological analysis of the rescued mice, fs-ko and wt, various organs were weighed after Bouin's fixation. In total, twelve fs-ko, five FS^{25}-ko.1, six FS^{25}-ko.2, five FS^{95}-ko.1, three FS^{95}-ko.2 and six wt were weighed for their organs. The details are described in Table IV.5 (Appendix IV). Furthermore, multiple comparisons of the organ weights between the different lines were performed and are described in Table IV.6 (Appendix IV).

Figure 5.6 The external genitalia and gross anatomy of urogenital system of fs-ko, wt, FS^{25}-ko.1, FS^{25}-ko.2, FS^{95}-ko.1 and FS^{95}-ko.2

All pictures shown here are from day 0 pups. (a) ~ (f) The pictures focus on the external genitalia. (a): fs-ko. (b): wt. (c): FS^{25}-ko.1. (d): FS^{25}-ko.2. (e): FS^{95}-ko.1. (f): FS^{95}-ko.2. Apparently, the external genitalia of fs-ko, FS^{25}-ko.1, FS^{25}-ko.2, FS^{95}-ko.1 and FS^{95}-ko.2 were aplastic or under-developed. (g) ~ (i) The pictures show the gross anatomy of urogenital organs from dissecting the post-Bouin's fixation sample of a male FS^{95}-ko.1. Although the pictures from other mouse lines are not shown here, they have been examined and considered to show no differences between them. K: kidney. U: ureter. B: urinary bladder. T: testis. V: vas deferens. S: seminal vesicle. P: prostate. There was no gross abnormality.

Figure 5.6

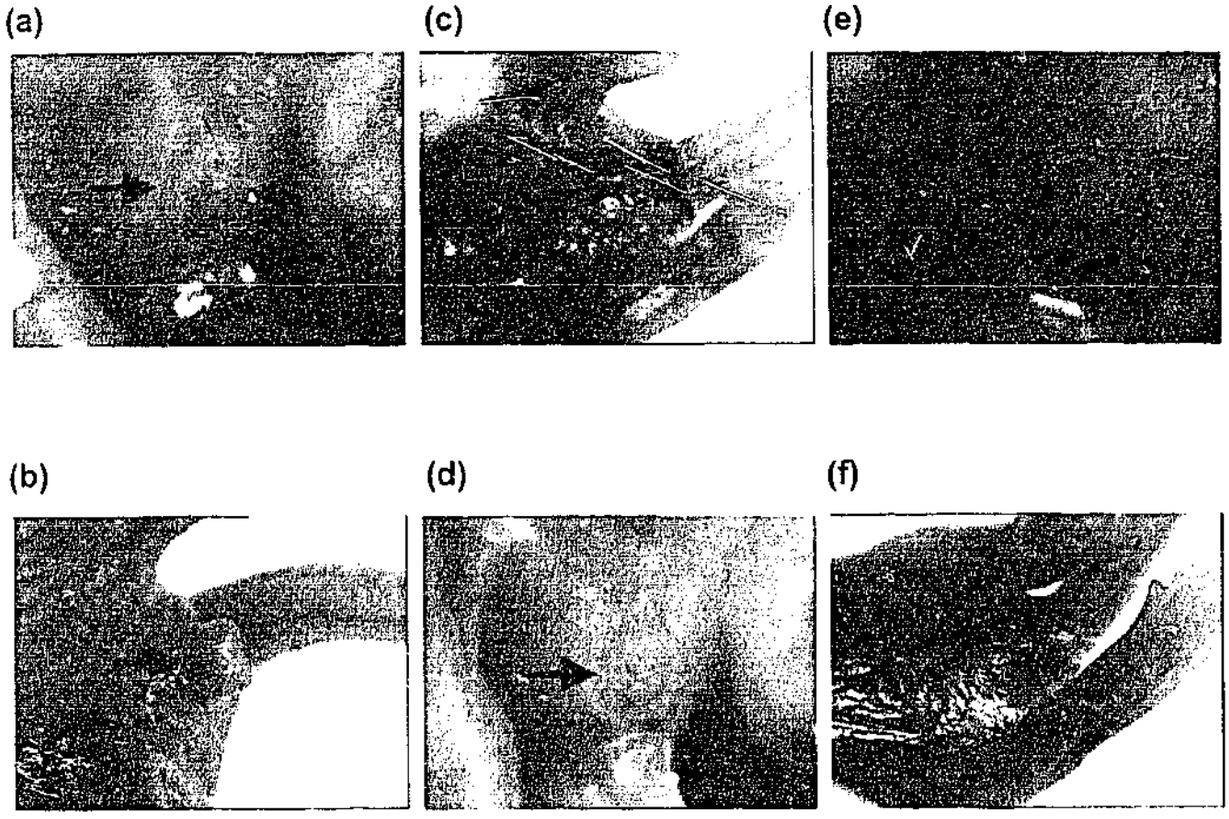

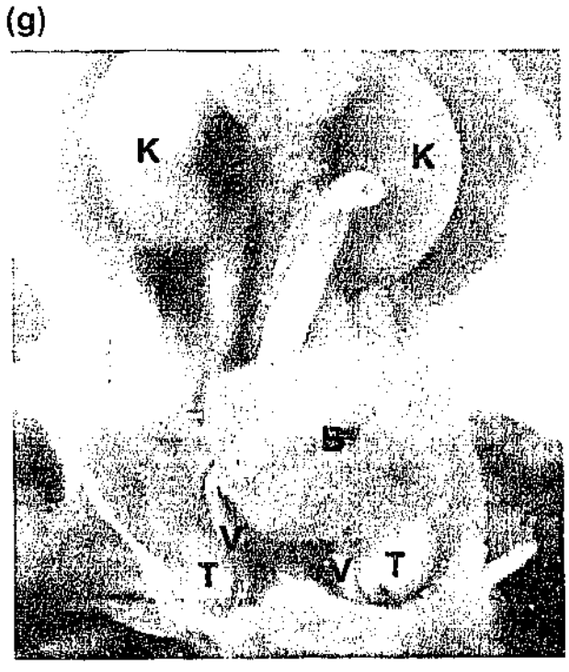

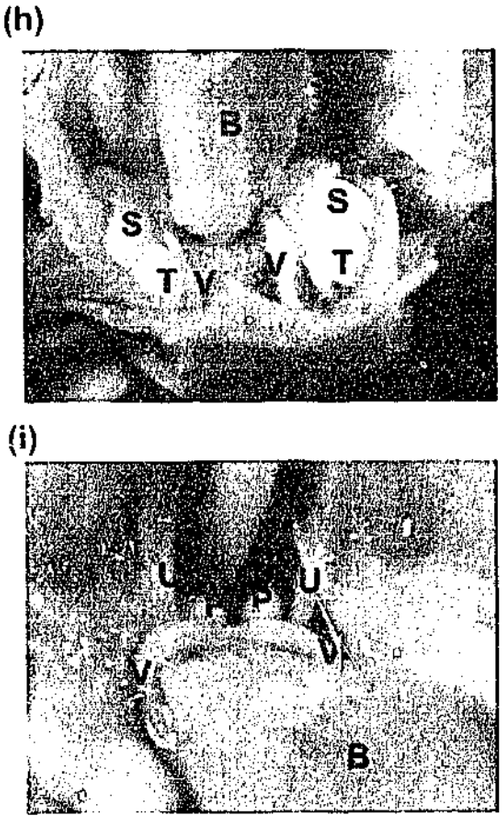

Various organs have been histologically analyzed to determine if there were differences between fs-ko, wt, FS^{25}-ko.1, FS^{25}-ko.2, FS^{95}-ko.1 and FS^{95}-ko.2. At least 3 pups from each line were examined. In general, there was no difference between FS^{25}-ko.1 and FS^{25}-ko.2. Likewise, FS^{95}-ko.1 and FS^{95}-ko.2 were not different. Furthermore, all the rescued mice with transgenes of different lengths appeared to be similar in almost all the slides that have been examined. It is was difficult to detect any difference in thyroid, thymus, spleen, kidney and skeletal muscle between the different lines. Qualitatively the size of the intercostal muscles appeared to be smaller in fs-ko compared to wt, while those of the rescued mice seemed to lie between both.

Liver:

Multiple comparisons of the weights of livers of fs-ko, wt, FS^{25}-ko.1, FS^{25}-ko.2, FS^{95}-ko.1 and FS^{95}-ko.2 revealed that at birth, the livers of fs-ko were significantly lighter than that of wt. Furthermore, the livers of wt were markedly heavier than that of fs-ko, FS^{25}-ko.1 and FS^{25}-ko.2. Although the weights of the livers of FS^{25}-ko.1 and FS^{25}-ko.2 were closer to that of fs-ko, and the weights of the livers of FS^{95}-ko.1 and FS^{95}-ko.2 were closer to that of wt, the weights of the livers of FS^{95}-ko.1 and FS^{95}-ko.2 did not show any statistical difference from those of the other lines due to the numbers of samples assessed (Figure 5.7).

However, the qualitative analysis of liver histology of each line failed to reveal any marked differences in the architecture and cytological features.

GI (gastrointestinal system):

The weights of GI, including stomach and bowels, of wt mice were significantly greater than those of fs-ko, FS^{25}-ko.1, FS^{25}-ko.2, FS^{95}-ko.1 and FS^{95}-ko.2. Moreover, there was no difference in weights of GI between the fs-ko, FS^{25}-ko.1, FS^{25}-ko.2, FS^{95}-ko.1 and FS^{95}-ko.2 lines (Figure 5.8).

Nevertheless, the qualitative analysis did not show any cytological difference between different lines.

Figure 5.7

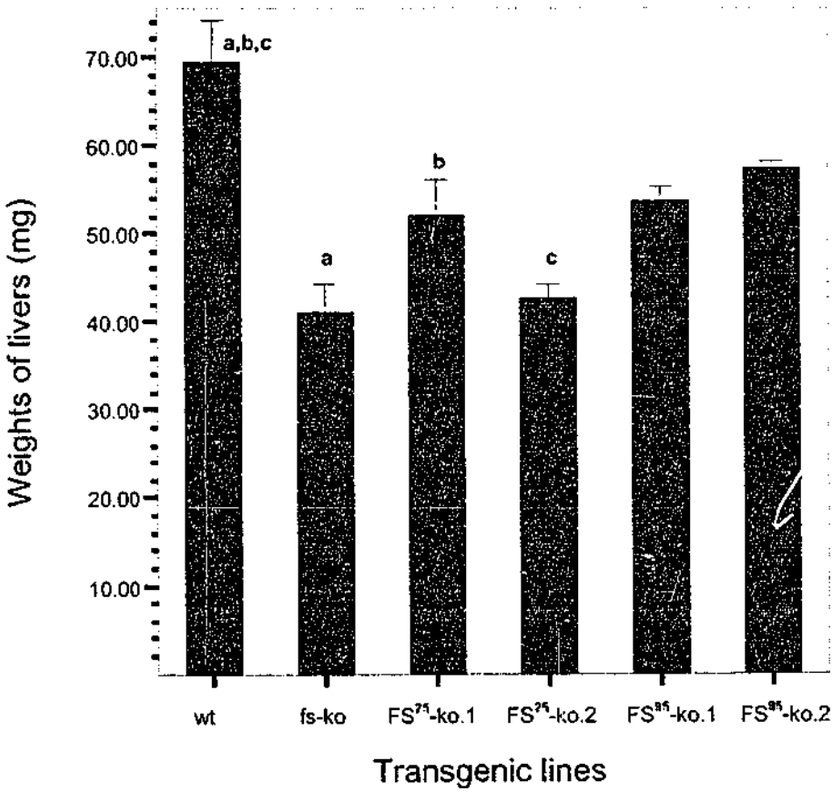

Figure 5.7 The weights of the livers of the lines wt, fs-ko and the rescued mice at birth

At birth, the livers of wt mice were heavier than those of fs-ko, FS^{25}-ko.1 and FS^{25}-ko.2. Four lines of the rescued mice did not significantly differ in the weights of livers. (a, b and c mean $p < 0.05$ between groups; error bars show standard error for mean, bars show means.).

Figure 5.8

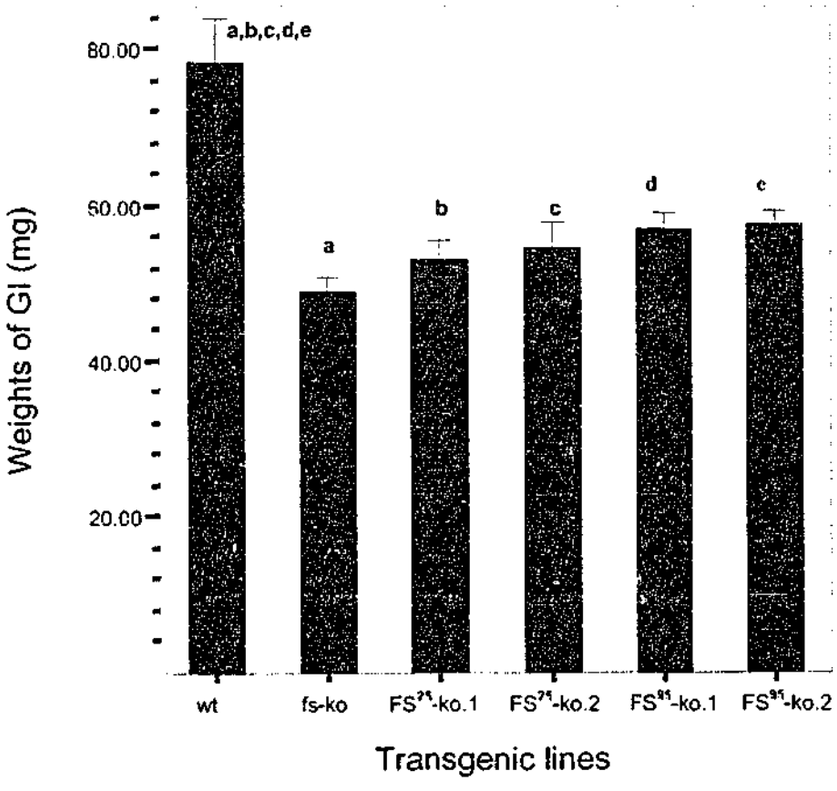

Figure 5.8 The weights of GI (stomach and bowels) of the lines wt, fs-ko and the rescued mice at birth

At birth, the GI of wt mice were heavier than those of fs-ko, FS^{25}-ko.1, FS^{25}-ko.2, FS^{95}-ko.1 and FS^{95}-ko.2. Four lines of the rescued mice and fs-ko did not significantly differ in the weights of GI. (a, b, c, d and e mean $p < 0.05$ between groups; error bars show standard error for mean, bars show means.).

Lung:

At birth, the lungs of fs-ko were significantly lighter than that of wt, FS^{95}-ko.1 and FS^{95}-ko.2, but not different from that of FS^{25}-ko.1 and FS^{25}-ko.2. Moreover, the lungs of wt were significantly heavier than fs-ko, FS^{25}-ko.1, FS^{25}-ko.2 and FS^{95}-ko.1, but not different from that of FS^{95}-ko.2 (Figure 5.9). There did not seem to be a consistent difference in the weights of the lungs of FS^{25}-ko and FS^{95}-ko lines, since the lungs of FS^{95}-ko.2 were heavier than that of FS^{25}-ko.2, but not different from that of FS^{25}-ko.1, and the lungs of FS^{95}-ko.1 were not different from that of both FS^{25}-ko.1 and FS^{25}-ko.2 in the weights.

The phenotypes of the lungs of the rescued mice were closer to that of wt than that of fs-ko, despite no differences between the rescued mice, except that the lungs of FS^{25}-ko.1 were more like that of fs-ko (Figure 5.10). The main differences between fs-ko and the rescued mice were the extent of the branching of bronchioles to form alveolar spaces and the thickness of the interalveolar septa between bronchioles. In the lung of fs-ko, the bronchioles appeared to branch less extensively and the interalveolar septa were also thicker compared to that of the rescued mice.

Heart:

Multiple comparisons of the weights of hearts of fs-ko, wt, FS^{25}-ko.1, FS^{25}-ko.2, FS^{95}-ko.1 and FS^{95}-ko.2 revealed that the hearts of wt were heavier than that of fs-ko. The weights of the hearts of the rescued mice were between that of fs-ko and wt, and were not significantly different from that of fs-ko or wt.

There appeared to be no qualitative differences in the structure of heart muscles between fs-ko, the rescued mice and wt. However, in the cardiac muscular layers of fs-ko, there appeared to be more degenerative or apoptotic muscle cells and less mitotic muscle cells compared to that of wt (Figure 5.11). Furthermore, the phenotypic features of the cardiac muscle cells of the rescued mice showed features in between the wt and fs-ko mice.

Figure 5.9

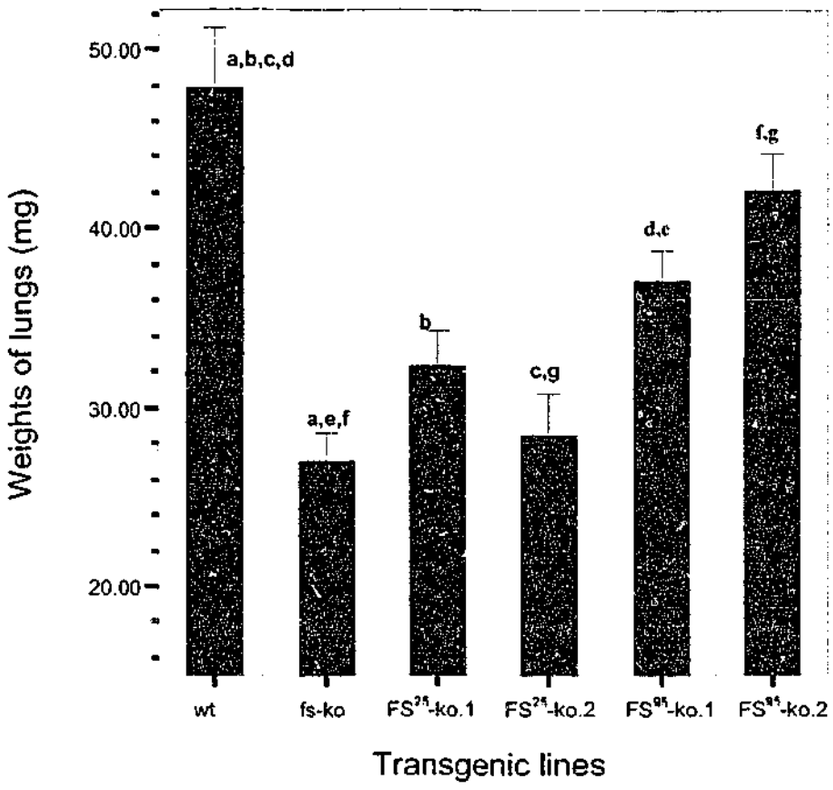

Figure 5.9 The weights of lungs of the lines wt, fs-ko and the rescued mice at birth

At birth, the lungs of wt mice were heavier than those of fs-ko, FS^{25}-ko.1, FS^{25}-ko.2 and FS^{95}-ko.1. The lungs of fs-ko were lighter than those of FS^{95}-ko.1 and FS^{95}-ko.2, but not different from those of FS^{25}-ko.1 and FS^{25}-ko.2. There was no consistent difference in the weights of lungs between four lines of the rescued mice since only the lungs of FS^{95}-ko.2 were significantly heavier than those of FS^{25}-ko.2. (a, b, c, d, e, f and g mean $p < 0.05$ between groups; error bars show standard error for mean, bars show means.).

Figure 5.10 'The phenotypes of the lung of fs-ko, wt, FS^{25}-ko.1, FS^{25}-ko.2, FS^{95}-ko.1 and FS^{95}-ko.2 at birth

The pictures show the lungs of fs-ko, wt and the four lines of the rescued mice. The slides were stained with hematoxylin and eosin (H&E). The pictures on the left were 4x magnified. The pictures on the right were 10x magnified. (a) & (b): wt. (c) & (d): fs-ko. (e) & (f): FS^{25}-ko.1. (g) & (h): FS^{25}-ko.2. (i) & (j): FS^{95}-ko.1. (k) (l): FS^{95}-ko.2. The striking difference between the wt and fs-ko is apparent both at low and high magnification. The "lacy" pattern (arrows) of the lung is poorly developed in the fs-ko due to the thickened interalveolar septa. A similar appearance is seen in FS^{25}-ko.1, but in the other lines, the structure of the lung more closely approaches that of the wt.

Figure 5.10

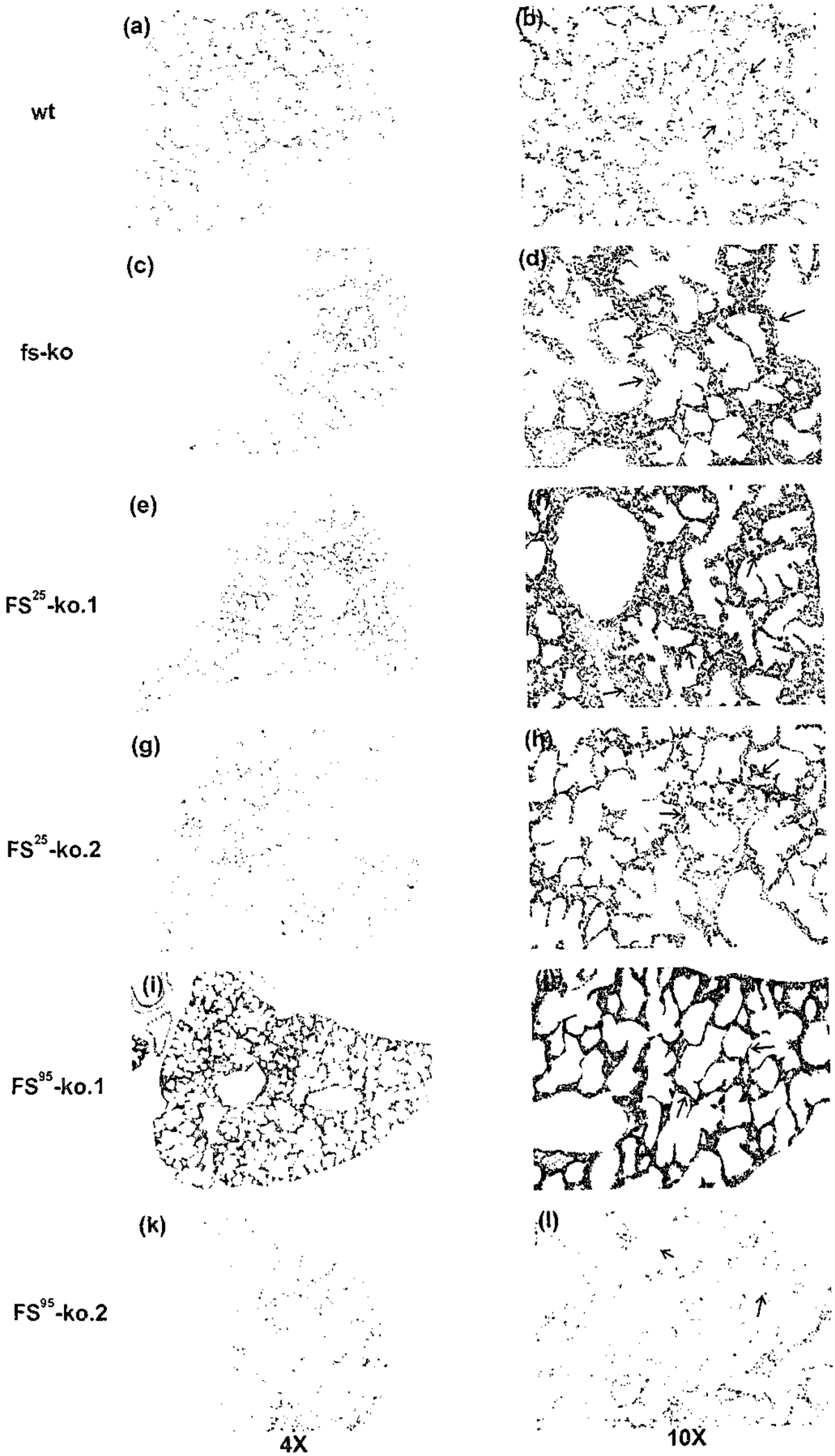
(a)
(b)
wt
(c)
(d)
fs-ko
(e)
(f)
FS25-ko.1
(g)
(h)
FS25-ko.2
(i)
(j)
FS95-ko.1
(k)
(l)
FS95-ko.2
4X
10X

Figure 5.11 The phenotypes of the testes and hearts of fs-ko, wt, FS^{25}-ko.1, FS^{25}-ko.2, FS^{95}-ko.1 and FS^{95}-ko.2 at birth

The pictures show the testes and hearts of fs-ko, wt and the four lines of the rescued mice. The slides were stained with hematoxylin and eosin (H&E) for hearts and periodic acid Schiff (PAS) for testes. The pictures on the left were 10x magnified and show the slides of testes. The pictures on the right were 40x magnified and show the slides of hearts. (a) & (b): wt. (c) & (d): fs-ko. (e) & (f): FS^{25}-ko.1. (g) & (h): FS^{25}-ko.2. (i) & (j): FS^{95}-ko.1. (k) (l): FS^{95}-ko.2. There did not appear to be any difference in testes between the lines. When the slides of hearts were examined under 40x magnification, it is obvious that in the cardiac muscle of wt, there were more mitotic cells and less degenerating cells, in contrast to the fs-ko, where there were more degenerating cells and very rare mitotic cells. In regard to this characteristic of cardiac muscle, the hearts of the rescued mice were more like those of wt than those of fs-ko ("M" means mitotic cells, "D" means degenerating cells).

Figure 5.11

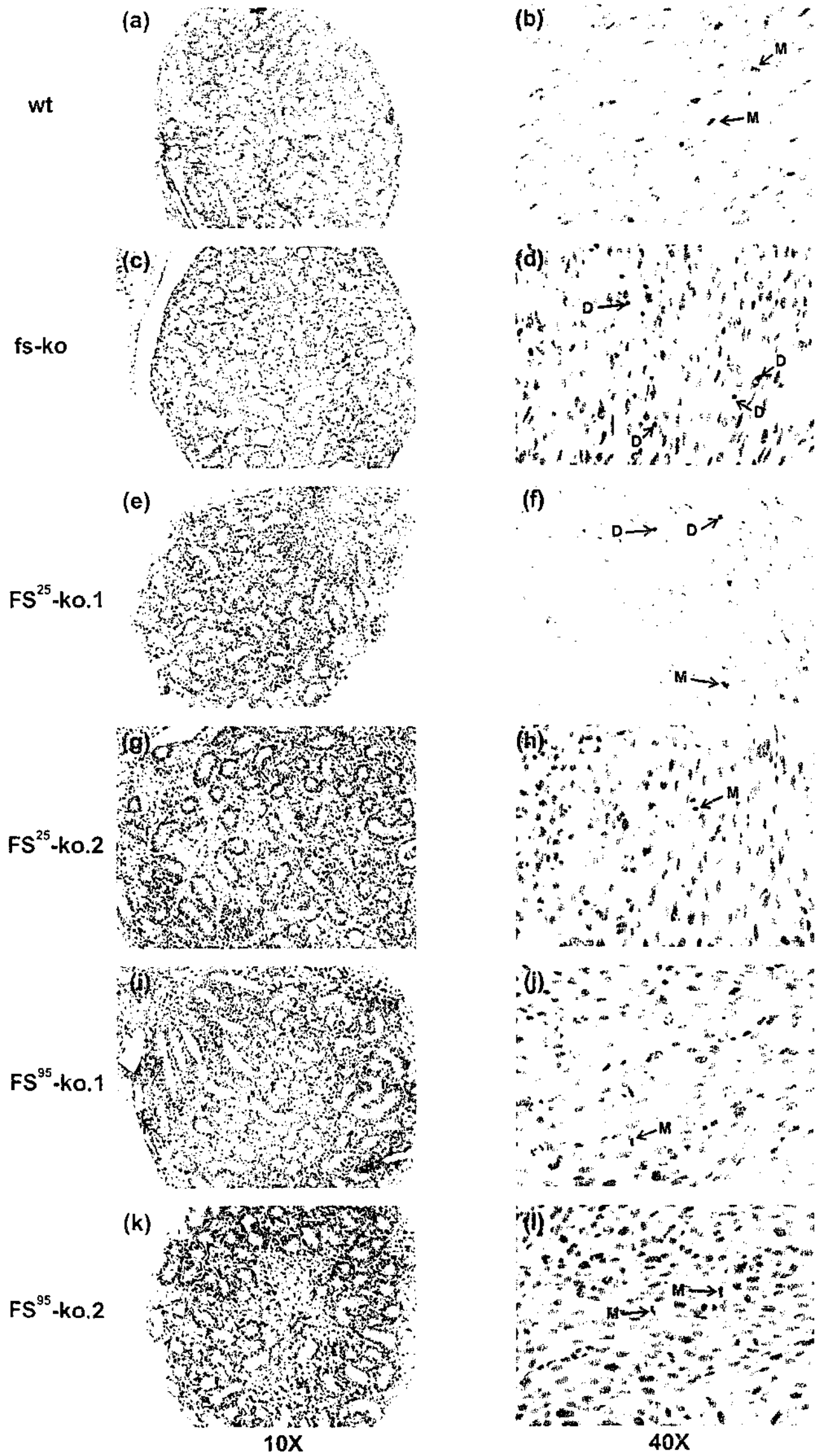
wt
fs-ko
FS25-ko.1
FS25-ko.2
FS95-ko.1
FS95-ko.2
(a)
(b)
(c)
(d)
(e)
(f)
(g)
(h)
(i)
(j)
(k)
(l)
M
D
10X
40X

Testis:

At birth, mouse testes were too small to obtain accurate measurements of weight.

The morphology of the testes in the fs-ko could not be distinguished from the wt. In addition, no differences were seen in the histology of the testes from the rescued mice (Figure 5.11).

Ovary:

As for testes, the weights of the mouse ovaries at birth were not measured.

In wt mice, the ovary is arranged into sex cords containing oocytes undergoing the leptotene, zygotene and pachytene (P) stages of meiosis. Some oocytes have progressed through to the diplotene (D) stages (Figure 5.12). In contrast, the oocyte numbers of fs-ko were remarkedly decreased compared to that of wt (Figure 5.12). In the ovaries of fs-ko, there were apparent patterns of sex cords, within most of which there were no oocytes. Some of the oocytes presented degenerative changes as shown by nuclear chromatin condensation and markedly eosinophilic cytoplasm. The small number of oocytes that were not degenerating were in leptotene to pachytene stages of the first meiosis. Only rare oocytes in the diplotene stage of the first meiosis can be seen. Taken together, the degeneration in the oocytes of fs-ko appeared to occur at the entry into the prophase of the first meiotic division. Qualitative analysis of the ovaries of FS^{25}-ko.1, FS^{25}-ko.2, FS^{95}-ko.1 and FS^{95}-ko.2 suggested appearances that were intermediate between the fs-ko and the wt (Figure 5.12). Quantitative studies will be required to confirm these observations.

Skin:

In the skin of fs-ko, most of the whole layer of the epidermis was thinner than that of wt (Figure 5.13). In addition, the epidermis of wt demonstrated a wavy contour, in contrast to that of the fs-ko which tended to be flatter, but quantitative studies would be required to confirm this observation. Moreover, the numbers of hair follicles in the skin of fs-ko seemed to be less than that of wt (Figure 5.13). For all these characteristics of skin

Figure 5.12 The phenotypes of the ovaries of fs-ko, wt, FS^{25}-ko.1, FS^{25}-ko.2, FS^{95}-ko.1 and FS^{95}-ko.2 at birth

These pictures show the ovaries of fs-ko, wt and the rescued mice on day 0 postpartum. The slides were stained with hematoxylin and eosin (H&E). The pictures were 40x magnified. (a) & (b): wt. (c) & (d): fs-ko. (e) & (f): FS^{25}-ko.1. (g) & (h): FS^{25}-ko.2. (i) & (j): FS^{95}-ko.1. (k) (l): FS^{95}-ko.2. Qualitative analysis indicates that the numbers of oocytes in the ovary of fs-ko were significantly decreased compared to the ovary of wt. In the wt the majority of oocytes were at the late pachytene (P) or diplotene (D) stage, whereas those oocytes present in the fs-ko were in the zygotene to pachytene stages. The remnants of degenerating oocytes can also be found in the ovary of fs-ko. There appeared to be more oocytes in the ovaries of the rescued mice than those of fs-ko; however, the oocyte numbers were still much lower in the ovaries of the rescued mice than those of wt. In addition, there seemed to be no difference in the oocyte numbers between the rescued mice (arrows indicate degenerating cells).

Figure 5.12

wt

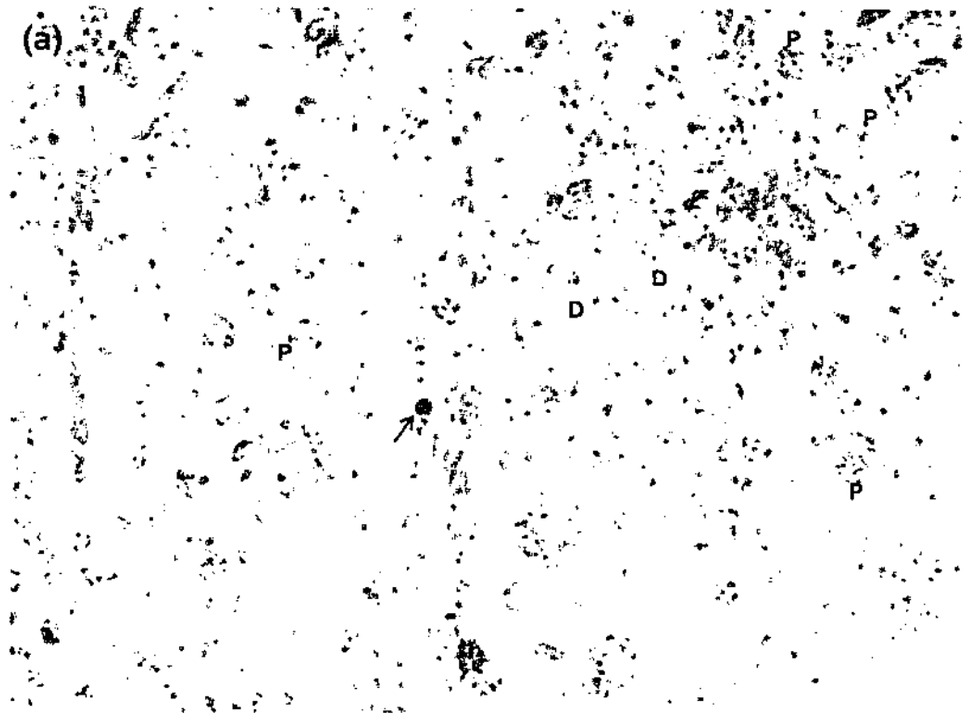

fs-ko

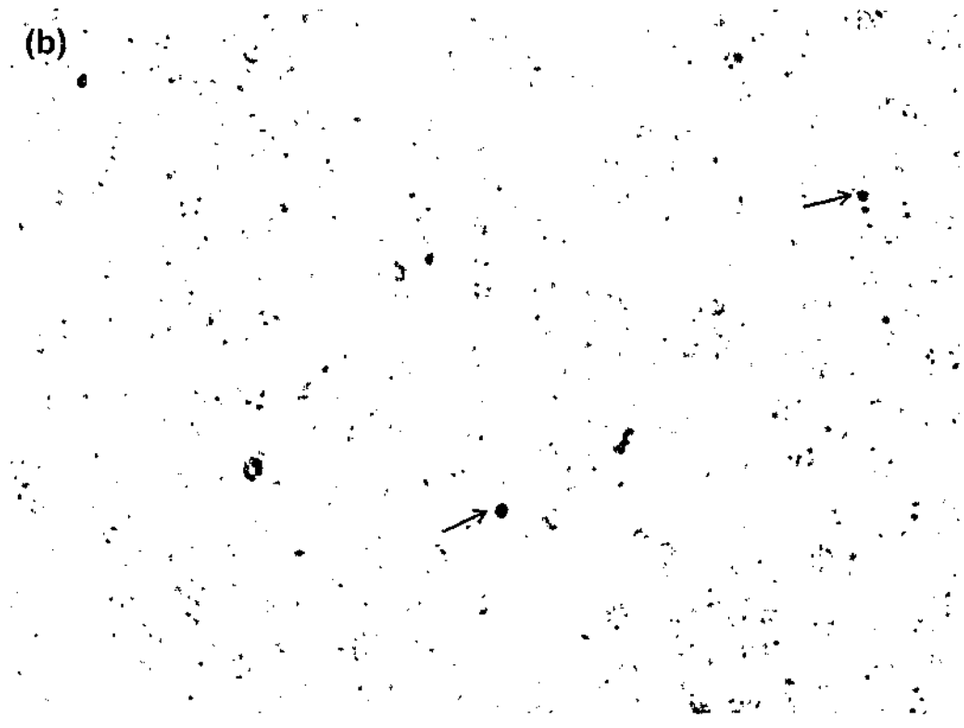

40X

Figure 5.12

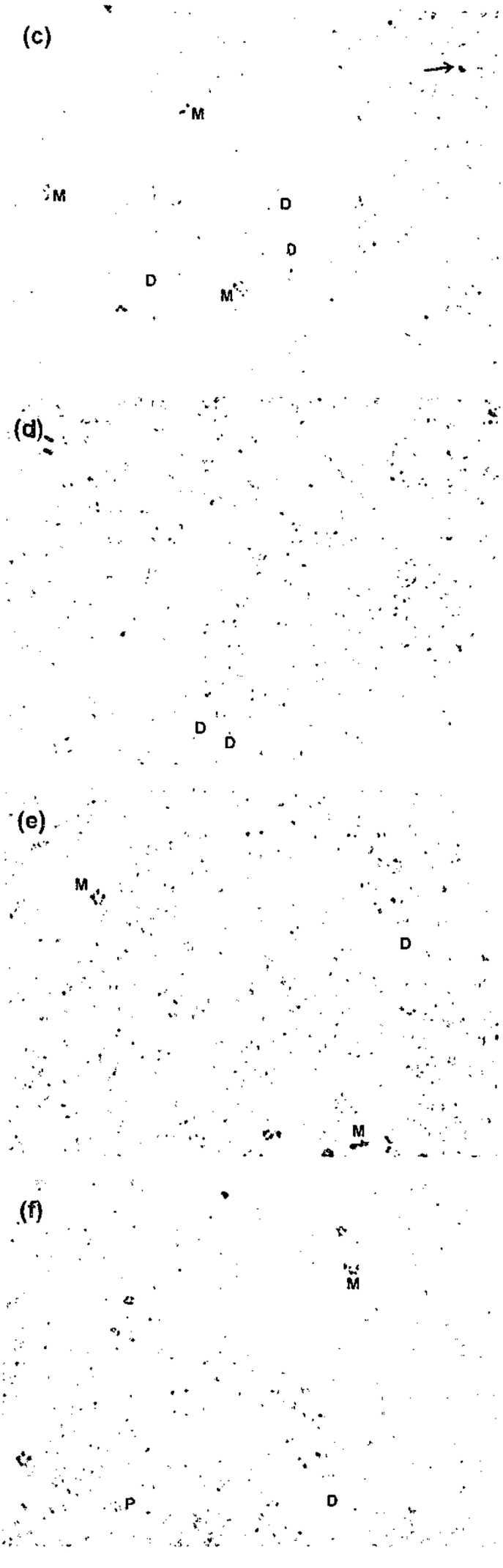

Figure 5.13 The skin of fs-ko, wt, FS^{25}-ko.1, FS^{25}-ko.2, FS^{95}-ko.1 and FS^{95}-ko.2 at birth

The pictures show the skin of fs-ko, wt and four lines of the rescued mice on day 0 postpartum, at 10x magnification. Comparison of the wt skin with the fs-ko skin revealed that the whole layer of the wt epidermis appeared to be thicker while the strata corneum and granulosum epidermidis of fs-ko were thicker. In addition, the contour of the skin of wt assumed a wavy pattern; in contrast, that of fs-ko displayed flatter. Furthermore, the numbers of hair follicles of the fs-ko seemed to be decreased compared to those of wt. Moreover, all four lines of the rescued mice had skin that was more similar to that of fs-ko although sometimes the skin of FS^{95}-ko.1 looked more similar to that of wt.

Figure 5.13

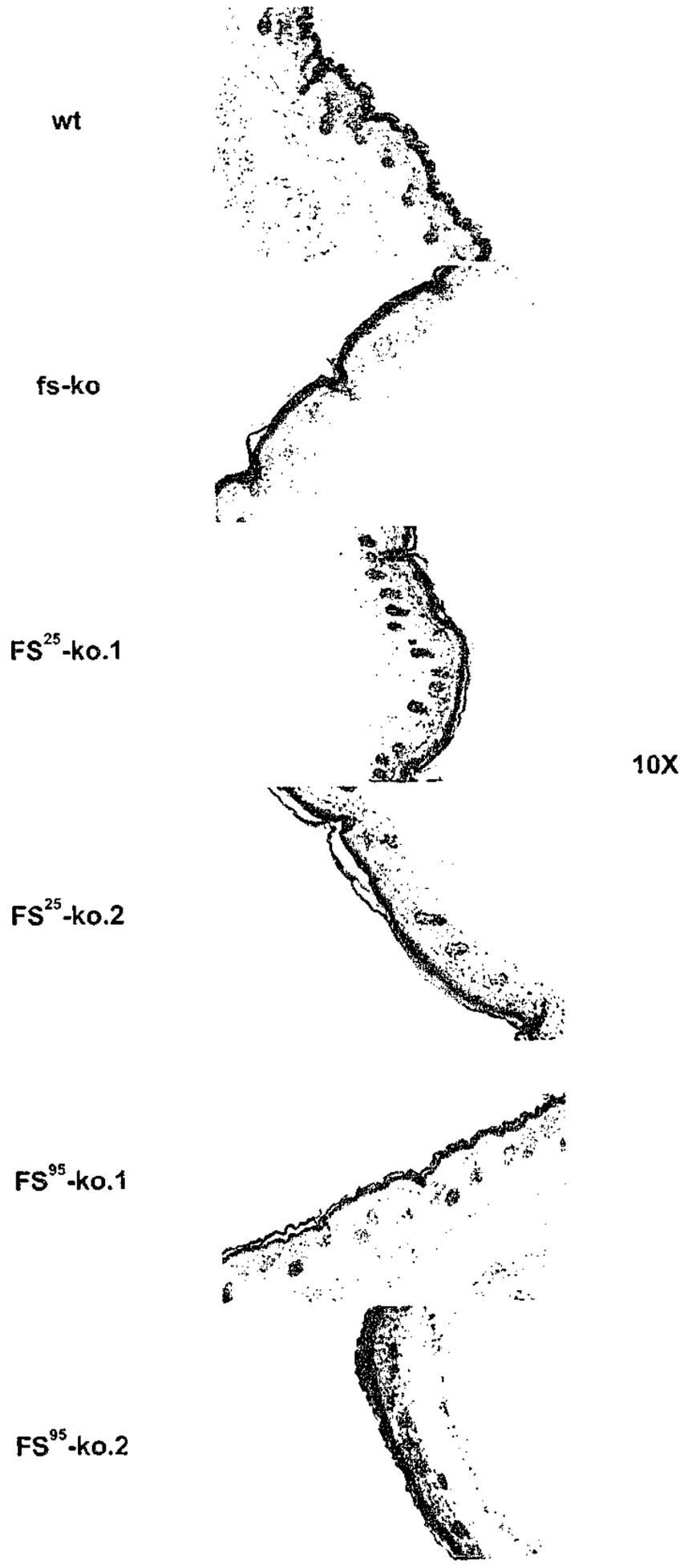

described above, the four lines of the rescued mice displayed appearances that were intermediate between the fs-ko and the wt, but tended to be more like that of fs-ko. There also appeared to be no differences between four lines of the rescued mice. These histological characteristics appear to be compatible to the gross appearances of the rescued mice where they still displayed shiny and taut skin, but which was looser and less shiny than the fs-ko skin.

Palate:

Cleft palate was detected in 1/3 of fs-ko, 0/3 of wt, 0/3 of FS^{25}-ko.1, 0/3 of FS^{25}-ko.2, 0/3 of FS^{95}-ko.1 and 1/3 of FS^{95}-ko.2 (Figure 5.14).

5.3.6 Human follistatin mRNA expressions in rescued mice

In order to compare the mRNA levels of human follistatin transgenes in different organs of the rescued mice to the mRNA levels of the mouse follistatin gene in wt mice at birth, real-time RT-PCR was used for the mRNA quantification. As such, human follistatin mRNA expression levels in the rescued mice were determined by calculating the ratios of the amounts of human follistatin mRNA to the amounts of mouse β actin to avoid sampling errors. Likewise, mouse follistatin mRNA expression levels in the wt mice were determined by the ratios of the amounts of mouse follistatin mRNA to the amounts of mouse β actin mRNA. For each line, three pups were used to obtain mRNA samples and do statistics. As a result, the follistatin mRNA expressions in heart, lung, liver, kidney, muscle and skin from each line are shown in Table IV.7 (Appendix IV).

Multiple comparisons between the different lines are described comprehensively in Table IV.8 (Appendix IV). There was no significant difference of follistatin mRNA expression between the rescued mouse lines FS^{25}-ko.1, FS^{25}-ko.2, FS^{95}-ko.1 and FS^{95}-ko.2 in the organs of heart, lung, liver, kidney, muscle and skin. Of note, compared to wt, the follistatin mRNA expression in muscle and skin of all four lines of the rescued mice were significantly lower, while the expression levels in heart, lung, liver and kidney revealed no difference between the wt and rescued mice (Figure 5.15).

Figure 5.14 The phenotypes of the palates of fs-ko, wt, FS^{25}-ko.1, FS^{25}-ko.2, FS^{95}-ko.1 and FS^{95}-ko.2

The pictures are showing whether there was a cleft palate in fs-ko, wt and four lines of the rescued mice on day 0 postpartum. There was a cleft palate shown in the slide of fs-ko, while the other lines had intact hard palates in the slides that have been examined.

Figure 5.14

Figure 5.15 Follistatin mRNA expression in heart, lung, liver, kidney, muscle and skin of the wt and rescued mice at birth

At birth, follistatin mRNA expression both in muscle and skin of four lines of the rescued mice was significantly and markedly lower than that of the wt mice, whereas there was no significant difference in that of heart, lung, liver and kidney between all the mouse lines. (Three mice were used for each line. The data is presented as computer scientific notation. For example, "4.0E-0.2" means "4.0×10^{-2}". The follistatin mRNA levels were the ratios of the copy numbers of human (in the rescued mice) or mouse (in the wt mice) follistatin mRNA to the copy numbers of mouse β actin mRNA in every sample to avoid sampling errors. a, b, c, and d mean $p < 0.05$ between groups; error bars show standard error for mean, bars show means.)

Figure 5.15

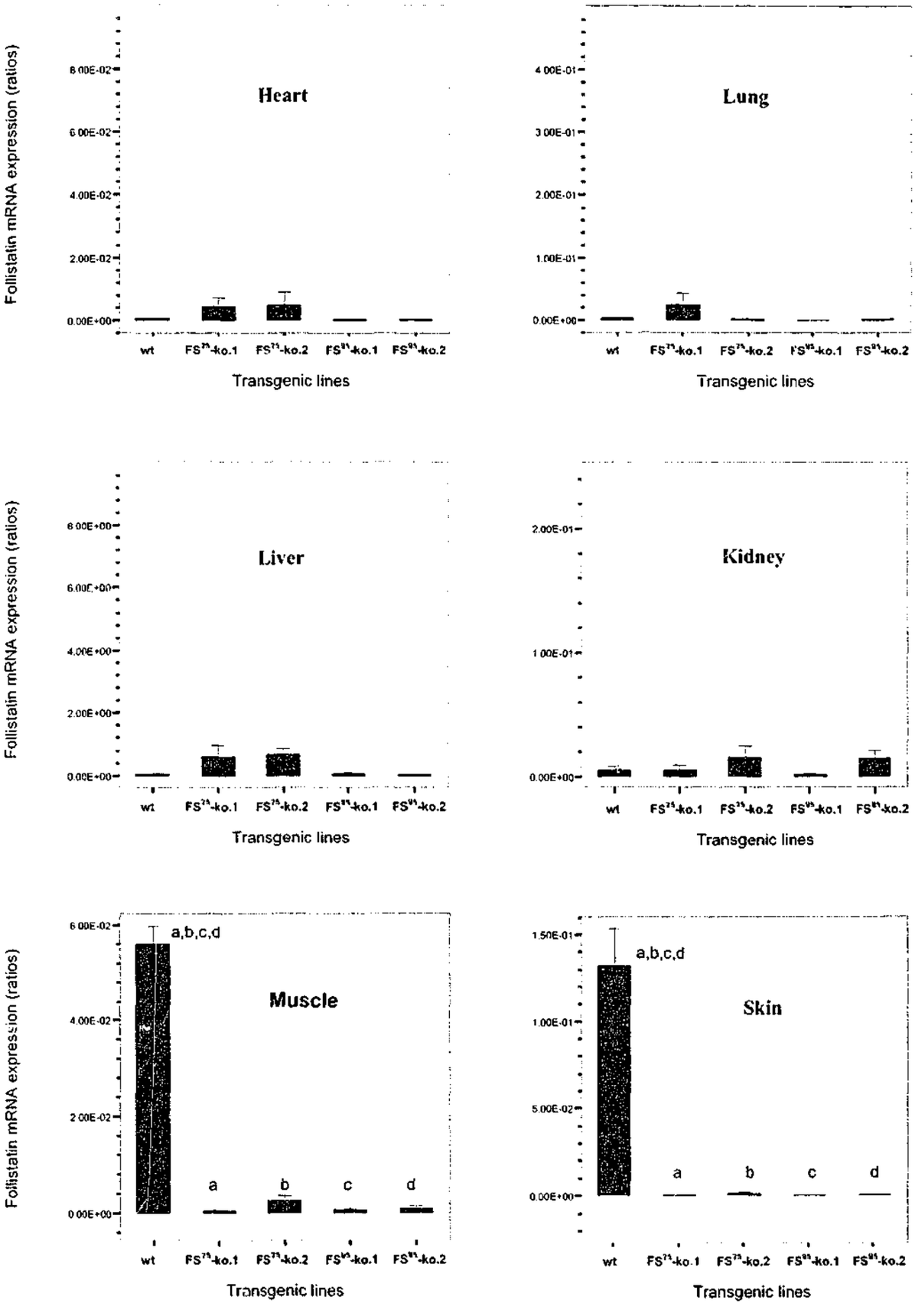
Follistatin mRNA expression (ratios)
Heart
Lung
Liver
Kidney
Muscle
Skin
a,b,c,d
a
b
c
d
wt
FS315-ko.1
FS315-ko.2
FS344-ko.1
FS344-ko.2
Transgenic lines

5.4 Discussion

To define the human follistatin locus and try to identify the essential elements required for appropriate expression of follistatin during development, the aim of the work presented in this chapter was to validate two genomic sequences of the human follistatin locus in the mouse follistatin knockout background. In other words, we were using two human genomic constructs with different lengths of the flanking regions of the follistatin gene to try to rescue the phenotypes of fs-ko. Unfortunately, both the 25 kb and 95 kb human follistatin transgenes did not prevent the fs-ko from the fate of neonatal death. However, observation of the phenotypes of the "rescued" mice and fs-ko does provide some important insights into the biology of follistatin, and some evidence of increased longevity, albeit brief, was seen in the rescued mice.

Interpretation of the data of follistatin mRNA quantification:

Quantification of follistatin mRNA expression in heart, lung, liver and kidney on day 0 after birth did not show any significant difference between the wt and four lines of the rescued mice, *i.e.* FS^{25}-ko.1, FS^{25}-ko.2, FS^{95}-ko.1 and FS^{95}-ko.2. In contrast, the follistatin mRNA levels in muscle and skin of the wt were significantly higher than that of the rescued mice ($p < 0.05$). These data raise the question as to why, despite mRNA levels of follistatin in the vital organs of the rescued mice being similar to those of the wt, the rescued mice could not survive for longer periods. There might be several potential explanations to this. First, the samples for determination of mRNA levels were from the day 0 pups. In effect this provides a profile of follistatin expression at one point in time. However, follistatin is tightly regulated during development. The evidence that mRNA levels of follistatin in the vital organs of the rescued mice at birth were similar to those of the wt does not mean the same levels of expression occurred at every critical stage during development. Second, there might be some critical tissues that may be associated with the survival of the rescued mice, but have not been checked. Third, the procedures for mRNA determination may have had some errors and alternate methods, such as RNase protection assays, may be required to reconfirm these data. However, since for each organ of each line the sample was from different individuals

and the experiments were performed independently, there is less chance that these data are incorrect. Furthermore, the insufficient expression of follistatin in muscle and skin of the rescued mice may be one of the pivotal causes that made the rescued mice different from the wt mice. Of note, at least, these data reveal that there may be critical regulatory elements that control follistatin mRNA expression and are not included within the 45 kb regions both upstream and downstream of the human follistatin gene used in these studies. Moreover, it may also suggest that the information contained within the 25 kb and 95 kb genomic sequences is similar for the expression of follistatin. Such a view was further supported by the evidence that there was no significant difference in the phenotypes of FS^{25}-ko and FS^{95}-ko. Alternately, the lower levels of follistatin in skin and muscle may reflect a species specific regulation of follistatin expression.

Potential causes of death in the rescued mice:

Clearly, observation of the rescued mice indicated that their respiratory and general movements were greater than the fs-ko and these factors contributed to their extended but still short survival. What then was responsible for their death 12-24 hours after birth? Several possibilities emerge. First, studies of mRNA expression of follistatin in the rescued mice at birth show significantly lower levels of mRNA in comparison to the muscle of wt mice. This observation raises the possibility that although their movements were more active than the fs-ko, the rescued mice still have a significant defect in skeletal muscle function. This defect may result in a limitation of sustained action of their respiratory muscles. More likely, however, is the possibility that their skeletal muscle function is insufficient to enable them to position themselves to suckle efficiently, leading to the absence of milk in their stomachs. The limited expression of the human transgene in muscle enables relatively unopposed action of two agents that can inhibit muscle development, namely myostatin and activin (Link and Nishi, 1997; Lee and McPherron, 2001). Further, follistatin can facilitate angiogenesis (Kozian, *et al.*, 1997), one of the key processes in organogenesis and the absence of this action may lead to growth retardation in general.

Second, although the histology of the lung in the rescued mice more closely resembled the wt, there was still observable thickening of the alveolar septa and a pattern suggesting that the terminal bronchioles branched less extensively. These changes were also supported by decreases in lung weights which were more obvious in the fs-ko and in the FS^{25}-ko mice, but less notable in the FS^{95}-ko lines. These changes may indicate subnormal lung function that may be incompatible with more vigorous movement and the required increase in oxygen.

Influence of follistatin on the lungs:

As discussed earlier, this work has identified pathological changes in the lungs of fs-ko mice which have not been described earlier. These changes, when added to the inability of these mice to expand their thoracic cavity due to inadequate skeletal muscle function, may represent the causes of death in these mice. The pattern observed histologically may indicate inadequate branching of the developing bronchial tree, leading to a decrease in lung mass and a limited alveolar space. Activin and follistatin have been shown to influence branching in several sites. Activin inhibits and follistatin stimulates branching in kidney and prostate (Cancilla, *et al.*, 2001; Maeshima, *et al.*, 2001). The unopposed action of activin in the fs-ko mice could influence lung development, leading to the observations in this thesis. Detailed quantitative histological studies are required to confirm these qualitative observations. As indicated in the earlier discussion, the increased lung weights in the FS^{95}-ko mice may contribute to their extended neonatal survival.

Influence of follistatin on liver and GI (stomach and bowels):

The preliminary analyses in histology of the liver and the GI tract failed to reveal any difference between wt, fs-ko and the rescued mice. However, the weights of these organs at birth showed significant differences between wt and fs-ko, and those of the rescued mice were closer to the fs-ko in terms of the weights of liver and GI. Although the size of organs may be in proportion to the body size of the mice, differences between the wt and fs-ko appear to be greater than expected for the decrease in body weight. This observation would be in keeping with the known action of activin as an

agent that causes apoptosis and decreased hepatic mass in adults (Kogure, *et al.*, 2000). Further, follistatin has been shown to block this action of activin and enhances regeneration of the liver after partial hepatectomy (Kogure, *et al.*, 1995). Finally, the liver develops by branching of a diverticulum derived from the mid-gut of the embryo and it is possible that activin limits the branching pattern.

Oogenesis and follistatin:

Another important phenotype of fs-ko and four lines of the rescued mice that has not been recognized in the original paper of follistatin knockout mice (Matzuk, *et al.*, 1995) is a significantly decreased numbers of oocytes in the perinatal ovaries. In some ovaries of fs-ko it was rare to see oocytes. Obviously, both human follistatin transgenes failed to rescue the ovarian phenotype of fs-ko, although the numbers of oocytes of the rescued mice appeared to be more than that of fs-ko. However, these conclusions will require quantitative stereological data. The essential role of follistatin in fetal oogenesis was further supported by the work of others in our Institute who were exploring the capacity of the ovary in fs-ko mice to undergo ovulation by transplantation to an immune deprived host (Snow *et al.*, personal communication). In their quantitative studies of ovarian morphology in the wt and fs-ko mice, they observed a marked decrease in the number of primary oocytes in the fs-ko mice. They also showed that despite a decreased number of oocytes in fetal ovaries of fs-ko, these remaining oocytes could develop into antral follicles when the ovaries of fs-ko were transplanted into the subcapsular space of kidneys of ovariectomized adult wt SCID mice. Follistatin has been recognized as an important factor modulating the ovarian function and folliculogenesis through interactions with some members of TGF-β superfamily (Knight and Glister, 2001; Otsuka, *et al.*, 2001; Lin, *et al.*, 2003). However, there was no published report implicating the role of follistatin in fetal oogenesis. Therefore, this finding is important and also broadens the understanding of follistatin biology.

While examining the day 0 testes of fs-ko and the rescued mice, there did not appear to be obvious abnormalities in male gametogenesis, pointing to the different roles of follistatin in male and female gametogenesis. This phenomenon can be further explained by the expression levels of follistatin in embryonic testes and ovaries. Using a

PCR-based cDNA subtraction technique to investigate expression differences that arise during gonadal sex differentiation, Menke and Page showed that follistatin is expressed at higher levels in XX gonads (Menke and Page, 2002). Further whole-mount *in situ* hybridization demonstrated that in embryonic gonads at E12.5, E13.5, E14.5, and E15.5, follistatin exhibited staining in ovaries; in contrast, no expression was detected in testes (Menke and Page, 2002). The expression of follistatin in the developing ovaries, but not with testes, suggests this pattern is crucial for ovarian development. This view is supported by the ovarian phenotype identified in the fs-ko mice, showing a depletion of oocytes. The histological analyses also indicated that this depletion of oocytes in fs-ko seemed to occur before or during the early phases of the prophase of the first meiotic division. Either follistatin is active directly on this process or, more likely, the expression of follistatin in the ovary blocks the actions of activin or BMPs, which would otherwise disrupt the entry into meiosis or survival of the oogonia. Further studies of the development of the ovaries in fs-ko mice prior to E18 are essential in understanding the pathogenesis of the ovarian lesion.

Development of genital tubercle-- a new insight into the context of follistatin:

In this chapter, agenesis or severe under-development of the genital tubercle was described in fs-ko and all four lines of the rescued mice. Since the development of the genital tubercle is a complex process, many aspects of which remain to be elucidated, this finding would provide a new direction for research into this process and a new potential action for the follistatin-activin system.

The genital tubercle (GT) is an anlage of the external genitalia for a penis in males and a clitoris in females. The external genitalia are made up of terminal appendage organs with endoderm-derived tubular structures, i.e. initially a urethral plate and later a urethral tube. The developing GT is composed of a urethral plate/tube together with mesenchyme and outer ectoderm. Currently, the processes of the murine fetal external genitalia are divided into two processes (Ogino, *et al.*, 2001). The first process is involved with the initial outgrowth of GT, which has been considered to be independent of steroid hormones. The second process is to create sexual dimorphism of the external

genitalia through further differentiation of GT, which is known in humans to be the result of the action of dihydrotestosterone, formed by the action of 5α reductase.

Accordingly, agenesis or hypoplasia of the GT in fs-ko or the rescued mice is very likely to result from the problems involved in the process of the initial outgrowth of GT, leading to nearly complete absence of the external genitalia. Despite the potential role of follistatin in the first process of external genitalia development, it remains unclear whether follistatin plays a role in the second stage of this process.

Several growth factors, including fibroblast growth factor (FGF) and Wnt, have been demonstrated to be active in the regulation of external genital development in mice (Yamaguchi, *et al.*, 1999; Haraguchi, *et al.*, 2000). Specially, FGF signaling plays a key regulatory component in orchestrating growth and differentiation of the GT (Haraguchi, *et al.*, 2000). Moreover, the Sonic hedgehog (Shh) signaling pathway has been shown in the urogenital sinus and in the distal tip of the urethral epithelium during murine external genitalia morphogenesis (Haraguchi, *et al.*, 2000). Importantly, Shh knockout mice displayed a complete absence of the formation of the external genitalia (Haraguchi, *et al.*, 2001), which is similar to that occurring in the external genitalia of fs-ko. Further analysis of gene expression in Shh knockout mice highlighted the roles of Shh in both induction and maintenance of gene expression in the GT (Perriton, *et al.*, 2002). It appeared that BMP-4 and FGF-8 need Shh for the maintenance of expression, but not initiation of their expression. In contrast, BMP-2, Wnt-5a and FGF-10 appeared to require Shh for the induction of their expression (Perriton, *et al.*, 2002). Since there is molecular evidence that follistatin interacts with BMP-2 and BMP-4 (Iemura, *et al.*, 1998), as well as being shown to be a bFGF-inducible gene (Kozian, *et al.*, 1997), it is likely that follistatin plays a role in the processes of the external genitalia development through interactions with BMP signaling, FGF signaling or/and Shh signaling pathway.

Summary and further directions:

In conclusion, observation of the phenotypes of fs-ko and the rescued mice provide new insights into the biology of follistatin. Both the 25 kb and 95 kb human genomic

transgenes could not rescue the fs-ko mice. However, alignment of the human and mouse follistatin loci will be studied further *in silico* in the next chapter (Chapter 6).

Chapter 6

In silico analysis of the human follistatin locus

Chapter Outline:

6.1 Introduction

In the previous chapters of the Result Section 2 (Chapter 4 ~ 5), the work was focused on the validation of two genomic sequences of the human follistatin locus in follistatin knockout mice by using transgenesis with the vectors PAC-FS and pNEB-FS. These kind of experiments can be considered as using an *in vivo* system (transgenic mice) to conduct a study of comparative genomics to further define the potential regulatory elements in the genomic sequences. In contrast, the work described in this chapter was to use an *in silico* system (computer) to analyze the human follistatin locus. The new term '*in silico*' has recently become a common reference to biological studies carried out in the computer, joining the traditional terms '*in vivo*' and '*in vitro*' to describe the location of experimental studies.

In view of the rationale that most of the important functional segments of genomic sequences will be conserved between species during evolution, comparative genomics provides not only estimates of when different species diverged, but also the opportunity to identify exons and functional segments of the noncoding regions, such as gene regulatory elements. However, the choice of species may be crucial to what needs to be identified during the genomic comparison. The most highly conserved sequences during evolution will be easier to identify by comparison of genomic sequences of more distant species in an attempt to avoid false positive results. In contrast, to reveal some conserved sequences that are being more quickly changed during the process of evolution, comparing closer species may be more informative to prevent false negative results. For example, the changes in amino acids leading to certain human diseases are more likely to occur at the conserved sites of the protein sequences that will be best identified by comparison with a distant species, such as the tiger pufferfish (*Fugu rubripes)* (Hedges and Kumar, 2002). Nevertheless, to reveal regulatory elements within genomic sequences, a closer species, such as mouse, may be a better choice (Hardison, 2000). Hence, in this chapter we chose the mouse as the species to compare with the human genomic sequences.

Recently, conserved noncoding sequences (CNSs) have been considered as reliable guides to gene regulatory elements (Hardison, 2000). Currently, the methodology to identify the gene regulatory elements has tended to compare the genomic sequences of the appropriate species followed by verifying the identified CNSs with *in vivo* or *in vitro* approaches (Ishihara, *et al.*, 2000; Loots, *et al.*, 2000; Qiu, *et al.*, 2001; Gottgens, *et al.*, 2002). The doubt about whether the CNSs can represent the potential gene regulatory elements has been further clarified by the numerous transgenic studies, showing that genomic transgenes could nearly mimic their natural expression patterns even when introduced into mice from various mammals (Lacy, *et al.*, 2000).

At the early stage of the experiments described in Chapter 4 ~ 5, the human and mouse genomic sequences of the follistatin locus were not available, so chronologically, functional analysis of two different-length human genomic sequences of the follistatin locus was first performed via an *in vivo* approach. However, it is still meaningful to do *in silico* analysis of the human follistatin locus at the later stage. The first reason is that the data from the computational analysis can be used as a supplement to the biological data produced in the previous chapters. The second reason is that the computational data may be able to shed light on the future directions of studies on this area. Therefore, this chapter was aimed to retrieve the human and mouse genomic sequences of the follistatin locus from the data resources, followed by the computational alignments of the sequences from these two species to try to identify CNS elements that may be the regulatory elements of the follistatin gene.

6.2 Experimental design & procedures

6.2.1 Acquiring the genomic sequences of the follistatin locus

The human and mouse genomic sequences of the follistatin loci were retrieved from the NCBI data base (http://www.ncbi.nlm.nih.gov/). Sequences were recruited contained the follistatin gene and its largest flanking regions up to the nearest identical genes for both human and mouse, based on the phenomenon that the gene orders of human and mouse are syntenic to each other in most situations. Another consideration for the size of the recruitment is that most of the essential regulatory elements tend to locate within the flanking regions of the genes.

6.2.2 Aligning human and mouse genomic DNA sequences

The alignment of the retrieved human and mouse genomic sequences was performed through Pipmaker (http://bio.cse.psu.edu). Pipmaker is an internet-based tool for aligning large genomic regions (Schwartz, *et al.*, 2000). This server can return an alignment, positions and percent identity of gap-free segments within that alignment, a percentage identity plot (pip) and the corresponding dot plot.

To avoid uninformative and time-consuming alignments among repeats, the first sequence (human sequences) was uploaded to RepeatMasker (http://ftp.genome.washington.edu/cgi-bin/RepeatMasker) to obtain the repeats file that was then submitted to Pipmaker together with the sequence files.

The conserved noncoding sequences (CNSs) were defined arbitrarily as having at least 100 bp that align without a gap and with at least 70% nucleotide identity (Loots, *et al.*, 2000).

6.3 Results

6.3.1 The sequences of the follistatin locus

Human genomic sequence of the follistatin locus:

The human genomic sequences of the follistatin locus were recruited from the Homo sapiens chromosome 5 genomic contig of the NCBI data base. The ACCESSION is NT_006431, REGION: 2958639.~ 3421212 and the VERSION of these DNA sequences is NT_006431.13; GI:29798426. The recruited region covers 462574 bp of genomic DNA sequences and contains the follistatin gene, its upstream sequence up to MOCS2 (molybdenum cofactor synthesis 2) (but not including the MOCS2 sequences), and its downstream sequence up to NDUFS4 (NADH dehydrogenase (ubiquinone) Fe-S protein 4) (but not including the NDUFS4 sequences). The reason to include this length of genomic sequences is because the order of the genes MOCS2, follistatin and NDUFS4 is syntenic with that of the mouse genome. Analysis of this region would provide some information into the control of systems which may be involved in the regulation of the expression of the follistatin gene. In addition, between the follistatin gene and MOCS2 there are three un-designated genes, *i.e.* LOC348963, LOC348962 and LOC257396 (Figure 6.1).

Mouse genomic sequence of the follistatin locus:

Likewise, the mouse genomic sequences of the follistatin locus were recruited from the Mus musculus chromosome 13 genomic contig, strain C57BL/6J of the NCBI data base. The ACCESSION is NT_039590, REGION: 22775330.~.23206821 and the VERSION of these DNA sequences is NT_039590.1; GI:28527136. The recruited region covers 431492 bp of genomic DNA sequences and contains the follistatin gene, its upstream sequence up to MOCS2 (but not including the MOCS2 sequences), and its downstream sequence up to NDUFS4 (but not including the NDUFS4 sequences). The reason to include this length of genomic sequences is because the order of the genes MOCS2, follistatin and NDUFS4 is syntenic with that of human genome. Analysis of this region

Figure 6.1

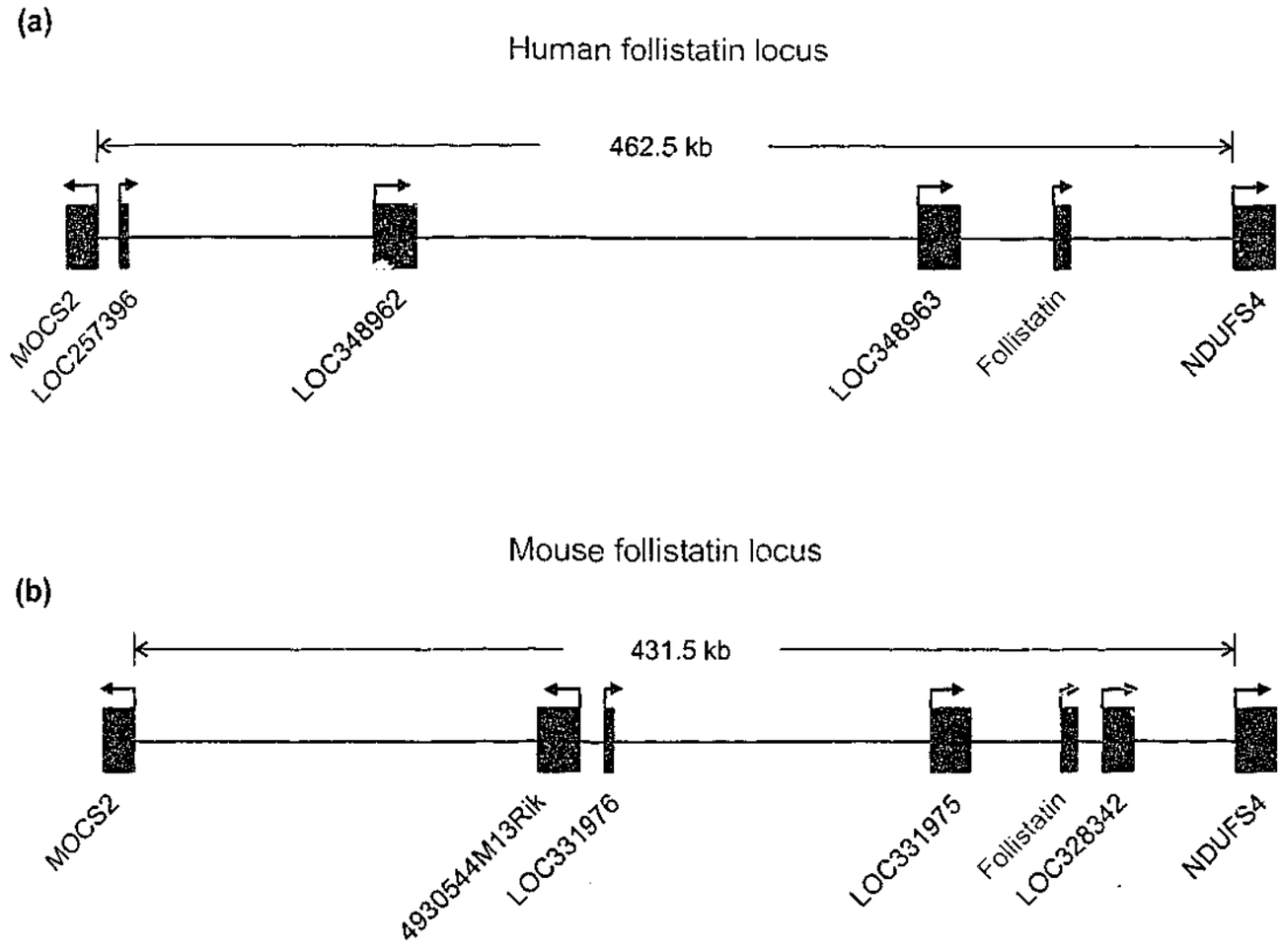

Figure 6.1 Human-mouse genome comparison of the follistatin loci

The figures show the locations of the segments of human and mouse genomes that were recruited for human-mouse sequence alignments. (a) The recruited sequence of the human follistatin locus includes the follistatin gene, its 382.3 kb upstream sequence and its 73.5 kb downstream sequence. (b) In mice, the recruited sequence of the mouse follistatin locus contains the mouse follistatin gene, its 361.3kb upstream sequence and its 64.5 kb downstream sequence. Interestingly, the genes MOCS2 and NDUFS4 are upstream and downstream of the follistatin gene, respectively, in both human and mouse genomes (a & b).

would provide some information into the control of expression of the follistatin gene. In addition, between the follistatin gene and MOCS2 there are three un-designated genes, *i.e.* 4930544M13Rik, LOC331976 and LOC331975, and between the follistatin gene and NDUFS4 there is one un-designated gene, LOC328342 (Figure 6.1).

6.3.2 Conserved noncoding sequences (CNSs) of the follistatin locus

For the pip (Figure 6.2), the program plots the position (in the first sequence, *i.e.* human sequence) and percent identity of each gap-free segment of the alignments. The bottom horizontal axis shows the positions of the retrieved human sequence whose length is 462574 bp, whereas the top horizontal axis is marked with the positions of repeats and exons. The vertical axis is defined as percent identity (50% ~ 100%). The segments with percent identity between 50% ~ 100% will be represented as dots in the strips of diagrams. For clearly recognition of CNS elements in the diagrams, red underlay was used for CNS elements (Figure 6.2). The locations of the sequences of two human transgenes, PAC-FS and pNEB-FS, can be checked in the diagram by the data that PAC-FS includes about 45 kb of upstream and downstream sequences of the follistatin gene as well as pNEB-FS includes about 16 kb of upstream and 3 kb of downstream sequences of the follistatin gene. Apparently, the vector PAC-FS covers all the upstream segment of the follistatin gene until the gene LOC348963, however, does not include all the downstream segment of it before the gene NDUFS4. The nine CNS elements that were not included in PAC-FS but were located in the downstream of the follistatin gene were described in Table 6.1.

Although the pip described above (Figure 6.2) provided compact and highly informative features of the first sequence (human) about the alignments, it did not convey the position of the interesting alignment in the second sequence (mouse). The dot plot (Figure 6.3) of the same alignments can supplement the requirement of this aspect of information. The horizontal axis was defined as the position of the human sequence (1 ~ 462574 bp), while the vertical axis was defined as the position of the mouse sequence (1 ~ 408941 bp). Red underlay indicates CNS elements. As a result, the positions of CNSs in mouse sequences can be approximately deduced from the positions of the dots on the red strips.

Figure 6.2 Percent identity plots comparing human and mouse sequences at the follistatin locus

The percent identity plot (pip) is a compact display of the results of aligning the human sequence with the mouse sequence at the follistatin locus. The icons below for the decoration on the top horizontal axis of pip represent exons and various repeat sequences. SINE: short interspersed nuclear elements. MIR: mammalian-wide interspersed repeat. LINE: long interspersed nuclear elements. LTR: long terminal repeat. UTR: untranslated region. The red underlay in the pip: represents CNS (conserved noncoding sequence) elements that are at least 100 bp without a gap and with at least 70% identity between two species. The following pages are the pips, in which the top horizontal axes are decorated with the icons below to indicate exons or various repeats, the base horizontal axes are for the positions of human sequence, the vertical axes are designated as percent identity. Only 50~100% identity is shown in the pips. The positions of the dots in the horizontal strips provide the information for conserved segments as well as their percent identity. In addition, CNS elements can be easily identified as red strips in the pips.

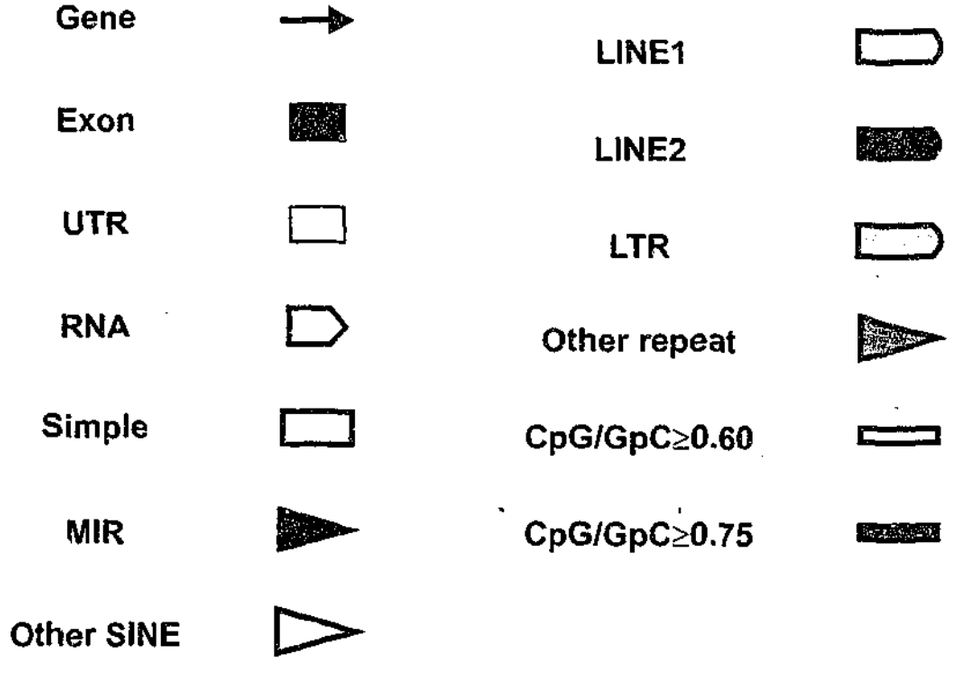

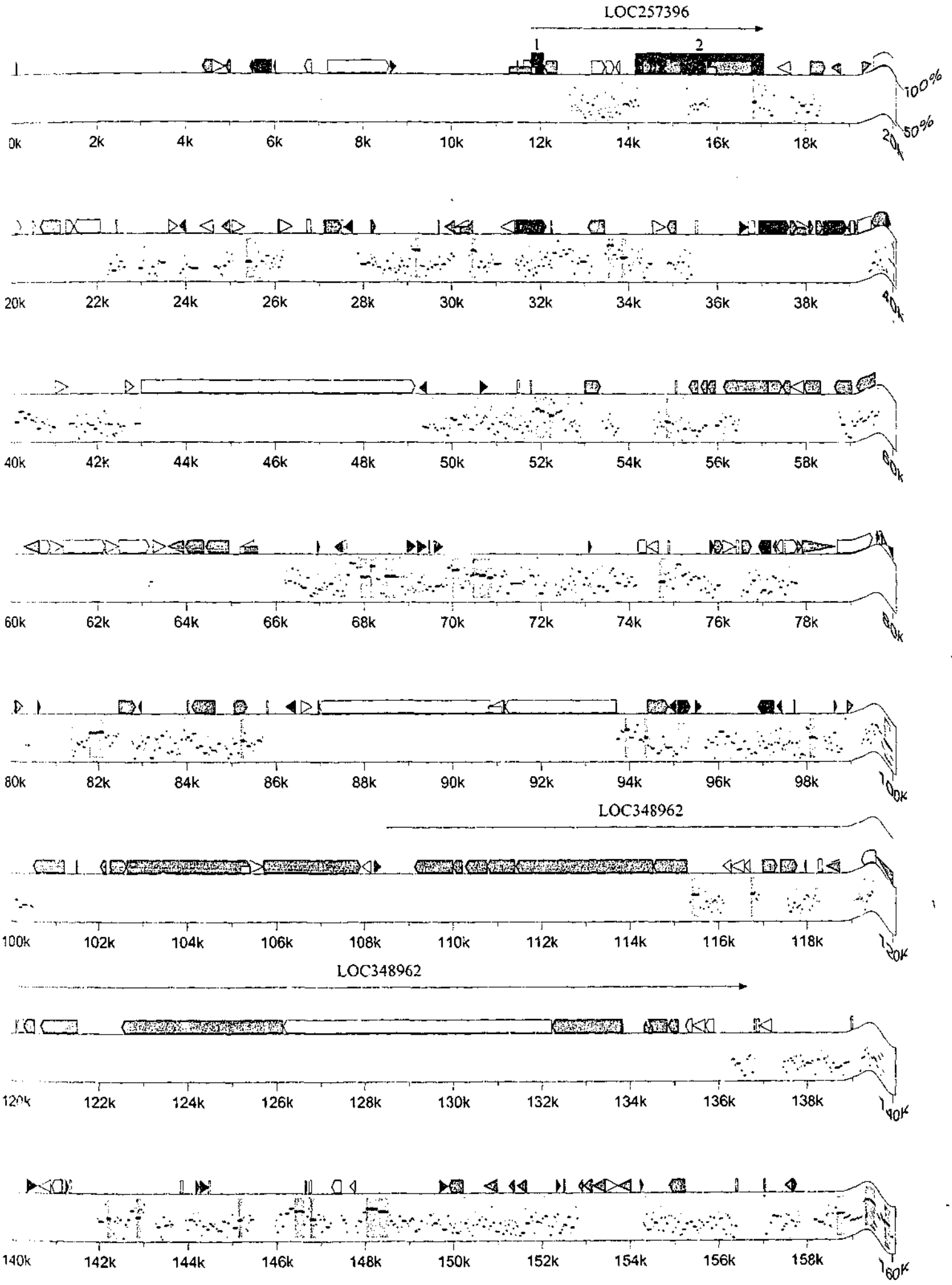
LOC257396
1
2
100%
50%
0k
2k
4k
6k
8k
10k
12k
14k
16k
18k
20k
22k
24k
26k
28k
30k
32k
34k
36k
38k
40k
42k
44k
46k
48k
50k
52k
54k
56k
58k
60k
62k
64k
66k
68k
70k
72k
74k
76k
78k
80k
82k
84k
86k
88k
90k
92k
94k
96k
98k
100k
LOC348962
102k
104k
106k
108k
110k
112k
114k
116k
118k
120k
LOC348962
122k
124k
126k
128k
130k
132k
134k
136k
138k
140k
142k
144k
146k
148k
150k
152k
154k
156k
158k
160k

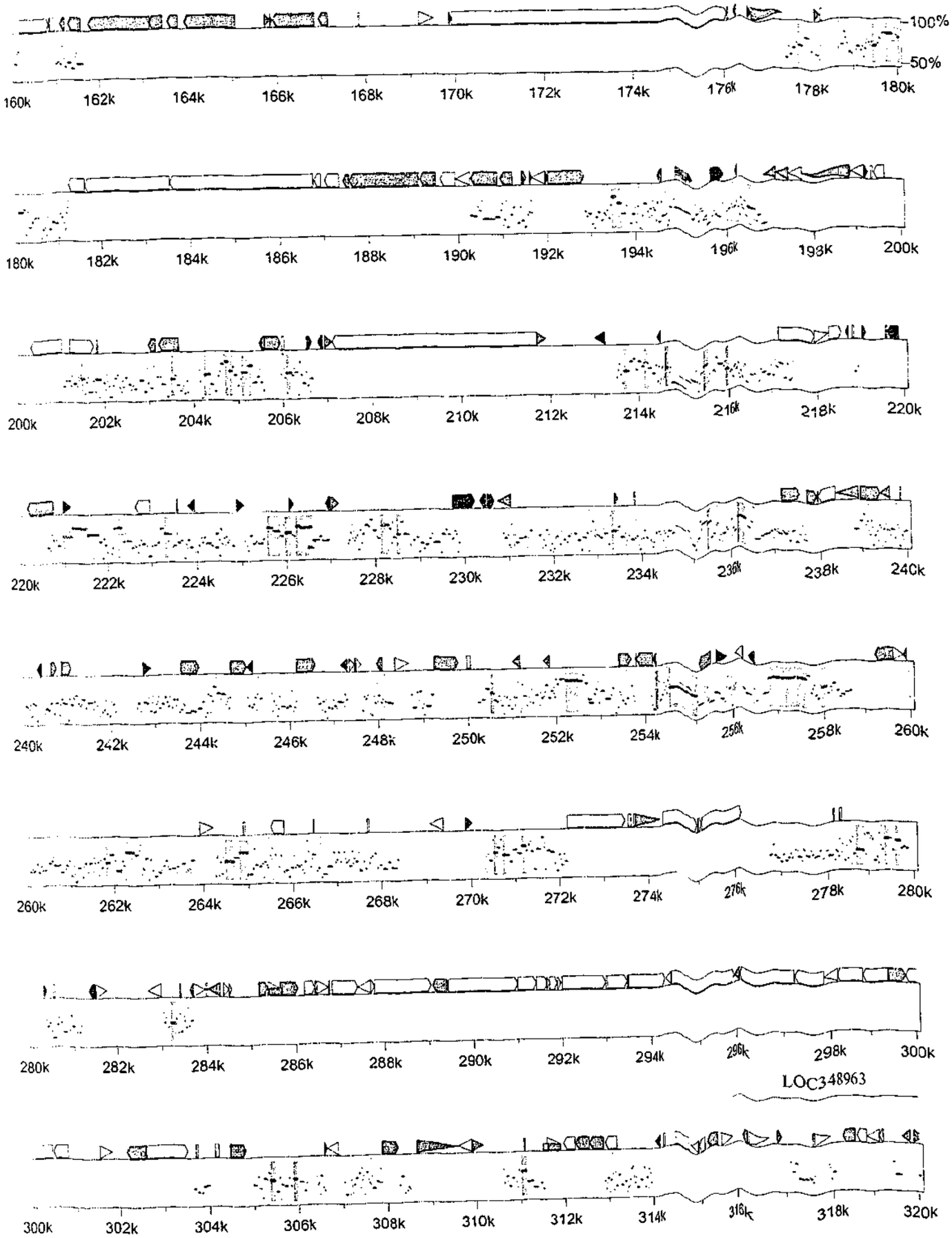
100%
50%
160k
162k
164k
166k
168k
170k
172k
174k
176k
178k
180k
182k
184k
186k
188k
190k
192k
194k
196k
198k
200k
202k
204k
206k
208k
210k
212k
214k
216k
218k
220k
222k
224k
226k
228k
230k
232k
234k
236k
238k
240k
242k
244k
246k
248k
250k
252k
254k
256k
258k
260k
262k
264k
266k
268k
270k
272k
274k
276k
278k
280k
282k
284k
286k
288k
290k
292k
294k
296k
298k
300k
LOC348963
302k
304k
306k
308k
310k
312k
314k
316k
318k
320k

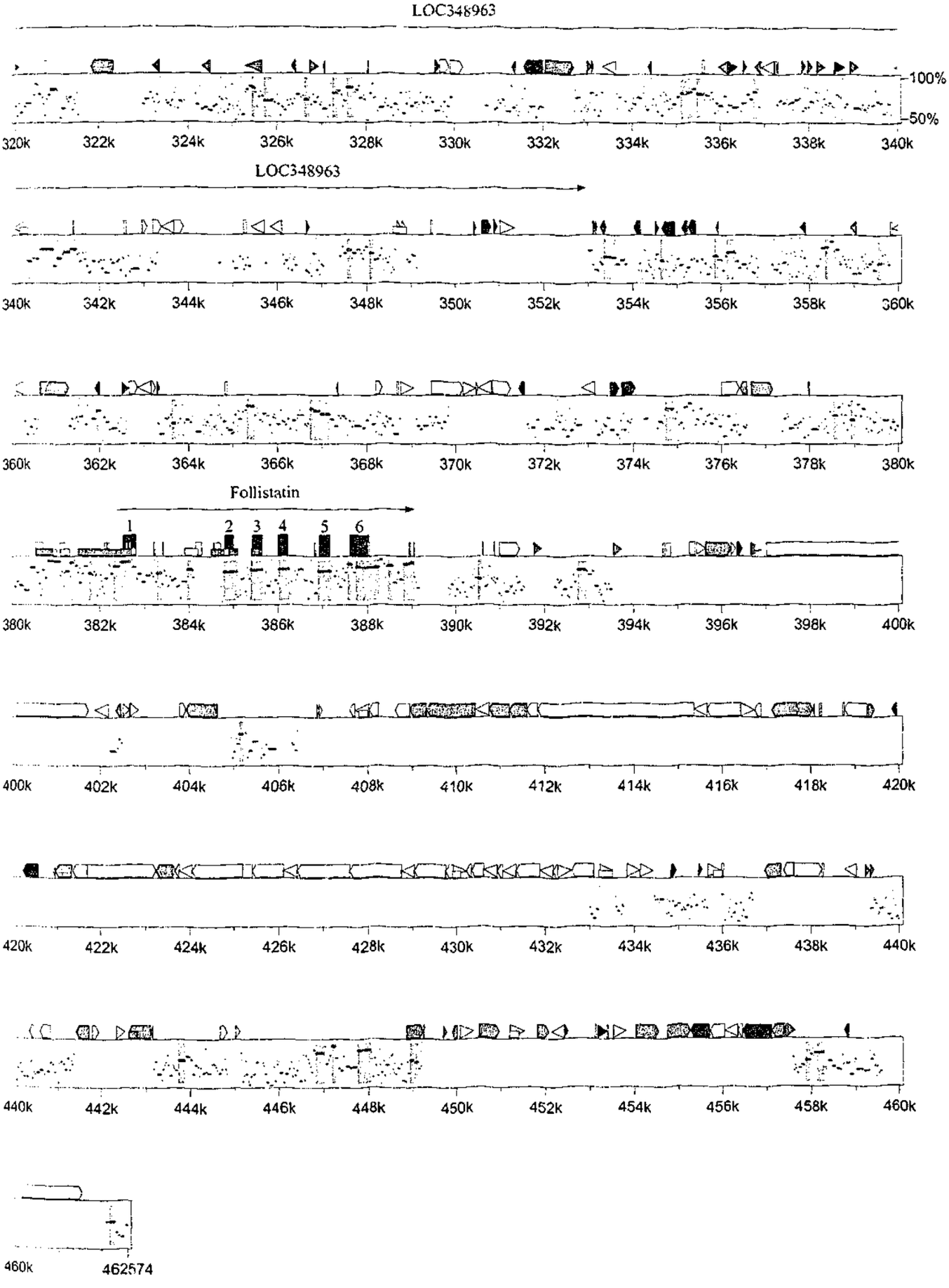
LOC348963
100%
50%
320k
322k
324k
326k
328k
330k
332k
334k
336k
338k
340k
LOC348963
340k
342k
344k
346k
348k
350k
352k
354k
356k
358k
360k
360k
362k
364k
366k
368k
370k
372k
374k
376k
378k
380k
Follistatin
1
2
3
4
5
6
380k
382k
384k
386k
388k
390k
392k
394k
396k
398k
400k
400k
402k
404k
406k
408k
410k
412k
414k
416k
418k
420k
420k
422k
424k
426k
428k
430k
432k
434k
436k
438k
440k
440k
442k
444k
446k
448k
450k
452k
454k
456k
458k
460k
460k
462574

Table 6.1 The CNS elements that are in the downstream sequence of the human follistatin gene and beyond the content of the vector PAC-FS in the recruited human genomic sequences.

The nucleotide location in the human locus	Identity	Length (bp)
457859-457981	78 %	123
458128-458302	87 %	175
462146-462302	79 %	157
443715-443894	79 %	180
446807-447020	88 %	214
447167-447284	96 %	118
447743-448055	91 %	313
448916-449016	79 %	101
449018-449129	76 %	112

Figure 6.3 Dot plot of the human-mouse alignment at the follistatin locus

The X-axis is designated as the positions of the human sequence. The Y-axis is designated as the positions of the mouse sequence. The dots represent the conserved segments in both sequences. The red strips are for CNSs in the human sequence. Therefore, the dots located in the red strips indicate CNS elements for both sequences.

Figure 6.3

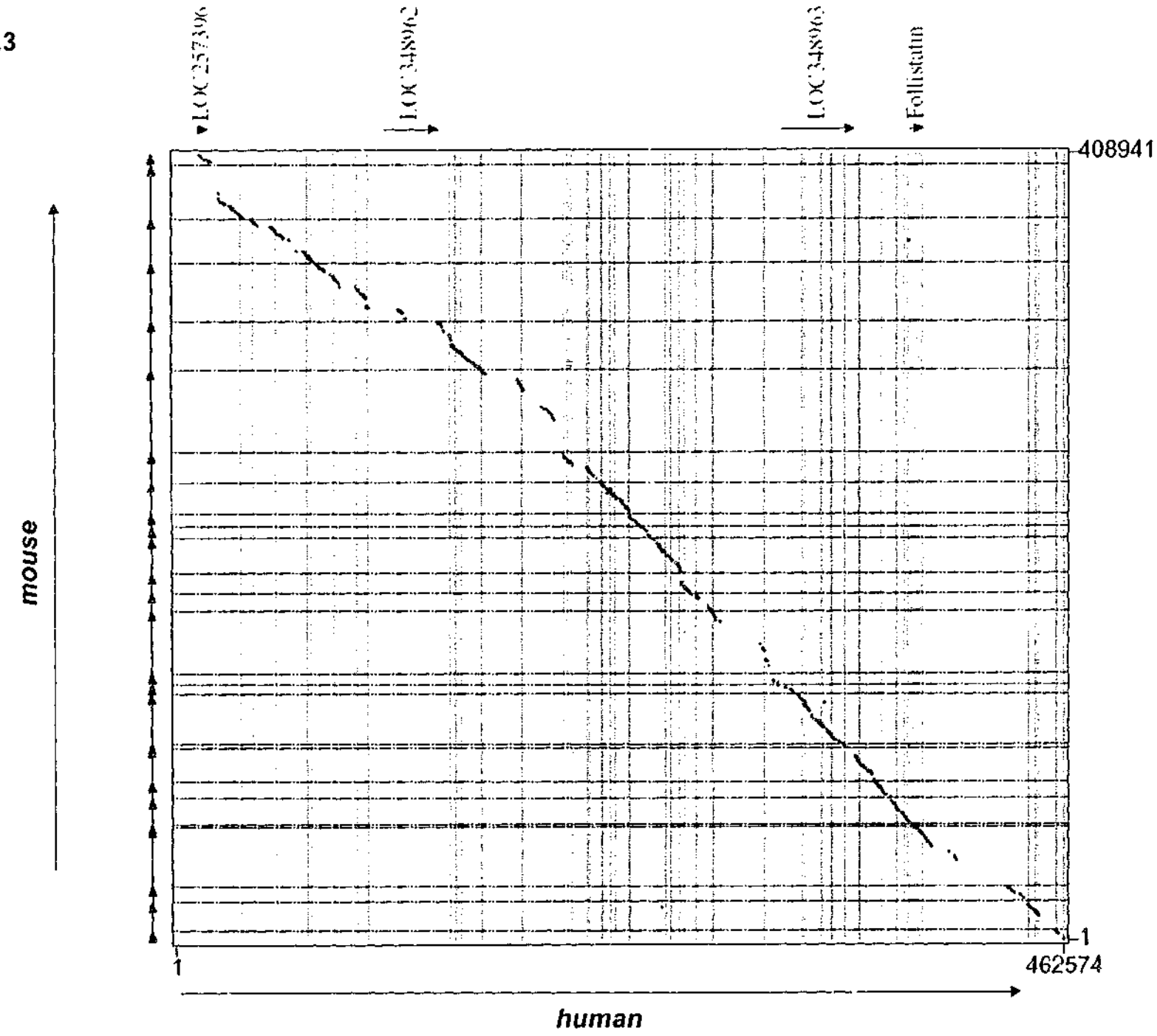
LOC253396
LOC348963
LOC348963
Follistatin
408941
1
462574
1
mouse
human

6.4 Discussion

The work described in this chapter has identified some CNS elements of the human follistatin locus. In view of the limited number of transcription factors compared with the total number of genes in a genome, it is possible that the transcriptional profiling for the coordinated gene regulation can be established through identifying common transcription factor binding sites in CNS elements. As discussed in Chapter 1, the molecular context of follistatin would be very complex; follistatin may behave as a mediator through which the associated TGF-β superfamily members interact with each other. As such, the CNS elements at the follistatin locus may be like a window through which we can have broader perspective about this complex system.

In light of the data described in Chapter 5 that FS-25 and FS-95 rescued mice cannot survive, it is reasoned that some regulatory element essential for appropriate expression of follistatin during the prenatal developmental period have been missed. Because for most genes the important regulatory elements usually locate within the upstream or downstream segments of sequences before the nearest neighboring genes, the missing elements may be just some of the nine CNS elements (Table 6.1) which even PAC-FS did not include. However, more experiments are required to prove this proposal. Moreover, there are some CNS elements located beyond the 16 kb upstream and within the 45 kb upstream of the follistatin gene, and also beyond the 3 kb downstream and within the 45 kb downstream of the follistatin gene. Based on the evidence that FS-25 and FS-95 rescued mice appeared not to have marked differences in their phenotypes, these CNS elements may not play an important role in follistatin expression during fetal development.

There is always a question as to the length of the genomic sequences that should be examined in studies on the regulation of eukaryotic gene expression. Some enhancers may be located more than 100 kb from the start of the gene, the expression of a gene in a gene cluster may be coordinated by the locus control region (LCR) (Grosveld, *et al.*, 1993) which is located some distance upstream of the gene cluster, and moreover, there even are epigenetic mechanisms and long-range control of gene expression by

chromatin structure (Geyer, 1997). The work described in this chapter was focused on the alignment of about 460 kb genomic sequences of the human follistatin locus and that of the mouse follistatin locus. Some CNS elements have been identified; however, further experiments are required to elucidate their functions.

Chapter 7

Construction of human follistatin isoform-specific transgenes

Chapter Outline:

7.1 Introduction

7.1.1 Aims

As discussed in the Introduction (Chapter 1), follistatin-288 and follistatin-315 have distinct biochemical properties, leading to the hypothesis that both isoforms may have different biological functions. Hence, dissecting the functions of both isoforms would further enhance our understanding of follistatin biology. Thus, we planned to create mice in which there was expression of only one follistatin isoforms.

To achieve this aim, the DNA engineering in the follistatin gene was attempted to delete the intron 5 for the follistatin-288 specific construct and to delete intron 5 plus exon 6a for the follistatin-315 specific construct (Figure 7.1). The basis of this design was to force the translation of either follistatin-288 or follistatin-315 (see Section 1.2.2).

Initially, two ways were considered to accomplish the DNA engineering in the follistatin gene. One is using the 'knock-in' technique to delete intron 5 or intron 5 plus exon 6a for follistatin-288 or follistatin-315, respectively, in the mouse genome; thereby the created homozygous knock-in mice would have only one of two isoforms. Alternatively, a transgene could be generated using the human follistatin locus. However, the human genomic sequence needs to be constructed by the technique of DNA engineering to generate two kinds of constructs of transgenes that were expected to be able to produce follistatin-288 or follistatin-315 *in vivo*. Taking advantage of the follistatin knockout mice that were already created by Matzuk's group (Matzuk, *et al.*, 1995), the mice carrying the isoform-specific transgenes in the mouse follistatin knockout background can be created after two steps of cross-breeding these transgenic mice with heterozygous follistatin knockout mice (using the heterozygous mutants is because homozygous follistatin mutants died soon after birth) (refer to Section 2.2.12).

Finally, the decision to create the transgenic mice rather than the knock-in mice was made. The first reason is that we may still be able to fulfill our purpose to separate two follistatin isoforms *in vivo* using transgenesis. The second reason is that the transgenic

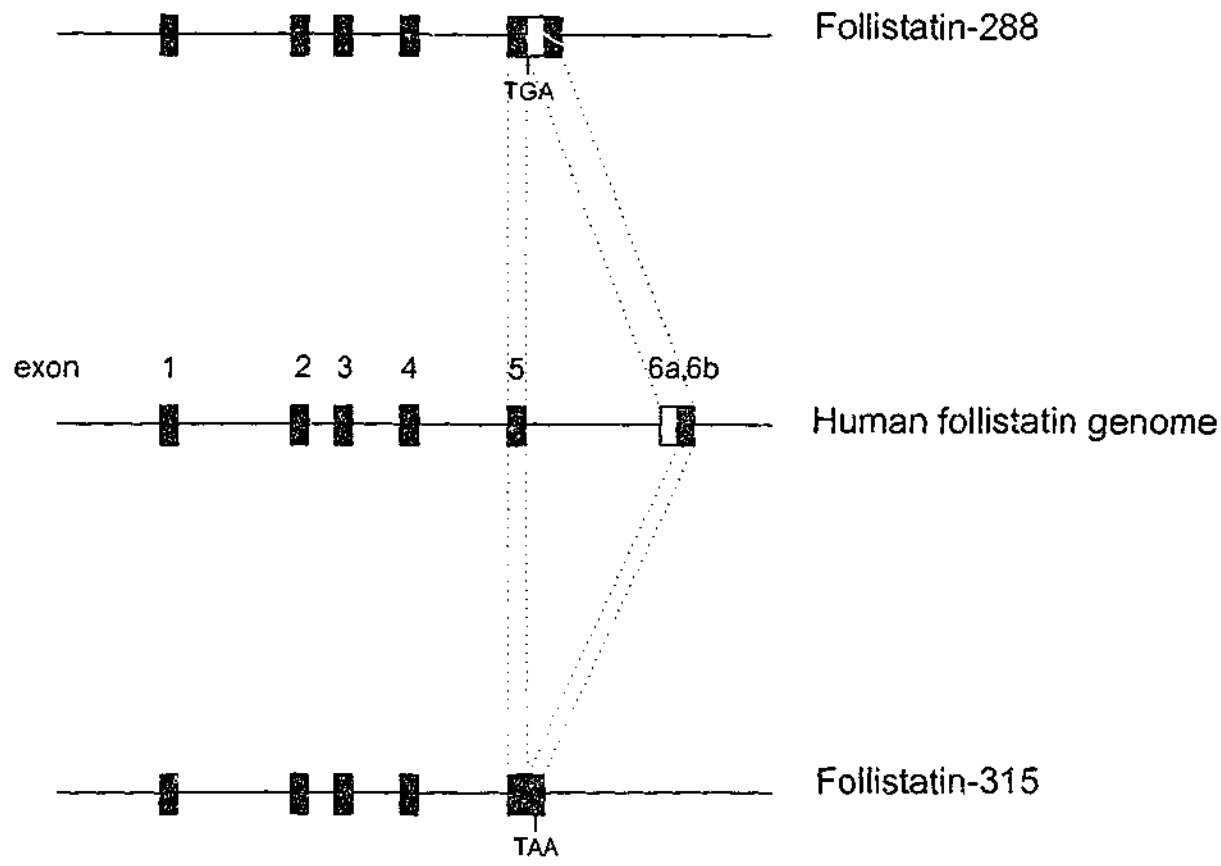

Figure 7.1 The aims of DNA engineering in genomic sequences to generate follistatin isoform-specific constructs

To generate a follistatin-288 specific genomic sequence that would force the production of follistatin-288 mRNA, the deletion of intron 5 was attempted to generate a stop codon (TGA) following the end of exon 5. Moreover, to generate a follistatin-315 specific genomic sequence that would force the production of follistatin-315 mRNA, the deletion of intron 5 plus exon 6a was attempted to allow the extension of C-terminal 27 amino acids and a stop codon (TAA) following the end of the sequence encoding this C-terminal extension.

models may be more useful than the knock-in models in future studies. For example, once the base vectors were generated and characterized, it would be relatively easy to incorporate point mutations into the follistatin transgene to study the biology of this gene. Moreover, insights would be obtained of the regulatory elements controlling the expression of the human follistatin gene.

Subsequently, the important question of what kind of constructs should be created arose. Because the expression of follistatin is under tight control during development (Feijen, *et al.*, 1994; Merino, *et al.*, 1999; Patel, *et al.*, 1999), an *in vivo* model that can express the follistatin in a physiological way would be most suitable. Thus we decided to use the natural regulatory elements that control follistatin expression. A human follistatin genomic sequence, spanning about 45 kb upstream and 45 kb downstream sequences and cloned in a PAC vector, was used for DNA engineering to create two isoform-specific transgenes. The PAC vector containing this length of the human follistatin locus was named as 'PAC-FS' (section 2.1.3). After PAC-FS was modified for the specific production of follistatin-288, it was designated as '**PAC-FSm1**'; whereas for follistatin-315, it was designated as '**PAC-FSm2**'.

7.1.2 The challenges

There are several challenges to achieve these aims. First, the PAC clone is very long making recombination difficult. It is susceptible to shearing during DNA preparation. Moreover, the ligation of the long DNA fragments and transforming them into the cells is also more difficult than for short DNA fragments. However, the most challenging aspect was how to design a strategy to engineer the long DNA, as it is really hard to find unique restriction sites in such a long sequence (about 95 kb of human genomic sequence plus about 15 kb of PAC vector sequence). Alternative methods do exist such as RARE (RecA assisted restriction endonuclease) cleavage (Callow, *et al.*, 1994), however the efficiency of this method is highly variable (JRM, personal communication). More recently, phage-based *Escherichia Coli* homologous recombination systems have been successfully developed (Copeland, *et al.*, 2001) which may have simplified our cloning strategy; however this technology was not available when I initiated this project. A major aid in completing this project was the publication

of the draft of the human genome sequence which enabled a complete restriction map of the follistatin locus to be assembled.

7.2 Experimental design & procedures

7.2.1 Mapping restriction sites

The upstream and downstream sequences of the human follistatin gene in the PAC-FS were obtained from the human genomic sequences of the follistatin locus recruited from the Homo sapiens chromosome 5 genomic contig of the NCBI data base (Accession: NT_006431). The software, Gene Construction Kit™ 2 (Textco, Inc., New Hampshire, USA), was used to map the restriction sites.

7.2.2 DNA cloning

The techniques of DNA cloning for the experiments described in this chapter are described in Section 2.2.2. PCR primers are detailed in Appendix III.

7.2.3 Pulsed field gel electrophoresis (PFGE)

Since PAC clones are very long, some of steps involved in DNA recombination required PFGE to separate long DNA in the gel. The technique for PFGE can be referred to the Section 2.2.2.3.

7.2.4 Experimental procedures

In a perspective of the whole plan, two arms of the experiments were proceeded at the same time: one for PAC-FSm1 (a follistatin-288 specific construct) and the other for PAC-FSm2 (a follistatin-315 specific construct). The modified parts (i.e. a deletion of intron 5 of the follistatin gene for PAC-FSm1 and a deletion of intron 5 plus exon 6a for PAC-FSm2) were progressively built up in some instances using short segments. The reason for applying the gradual increase of the segment size in which the modified parts are located was that suitable unique restriction sites could not be found. As a result, different restriction sites have to be used step by step. When the segment was long enough, the DNA engineering was shifted to the PAC based manipulation. After

completing the DNA engineering for PAC-FSm1 and PAC-FSm2, the DNA for both constructs was purified, quantified and validated for use in microinjection.

7.3 Results

7.3.1 Maps of DNA engineering for PAC-FSm1 and PAC-FSm2

This section describes the maps (Figures 7.2, 7.3 and 7.4) required for DNA engineering of follistatin isoform-specific transgenes in the PAC-FS vector. As mentioned before, PAC-FS includes the human follistatin gene as well its 45 kb upstream and 45 kb downstream sequences. The modified PAC-FS vector specific for follistatin-288 was designated as PAC-FSm1 and the modified PAC-FS vector specific for follistatin-315 was designated as PAC-FSm2.

In the maps, there are several terms representing different fragments which need to be defined to facilitate the description of the cloning steps. 'S1' is the segment that contains the 16 kb upstream sequence and exon 1, and is cut from the PAC-FS with the restriction endonucleases SacI (figure 7.2b). 'S2' contains the remainder of the follistatin gene and its 3 kb down stream sequence with SacI and PacI sites on either end (Figure 7.2b). Thus S1 plus S2 is actually the whole cloned DNA fragment in the pNEB-FS that has been assembled in Chapter 4. 'S3' and 'S4' are the segments within S2. S3 contains a 1.8 kb sequence with the sites of EcoRI and HindIII on both its edges (Figure 7.2c), whereas S4 contains a 2.6 kb sequence with the sites of EcoRV and NcoI on both its edges (Figure 7.2a). Further, 'm1' means the main part of the fused fragment of exon 5, exon 6a and exon 6b which is 546 bp in length, with the sites of EcoRV and XbaI on both its edges (Figure 7.2d). 'm2', however, means the main part of the fused fragment of exon 5 and exon 6b which is 282 bp in length, with the sites of EcoRV and XbaI on both its edges as well (Figure 7.2e). As will be mentioned later, m1 is specific for follistatin-288, whereas m2 is specific for follistatin-315.

In addition, 'S5' is 18 kb in length and contains all of S2 as well as some sequences that are beyond the scope of S2 (Figure 7.3b) but still within PAC-FS. Further, 'S5' has the sites of AscI and BamHI on both its ends.

Figure 7.2 The maps for constructing the follistatin isoform-specific transgenes: S1, S2, S3, S4, m1 and m2

The maps shown here were required for the experiments of DNA recombination in the smaller vectors, *i.e.* pNEB193 and pSL1180. (b) **S1** represents a segment containing exon 1 of the follistatin gene and a 16 kb upstream sequence with both flanking sites of SacI. **S2** is a segment that contains a 9 kb sequence downstream of S1 and has the flanking restriction sites of SacI and PacI. (c) **S3** is virtually a 1.8 kb segment within S2 that contains exon 5 and exon 6 and has the flanking restriction sites of EcoRI and HindIII. (a) **S4** is also a segment within S2 that spans 2.6 kb with its flanking sites of EcoRV and NcoI. (d) **m1** is a fused segment of exon 5, exon 6a and exon 6b with its flanking sites of EcoRV and XbaI. (e) However, **m2** is a fused segment of exon 5 and exon 6b with its flanking sites of EcoRV and XbaI.

Figure 7.2

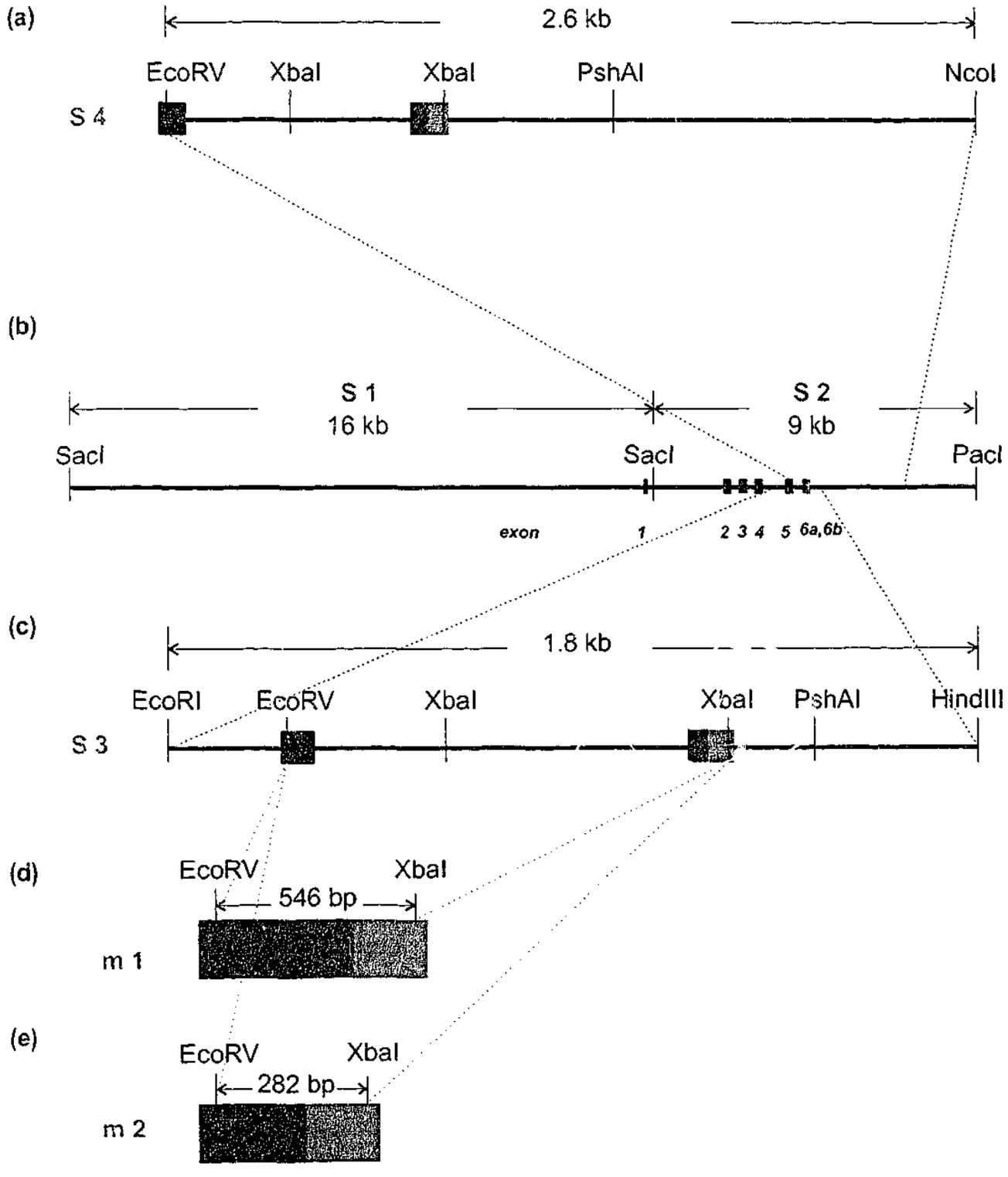
(a)
2.6 kb
EcoRV
XbaI
XbaI
PshAI
NcoI
S 4
(b)
S 1
16 kb
S 2
9 kb
SacI
SacI
PacI
exon
1
2 3 4
5
6a,6b
(c)
1.8 kb
EcoRI
EcoRV
XbaI
XbaI
PshAI
HindIII
S 3
(d)
EcoRV
XbaI
546 bp
m 1
(e)
EcoRV
XbaI
282 bp
m 2

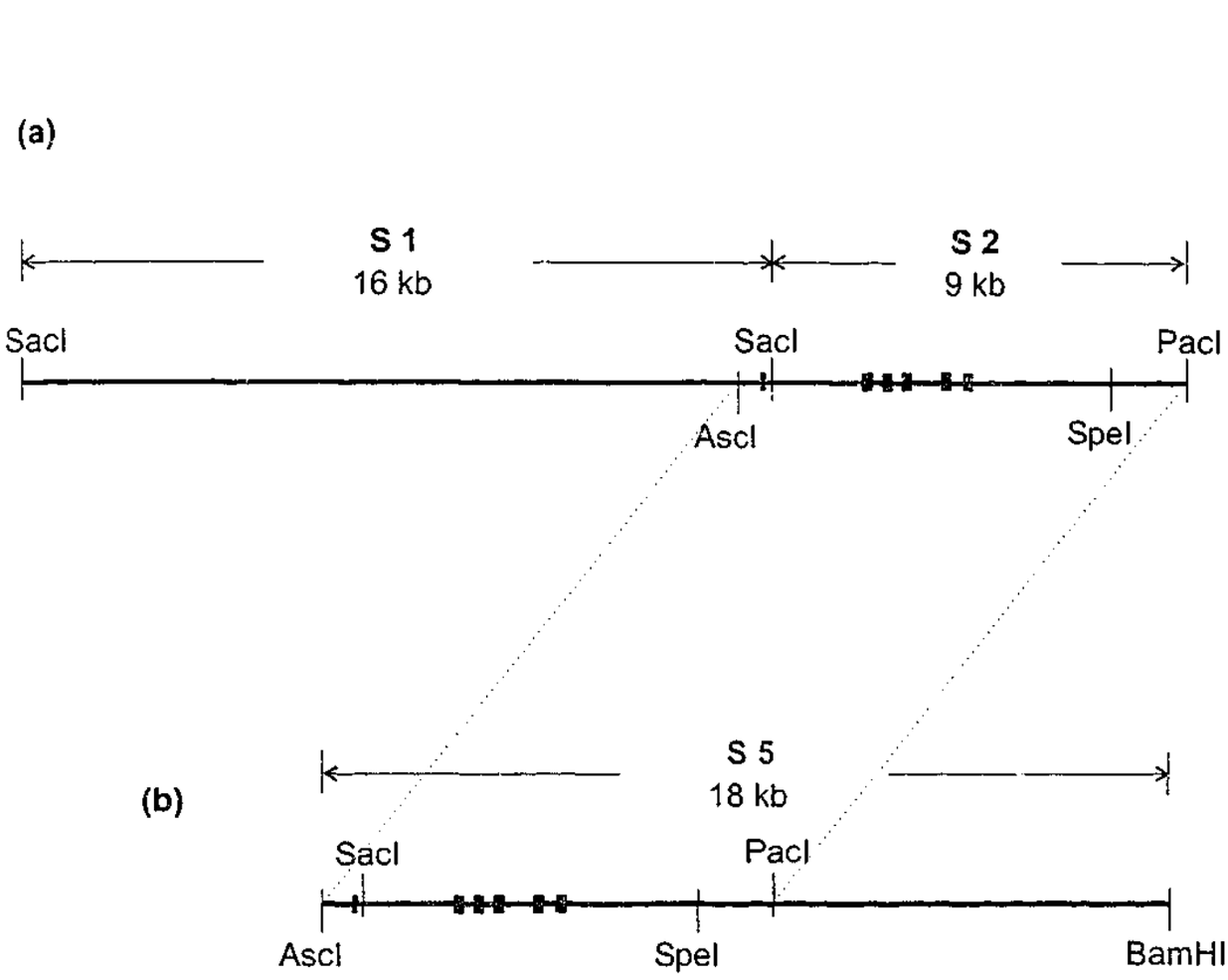

Figure 7.3 The maps for constructing the follistatin isoform-specific transgenes -- S5

(a) & (b) show that **S5** contains all of S2 as well as a short sequence upstream of S2 and a 9 kb segment downstream of S2.

In contrast to the maps in Figures 7.2 and 7.3 that were required for DNA recombination in the vectors pNEB 193 and pSL 1180, the map in Figure 7.4 was required for DNA manipulation in the PAC vector. Six restriction endonucleases that were used for DNA engineering in the PAC-FS are as follows: BsiWI, SpeI, NotI, BamHI, AscI and AatII.

To prevent single-nucleotide polymorphisms from disturbing the strategy of DNA engineering, every required restriction site was confirmed before beginning the DNA engineering.

7.3.2 Construction of human follistatin isoform-specific transgenes in PAC-FS: PAC-FSm1 and PAC-FSm2

This section will present the results of DNA engineering procedures to construct the human follistatin isoform-specific transgenes step by step.

7.3.2.1 Cloning m1 and m2 into the pCRII vector

RT-PCR for m1 and m2:

One μg of human testis total RNA (BD Biosciences Clontech, CA, USA) was used for the first strand of cDNA synthesis of reverse transcription using RNase H$^-$ reverse transcriptase, Superscript^{TM}II (Life Technologies) (figure 7.5a). The protocol for reverse transcription is found in Section 2.2.4. Two μl of the first strand reaction was used for the PCR reaction (Section 2.2.5.1). The PCR reaction was run with the primers, fs-i-F and fs-i-R-1, and *Taq* DNA polymerase (Figure 7.5b).

Cloning m1 and m2 into the pCRII vector:

The PCR reaction was electrophoresed and the predicted products of PCR reactions, 396 bp and 660 bp, were excised from the low melting temperature (LMT) gel. The target bands were then cloned into the pCRII vector (Invitrogen) by TA cloning technique and in-gel ligation method (Section 2.2.2.6 & 2.2.2.8) (Figure 7.5c). The new formed vectors were designated as pCR-m1 and pCR-m2 for the segments m1 and m2,

Figure 7.4 The maps for constructing the follistatin isoform-specific transgenes -- PAC-FS and S5

(a) **PAC-FS**, about 110 kb, is depicted with 6 restriction endonucleases (BsiWI, SpeI, NotI, BamHI, AscI and AatII). The area in which the exons of the follistatin gene are located is colored purple. (b) The position of **S5** in PAC-FS is shown here. S5 is a segment that was used to extend and incorporate the follistatin isoform specific modifications into the follistatin PAC clone from a smaller genomic fragment.

Figure 7.4

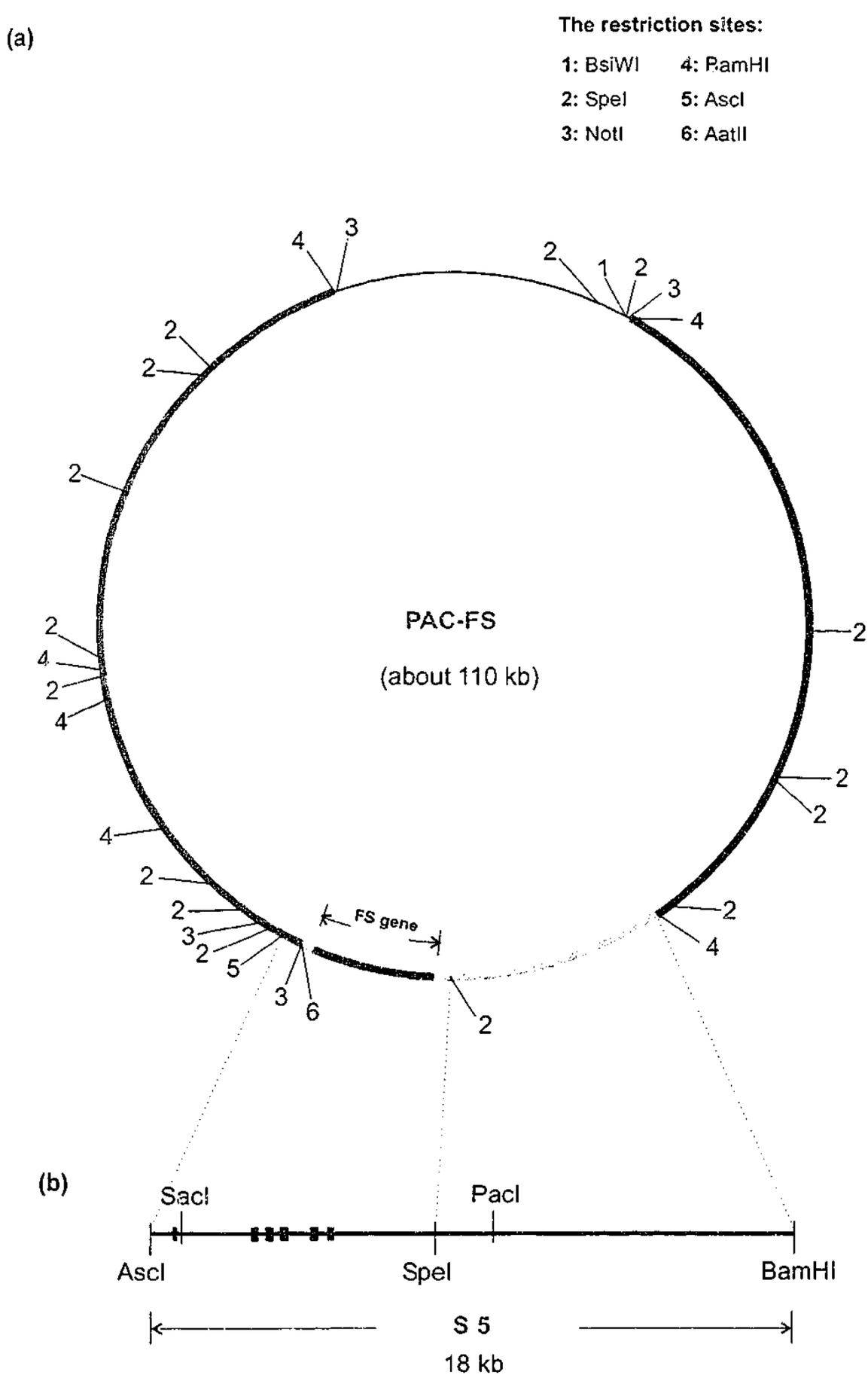
(a)
The restriction sites:
1: BsiWI
2: SpeI
3: NotI
4: BamHI
5: AscI
6: AatII
PAC-FS
(about 110 kb)
FS gene
(b)
SacI
PacI
AscI
SpeI
BamHI
S 5
18 kb

Figure 7.5 Cloning m1 and m2 into the pCRII vector

(a) Human testis total RNA was used for reverse transcription. (b) PCR reaction with Taq DNA polymerase was then performed targeting the segments of alternative mRNA splicing of the follistatin gene in the cDNA sequences. (c) The PCR products were consequently used for TA cloning in the pCRII vector. (d) After transformation, the clones hosting **m1** or **m2** were detected with PCR based screen.

Figure 7.5

(a) Total RNA of human testis

Reverse transcription

cDNA

(b) PCR with primers targeting the fragment of alternative splicing of the follistatin gene

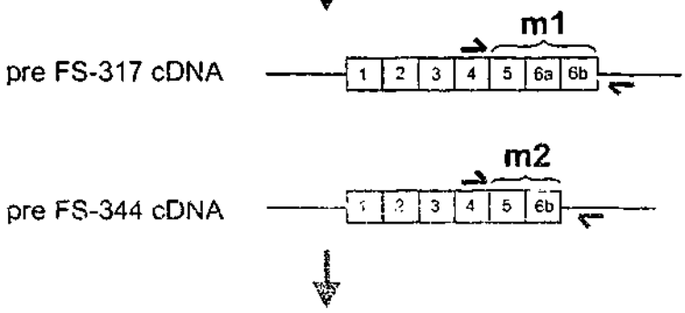

(c) PCR products (m1 & m2) were ligated into the pCRII vector by TA cloning technique.

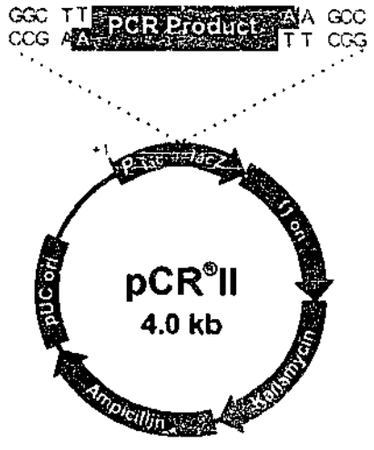

The ligation reaction mixture was transformed into DH5α cells, which were then grown on agar.

(d) Screening the colonies by PCR

respectively. The ligation reaction was further transformed into DH5α cells (Section 2.2.2.9.1). The cells were then grown on LB agar with kanamycin at 37°C overnight. After that, PCR screening of colonies was performed with the primers, fs-i-F and fs-i-R-1 (Figure 7.5d). Six colonies for pCR-m1 and pCR-m2 were picked for further growing. Following that, glycerol stocks and DNA mini-preps of pCR-m1 and pCR-m2 were made. The DNA of three clones for both pCR-m1 and pCR-m2 was then sent to be sequenced. The clones with the correct sequences were kept for further experiments.

7.3.2.2 Cloning S3 into the pNEB193 vector

Acquisition of S3 from pNEB-S2:

pNEB-S2 (Figure 7.6a & Section 4.3.2.2) and pNEB193 (Figure 7.6b) were cut with double digestion of EcoR1 and HindIII, releasing S3 from pNEB-S2 as well as linearizing and preparing pNEB193 for ligation with S3 (Figures 7.6c & d).

Ligation and transformation:

The digestion reactions were then electrophoresed in agarose gel. The target bands, S3 (1.8 kb) and pNEB193 (2.7 kb), were entrapped in LMT gel (Figure 7.6e). DNA extraction of the target bands was performed by digesting the LMT gel with β-agarase I (New England BioLabs). Subsequently, a ligation reaction was set up for S3 and linearized pNEB193 with the ratio of 1:1 between the insert and the vector at room temperature overnight. The newly formed vector was designated as pNEB-S3 The INVαF′ cells were grown on LB agar containing ampicillin at 37°C overnight, after being transformed by the ligation reaction (Figure 7.6f). PCR screening of colonies was made with the primers, fol.5.F and fol.5.R. Several positive colonies were obtained (Figure 7.6g). Two colonies were chosen for glycerol stocks and DNA mini-preps for further experiments.

Figure 7.6 Cloning S3 into the pNEB193 vector

(a) & (b) pNEB-S2 and pNEB193 were double digested with EcoRI and HindIII. That released **S3** (1.8 kb) from pNEB-S2 and linearized **pNEB193** (2.7 kb) (c & d). The digestion reaction mixture was then electrophoresed in the gel (e). S3 and the linearized pNEB193 were ligated together to form **pNEB-S3** (f). After transformation, the desired clones were detected by PCR based screening (g).

Figure 7.6

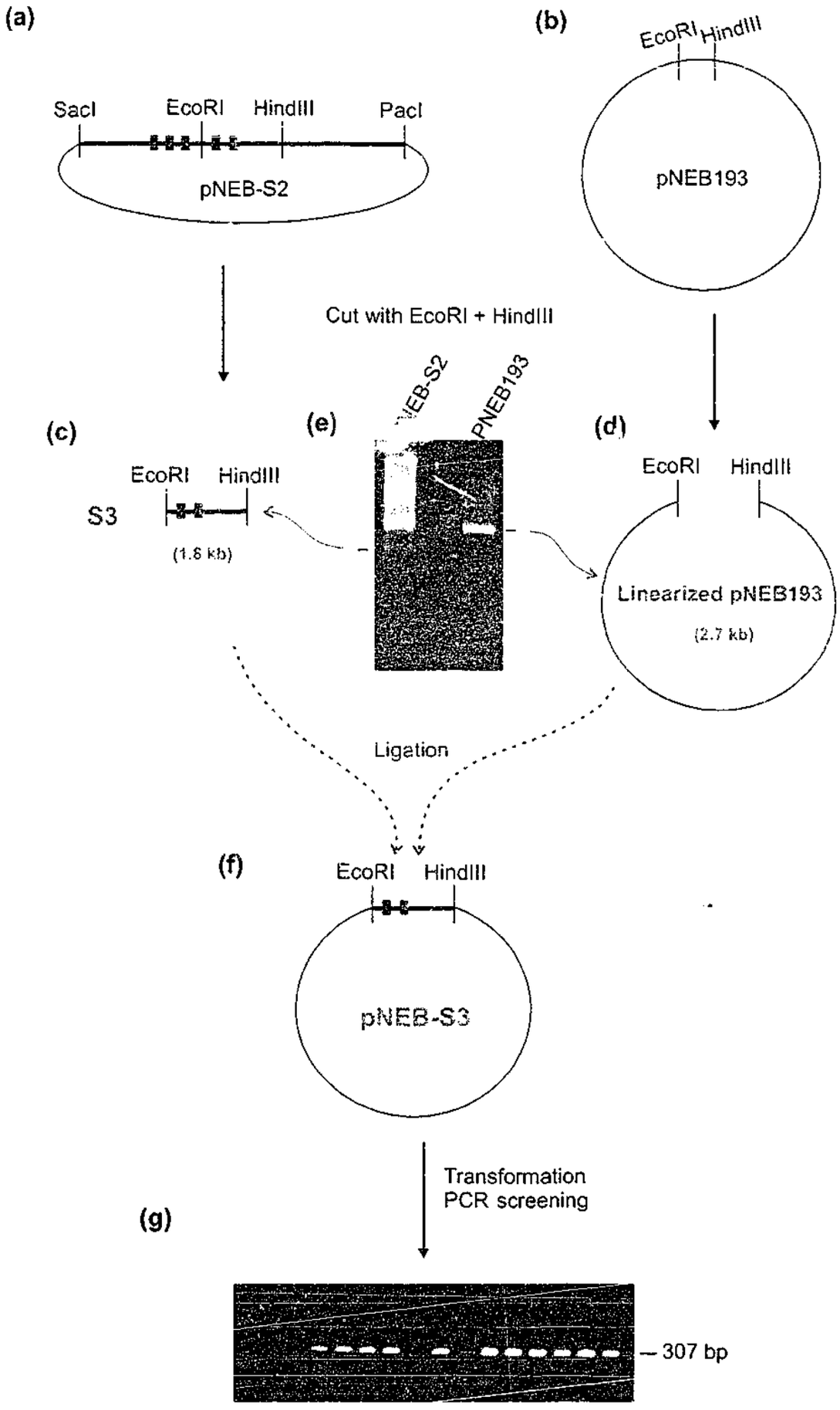
(a)
SacI
EcoRI
HindIII
PacI
pNEB-S2
(b)
EcoRI
HindIII
pNEB193
Cut with EcoRI + HindIII
(c)
EcoRI
HindIII
S3
(1.6 kb)
(e)
pNEB-S2
pNEB193
(d)
EcoRI
HindIII
Linearized pNEB193
(2.7 kb)
Ligation
(f)
EcoRI
HindIII
pNEB-S3
Transformation
PCR screening
(g)
307 bp

7.3.2.3 Cloning S4 into the pSL1180 vector

Acquisition of S4 from pNEB-S2:

pNEB-S2 (Figure 7.7a & Section 4.3.2.2) and pSL1180 (Figure 7.7b) were double digested with EcoRV and NcoI. This released S4 from pNEB-S2 and also linearized pSL1180 (Figure 7.7c & d).

Ligation and transformation:

The target bands, S4 (2.6 kb) and linearized pSL1180 (3.4 kb), were obtained via electrophoresis of the digestion reaction mixtures (Figure 7.7e). DNA extraction was then performed by QIAquick Gel Extraction kits (QIAGEN, Vic., Australia). Subsequently, a ligation reaction was set up for S4 and linearized pSL1180 with the ratio of 1:1 between the insert and the vector at 16°C overnight. The newly formed vector was designated as pSL-S4 (Figure 7.7f). The DH5α cells were grown on LB agar containing ampicillin at 37°C overnight, after being transformed by the ligation reaction. PCR screening of colonies was made with the primers, fs-x-F and fs-i-R-2. Several positive colonies were obtained (Figure 7.7g). Three colonies were chosen for glycerol stocks and further DNA mini-prep.

7.3.2.4 Assembly of pNEB-S3m1 and pNEB-S3m2

Restriction digestion:

pCR-m1, pCR-m2 (Section 7.3.2.1) and pNEB-S3 (Section 7.3.2.2 & Figure 7.8a) were double digested with EcoRV and XbaI. This released m1 (Figure 7.8b) and m2 (Figure 7.8d) as well as cutting the segment intended to be modified from pNEB-S3 (Figure 7.8c). The digestion reactions were then electrophoresed. The target bands, 546 bp, 3.4 kb and 282 bp, were obtained in LMT gel (Figures 7.8e, f & g).

Figure 7.7 Cloning S4 into the pSL1180 vector

(a) & (b) pNEB-S2 and pSL1180 were double digested with EcoRV and NcoI. That released **S4** from pNEB-S2 and linearized **pSL1180** (c & d). S4 and the linearized pSL1180 were then obtained from electrophoresis of the digestion reaction mixtures(e). Consequently, the ligation of S4 with the linearized pSL1180 led to the new vector, **pSL-S4** (f). After transformation with the ligation reaction mixture, the desired clones were obtained via PCR based screening (g).

Figure 7.7

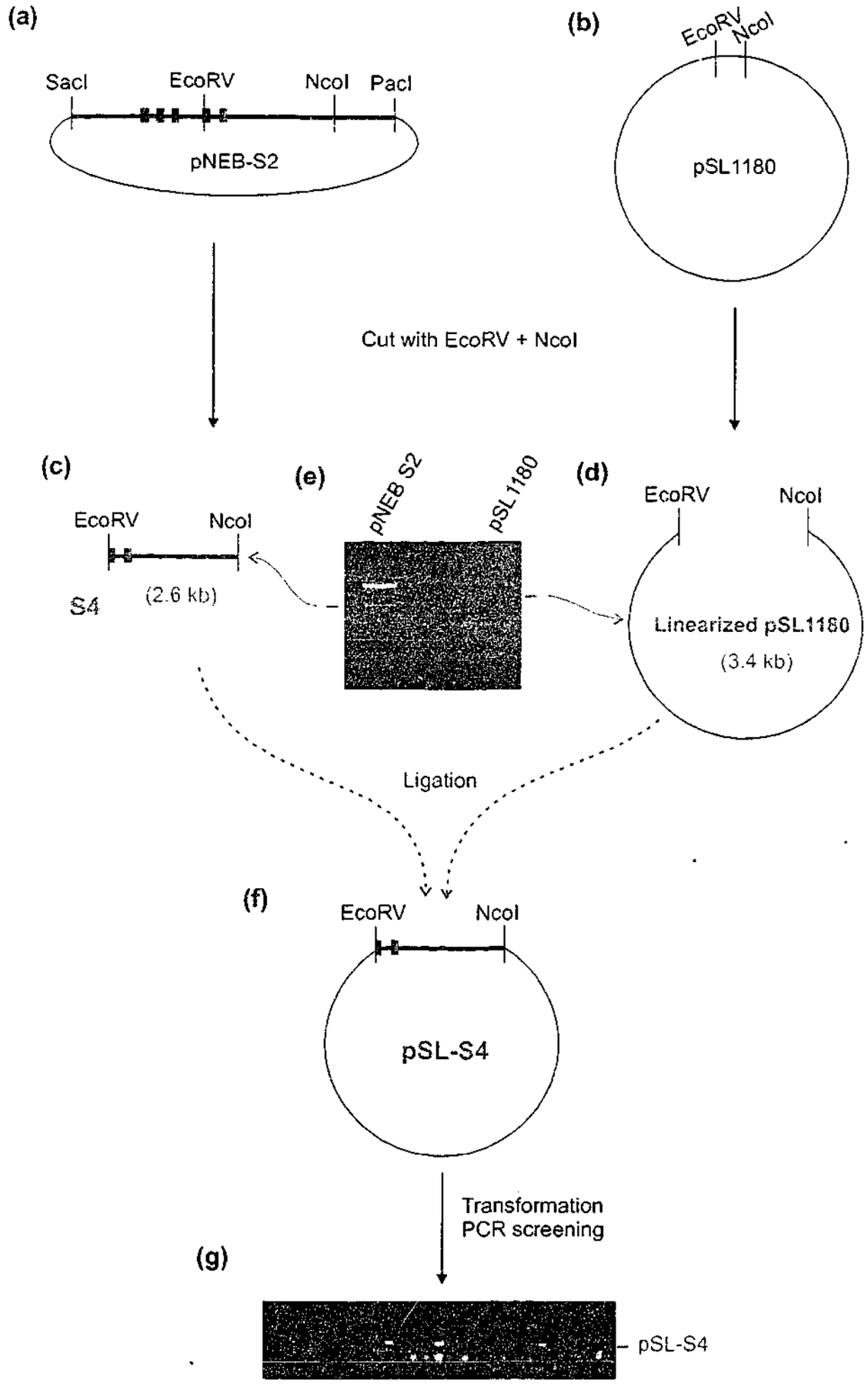
(a)
SacI
EcoRV
NcoI
PacI
pNEB-S2
(b)
EcoRV
NcoI
pSL1180
Cut with EcoRV + NcoI
(c)
EcoRV
NcoI
S4
(2.6 kb)
(e)
pNEB S2
pSL1180
(d)
EcoRV
NcoI
Linearized pSL1180
(3.4 kb)
Ligation
(f)
EcoRV
NcoI
pSL-S4
Transformation
PCR screening
(g)
pSL-S4

Figure 7.8 Assembly of pNEB-S3m1 and pNEB-S3m2

pCR-m1, pCR-m2 and pNEB-S3 (a) were double digested with EcoRV and XbaI. That released m1 (b), m2 (d) as well as cutting the segment intended to be modified from pNEB-S3 (c). Consequently, m1, m2 and the linearized pNEB-S3 were obtained via electrophoresis (e, f & g). Two sets of ligation reactions were performed to form pNEB-S3m1 and pNEB-S3m2, respectively (h & J). Further, following transformation, the desired clones were obtained via PCR based screening (i & k).

Figure 7.8

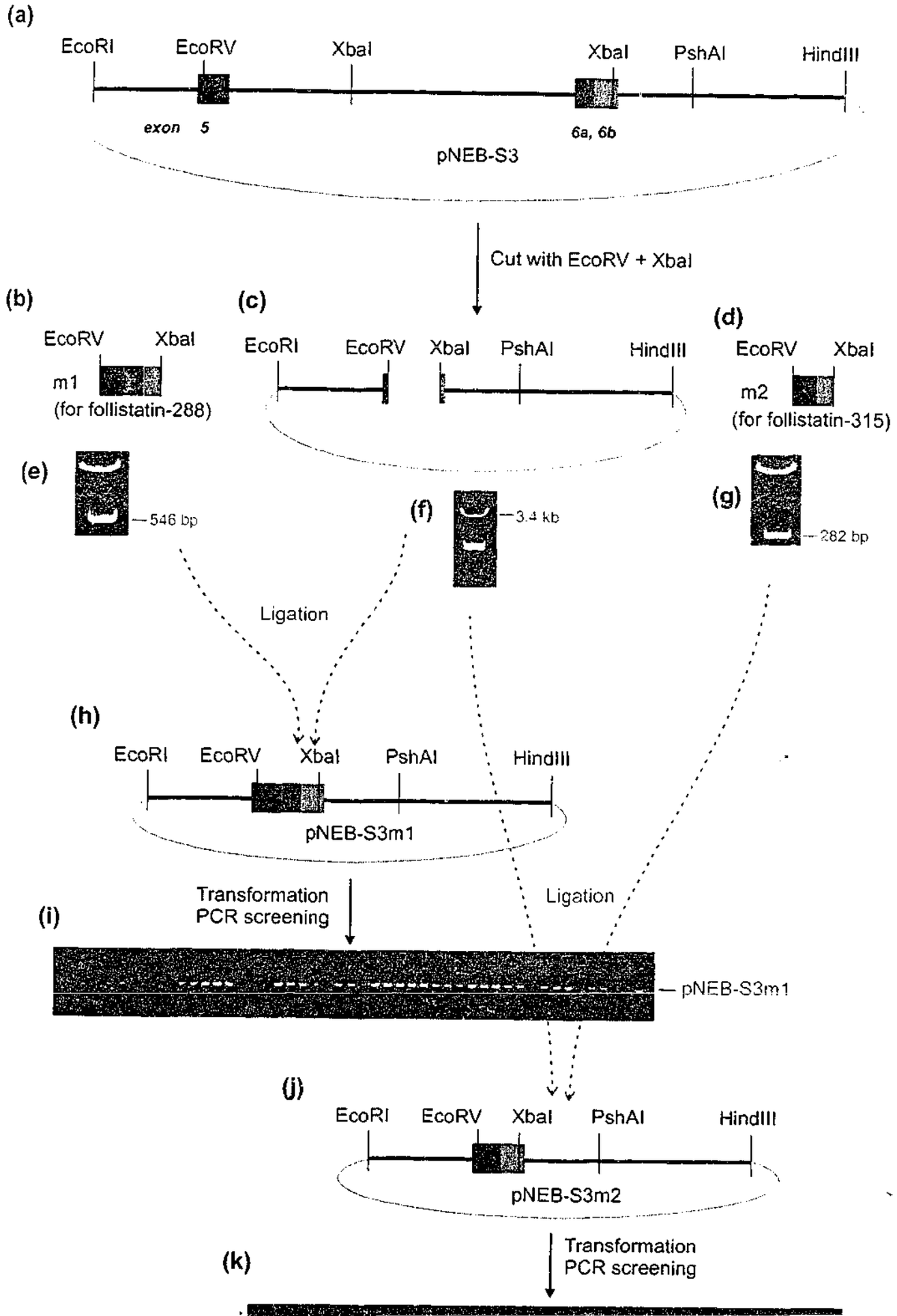
(a)
EcoRI
EcoRV
XbaI
XbaI
PshAI
HindIII
exon 5
6a, 6b
pNEB-S3
Cut with EcoRV + XbaI
(b)
EcoRV
XbaI
m1
(for follistatin-288)
(c)
EcoRI
EcoRV
XbaI
PshAI
HindIII
(d)
EcoRV
XbaI
m2
(for follistatin-315)
(e)
546 bp
(f)
3.4 kb
(g)
282 bp
Ligation
(h)
EcoRI
EcoRV
XbaI
PshAI
HindIII
pNEB-S3m1
Transformation
PCR screening
Ligation
(i)
pNEB-S3m1
(j)
EcoRI
EcoRV
XbaI
PshAI
HindIII
pNEB-S3m2
Transformation
PCR screening
(k)

Ligation, transformation and PCR screening:

Two ligation reactions (one for m1, the other for m2) were set up with T_4 DNA ligase to form the new vectors pNEB-S3m1 and pNEB-S3m2, respectively (Figures 7.8h & j). Transfer of the ligation products into cells was done by transforming electrocompetent DH10B cells. Following that, DH10B cells were grown on LB agar containing ampicillin at 37°C overnight. Further, PCR screening for the desired colonies was made with the primers, fol.5.F and fs-i-R-1. Several positive colonies were obtained (Figures 7.8i & k). Two positive colonies were chosen from each of pNEB-S3m1 and pNEB-S3m2 groups to be grown up for glycerol stocks and further experiments.

7.3.2.5 Assembly of pSL-S4m1 and pSL-S4m2

Restriction digestion:

pNEB-S3m1, pNEB-S3m2 (Section 7.3.2.4 & Figures 7.9a, c) and pSL-S4 (Section 7.3.2.3 & Figure 7.9b) were double digested with EcoRV and PshAI. This released S3m1 and S3m2 from the vectors (Figures 7.9d & f) as well as cut off the segment intended to be modified from pSL-S4 (Figures 7.9e). The digestion reactions were then electrophoresed. The target bands, 707 bp, 4.8 kb and 443 bp, were obtained in LMT gel (Figures 7.9g, h & i). DNA extraction from gel was made with QIAquick Gel Extraction kits (QIAGEN).

Ligation, transformation and PCR screening:

Two ligation reactions (one for m1, the other for m2) were set up with T_4 DNA ligase at cyclic temperature (Section 2.2.2.7) to form two new vectors pSL-S4m1 and pSL-S4m2, respectively (Figures 7.9j & k). Transfer of the ligation products into cells was done by transforming electrocompetent DH10B cells. Following that, DH10B cells were grown on LB agar containing ampicillin at 37°C overnight. Further, PCR screening for the desired colonies was made with the primers, S4-M-F and fs-i-R-2. Several positive colonies were obtained (Figure 7.9l). Two positive colonies were chosen from each of pSL-S4m1 and pSL-S4m2 groups to be grown up for glycerol stocks and further experiments.

Figure 7.9 Assembly of pSL-S4m1 and pSL-S4m2

(a, b & c) pNEB-S3m1, pNEB-S3m2 and pSL-S4 were double digested with EcoRV and PshAI. That released S3m1 (d), S3m2 (f) from the vectors as well as cutting the segment intended to be modified from pSL-S4 (e). Following electrophoresis of these digestion reactions, the target bands that were 707 bp, 443 bp and 4.8 kb for S3m1, S3m2 and the linearized pSL-S4, respectively were obtained (g, h & i). Consequently, two sets of ligation reactions were performed to form pSL-S4m1 (j) and pSL-S4m2 (k). After transformation, the desired clones were obtained via PCR based screening with primers of S4-M-F and fs-i-R-2 (l).

Figure 7.9

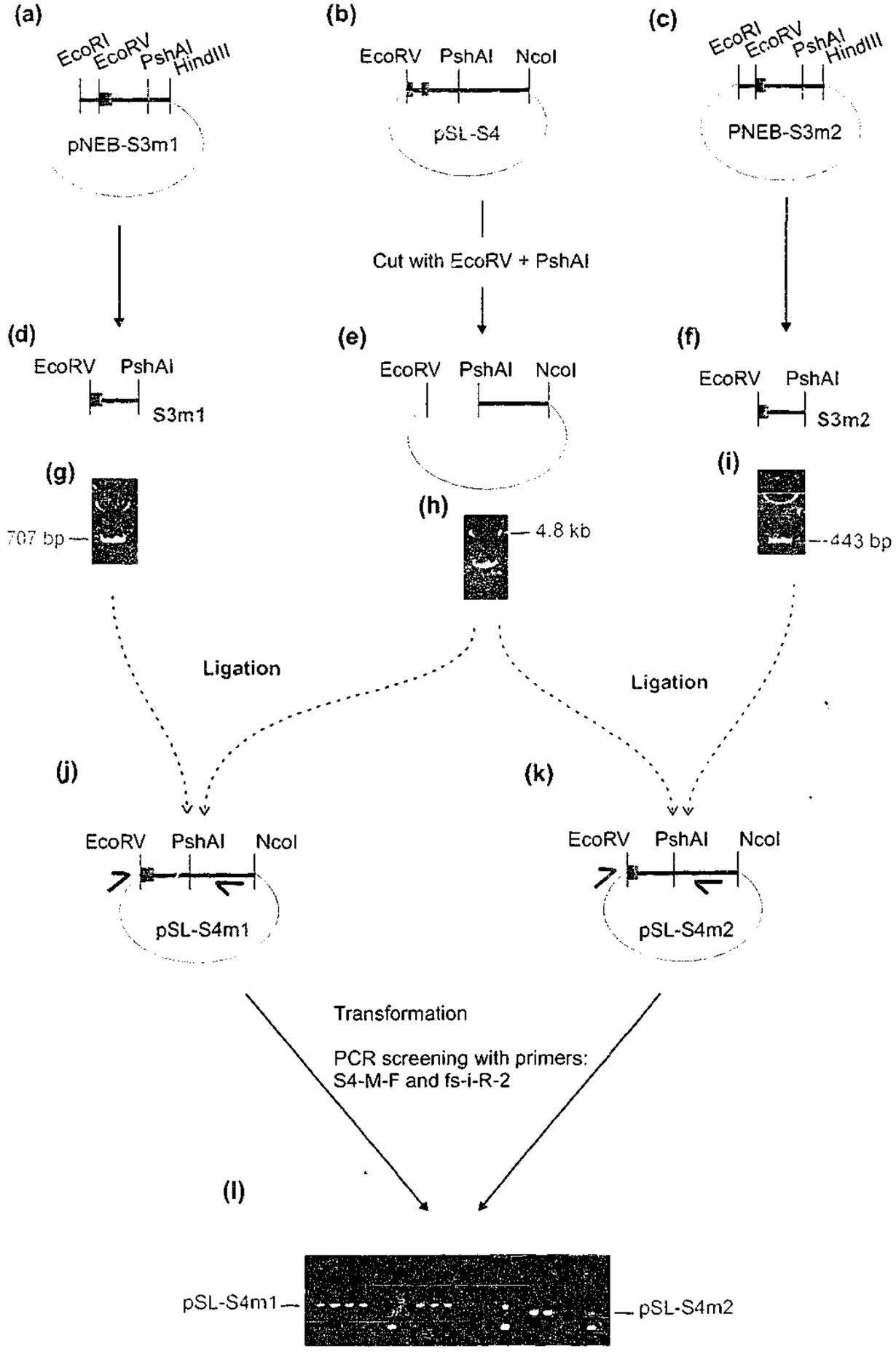
(a)
EcoRI
EcoRV
PshAI
HindIII
pNEB-S3m1
(b)
EcoRV
PshAI
NcoI
pSL-S4
(c)
EcoRI
EcoRV
PshAI
HindIII
PNEB-S3m2
Cut with EcoRV + PshAI
(d)
EcoRV
PshAI
S3m1
(e)
EcoRV
PshAI
NcoI
(f)
EcoRV
PshAI
S3m2
(g)
707 bp
(h)
4.8 kb
(i)
443 bp
Ligation
Ligation
(j)
EcoRV
PshAI
NcoI
pSL-S4m1
(k)
EcoRV
PshAI
NcoI
pSL-S4m2
Transformation
PCR screening with primers:
S4-M-F and fs-i-R-2
(l)
pSL-S4m1
pSL-S4m2

7.3.2.6 Assembly of pNEB-S2m1 and pNEB-S2m2

Restriction digestion:

pSL-S4m1, pSL-S4m2 (Section 7.3.2.5 & Figures 7.10a, c) and pNEB-S2 (Section 4.3.2.2 & Figure 7.10b) were double digested with EcoRV and NcoI. This released S4m1 and S4m2 from the vectors (Figures 7.10d & f) as well as cutting the segment intended to be modified from pNEB-S2 (Figure 7.10e). The digestion reactions were then electrophoresed. The target bands, 2.2 kb, 9.4 kb and 1.9 kb, were obtained in LMT gel (Figures 7.10g, h & i). DNA extraction from gel was made with β-agarase I (Section 2.2.2.4).

Ligation, transformation and PCR screening:

Two ligation reactions (one for m1, the other for m2) were set up with T_4 DNA ligase at cyclic temperature (Section 2.2.2.7) to form two new vectors pNEB-S2m1 and pNEB-S2m2, respectively (Figures 7.10j & k). Transfer of the ligation products into cells was done by transforming electrocompetent DH10B cells. Following that, DH10B cells were grown on LB agar containing ampicillin at 37°C overnight. Further, PCR screening for the desired colonies was made with the primers, fol.5.F and fs-i-R-1. Several positive colonies were obtained (Figure 7.10l). Two positive colonies were chosen from each of pNEB-S2m1 and pNEB-S2m2 groups to be grown up for glycerol stocks and further experiments.

7.3.2.7 Assembly of pNEB-FSm1 and pNEB-FSm2

Restriction digestion:

pNEB-S2m1, pNEB-S2m2 (Section 7.3.2.6 & Figures 7.11a, c) and pNEB-S1 (Section 4.3.2.3 & Figure 7.11b) were digested with the restriction endonuclease SacI, resulting in the release of S1 (Figure 7.11e) from pNEB-S1 and the linearization of pNEB-S2m1, pNEB-S2m2 (Figures 7.11d &f). The digestion reactions were then electrophoresed. The target bands that were 12 kb, 16 kb and 12 kb for pNEB-S2m1, S1 and pNEB-

Figure 7.10 Assembly of pNEB-S2m1 and pNEB-S2m2

(a, b & c) pSL-S4m1, pSL-S4m2 and pNEB-S2 were double digested with EcoRV and NcoI. That released S4m1 (d), S4m2 (f) from the vectors as well as cutting the segment intended to be modified from pNEB-S2 (e). Following electrophoresis of these digestion reactions, the target bands that were 2.2 kb, 1.9 kb and 9.4 kb for S4m1, S4m2 and the linearized pNEB-S2, respectively were obtained (g, h & i). Consequently, two sets of ligation reactions were performed to form pNEB-S2m1 (j) and pNEB-S2m2 (k). After transformation, the desired clones were obtained via PCR based screening with primers of fol5.F and fs-i-R-1 (l).

Figure 7.10

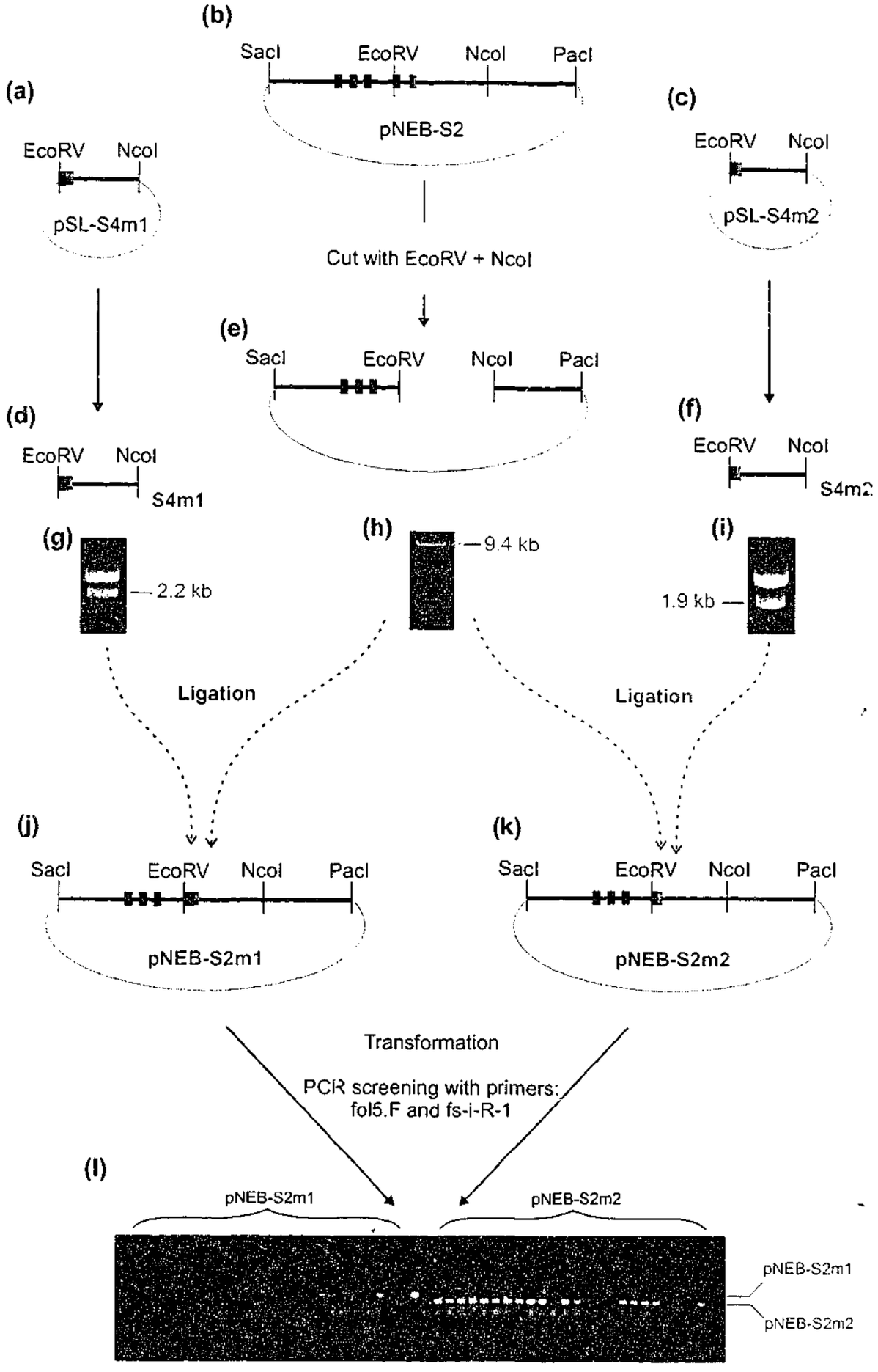
(a)
EcoRV
NcoI
pSL-S4m1
(b)
SacI
EcoRV
NcoI
PacI
pNEB-S2
Cut with EcoRV + NcoI
(c)
EcoRV
NcoI
pSL-S4m2
(d)
EcoRV
NcoI
S4m1
(e)
SacI
EcoRV
NcoI
PacI
(f)
EcoRV
NcoI
S4m2
(g)
2.2 kb
(h)
9.4 kb
(i)
1.9 kb
Ligation
Ligation
(j)
SacI
EcoRV
NcoI
PacI
pNEB-S2m1
(k)
SacI
EcoRV
NcoI
PacI
pNEB-S2m2
Transformation
PCR screening with primers:
fol5.F and fs-i-R-1
(l)
pNEB-S2m1
pNEB-S2m2
pNEB-S2m1
pNEB-S2m2

Figure 7.11 Assembly of pNEB-FSm1 and pNEB-FSm2

(a, b & c) pNEB-S2m1, pNEB-S2m2 and pNEB-S1 were cut with SacI to release S1 (e), and linearize pNEB-S2m1 (d) and pNEB-S2m2 (f). Consequently, the digestion reactions were electrophoresed. The target bands, 12 kb, 16 kb and 12 kb, were used for ligation reactions (g, h & i). Two sets of ligation reactions were then made to form the two new vectors, pNEB-FSm1 and pNEB-FSm2 (j & k). After transformation, the desired clones were obtained via PCR based screening (l & m).

Figure 7.11

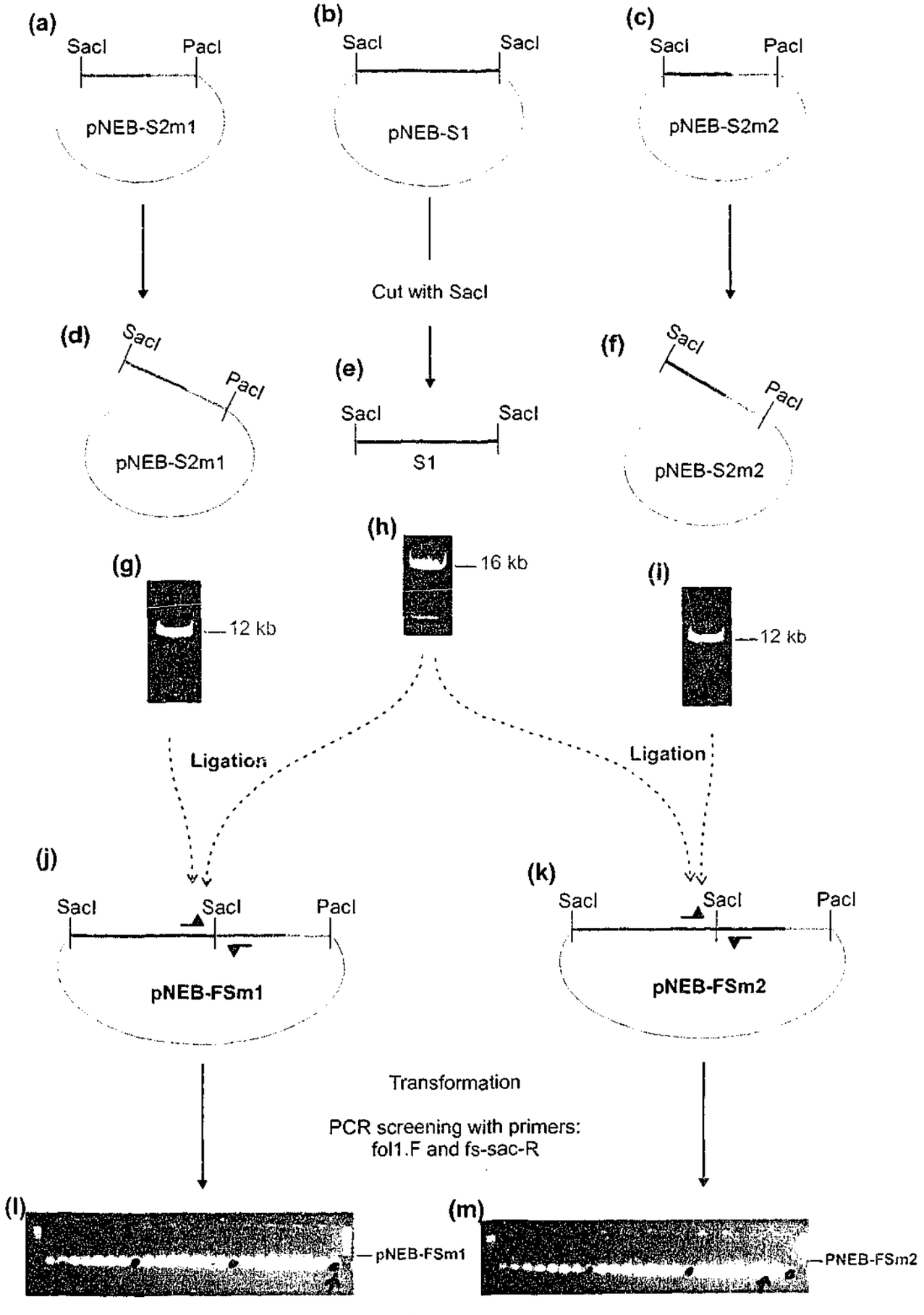
(a)
SacI
PacI
pNEB-S2m1
(b)
SacI
SacI
pNEB-S1
(c)
SacI
PacI
pNEB-S2m2
Cut with SacI
(d)
SacI
PacI
pNEB-S2m1
(e)
SacI
SacI
S1
(f)
SacI
PacI
pNEB-S2m2
(g)
12 kb
(h)
16 kb
(i)
12 kb
Ligation
Ligation
(j)
SacI
SacI
PacI
pNEB-FSm1
(k)
SacI
SacI
PacI
pNEB-FSm2
Transformation
PCR screening with primers:
fol1.F and fs-sac-R
(l)
pNEB-FSm1
(m)
PNEB-FSm2

S2m2, respectively, were obtained in LMT gel (Figures 7.11g, h & i). DNA extraction from the gel was achieved with β-agarase I (Section 2.2.2.4).

Ligation, transformation and PCR screening:

Two ligation reactions (one for m1, the other for m2) were set up with T_4 DNA ligase at cyclic temperature (Section 2.2.2.7) to form two new vectors, pNEB-FSm1 and pNEB-FSm2 (Figures 7.11j & k). Transfer of the ligation products into cells was done by transforming electrocompetent DH10B cells (Section 2.2.2.9.2). Following that, DH10B cells were grown on LB agar containing ampicillin at 37°C overnight. Further, PCR screening for the desired colonies was made with the primers, fol.1.F and fs-sac-R. Several positive colonies were obtained (Figures 7.11l & m). Two positive colonies were chosen from each of pNEB-FSm1 and pNEB-FSm2 groups to be grown up for glycerol stocks and further experiments.

7.3.2.8 Cloning S5 into the pNEB193 vector

Acquisition of S5 from PAC-FS:

PAC-FS (Section 4.3.1 & Figure 7.12b) and pNEB193 (Figure 7.12c) were double digested with AscI and BamHI, releasing S5 (Figure 7.12d) from PAC-FS as well as linearizing and preparing pNEB193 for ligation with S5 (Figure 7.12e).

Ligation and transformation:

The digestion reactions were then electrophoresed in the agarose gel. The target bands, S5 (18 kb) and pNEB193 (3 kb), were entrapped in LMT gel (Figures 7.12f & g). DNA extraction of the target bands was performed using β-agarase I (Section 2.2.2.4). Subsequently, a ligation reaction was set up for S5 and linearized pNEB193 with the ratio of 1:1 between the insert and the vector and with T_4 DNA ligase at cyclic temperature (Section 2.2.2.7) to make a new vector, pNEB-S5 (Figure 7.12h). The DH5α cells were grown on LB agar containing ampicillin at 37°C overnight, following transformation by the ligation reaction. PCR screening of colonies was made with the primers, 1.5Down.AF and 1.5Down.AR. Several positive colonies were obtained

Figure 7.12 Cloning S5 into the pNEB193 vector

(a) The restriction sites shown in this figure are labeled with numbers 1 ~ 6: 1, BsiWI; 2, SpeI; 3, NotI; 4, BamHI; 5, AscI; 6, AatII. (b & c) PAC-FS and pNEB193 were double digested with AscI and BamHI to release S5 (d) from PAC-FS and linearize pNEB193 (e). The digestion reaction was then electrophoresed. Consequently, the target bands, 18 kb and 3 kb, were obtained (f & g). The DNA from these bands was further used to set up the ligation reaction to make a new vector, pNEB-S5 (h). After transformation, the desired clones were obtained via a PCR based screening (i).

Figure 7.12

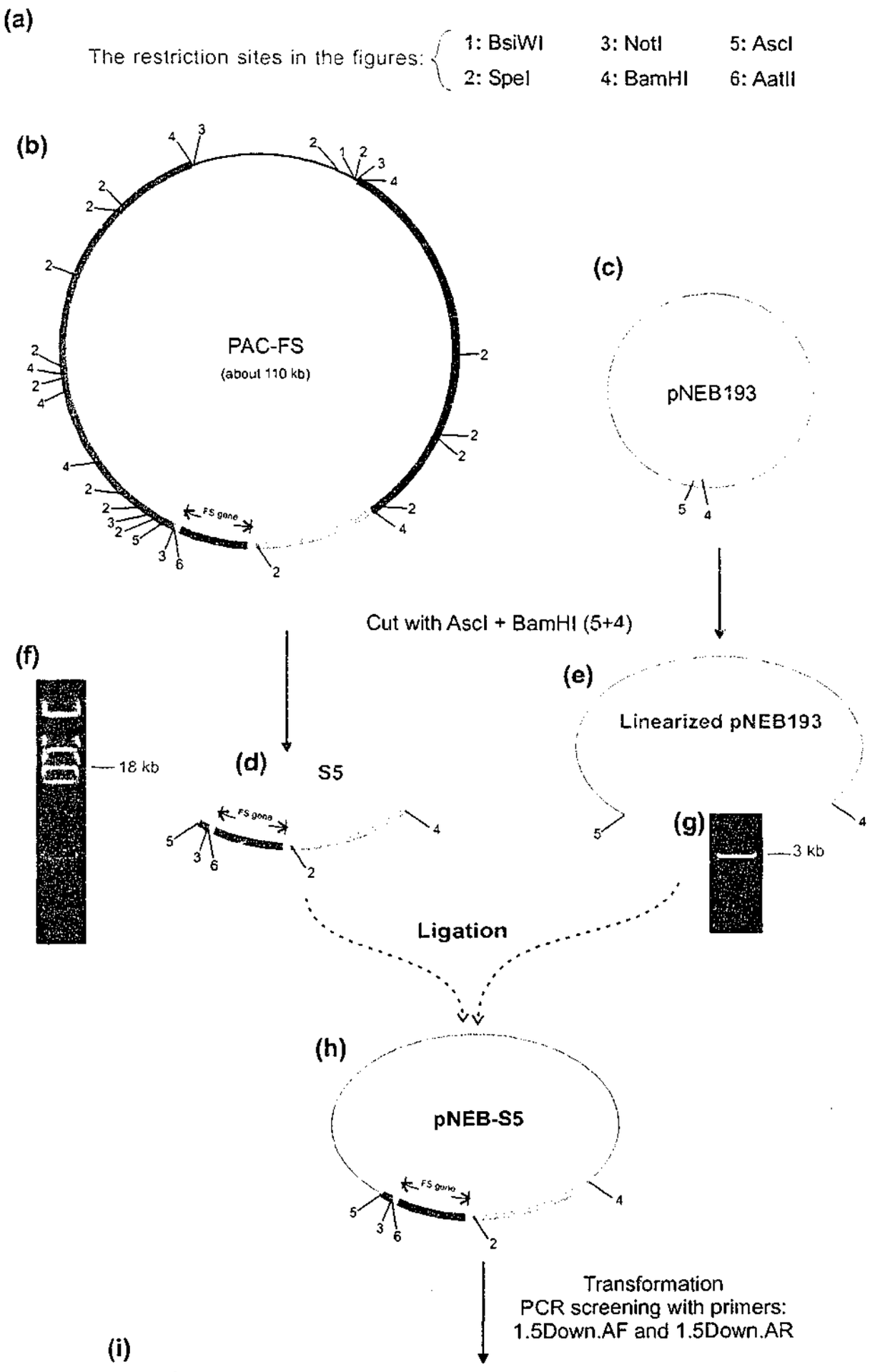
(a)
The restriction sites in the figures:
1: BsiWI
2: SpeI
3: NotI
4: BamHI
5: AscI
6: AatII
(b)
PAC-FS
(about 110 kb)
FS gene
(c)
pNEB193
Cut with AscI + BamHI (5+4)
(e)
Linearized pNEB193
(f)
18 kb
(d)
S5
FS gene
(g)
3 kb
Ligation
(h)
pNEB-S5
FS gene
Transformation
PCR screening with primers:
1.5Down.AF and 1.5Down.AR
(i)

(Figure 7.12i). Two colonies were chosen for glycerol stocks and further DNA mini-preps.

7.3.2.9 Assembly of pNEB-S5.m1 and pNEB-S5.m2

Restriction digestion:

pNEB-FSm1, pNEB-FSm2 (Section 7.3.2.7 & Figures 7.13b, d) and pNEB-S5 (Section 7.3.2.8 & Figure 7.13c) were double digested with AscI and SpeI. This released the segments (Figures 7.13e & g) from pNEB-FSm1 and pNEB-FSm2 that would be used to exchange the corresponding segment in S5 to get the isoform specific fragments extended to S5. At the same time, the digestion reaction cut off the segment intended to be modified from pNEB-S5 (Figure 7.13f), thereby allowing the linearized and digested pNEB-S5 to be available for use in the ligation reaction with the segments from pNEB-FSm1 and pNEB-FSm2 (Figures 7.13e & g). The digestion reactions were then electrophoresed. The target bands, 7 kb, 14 kb and 7 kb, for further ligation reactions were obtained in LMT gel (Figures 7.13h, i.& j). DNA extraction from the gel was made with β-agarase I (Section 2.2.2.4).

Ligation, transformation and PCR screening:

Two sets of ligation reactions (one for m1, the other for m2) were performed with T_4 DNA ligase at 16°C overnight to make two new vectors, pNEB-S5.m1 and pNEB-S5.m2 (Figures 7.13k & l). Transfer of the ligation products into cells was done by transforming DH5α cells. Following that, DH5α cells were grown on LB agar containing ampicillin at 37°C overnight. Further, PCR screening for the desired colonies was made with the primers, fs-56-F and fs-i-R-2. Several positive colonies were obtained (Figures 7.13m & n). Three positive colonies were chosen from each of pNEB-S5m1 and pNEB-S5m2 groups to be grown up for glycerol stocks and further experiments.

Figure 7.13 Assembly of pNEB-S5.m1 and pNEB-S5.m2

(a) The restriciton sites are represented with numbers 1 ~ 6. (b, c & d) pNEB-FSm1, pNEB-FSm2 and pNEB-S5 were double digested with AscI and SpeI. That released the segments (e & g) from pNEB-FSm1 and pNEB-FSm2 as well as cutting the corresponding segment intended to be modified from pNEB-S5 (f). The target bands that were 7 kb, 14 kb and 7 kb in length for further ligation were obtained through electrophoresis (h, i & k). Two sets of ligation reactions were performed to make two new vectors, pNEB-S5.m1 and pNEB-S5.m2 (k & l). After transformation with the ligation reactions, the desired clones were obtained via PCR based screening (m & n).

Figure 7.13

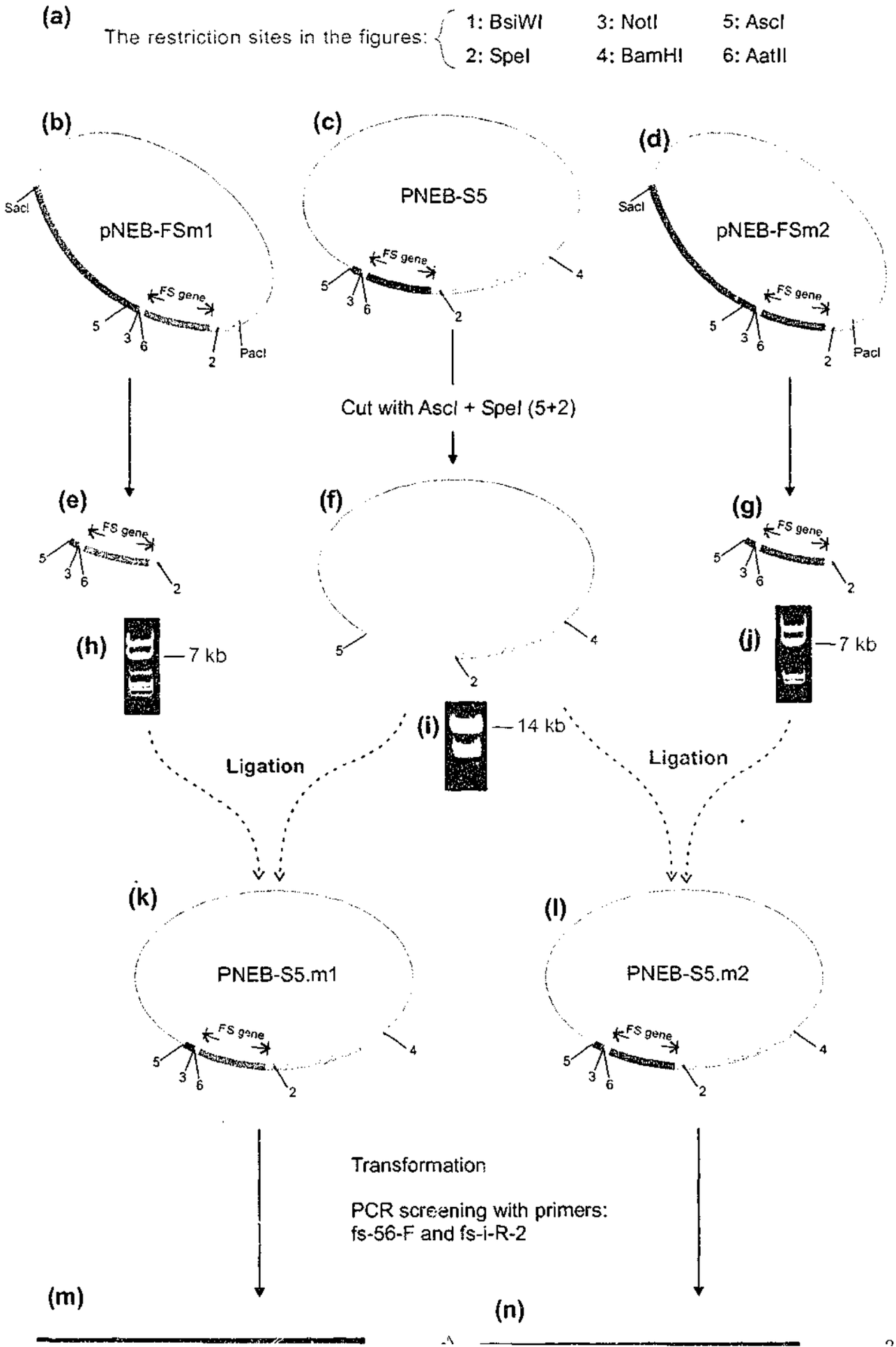
(a)
The restriction sites in the figures:
1: BsiWI
2: SpeI
3: NotI
4: BamHI
5: AscI
6: AatII
(b)
SacI
pNEB-FSm1
FS gene
5
3
6
2
PacI
(c)
PNEB-S5
FS gene
5
3
6
2
4
(d)
SacI
pNEB-FSm2
FS gene
5
3
6
2
PacI
Cut with AscI + SpeI (5+2)
(e)
FS gene
5
3
6
2
(f)
5
4
2
(g)
FS gene
5
3
6
2
(h)
7 kb
(i)
14 kb
(j)
7 kb
Ligation
Ligation
(k)
PNEB-S5.m1
FS gene
5
3
6
2
4
(l)
PNEB-S5.m2
FS gene
5
3
6
2
4
Transformation
PCR screening with primers:
fs-56-F and fs-i-R-2
(m)
(n)

7.3.2.10 Assembly of PAC-1/4Step

Restriction digestion:

PAC-FS (Section 4.3.1 & Figure 7.14b) was cut with the restriction endonuclease NotI, resulting in the release of three fragments from PAC-FS (Figures 7.14c, d & e). These three fragments were separated by pulsed field gel electrophoresis (PFGE) (Section 2.2.2.3). The two target bands that were 52 kb and 15 kb in size for further ligation were obtained in LMT gel (Figure 7.14f).

Ligation, transformation and PCR screening:

The in-gel ligation reaction (Section 2.2.2.6) was set up with T_4 DNA ligase at 16°C overnight to make a new vector, PAC-1/4Step (Figure 7.14g). Transfer of the ligation products into cells was done by transforming electrocompetent DH10B cells. Following that, DH10B cells were grown on LB agar containing kanamycin at 37°C overnight. Further, PCR screening for the desired colonies was made with the primers, prim-4steps-3F and prim-4steps-3R. One positive colony was obtained (Figure 7.14h). The positive colony was then grown up for glycerol stocks and further experiments.

7.3.2.11 Assembly of PAC-2/4Step.m1 and PAC-2/4Step.m2

Restriction digestion:

pNEB-S5.m1, pNEB-S5.m2 (Section 7.3.2.9 & Figures 7.15b, d) and PAC-1/4Step (Section 7.3.2.10 & Figure 7.15c) were double digested with AatII and BamHI. This released the most parts of the modified S5 segments from pNEB-S5.m1 and pNEB-S5.m2 (Figures 7.15e & g) as well as the backbone of PAC vector from PAC-1/4Step (Figure 7.15f). The digestion reactions were then electrophoresed by PFGE. The target bands that were 18 kb, 15 kb and 18 kb in size for further ligations were obtained in LMT gel (Figures 7.15h, i.& j).

Figure 7.14 Assembly of PAC-1/4Step

(a) The restriction sites shown in this figure are labeled with numbers 1 ~ 6. (b) PAC-FS was digested with NotI into three fragments (c, d & e), which were further separated through pulsed field gel electrophoresis (f). The target bands that were 52 kb and 15 kb in size were then used for the ligation reaction to make a new vector, PAC-1/4Step (g). After transformation with the ligation reaction, the desired clone was obtained via a PCR based screening (h).

Figure 7.14

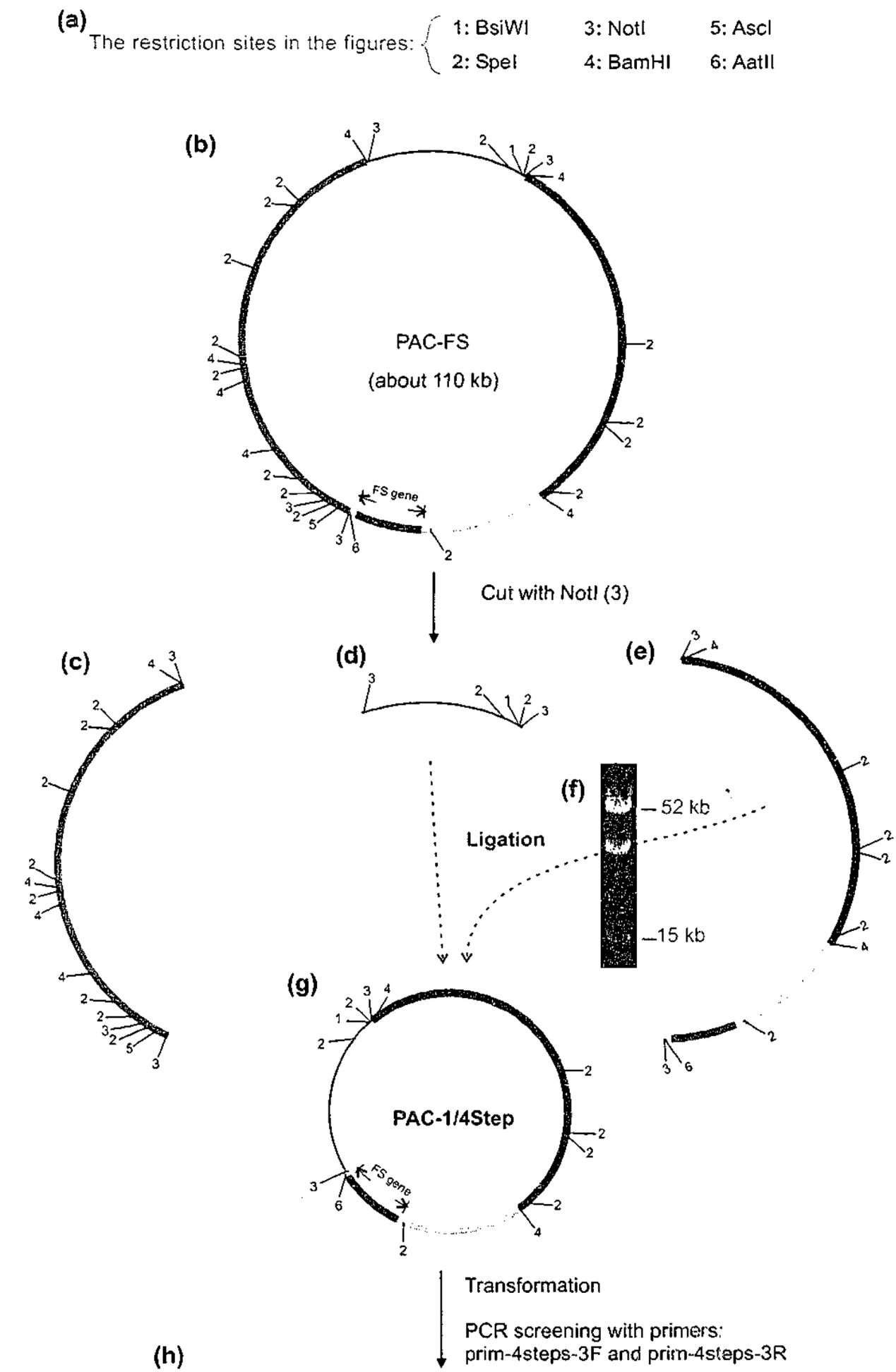
(a)
The restriction sites in the figures:
1: BsiWI
2: SpeI
3: NotI
4: BamHI
5: AscI
6: AatII
(b)
PAC-FS
(about 110 kb)
FS gene
Cut with NotI (3)
(c)
(d)
(e)
(f)
52 kb
15 kb
Ligation
(g)
PAC-1/4Step
FS gene
Transformation
PCR screening with primers:
prim-4steps-3F and prim-4steps-3R
(h)

Figure 7.15 Assembly of PAC-2/4Step.m1 and PAC-2/4Step.m2

(a) The restriction sites shown in this figure are labeled with numbers 1 ~ 6. (b, c & d) pNEB-S5.m1, pNEB-S5.m2 and PAC-1/4Step were double digested with AatII and BamHI. That released most of the modified S5 fragments from pNEB-S5.m1 and pNEB-S5.m2 (e & g) as well as the backbone of PAC vector from PAC-1/4Step (f). The DNA of these 3 fragments was obtained from the target bands (18 kb, 15 kb and 18 kb in size) through pulsed field gel electrophoresis (h, i & j). Two sets of ligation reactions were performed to make two new vectors, PAC-2/4Step.m1 and PAC-2/4Step.m2 (k & l). After transformation of ligation reactions, the desired clones were obtained via PCR based screening (m).

Figure 7.15

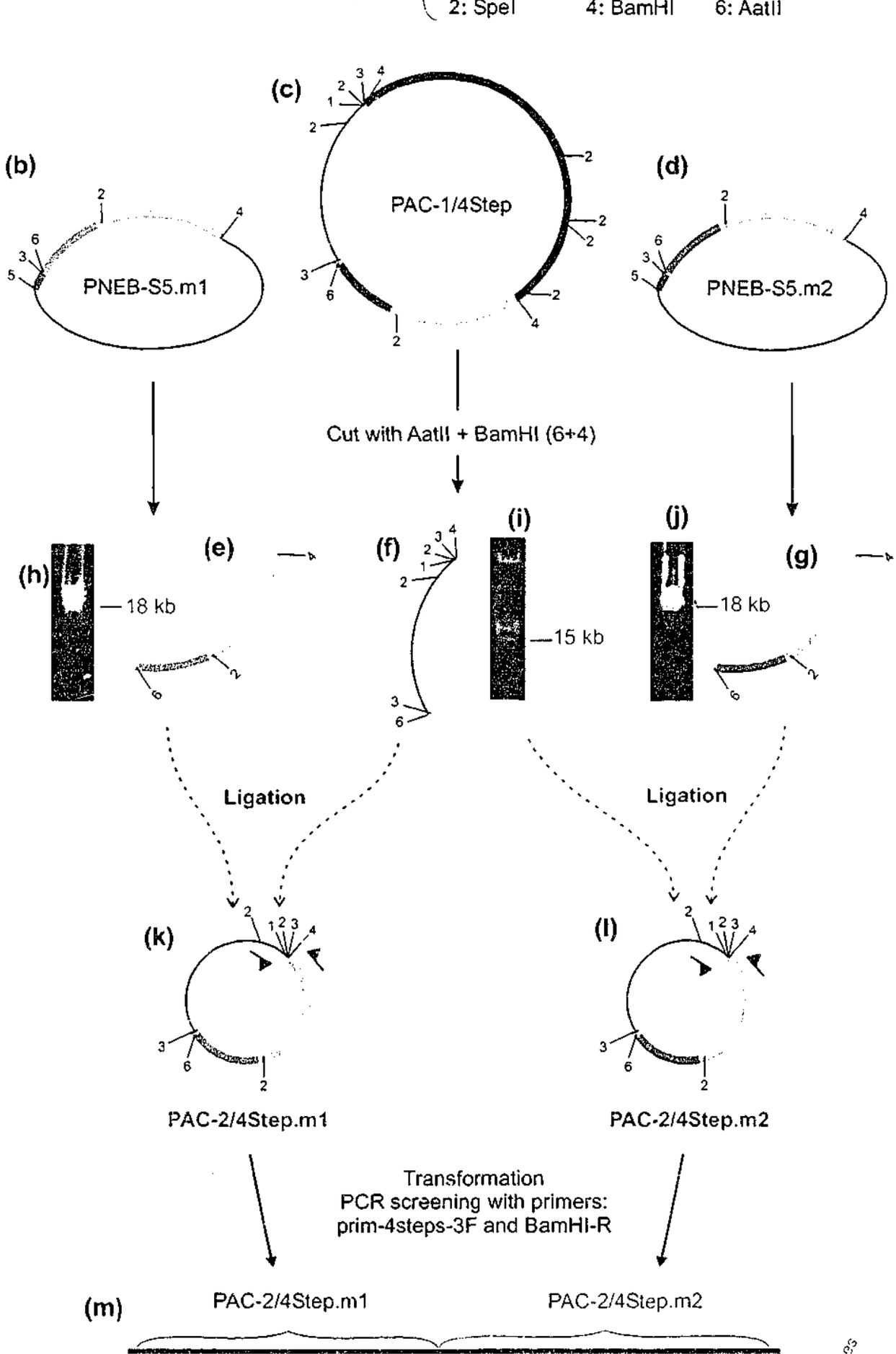
(a)
The restriction sites in the figures:
1: BsiWI
2: SpeI
3: NotI
4: BamHI
5: AscI
6: AatII
(b)
PNEB-S5.m1
(c)
PAC-1/4Step
(d)
PNEB-S5.m2
Cut with AatII + BamHI (6+4)
(e)
(f)
(g)
(h)
18 kb
(i)
15 kb
(j)
18 kb
Ligation
Ligation
(k)
(l)
PAC-2/4Step.m1
PAC-2/4Step.m2
Transformation
PCR screening with primers:
prim-4steps-3F and BamHI-R
(m)
PAC-2/4Step.m1
PAC-2/4Step.m2

Ligation, transformation and PCR screening:

Two in-gel ligation reactions (one for m1, the other for m2) were set up with T_4 DNA ligase at 16°C overnight to make two vectors, PAC-2/4Step.m1 and PAC-2/4Step.m2 (Figures 7.15k & l). Transfer of the ligation products into cells was done by transforming electrocompetent DH10B cells. Following that, DH10B cells were grown on LB agar containing kanamycin at 37°C overnight. Further, PCR screening for the desired colonies was made with the primers, prim-4steps-3F and BamHI-R. Several positive colonies were obtained (Figure 7.15m). Four positive colonies were chosen from each of PAC-2/4Step.m1 and PAC-2/4Step.m2 groups to be grown up for glycerol stocks and further experiments.

7.3.2.12 Assembly of PAC-3/4Step.m1 and PAC-3/4Step.m2

Restriction digestion:

PAC-2/4Step.m1, PAC-2/4Step.m2 (section 7.3.2.11 & figure 7.16b, d) and PAC-1/4Step (Section 7.3.2.10 & Figure 7.16c) were cut with the restriction endonuclease BamHI. This linearized PAC-2/4Step.m1 and PAC-2/4Step.m2 (Figures 7.16e & g) as well as released a segment required for further ligation from PAC-1/4Step (Figure 7.16f). The digestion reactions were then electrophoresed by PFGE. The 3 target bands that were 33.5 kb in size for further ligation reactions were obtained in LMT gel (Figures 7.16h, i.& j).

Ligation, transformation and PCR screening:

Two in-gel ligation reactions (one for m1, the other for m2) were set up with T_4 DNA ligase at 16°C overnight to make two new vectors, PAC-3/4Step.m1 and PAC-3/4Step.m2 (Figures 7.16k &l). Transfer of the ligation products into cells was done by transforming electrocompetent DH10B cells. Following that, DH10B cells were grown on LB agar containing kanamycin at 37°C overnight. Further, PCR screening for the desired colonies was made with the primers, prim-4steps-3F and prim-4steps-3R. Several positive colonies were obtained (Figures 7.16m & n). Six positive colonies were

Figure 7.16 Assembly of PAC-3/4Step.m1 and PAC-3/4Step.m2

(a) The restriction sites shown in this figure are labeled with numbers 1 ~ 6. (b, c & d) PAC-2/4Step.m1, PAC-2/4Step.m2 and PAC-1/4Step were digested with BamHI. That linearized PAC-2/4Step.m1 and PAC-2/4Step.m2 (e & g) as well as releasing a segment required for further ligation reactions from PAC-1/4Step (f). These 3 segments were obtained from the gel through pulsed field gel electrophoresis (h, i & j). Two sets of ligation reactions were performed to make two new vectors, PAC-3/4Step.m1 and PAC-3/4Step.m2 (k & l). After transformation of ligation reactions, the desired clones were obtained via PCR based screening (m & n).

Figure 7.16

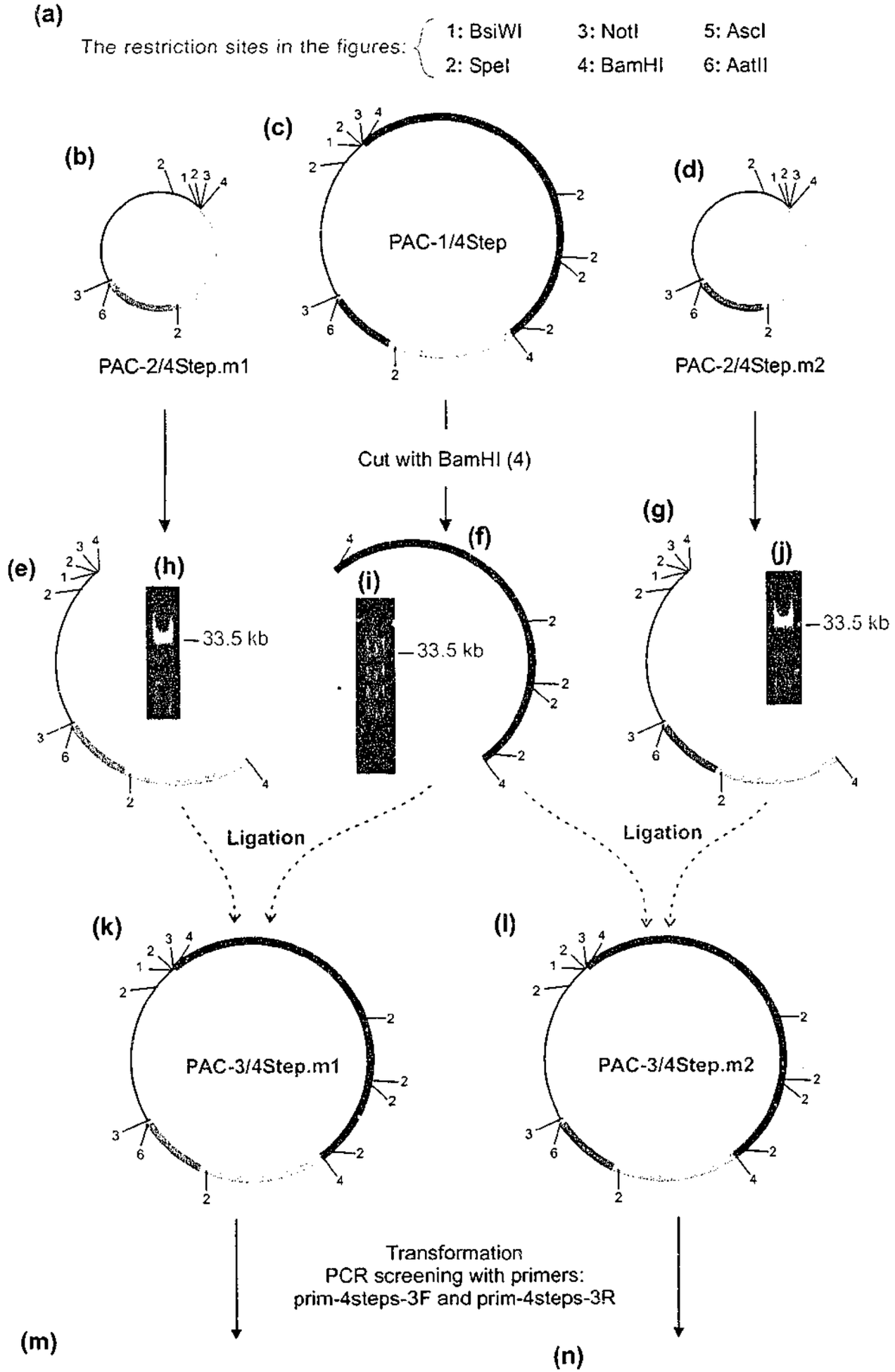
(a)
The restriction sites in the figures:
1: BsiWI
2: SpeI
3: NotI
4: BamHI
5: AscI
6: AatII
(b)
PAC-2/4Step.m1
(c)
PAC-1/4Step
(d)
PAC-2/4Step.m2
Cut with BamHI (4)
(e)
(h)
33.5 kb
(f)
(i)
33.5 kb
(g)
(j)
33.5 kb
Ligation
Ligation
(k)
PAC-3/4Step.m1
(l)
PAC-3/4Step.m2
Transformation
PCR screening with primers:
prim-4steps-3F and prim-4steps-3R
(m)
(n)

chosen from each of the PAC-3/4Step.m1 and PAC-3/4Step.m2 groups to be grown up for glycerol stocks and further experiments.

7.3.2.13 Assembly of PAC-FSm1 and PAC-FSm2

Restriction digestion:

PAC-3/4Step.m1, PAC-3/4Step.m2 (Section 7.3.2.12 & Figures 7.17b, d) and PAC-FS (Section 4.3.1 & Figure 7.17c) were double digested with BsiWI and AatII. This cut off the backbone sequence of the PAC vector from PAC-3/4Step.m1 and PAC-3/4Step.m2 (Figures 7.17e & g) as well as releasing a segment required for the final ligation from PAC-FS (Figure 7.17f). The digestion reactions were then electrophoresed by PFGE. The target bands that were 51 kb, 56 kb and 51 kb in size for further ligation reactions were obtained in LMT gel (Figures 7.17h, i.& j). DNA extraction from gel was made with β-agarase I (Section 2.2.2.4).

Ligation, transformation and PCR screening:

Two ligation reactions (one for m1, the other for m2) were set up with T_4 DNA ligase at cyclic temperature (Section 2.2.2.7) to complete the final constructs, PAC-FSm1 and PAC-FSm2 (Figures 7.17k &l). Transfer of the ligation products into cells was done by transforming the electrocompetent DH10B cells (Section 2.2.2.9.2). Following that, DH10B cells were grown on LB agar containing kanamycin at 37°C overnight. Further, PCR screening for the desired colonies was made with the primers, prim-4steps-3F and prim-4steps-3R. Several positive colonies were obtained (Figures 7.17m & n). Six positive colonies were chosen from each of PAC-FSm1 and PAC-FSm2 groups to be grown up for glycerol stocks and further experiments.

7.3.3 Preparation of constructs for microinjection

7.3.3.1 Purification

After large-scale preparation of PAC DNA from bacterial cells (Section 2.2.1.3), PAC DNA was further cleaned with chromatography on Qiagen resin (Section 2.2.1.8). Then

Figure 7.17 Assembly of PAC-FSm1 and PAC-FSm2

This figure shows the final step of DNA engineering for isoform specific constructs. (a) The restriction sites shown in this figure are labeled with numbers 1 ~ 6. (b, c & d) PAC-3/4Step.m1, PAC-3/4Step.m2 and PAC-FS were double digested with BsiWI and AatII into 3 fragments (e, f & g) required for further ligation reactions. These 3 fragments of DNA that were 51 kb, 56 kb and 51 kb in size were then obtained through pulsed field gel electrophoresis (h, i & j). Consequently, two sets of ligation reactions were performed to make two final constructs, PAC-FSm1 and PAC-FSm2 (k & l). After transformation of ligation reactions, the desired clones hosting the final constructs were obtained via PCR based screening (m & n).

Figure 7.17

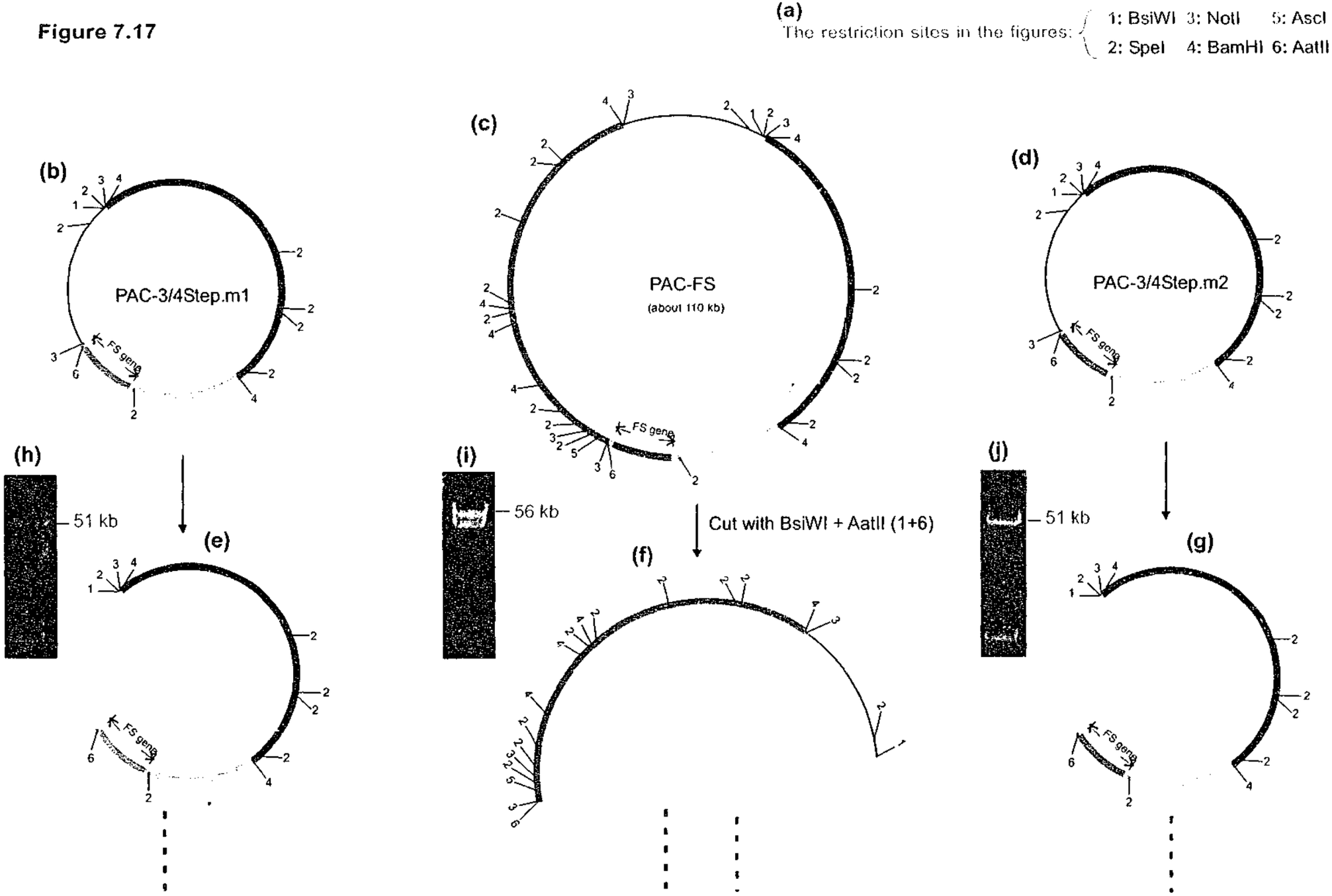
(a)
The restriction sites in the figures:
1: BsiWI 3: NotI 5: AscI
2: SpeI 4: BamHI 6: AatII
(b)
PAC-3/4Step.m1
FS gene
(c)
PAC-FS
(about 110 kb)
FS gene
(d)
PAC-3/4Step.m2
FS gene
(h)
51 kb
(e)
FS gene
(i)
56 kb
Cut with BsiWI + AatII (1+6)
(f)
(j)
51 kb
(g)
FS gene

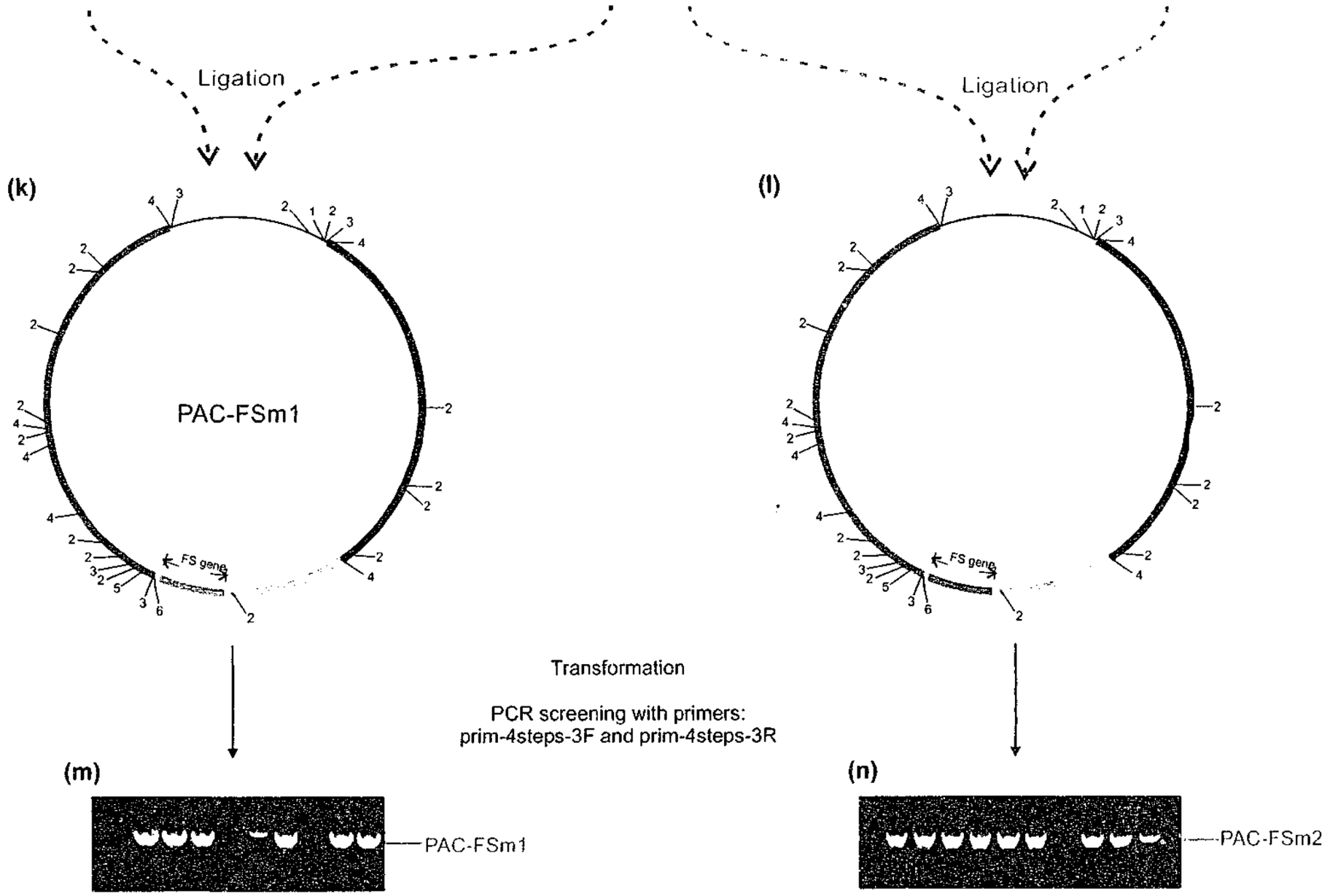
Ligation
Ligation
(k)
(l)
PAC-FSm1
FS gene
FS gene
Transformation
PCR screening with primers:
prim-4steps-3F and prim-4steps-3R
(m)
(n)
PAC-FSm1
PAC-FSm2

drop dialysis was performed to allow the DNA to be dissolved in the appropriate buffer solution for microinjection.

7.3.3.2 Quantification and validation

Spectrophotometry was used to quantify the amounts of prepared DNA. The reading at 260 nm allows calculation of the concentration of DNA. An OD of 1 corresponds to 50 µg/ml for double-strand DNA. Consequently, PAC-FSm1 and PAC-FSm2 were further validated by several restriction digestions to check if rearrangement of DNA occurred during the DNA engineering processes. Also, several PCR reactions were performed to check the areas of isoform specific modification (Figure 7.18). All data showed that no errors had occurred.

Figure 7.18 Checking PAC-FSm1 and PAC-FSm2

(a) Using restriction digestion to check PAC-FSm1 and PAC-FSm2. The DNA in lanes 1, 4, 7, 10 was from PAC-FS. The DNA in lanes 2, 5, 8, 11 was from PAC-FSm1. The DNA in lanes 3, 6, 9, 12 was from PAC-FSm2. Lanes 1,2,3 were from the digests of BamHI. Lanes 4, 5, 6 were from the digests of PacI. Lanes 7, 8, 9 were from the digests of AatII. Lanes 10, 11, 12 were from the digests of SwaI. The gel picture shows that the patterns of PAC-FSm1 and PAC-FSm2 were similar to those of PAC-FS, indicating that the sequences of PAC-FSm1 and PAC-FSm2 were grossly correct. (b) For checking the modified parts of PAC-FSm1 and PAC-FSm2, five pairs of primers were used for PCR reactions. The samples in lanes 1, 5, 9, 13, 17 were from PAC-FS. The samples in lanes 2, 6, 10, 14, 18 were from PAC-FSm1. The samples in lanes 3, 7, 11, 15, 19 were from PAC-FSm2. The samples in lanes 4, 8, 12, 16, 20 were the negative control. (c) The pair of primers for lanes 1, 2, 3, 4 were fol.1.F and fol.1.R. The pair of primers for lanes 5, 6, 7, 8 were fol.5.F and fol.5.R. The pair of primers for lanes 9, 10, 11, 12 were fs-56-F and fs-i-R-2. The pair of primers for lanes 13, 14, 15, 16 were prim-4steps-2F and prim-4steps-2R. The pair of primers for lanes 17, 18, 19, 20 were prim-4steps-3F and prim-4steps-3R. They all showed the correct sized bands (b).

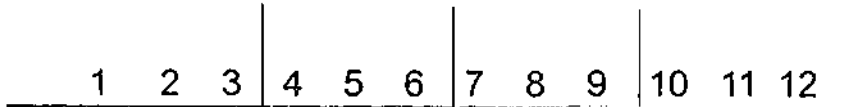

Figure 7.18

(b)

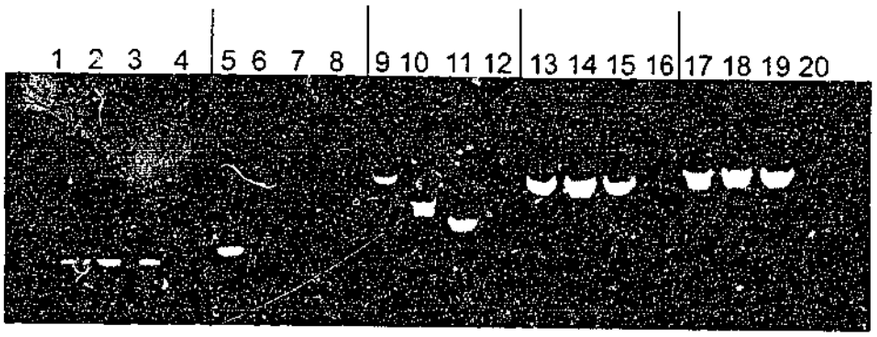

(c)

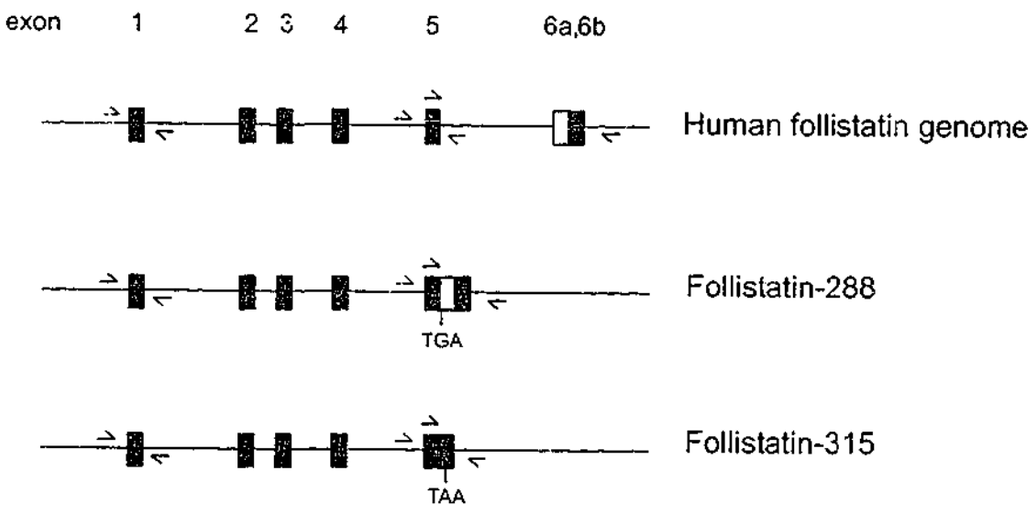

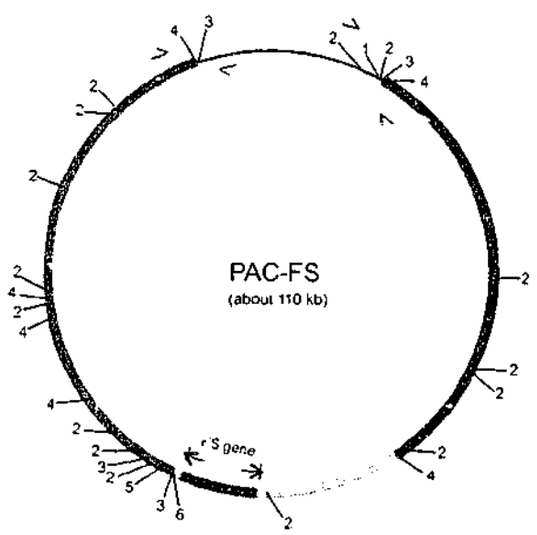

The primers used in (b):

	Lanes
⇌	1,2,3,4
⇌	5,6,7,8
⇌	9,10,11,12
⇌	13,14,15,16
⇌	17,18,19,20

7.4 Discussion

In this chapter, DNA engineering to assemble the two follistatin isoform-specific constructs in an approximately 95 kb human follistatin genomic sequence was achieved. Of the two constructs, one was devoid of intron 5 of the follistatin gene, forcing the production of mRNA for follistatin-288; the other was devoid of intron 5 and exon 6b of the follistatin gene, forcing the production of mRNA for follistatin-315.

Basically, it is difficult to remove several hundred base pairs in more 100 kb of DNA sequence. First, there has to be a good planning to know how to make the construct, since it is usually difficult to find suitable restriction sites to do DNA recombination in a direct way. A delicate strategy was designed to overcome this problem. Secondly, while doing DNA cloning, DNA of more than 30 ~ 40 kb in length is actually hard to separate in normal electrophoresis. PFGE with appropriate conditions was used to resolve this problem. Thirdly, very long DNA can be sheared easily and is often harder to ligate and transfer into cells during DNA cloning. Careful attention to detail was required to deal with these problems.

In conclusion, the work presented in this chapter was DNA engineering to construct the two follistatin isoform-specific transgenes in a 95 kb human genomic sequence of the follistatin locus. Both constructs include the human follistatin gene and its 45 kb upstream and 45 kb downstream flanking sequences, in addition to the 15 kb backbone sequence of the PAC vector. Subsequently, the two constructs were used for pronuclear microinjection to generate two kinds of transgenic lines (Chapter 8).

Chapter 8

Initial characterization of the phenotypes of the human follistatin isoform-specific mouse models

Chapter Outline:

8.1 Introduction

The importance of follistatin in regulating developmental, reproductive and non-reproductive processes is well recognized based on its role as an activin-binding protein. However, the scope of follistatin biology has recently broadened by data indicating that follistatin can regulate the biology of a number of other members of TGF-β superfamily (Fainsod, *et al.*, 1997; Iemura, *et al.*, 1998; Lee and McPherron, 2001; Otsuka, *et al.*, 2001). The follistatin knockout mice (FS-ko) are born with several developmental defects and die soon after birth due to breathing difficulties (Matzuk, *et al.*, 1995). This knockout model further highlights the importance of follistatin biology. Unfortunately, application of this *in vivo* model to study the role of follistatin in physiology is limited.

Follistatin is widely expressed as two separate isoforms: follistatin-288 and follistatin-315. The biology of each isoform is poorly understood although follistatin-315 is the likely circulating form while follistatin-288 appears to be bound to heparin-sulphate proteoglycans (Sugino, *et al.*, 1993; Schneyer, *et al.*, 1996). Follistatin-315 is expressed at approximately 20 times the level of follistatin-288 (Michel, *et al.*, 1990). A number of questions need to be addressed. Why do follistatin isoforms have such distinct biochemical characteristics? What is the biological significance of these isoforms? Are expression levels of the isoforms critical for biological functions? All these questions are essential to enable further understanding of the biology of follistatin.

In addition, several studies are exploring the clinical application of various aspects of follistatin biology. Follistatin may be useful to facilitate regeneration of the renal tubules after renal damage (Maeshima, *et al.*, 2001) and may have a role in promoting liver regeneration after partial hepatectomy (Kogure, *et al.*, 1998). Follistatin may be used in treating muscular atrophy since follistatin can potentiate hyperplasia and hypertrophy of muscle cells (Lee and McPherron, 2001) and studies indicate that follistatin may be helpful in reducing the scar formation after surgery (Wankell, *et al.*, 2001). However, clarification of the biology of follistatin isoforms would be valuable before these potential clinical uses can be developed. For instance, information is

required as to which isoform should be used in some specific situations as well as what should be the relative ratio of both isoforms should be to get the best results.

To further address the role of follistatin, the aim of the studies described in this Chapter was to establish models in which each of the follistatin isoforms was specifically expressed. To achieve this aim, constructs were created to express human follistatin-288 or follistatin-315 driven by the regulatory elements located in the 95 kb genomic sequence of the human follistatin locus. The transgene constructs, PAC-FSm1 (for follistatin-288) and PAC-FSm2 (for follistatin-315) (Chapter 7), were used to establish transgenic lines. Further, these transgenic mouse lines were crossed onto the mouse follistatin knockout background to generate "rescued mice" in which both follistatin isoforms have been separated. Subsequently, the distinct functions of both isoforms can be studied using these isoform-specific mouse models.

8.2 Experimental design & procedures

8.2.1 Experimental animals

FVB mice used for pronuclear microinjection were obtained from the Animal Resources Centre, Western Australia (ARC-WA). The C57/129 hybrid mice heterozygous for the deleted follistatin allele (Matzuk *et al.*, 1995) were used in the cross-breeding experiments. This study was approved by the Animal Ethics Committee of Monash University (MMCA 1999/18 and MMCA 2001/03) and conforms to the conditions laid down by the NH&MRC/CSIRO/AAC Australian Code of Practice for the Care and Use of Animals for Scientific Purposes (1997).

8.2.2 Pronuclear microinjection of transgenic DNA

The preparation of the DNA of transgenes, *i.e.* PAC-FSm1 and PAC-FSm2, for microinjection was described in Section 7.3.3. The methods associated with microinjection, *i.e.* hormonal stimulation and mating, embryo collection, DNA microinjection and embryo transfer, were outlined in Sections 2.2.10.2 ~ 2.2.10.6.

8.2.3 Procedures for genotyping

Genomic DNA was isolated from mouse tails (referred to Section 2.2.1.7) and then was used for genotyping. Four pairs of PCR primers, '10kb-UP.AF & R', '5kb-UP.AF & R', 'Southern.AF & R', and '1.5kb-DOWN.AF & R', were used for detecting the founders produced by the pronuclear microinjection of zygotes. 10kb-UP.AF & R and 5kb-UP.AF & R were targeting the sites about 10 kb upstream and 5 kb upstream of the human follistatin gene, respectively. Southern.AF & R was targeting the site within the follistatin gene and 1.5kb-DOWN.AF & R was targeting the site about 1.5 kb downstream of the follistatin gene. In addition, the characteristics of these four pairs of PCR primers can be referred to in Table 5.1. The conditions used for these PCRs were set up as described in Section 2.2.5.1.

For genotyping the offspring from cross-breeding, genomic DNA was isolated from mouse tails (referred to Section 2.2.1.7). Three pairs of primers, human.FS.2F & R, mouse.FS.2F & R and hHPRT.3F & R, were used to identify pups with different genetic backgrounds via PCR reactions. Human.FS.2F & R was targeting the site within the human follistatin gene, whereas mouse.FS.2F & R was targeting the site within the mouse follistatin gene. hHPRT.3F & R was targeting the site within the replacement cassette for the mouse follistatin gene in follistatin knockout mouse genome. Further, the characteristics of these primers were tabulated in Table 5.2. The conditions for the PCR reactions for these three pairs of primers were summarized in Section 5.2.3.

8.2.4 The generation of rescued mice

These transgenic mice carrying the human follistatin transgenes were crossed with the follistatin knockout heterozygotes via two steps of cross-breeding (referred to in Section 2.2.12), to generate "rescued" mice since the follistatin knockout homozygotes die soon after birth: rescued mice represent the mice that expressed the human follistatin transgenes, in the absence of the endogenous mouse gene.

8.2.5 General characterization

To maintain the transgenic lines and further use the transgenic lines to cross onto the follistatin knockout background, the mating of founders with wild-type mice (wt) was set up. Weights at birth and weaning time were recorded for 3 litters of each line. Gross examination was performed including assessment of their appearance, movement and eating behavior. Fertility was also checked, based on whether there were offspring from the matings of transgenic mice with wt mice.

For the follistatin isoform-specific rescued mice, the newborn pups were generally characterized by their appearance, weights, crown-rump length (CRL), breathing ability and survival rates. CRL was a length measured from the top of the head to the base of the tail. If the rescued pups were able to survive, the observations would then continue.

8.2.6 Statistics

SPSS® 11.0 (SPSS Inc., Chicago, USA) was the statistical software used to do the statistical analyses. Comparisons between multiple data sets were performed using one-way ANOVA followed by Tukey's post-hoc test. Differences between groups were deemed significant where $p < 0.05$.

8.2.7 Experimental design

The introduction of transgenes into the mouse genome was performed by pronuclear microinjection. The transgenic founders were then mated with wt mice to establish independent transgenic lines. The transgenic mouse lines were subsequently crossed onto the mouse follistatin knockout background by two steps of cross-breeding to generate "rescued mice". Initial characterization of the phenotypes of the follistatin isoform-specific models is presented in this chapter.

To simplify the following description, various labelings were used to designate the different mouse lines:

- wt: wild-type mice
- fs-ko: follistatin knockout mice
- FS^{95}-288-wt: mice carrying 95 kb human follistatin transgenes which specifically express human follistatin-288 in the mouse wild-type background
- FS^{95}-315-wt: mice carrying 95 kb human follistatin transgenes which specifically express human follistatin-315 in the mouse wild-type background
- FS^{95}-288-ko: mice carrying 95 kb human follistatin transgenes which specifically express human follistatin-288 in the mouse follistatin knockout background
- FS^{95}-315-ko: mice carrying 95 kb human follistatin transgenes which specifically express human follistatin-315 in the mouse follistatin knockout background

8.3 Results

8.3.1 Pronuclear microinjection data

For the PAC-FSm1 vector that was constructed in an attempt to express follistatin-288 only, as well as containing a 95 kb genomic sequence of the human follistatin locus and a 15 kb backbone sequence of the PAC vector, 359 eggs in total at the pronuclear stage were collected for microinjection. Following that, 211 embryos that looked healthy at the one-cell stage were transferred into the oviducts of the foster mice and 8 pups were born.

Similarly, for the PAC-FSm2 vector that was constructed in order to express follistatin-315 only, as well as containing a 95 kb genomic sequence of the human follistatin locus and a 15 kb backbone sequence of the PAC vector, 810 eggs in total were collected for microinjection. Subsequently, 545 embryos at the one-cell stage that looked healthy were transferred into the oviducts of the foster mice and 48 pups were born (Table 8.1).

8.3.2 Transgenic founders

Three transgenic founders (2 females, 1 male), designated as FS^{95}-288-wt.1, FS^{95}-288-wt.2 and FS^{95}-288-wt.3, were obtained from the pronuclear microinjection of the PAC-FSm1 vector; for the PAC-FSm2 vector, one transgenic founder was obtained (female), designated as FS^{95}-315-wt.1 (Table 8.1, Figure 8.1).

8.3.3 Transgenic lines carrying transgenes in wild-type background appear normal

Independent transgenic lines were generated by crossing founders with wild-type FVB mice. Offspring from the lines FS^{95}-288-wt.1, FS^{95}-288-wt.2, FS^{95}-288-wt.3 and FS^{95}-315-wt.1 and wild-type (wt) showed no differences in appearance (normal whiskers, fur, tails, eyes *etc.*) and normal daily activities. They were also all fertile. Weights at birth and at weaning time were not statistically different between each line and wt, based on

Table 8.1 Pronuclear microinjection data for the transgene constructs PAC-FSm1 and PAC-FSm2

Construct	No. of zygotes of pronuclear microinjection	No. of 1-cell embryos transferred	No. of fosters used	No. of pups born	No. of founders
PAC-FSm1	359	211	11	8	3
PAC-FSm2	810	545	23	48	1

Figure 8.1 Genotyping for detecting transgenic founders

This figure shows the genotyping evidence for detecting transgenic founders. (-) means the negative control. (+) means the positive control. Four pairs of PCR primers, 10kb-UP-AF & R, 5kb-UP-AF & R, Southern.F & R and 1.5 kb-DOWN-AF & R, are targeting the sites 10 kb upstream of, 5 kb upstream of, within, and 1.5 kb downstream of the human follistatin gene, respectively. (a) ~ (d) are the gel pictures for screening the transgenic founders carrying the PAC-FSm1 vector. (e) ~ (h) are the gel pictures for screeing the transgenic founders carrying the PAC-FSm2 vector. (a) & (e) are using the primer pair of 10kb-UP-AF & R; (b) & (f) are using the primer pair of 5kb-UP-AF & R; (c) & (g) are using the primer pair of Southern.F & R; (d) & (h) are using the primer pair of 1.5 kb-DOWN-AF & R. Thus, there are three founders from the PAC-FSm1 vector and one founder from the PAC-FSm2 vector.

Figure 8.1

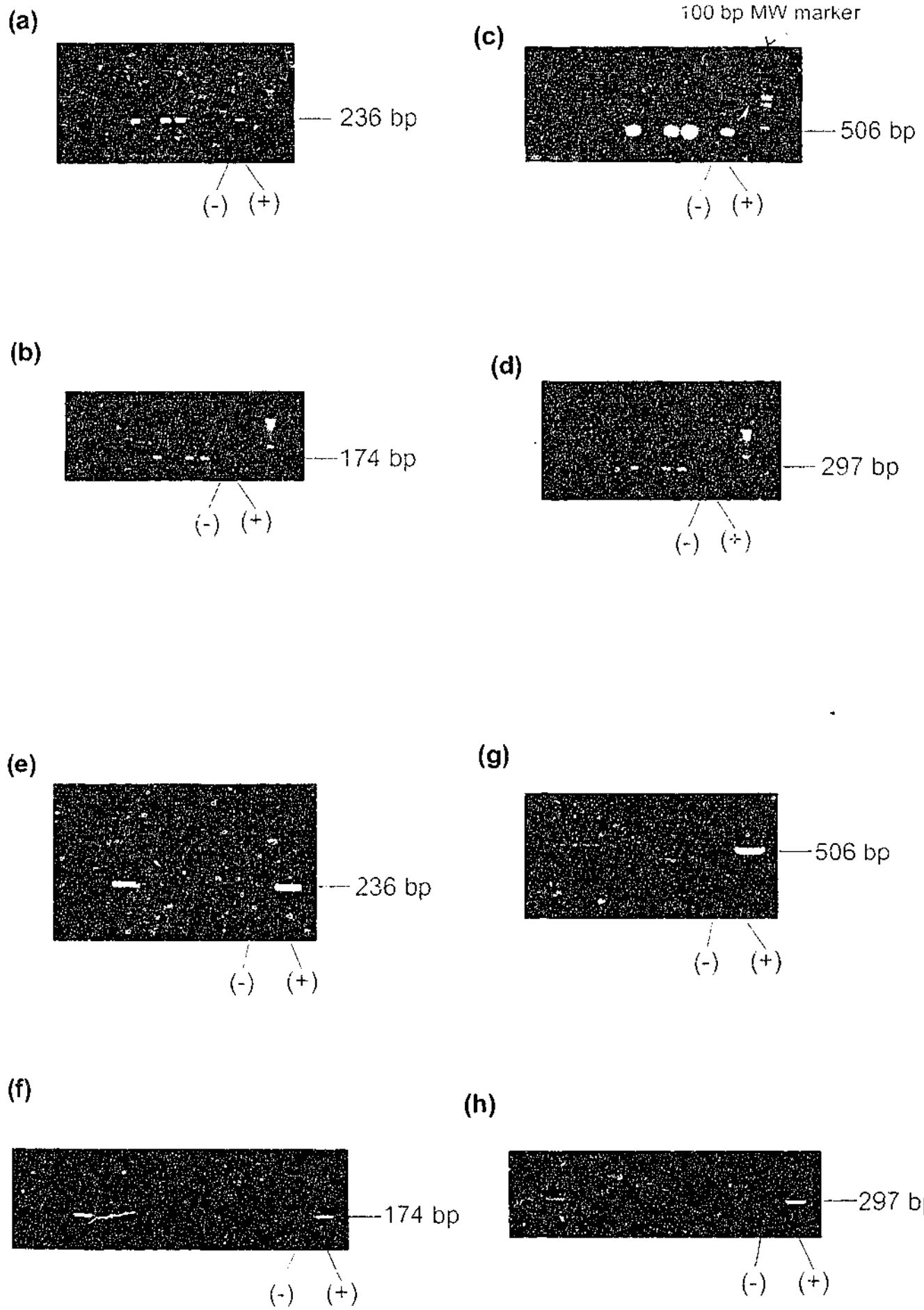
(a)
236 bp
(-) (+)
(b)
174 bp
(-) (+)
(c)
100 bp MW marker
506 bp
(-) (+)
(d)
297 bp
(-) (+)
(e)
236 bp
(-) (+)
(f)
174 bp
(-) (+)
(g)
506 bp
(-) (+)
(h)
297 bp
(-) (+)

the data of 3 litters from each line (Table 8.2). Thus, transgenic mice of the lines FS^{95}-288-wt.1, FS^{95}-288-wt.2, FS^{95}-288-wt.3 and FS^{95}-315-wt.1 were grossly normal.

8.3.4 Weights and crown-rump length (CRL) of follistatin isoform-specific rescued mice at birth

Follistatin isoform-specific rescued mice are designated as follows:

i) Follistatin-288 specific rescued mice: **FS^{95}-288-ko.1** and **FS^{95}-288-ko.2** represent the rescued mouse lines from the transgenic lines FS^{95}-288-wt.1 and FS^{95}-288-wt.2, respectively.

ii) Follistatin-315 specific rescued mice: **FS^{95}-315-ko.1** represents the rescued mouse line from the transgenic line FS^{95}-315-wt.1.

The lines FS^{95}-288-ko.1 and FS^{95}-288-ko.2 were no different from fs-ko in weight and CRL at birth, while they were smaller than wt. In contrast, the line FS^{95}-315-ko.1 was bigger than fs-ko, FS^{95}-288-ko.1 and FS^{95}-288-ko.2 in weight and CRL at birth; at the same time, FS^{95}-315-ko.1 was similar to wt in both weight and CRL at birth (Table 8.3).

8.3.5 Gross examination of follistatin isoform-specific rescued mice at birth

From gross examination, FS^{95}-288-ko.1 and FS^{95}-288-ko.2 are similar to FS^{95}-ko.1 and FS^{95}-ko.2 (referred to Chapter 5) (Figure 8.2a). FS^{95}-ko carries the 95 kb genomic sequence (PAC-FS) of the human follistatin locus, which was used as a base to delete intron 5 to make a transgene construct (PAC-FSm1) for FS^{95}-288-ko (see Chapters 4 and 7). FS^{95}-288-ko displayed better respiratory function as indicated by their pink skin color, in contrast to fs-ko which always showed respiratory distress with purple skin color at birth (Figures 8.2a,b). FS^{95}-288-ko was also more active and moved more freely than fs-ko. FS^{95}-288-ko lived for about 12 hours longer than FS-ko which usually died within 1~2 hours after birth. However, in other aspects, FS^{95}-288-ko was quite similar to fs-ko. They were much smaller than wt pups (Figure 8.2b). They had disoriented whiskers, taut and shiny skin and a flatter urogenital tubercle (Figures 8.2c,d,e,f). Further, no milk was observed in their stomachs (Figure 8.2).

Table 8.2 Weights at birth and at weaning time of transgenic mice and their wild-type littermates

Mouse line	Number	Mean ± standard deviation (at birth) (gm)	Mean ± standard deviation (at weaning) (gm)
FS^{95}-288-wt.1	15	1.28 ± 0.09	9.33 ± 0.34
FS^{95}-288-wt.2	13	1.27 ± 0.04	9.31 ± 0.31
FS^{95}-288-wt.3	11	1.30 ± 0.06	9.38 ± 0.33
FS^{95}-315-wt.1	12	1.28 ± 0.08	9.33 ± 0.36
Wild-type	45	1.29 ± 0.08	9.35 ± 0.35

Table 8.3 Weights and crown-rump lengths (CRL) at birth of rescued mouse lines and their wild-type and knockout littermates

Mouse line	Number	Weights (gm) (mean ± standard deviation)	CRL (cm) (mean ± standard deviation)
FS^{95}-288-ko.1	9	1.11 ± 0.11 [d]	2.12 ± 0.13 [c, e]
FS^{95}-288-ko.2	9	1.12 ± 0.09 [c]	2.11 ± 0.17 [d, f]
FS^{95}-315-ko.1	7	1.19 ± 0.07 [a]	2.49 ± 0.07 [a, c, f]
fs-ko	10	1.01 ± 0.10 [a, b]	2.02 ± 0.08 [a, b]
wt	10	1.29 ± 0.09 [b, c, d]	2.63 ± 0.08 [b, c, d]

(a, b, c, d, e and f represent statistical significance of $p < 0.05$.)

Figure 8.2 The phenotypes of FS^{95}-288-ko at birth

The figure shows some phenotypes of FS^{95}-288-ko at birth. (A) FS^{95}-288-ko is similar to fs-ko in size. However, fs-ko displayed early respiratory distress whereas FS^{95}-288-ko appeared to breathe well in the initial stages. In (a) the fs-ko was dying while both FS^{95}-288-ko were still active and their skin color still reflected enough oxygen in circulation. (b) The gross sizes of FS^{95}-288-ko and wt can be compared in this figure. Although FS^{95}-288-ko was smaller than wt, they moved as actively as wt. In addition, the skin of FS^{95}-288-ko was as taut and shiny as that of fs-ko. (c) & (d) The whiskers of FS^{95}-288-ko were disoriented compared to wt whose whiskers were straight (red arrows). (e) & (f) The urogenital tubercle of FS^{95}-288-ko was flat; in contrast, the genital tubercle of wt was quite obvious (red arrows).

Figure 8.2

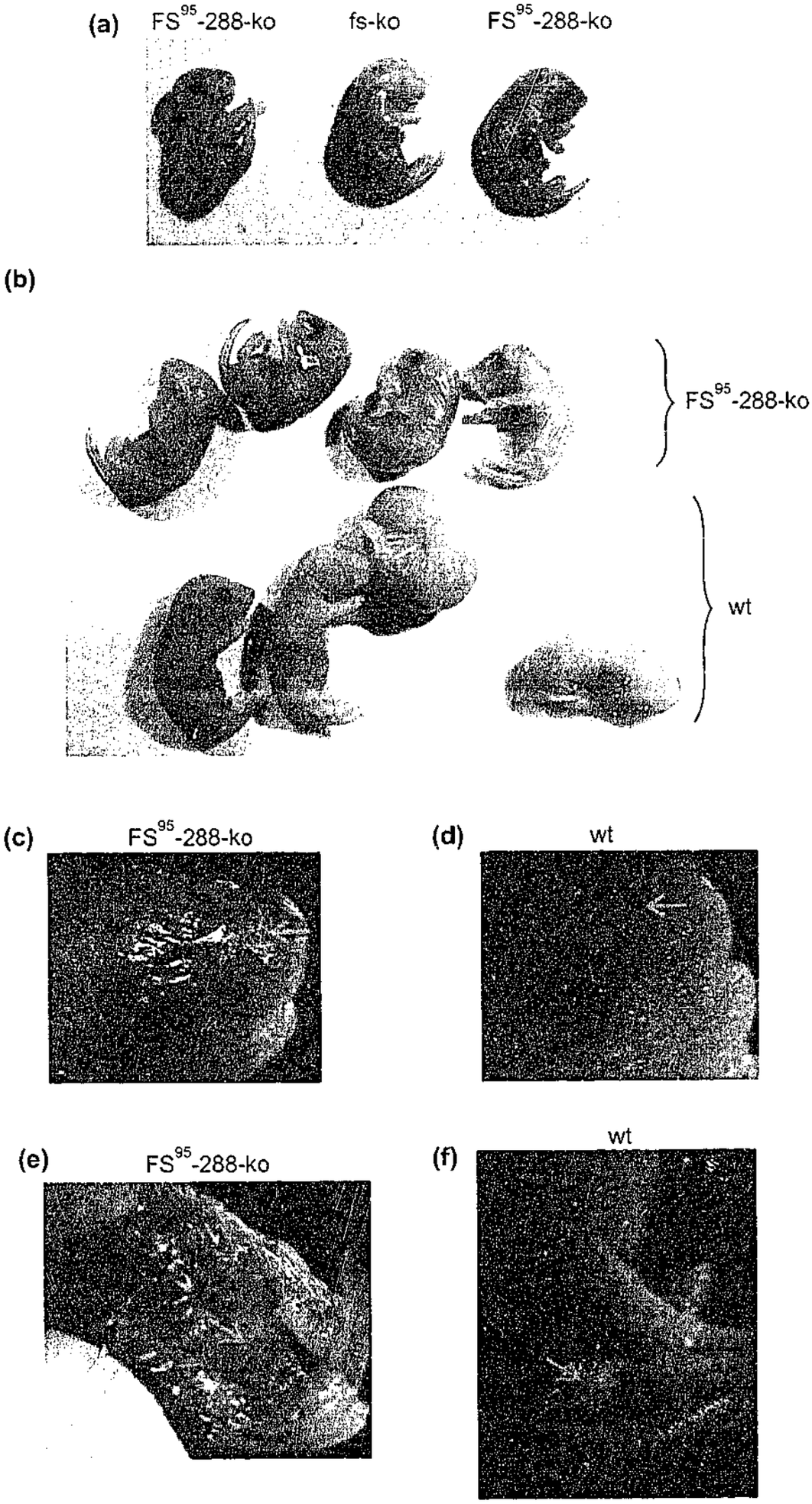
(a)
FS95-288-ko
fs-ko
FS95-288-ko
(b)
FS95-288-ko
wt
(c)
FS95-288-ko
(d)
wt
(e)
FS95-288-ko
(f)
wt

Interestingly and surprisingly, FS^{95}-315-ko.1 looked quite different from FS^{95}-288-ko and fs-ko. Their sizes were similar to wt pups (Figure 8.3a). Some of them still had slightly disoriented whiskers (Figure 8.3b). Their skin looked normal, without the taut and shiny characteristics of the skin of the fs-ko (Figure 8.3a). Further, the genital tubercle in FS^{95}-315-ko.1 was more obvious than that of the FS^{95}-288-ko and fs-ko mice, but was still flatter than that of the wt pups (Figure 8.3d). The tails of FS^{95}-315-ko.1 were similar to wt pups in length at birth. Afterwards, the tips of the FS^{95}-315-ko.1 started to display a red color and became shorter than that of wt (Figures 8.3a and 8.4i). Importantly, FS^{95}-315-ko.1 appeared as active as wt pups and milk could be easily identified in their stomachs (Figure 8.3).

8.3.6 Follistatin-315 specific genomic transgene prevented the neonatal fatality of follistatin knockout mice in contrast to follistatin-288 transgene

Of note, FS^{95}-315-ko.1 survived, in remarkable contrast to FS^{95}-288-ko that died around one day after birth. Some other interesting phenotypes became apparent as FS^{95}-315-ko.1 pups developed. First, they grew more slowly than wt pups (Figure 8.4a). Their tails were shorter compared to their body size (Figure 8.4a). Importantly, the tips of their tails were usually red and showed small nodules along the tip of the tail (Figure 8.4h). The red color at the tip of their tails sometime became black in color (Figures 8.4i, j,k), implying a gangrenous change due to compromised blood supply. At about 10 days of age, a parting of their hair appeared in the midline of the dorsum of their heads and backs but then disappeared by 3 weeks of age (Figure 8.4f). The disoriented whisker pattern became less obvious with age. The penis and clitoris looked normal (Figure 8.4e), although they seemed smaller than those of wt mice. Further, they had microphthalmia (Figure 8.4c). FS^{95}-315-ko.1 males proved to be fertile and appeared to be able to live up to 2 ~ 3 months. However, FS^{95}-315-ko.1 females appeared infertile although they did mate (Figure 8.4).

Figure 8.3 The phenotypes of FS^{95}-315-ko at birth

The figure shows some phenotypes of FS^{95}-315-ko at birth. (a) The four pups on the left side of the figure were FS^{95}-315-ko and the right one was wt. Obviously, they were similar in sizes and skin textures. (b) & (c) Some of whiskers of FS^{95}-315-ko still appeared disoriented but were less curly than those of FS^{95}-288-ko shown in Figure 8.2. In contrast, the whiskers of wt were straight (black arrows). (d) & (e) The urogenital tubercle of FS^{95}-315-ko was much flatter than that of wt (black arrows).

Figure 8.3

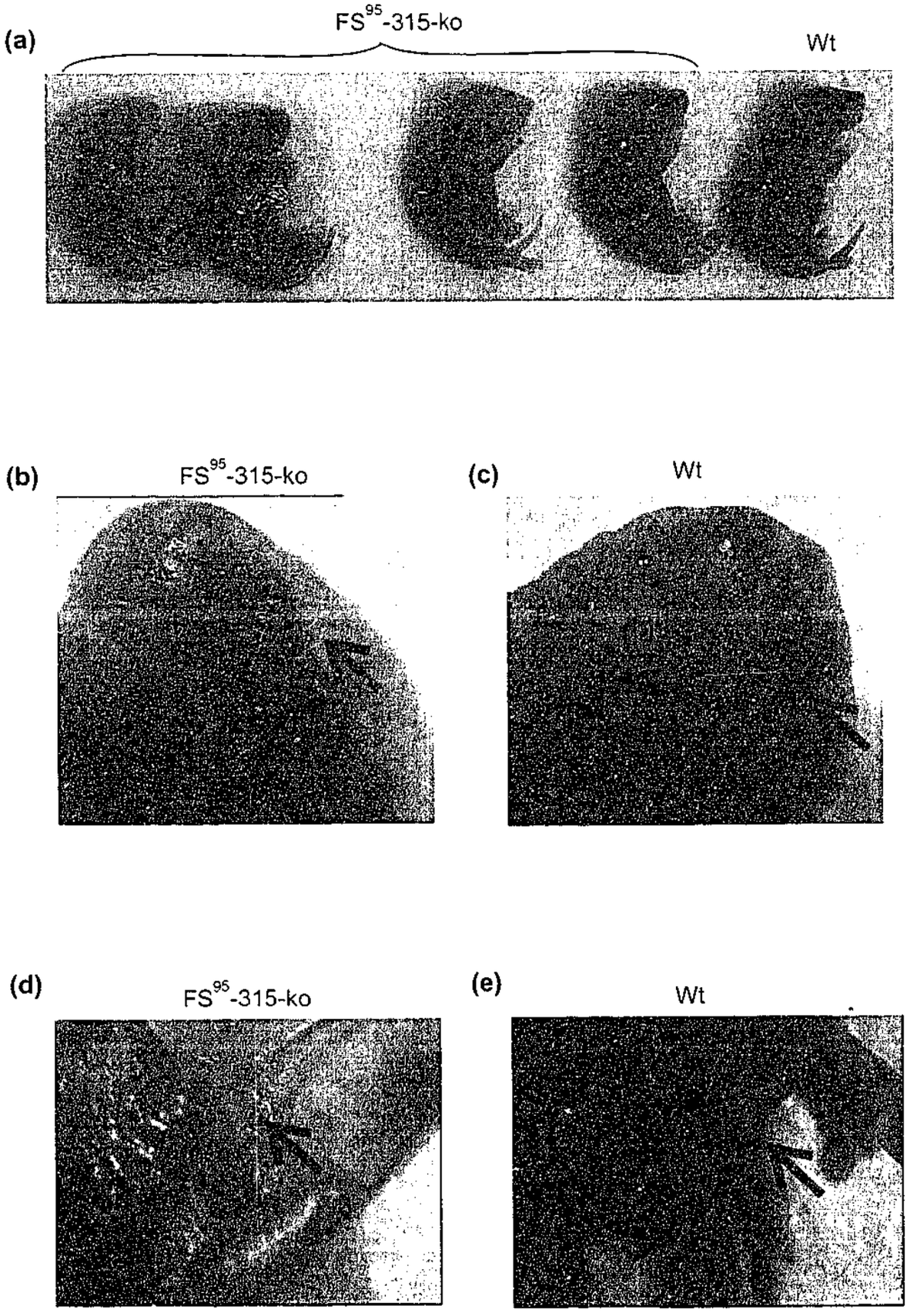

Figure 8.4 The phenotypes of FS^{95}-315-ko on day 10 and afterwards

The figures show some phenotypes of FS^{95}-315-ko. (a) The left one was wt and the right one was FS^{95}-315-ko. FS^{95}-315-ko was smaller in body size and its tail was shorter compared to wt on day 10 after birth. (b) In addition, on day 10 when pups had not yet opened their eyes, the eyelids of FS^{95}-315-ko (the left one in the figure) revealed a fissure above the normal fissure of the eyelid that wt (the right one in the figure) did not have. At three weeks of age, FS^{95}-315-ko displayed microphthalmia (small eyes) (c), compared to wt (d). Although the urogenital tubercles of FS^{95}-315-ko were flatter than wt shown in Figure 8.3, the male of FS^{95}-315-ko (e) had normal external genitalis at three weeks of age. Interestingly, on day 10, FS^{95}-315-ko (f) displayed a hair part pattern on its upper dorsum while wt (g) did not. This hair part pattern then disappeared gradually and could not be recognized at three weeks of age. Of note, the tail phenotypes were distinct between FS^{95}-315-ko and wt. On day 2 ~ 3, FS^{95}-315-ko (i) started to reveal a red-black color in the tip of its tail. On day 10, the tail of FS^{95}-315-ko (the right one in (h)) was remarkably shorter than that of wt (the left one in (h)). At the same time, the tip of FS^{95}-315-ko displayed red color and several small red nodules (h). Gradually, the tip of FS^{95}-315-ko became black, implying a gangrenous change (j). Eventually, this black part of the tail tip of FS^{95}-315-ko fell off and the tail became shorter (k).

Figure 8.4

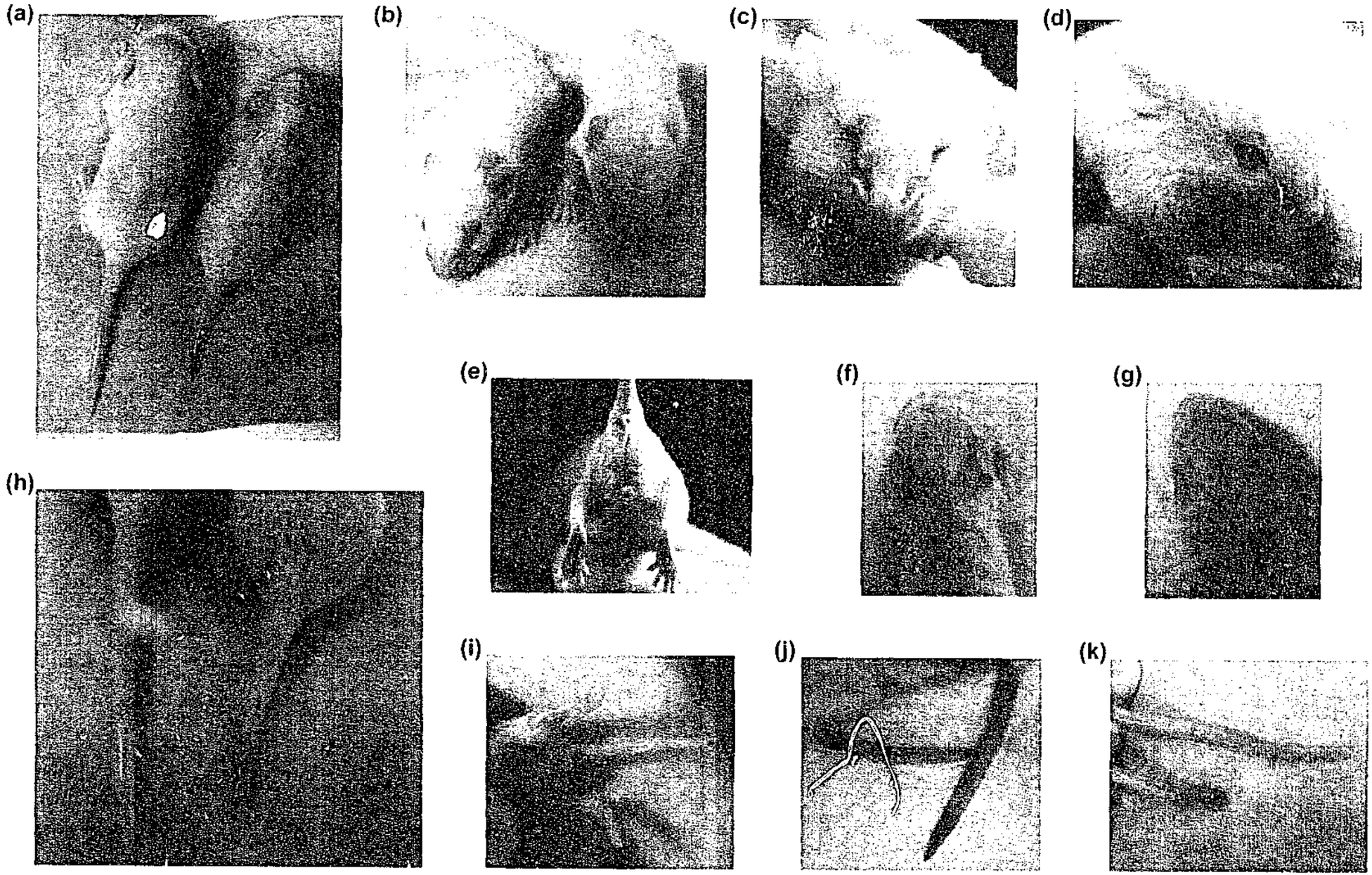

8.4 Discussion

8.4.1 Distinct functions of follistatin isoforms

The most stunning data of this thesis is that the human follistatin-315 specific transgene can prevent the neonatal death of FS-ko mice, while the human follistatin-288 specific transgene could not. This presents clear evidence that both follistatin isoforms have distinct functions in some aspects of follistatin biology. The only caution to this conclusion at this stage is that so far only one FS^{95}-315-wt transgenic line has been generated. Attempts are being made to generate further lines.

It is worthy to note again that the transgenes used to create both follistatin isoform-specific models were using a 95 kb genomic sequence of the human follistatin locus as a basis to perform the DNA engineering (referred to Chapter 7). The flanking regions of both isoform-specific transgenes are exactly the same. In other words, the natural regulatory elements within the transgene constructs that drive follistatin expression *in vivo* are the same in both the follistatin-288 specific and the follistatin-315 specific transgenes. Thus, in theory, FS^{95}-288-ko and FS^{95}-315-ko should have similar levels of follistatin and the difference is that only follistatin-288 is expressed in FS^{95}-288-ko and only follistatin-315 is expressed in FS^{95}-315-ko. The results presented clearly indicate that the FS^{95}-315-ko line can survive but not the FS^{95}-288-ko mice. What is the possible reason for this difference? The reason may be that follistatin-288 has a much higher affinity to heparan sulfate proteoglycans present in plasma membranes of cells in comparison to follistatin-315, leading to the relatively easy diffusion for follistatin-315 to reach the target sites. Therefore, follistatin-315 was still able to efficiently exert most of its biological functions in FS^{95}-315-ko. This rescue occurs despite probable under-expression of follistatin both in FS^{95}-288-ko and in FS^{95}-315-ko (because follistatin was under-expressed in FS^{95}-ko described in Chapter 5). As a result, despite the emphasis on the efficiency of follistatin-288 in a number of papers, it may be just the opposite in physiological situations. Follistatin-315 may be more physiologically efficient than follistatin-288, although the biochemical data *in vitro* just showed the reverse. Of course, an alternate explanation may be that follistatin-288 and follistatin-315 have just

different actions at the cellular levels, however, no published reports have addressed this point.

Another important question raised here is that of why the FS^{95}-ko cannot survive while FS^{95}-315-ko can survive. As mentioned above, FS^{95}-ko and FS^{95}-315-ko should express similar levels of follistatin. Further, FS^{95}-ko expresses both follistatin-288 and follistatin-315, the amounts of which would be 20 times the amount of follistatin-288 based on the published data (Michel, *et al.*, 1990), so the levels of follistatin-315 in FS^{95}-ko should be quite similar to those in FS^{95}-315-ko. If so, why are the phenotypes of FS^{95}-ko so different from those of FS^{95}-315-ko? One possible explanation is that follistatin-288 is, in some unknown way, counter-acting the biological actions of follistatin-315. To test this, both transgenic lines are being currently crossed onto the follistatin knockout background to generate doubly rescued mice with the prediction that these mice will also be unable to survive if this hypothesis is correct.

8.4.2 Phenotypes of follistatin-315 and follistatin-288 rescued mice: new insights into the biology of follistatin

Unfortunately, the two lines of FS^{95}-288-ko did not survive, so we cannot continue observing the postnatal development on the follistatin-288 specific models. Based on the data of FS^{95}-ko described in Chapter 5, the regulatory elements within the transgene constructs did not drive enough follistatin expression in every organ of the rescued mice, leading to failure to rescue the fs-ko phenotypes. Because the vector PAC-FSm2 contains the same flanking regions as the vector PAC-FS, it is reasonable to consider that FS^{95}-315-ko may express similar follistatin levels to FS^{95}-ko. As such, some of FS^{95}-315-ko phenotypes may support the point that follistatin-315 alone could reverse the effects of the follistatin knockout, whereas other phenotypes may represent the effects of follistatin under-expression or deficiency. Importantly, some interesting phenotypes of FS^{95}-315-ko occurred gradually during postnatal development. As a whole, this model provides new insights into the biology of follistatin.

Firstly, FS^{95}-315-ko has overcome growth restriction that was revealed in fs-ko, FS^{25}-ko, FS^{95}-ko and FS^{95}-288-ko. That may also be the main reason why FS^{95}-315-ko can

survive. Intra-uterine growth retardation has been an important and complex area of research. In view of the data presented in this thesis, there seems little doubt that follistatin is involved in the process of growth through mechanisms that remain unclear. Further, follistatin-315 may be more potent or pivotal in reversing the phenotype of growth restriction from the influence of the follistatin knockout, compared to follistatin-288.

My data also indicates that follistatin-315 is also able to reverse the phenotype of shiny and taut skin from the effects of the follistatin knockout. In contrast, follistatin-288 appears not to be able to have this kind of effect based on the phenotypes of FS^{95}-288-ko. This indicates that both follistatin isoforms may have distinct biological roles in skin.

In FS^{95}-315-ko, their whiskers were less disoriented and their urogenital tubercles were more obvious compared to fs-ko or FS^{95}-288-ko. However, when the FS^{95}-315-ko pups grew up, these phenotypes became less obvious and were more like that of wt mice. This may suggest that follistatin-315 can partially rescue these two phenotypes of fs-ko at the initial stage and that follistatin may not be so important at the later stage, or probably other factors can replace the role of follistatin in the meantime.

Other interesting phenotypes that developed gradually after birth in FS^{95}-315-ko are a hair parting pattern of the dorsum, microphthalmia and the defect of vasculogenesis and angiogenesis of their tails. These phenotypes may represent the results from the inability of follistatin-315 to rescue the effects of fs-ko or from the under-expression of follistatin-315 in FS^{95}-315-ko. As far as I know, the data presented in this chapter may be the first evidence suggesting the involvement of follistatin in eye development. Further, it may be the first *in vivo* evidence showing the role of follistatin in the processes of vasculogenesis and angiogenesis, although some *in vitro* studies have indicated the potential role of follistatin in angiogenesis (Kozian, *et al.*, 1997). In addition, it is unclear if the hair parting pattern of the dorsum of FS^{95}-315-ko presents some important information in the biology of follistatin.

The FS^{95}-315-ko females appear to be infertile because of the observation that no pregnancy has been found after 4~5 months of setting up the matings. Detailed experiments are required to decipher the mechanisms behind this.

8.4.3 Summary and future directions

The distinct phenotypes between FS^{95}-288-ko and FS^{95}-315-ko imply that both follistatin isoforms are different in some aspects of their actions. Through this study, the specific actions of the follistatin isoforms are starting to be uncovered. The transgenic mice that have been generated in this thesis offer the possibility to answer some of the questions regarding the biology of the follistatin isoforms. Why do we need two follistatin isoforms in our bodies? Which isoform is more competent physiologically; do both isoforms function antagonistically or synergistically? Do they have any functions that one of them holds but the other lacks? Is the relative ratio of these isoforms important for maintaining normal biological functions? How is this ratio regulated? Apparently, the follistatin isoforms are not functionally redundant to each other. Furthermore, the phenotypes of FS^{95}-315-ko broaden the research areas of follistatin biology. In addition to the areas discussed in Chapter 1, follistatin is quite probably involved in the development of eyes, the processes of vasculogenesis or/and angiogenesis, the development of genital tubercle, female infertility and the processes of growth restriction.

Because of the limited duration of my PhD program, the thesis represents a preliminary analysis of the phenotypes of human follistatin isoform-specific mouse models but not all detailed studies on them. Unequivocally, ongoing work will find more potentially interesting phenotypes that cannot be detected by gross examination, as well as elucidate more intriguing points of follistatin biology.

Currently, a new independent follistatin-315 specific transgenic line is being established. Moreover, to test the hypothesis that follistatin-288 is mitigating the actions of follistatin-315, both transgenic lines are being crossed onto the FS knockout background to generate doubly rescued mice. In addition, detailed histological analyses for both isoform-specific models are in progress. Further, development of a technique

that can quantify the mRNA expression levels of a single specific isoform for these models is also required.

Chapter 9

General Discussion

While the isolation and characterization of follistatin as an activin binding protein has been known for more than ten years, many aspects of the biology of follistatin still continue to emerge from ongoing research. Certainly, many of the biological effects of follistatin can be explained by its capacity to bind and neutralize the actions of activin. Indeed, the widespread effects of activin in a diversity of systems have highlighted the significance of follistatin biology and many papers indicate that these actions of follistatin involve autocrine/paracrine processes affecting the physiology of many systems such as reproduction, development, vascular biology, inflammation, fibrosis and wound healing (Chang, *et al.*, 2002; Welt, *et al.*, 2002; Lin, *et al.*, 2003).

Recent papers, however, have considerably broadened the field of follistatin biology. Emerging compelling evidence supports the interaction of follistatin with some of the TGF-β superfamily members other than activin. For example, BMP-2, 4, 7 and 15, myostatin (GDF-8) and GDF-11 have been implicated as targets to which follistatin can bind (Iemura, *et al.*, 1998; Lee and McPherron, 2001; Otsuka, *et al.*, 2001). Owing to the structural similarity of the TGF-β superfamily members, it is possible that more members which interact with follistatin will be identified in the near future. Furthermore, the signaling pathways of the TGF-β superfamily members have been demonstrated to cross-talk with the signaling pathways of other families (Massagué and Wotton, 2000; Zimmerman and Padgett, 2000), complicating the potential influence of follistatin in normal biological functions. Considering the complex context in which follistatin acts, studies in this thesis set out to establish genetically engineered mouse models in an attempt to study the biology of follistatin in an *in vivo* context providing more physiologically relevant models than *in vitro* experiments. The studies reported in this thesis extend our knowledge of the defects seen in the fs-ko mice which die at birth.

They also provide a variety of new concepts that enhance our understanding of the biology of this protein.

From my "rescue" experiments using human follistatin isoform-specific transgenes, one of the striking results is that FS^{95}-315-ko mice can survive in contrast to FS^{95}-288-ko, indicating the distinct physiological roles of follistatin isoforms. In view of the distinct biochemical characteristics of follistatin isoforms (follistatin-288 is a membrane-bound form, whereas follistatin-315 is a circulating form), it was hypothesized that they may also have distinct biological functions. Such a view is supported by the results in this thesis and has extended our understanding of this molecule.

Another important emerging concept from my "rescue" experiments is the possibility that follistatin-288 may counter-act the effects of follistatin-315 at certain times and in some physiological systems during development. Such a view is raised from the observation of the phenotypes of FS^{95}-ko, FS^{95}-288-ko and FS^{95}-315-ko. These three models harbor one of three different human genomic constructs in the mouse follistatin knockout background that have the same natural flanking regions of the human follistatin gene but contain different lengths of sequences between exon 5 and exon 6 of the follistatin gene (Figure 7.1). As such, in theory, these three transgenic models should express the same levels of follistatin directed by the natural regulatory elements located in the flanking regions of the follistatin gene. Nevertheless, in FS^{95}-288-ko and FS^{95}-315-ko there are only follistatin-288 and follistatin-315 expressed, respectively, and in FS^{95}-ko both follistatin-288 and follistatin-315 are expressed, presumably in a ratio controlled by the natural regulatory elements. Therefore, the evidence that both FS^{95}-ko and FS^{95}-288-ko could not survive, in contrast to FS^{95}-315-ko, suggests not only that follistatin-315, but not follistatin-288, may be an essential isoform for survival, but also that follistatin-288 may have blocked or inhibited the actions of follistatin-315 in FS^{95}-ko mice, leading to the inability of follistatin-315 to rescue FS^{95}-ko mice from the fate of neonatal death of the fs-ko mice. Alternatively, follistatin-288 may not antagonize the actions of follistatin-315 directly. Instead, each follistatin isoform may have some specific targets and the resultant phenotypes of FS^{95}-ko reflect the aggregate of these actions. Together all the evidence suggests that there may be a

regulatory system that controls some important developmental processes by modulating the relative expression of follistatin isoforms.

Although the concept raised in this thesis, that follistatin isoforms may have distinct biological functions, could change the directions of research in the biology of follistatin in the near future, it is not unusual that protein isoforms arising from alternative splicing could have distinct and even antagonistic functions. For example, the short isoform of the tumor suppressor p53 (p44) has distinct functions from p53 and an altered ratio of expression of p44 and p53 led to disruption of maternal-fetal communication during pre-implantation embryogenesis, which could further cause the growth retardation of embryos (Gluba, *et al.*, 2003). Likewise, two splice variants of the Wilms' tumor suppressor gene *Wt1*, -KTS and +KTS isoforms, differ in their ability to bind to specific DNA sequences in target genes. Moreover, the genetic models with a reduction of -KTS or +KTS isoforms demonstrate that these two splice variants have distinct functions during sex determination and nephron formation (Hammes, *et al.*, 2001). As such, alternative splicing of mRNA allows individual genes to produce many gene products with different functions. About 59% of human genes generate multiple mRNAs by alternative splicing (Lander, *et al.*, 2001), and about 80% of alternative splicing results in changes in the encoded protein (Modrek and Lee, 2002), indicating what is likely to be the primary source of human proteomic diversity. Through alternative splicing, the complexity of functions of individual genes can be increased to refine their actions and further tightly control developmental processes.

Our follistatin-288 specific mice, FS^{95}-288-ko, died within one day after birth, whereas the follistatin-315 specific mice, FS^{95}-315-ko, overcame the fate of neonatal death of fs-ko. The observation of the phenotypes of FS^{95}-315-ko revealed some important developmental processes, with which follistatin appears to be associated. First, FS^{95}-315-ko displayed much improvement in the growth retardation seen in fs-ko as well as increasing the capacity for movement in comparison with the fs-ko mice. In my view, this was the most important process that made FS^{95}-315-ko different from fs-ko and enabled it to survive. Recently, myostatin (GDF-8) has been demonstrated to function as a negative regulator of skeletal muscle mass, and follistatin can bind to myostatin and suppress its actions (McPherron, *et al.*, 1997; Lee and McPherron, 2001). This could

explain why there was a decrease in intercostal muscle mass of fs-ko (Matzuk, *et al.*, 1995). However, the myostatin knockout mice did not show changes in their body size (personal communication with Dr. Se-Jin Lee). Thus, it seems unlikely that the general growth retardation of fs-ko mice was just due to loss of antagonism of follistatin to myostatin. Moreover, the role of follistatin in growth retardation has not been addressed thoroughly. The data presented in this thesis reveal that follistatin-315 alone may be enough to exert the normal function of follistatin to the point of avoiding growth retardation. Nevertheless, the mechanisms involved need to be further clarified, especially the possibilities of the interactions of follistatin with growth hormone and/or insulin-like growth factor (IGF) family. In this context, follistatin has been localized to the somatotrophs in the pituitary gland (Kaiser, *et al.*, 1992).

To our surprise, FS^{95}-315-ko mice exhibit microphthalmia, a finding that has not been related to the functions of follistatin. Detailed studies need to be performed in this important area of research. In the early exploration of this phenomenon, preliminary observations (Figure 8.3 & Figure 8.4) revealed that the sizes of the eyes of wt and FS^{95}-315-ko seemed similar but displayed different sizes after they opened their eyes at about three weeks of age. This evidence may imply that disruption in the normal balance between apoptosis and proliferation occurred (*i.e.* the apoptotic process overwhelmed the proliferation process) in the eyes of FS^{95}-315-ko after their birth. It appears reasonable to consider this aspect of function of follistatin from the viewpoint of its interaction with some members of the TGF-β superfamily. Pax6 is a member of the Pax family of transcription factors, containing two DNA-binding motifs, the paired domain and paired-type homeodomain (Chow and Lang, 2001). Pax6 is required for normal eye development. A decrease in Pax6 activity causes small eyes in mice and rats, whereas overexpression of Pax6 leads to a severe eye phenotype (Chow and Lang, 2001). BMP-7 plays an important role in the early stages of lens development where it functions upstream of Pax6 and cooperates with FGF receptor signaling (Chow and Lang, 2001). Moreover, BMP-7 null mutants displayed a variable eye phenotype from microphthalmia to anophthalmia (Chow and Lang, 2001). BMP-4 has also been implicated in lens development and differentiation; however the expression of Pax6 in BMP-4 null mutants is normal in contrast to that of BMP-7 (Chow and Lang, 2001). The eye phenotypes of FS^{95}-315-ko may reflect the imbalance of actions of some

members of the TGF-β superfamily owing to the inappropriate expression of follistatin isoforms.

Another important process, in which follistatin may be involved, pinpointed by observation of the phenotypes of FS^{95}-315-ko, is the process of vasculogenesis and/or angiogenesis. As FS^{95}-315-ko mice grew up, the tips of their tails displayed a gangrenous change, and then fell off, resulting in shorter tails in comparison to those of wt mice. It appears that the disruption of vasculogenesis and/or angiogenesis caused the inability of the tails of FS^{95}-315-ko to grow longer. To our knowledge, this is the first time follistatin has been shown to be involved in the process of vasculogenesis and/or angiogenesis in an *in vivo* model, although follistatin has also been demonstrated to induce angiogenesis *in vitro* (Kozian, *et al.*, 1997). This phenotype of the tails of FS^{95}-315-ko may imply that follistatin-288 is essential for angiogenesis, or the expression levels of follistatin-315 were not enough to facilitate a normal process of angiogenesis. Further, the insufficiency of follistatin in fs-ko mice may contribute to the disruption of vasculogenesis and/or angiogenesis during development, which would further lead to their growth retardation.

In addition, observations of fs-ko and the rescued mice provided insights into various areas of the biology of follistatin. First, follistatin-315, but not follistatin-288, is essential for normal development of skin and hair follicles. Secondly, follistatin is involved in the development of genital tubercles. In addition, follistatin is required for normal fetal oogenesis. Moreover, follistatin is critical for normal lung development, perhaps through a role in the branching morphogenesis of the respiratory tracts. Furthermore, follistatin is an important factor in promoting liver growth and development based on the significant difference in the liver masses of the fs-ko and wt mice at birth.

Because of the importance of the regulation of follistatin expression, the first attempt to define the human follistatin locus and identify the regulatory elements required for the appropriate expression of follistatin during development was performed to validate the 25 kb and 95 kb genomic sequences of the human follistatin locus in the mouse follistatin null background. Based on the phenotypes of FS^{25}-ko and FS^{95}-ko, it suggests

that there may be some essential elements beyond the 45 kb sequences both upstream and downstream of the human follistatin gene. Moreover, there appears to be similar information contained in the 25 kb and 95 kb genomic sequences for the regulation of follistatin expression. However, in these experiments, the possibility of species differences should be taken into consideration before definitive conclusions can be reached.

In addition to exploring the influence of follistatin on the whole body in this thesis, the potential autocrine/paracrine role of follistatin in testis development was also investigated by transplanting fetal testes into the ears of castrated RAG adult mice. Since the grafted testes 8~9 weeks after transplantation showed full stages of spermatogenesis both in wild-type (wt) and follistatin null (fs-ko) testes, and follistatin could also be demonstrated in the testes of fs-ko by immunohistochemistry, it was proposed that circulating follistatin-315 from the host could provide any actions of follistatin required for the postnatal development of testes. Such a view is supported by our follistatin-315 specific model where the male mice carrying only human genomic follistatin-315 transgenes but no mouse endogenous follistatin gene had normal testis development and were fertile. However, the possibility that follistatin may not be required for postnatal testicular development cannot be excluded, although such a view is not consistent with studies of the overexpression of the βA subunit in the studies of Tanimoto *et al* (Tanimoto, *et al.*, 1999) and the testicular damage seen in mice that overexpressed follistatin (Guo, *et al.*, 1998).

In conclusion, the work presented in this thesis provides insights into new fields of follistatin biology that have not been reported earlier. At the same time, it highlights the importance of follistatin and recognizes the potential complex context in which this molecule functions. The biology of follistatin cannot be full understood by only considering this molecule as a binding protein of activin. This thesis has broadened our understanding of the biology of follistatin. Most importantly, this thesis proposes an important concept that follistatin isoforms have distinct functions and the appropriate expression of both isoforms may be critical during development and normal cellular function. Therefore, the biology of follistatin could be considered as the biology of follistatin ISOFORMS.

- Appendix I -

Solutions referred to in Chapter 2 (Materials and methods)

Bouin's fixative

714ml of saturated picric acid, 238ml of 37% formalin solution, 48ml of glacial acetic acid

Church buffer

1% (w/v) bovine serum albumin (BSA), 1mM EDTA, 0.5M phosphate buffer (0.5M phosphate buffer is 134g of Na_2HPO_4-$7H_2O$, 4ml of 85% H_3PO_4, H_2O to 1 L), 7% (w/v) SDS

DAB-H_2O_2 solution

Add 10µl of 3% H_2O_2 to 1ml Diaminobenzene (DAB).

DEPC-treated water

0.1% diethyl pyrocarbonate in dH_2O

Ear clip lysis buffer

10mM Tris (pH8.3), 50mM NaCl, 0.2% (v/v) Tween20, 19µg of proteinase K

KSOM

95mM NaCl, 2.5mM KCl, 0.35mM KH_2PO_4, 0.2mM $MgSO_4$-$7H_2O$, 1.71mM $CaCl_2$-$2H_2O$, 25mM $NaHCO_3$, 10mM Na lactate, 0.2mM Na pyruvate, 0.2mM Glucose, 1mM Glutamine, 0.01mM EDTA, 1mg/ml BSA

Luria-Bertani (LB) medium

10g bacto-trypton, 5g bacto-yeast extract, 5g NaCl in 1 litre (L) of dH_2O, pH7.0

LB agar

1 L of LB medium, 15 g agar

M2 medium

94.66mM NaCl, 4.78mM KCl, 1.71mM $CaCl_2$-$2H_2O$, 1.19mM KH_2PO_4, 1.19mM $MgSO_4$-$7H_2O$, 4.15mM $NaHCO_3$, 20.85mM HEPES, 23,28mM sodium lactate, 0.33mM sodium pyruvate, 5.56mM glucose, 4mg/ml BSA, 60μg/ml penicillin G potassium salt, 50μg/ml streptomycin sulphate, 10μg/ml phenol red

Mouse-tail lysis buffer I

100 mM Tris-Cl (pH 8.5), 5 mM EDTA (pH 8.0), 200 mM NaCl, 0.2% (w/v) SDS, 100 μg/ml proteinase K

PBS

8g NaCl, 0.2g KCl, 1.44g Na_2HPO_4, 0.24g KH_2PO_4 in 1 L of dH_2O, pH7.4

QBT buffer

750mM NaCl, 50mM 3[N-morpholino]propanesulfonic acid(MOPS) (pH7.0), 15% (v/v) isopropanol, 0.15% (v/v) Triton X-100

SOC medium

20g bacto-tryptone, 5g bacto-yeast extract, 0.5g NaCl, 20mM glucose

Solution D

4M guanidinium thiocyanate, 25mM sodium citrate, pH7.0, 0.5% sodium lauryl sarcosinate, 0.1M β-Mercaptoethanol

SSC

175.3g NaCl, 88.2g sodium citrate in 1 L of dH_2O, pH7.0

TAE

40mM Tris-acetate, 1mM EDTA, pH8.0

5x TBE buffer

54g of Tris base, 27.5g of boric acid, 20ml of 0.5M EDTA, pH8.0, in 1 L of dH_2O

TBS (Tris-buffered saline)

Dissolve 8g of NaCl, 0.2g of KCl, and 3g of Tris base in 800ml of dH_2O. Add 0.015g of phenol red and adjust the pH to 7.4 with HCl. Add dH_2O to 1 L. Store the buffer at room temperature after autoclaving.

TE

10mM Tris-Cl, pH8.0, 1mM EDTA, pH8.0

- Appendix II -

Manufacturers of reagents

American Tissue Culture Collection	Rockville, MD, USA
Amersham	Buckinghamshire, UK
Applied Biosystems	CA, USA
Beckman	Palo Alto, CA, USA
Biorad	Richmond, CA, USA
Boehringer Mannheim Biochem	Mannheim, Germany
Clontech	Palo Alto, CA, USA
CSL	Parkville, VIC, Australia
DYNAL BIOTECH ASA	OSLO, Norway
Geneset Pacific Pty. Ltd	Lismore, Australia
GibcoBRL	Ontario, Canada
Histolabs	Riverstone, NSW, Australia
Invitrogen	Carlsbad, CA, USA
New England Biolabs	Beverly, MA, USA
Pharmacia	Uppsala, Sweden
Promega	Madison, WI, USA
Qiagen	Hilden, Germany
Sigma Genosys	Castle Hill, NSW, Australia
Stratagene	La Jolla, CA, USA

- Appendix III -

Sequences of PCR primers

Name	Sequence: (5'- 3')	Tm (°C)
Fol1.F	U: 5' TCTGCCAGTTCATGGAGGAC 3'	61.2
Fol1.R	D: 5' CGAGCTCCAAACTCAGTTCC 3'	59.9
Fol2.F	U: 5' ACTGCTCACTCACCCACCTC 3'	60.3
Fol2.R	D: 5' CTGCAAGTTGGGAAGAAGGA 3'	60.3
Fol3.F	U: 5' ACTGCCTGGCTCTGGTTTTA 3'	59.8
Fol3.R	D: 5' GGAGGGGACAGATCCAGTCT 3'	60.4
Fol4.F	U: 5' TGTGTTTCCTTCTTTGTTCCAG 3'	59.2
Fol4.R	D: 5' TTTTTCCTTCCTCAATCCAGAA 3'	60.0
Fol5.F	U: 5' GGGGATATGGGGAAATCAGT 3'	59.8
Fol5.R	D: 5' GGCAGCAAGGTTAAAAATCG 3'	59.7
Fs-insertion F	U: 5' CTGCTGGGCAGATCTATTGG 3'	60.7
Fs-insertion R-1	D: 5' CAAAGGCTATGTGAACACTGAA 3'	57.9
Fs-insertion R-2	D: 5' GGGAGACAGATGAGTGAGTGAA 3'	59.3
HPRT-F	U: 5' TGCTCGAGATGTGATGAAGG 3'	59.9
HPRT-R	D: 5' TCCCCTGTTGACTGGTCATT 3'	60.3
HPRT-2F	U: 5' GACCAGTCAACAGGGGACAT 3'	59.8
HPRT-2R	D: 5' AACACTTCGTGGGGTCCTTT 3'	60.7
hHPRT.3F	U: 5' TGCTGACCTGCTGGATTACA 3'	60.4
hHPRT.3R	D: 5' CTGCATTGTTTTGCCAGTGT 3'	59.7
FS-MO-F	U: 5' TGCCACCTGAGAAAGGCTAC 3'	60.4
FS-MO-R	D: 5' TGCAAGTTTGTTGAAAGTGGA 3'	59.4
fs-X-F	U: 5' TGTTCAGTGTTCACATAGCCTTT 3'	58.8
fs-56-F	U: 5' TCCTCAGGTGTGCTACTGGA 3'	59.4

fs-56-R	D: 5' TCAGGTTTTACGGGCAGATT 3'	59.6
pNEB193-R	D: 5' CCTGCAGGTTTAAACAGTCG 3'	58.4
pNEB193-F	U: 5' TAAAACGACGGCCAGTGAAT 3'	60.5
fs-Sac-R	D: 5' CAAACCCCCAGGTTTTCTTT 3'	60.2
S4-m-F	U: 5' CGCAAATTTAAAGCGCTGAT 3'	60.4
S4-m-R	D: 5' TCCAGTAGCACACCTGAGGA 3'	59.4
pCR2.1/F	U: 5' ATGACCATGATTACGCCAAG 3'	58.2
pCR2.1/R	D: 5' CGGCCAGTGAATTGTAATACG 3'	60.2
10kb-UP-A.F	U: 5' GTGGCCTTCTGGAGACTGAG 3'	60
10kb-UP-A.R	D: 5' CATGATGGCACGAACCTGTA 3'	60.5
10kb-UP-B.F	U: 5' GTTTACCCTCACTCCAGGC 3'	60.1
10kb-UP-B.R	D: 5' CACTTAAACCTGGGAGGTG 3'	59.4
5kb-UP-A.F	U: 5' AACATCCCCATTCTAAGGCA 3'	59.3
5kb-UP-A.R	D: 5' GCCTTGCTTTCCCCTTTAAT 3'	59.5
5kb-UP-B.F	U: 5' AACATCCCCATTCTAAGGC 3'	59.3
5kb-UP-B.R	D: 5' TTTTATTGCCTTGCTTTCC 3'	59.1
Intron1-A.F	U: 5' TTAAAAAGGGGGAAGAGGGA 3'	59.8
Intron1-A.R	D: 5' GGCAGAGCCTCTCCTCTAAA 3'	58.7
Intron1-B.F	U: 5' TTAAAAAGGGGGAAGAGGG 3'	59.8
Intron1-B.R	D: 5' CTTTCGAAATCTCCGAGGG 3'	59.7
Southern-F	U: 5' CTGGGTCACTGGTAACTGACATT 3'	60.3
Southern-R	D: 5' GAGTCCTACCTTTACAGGGGATG 3'	60.2
1.5kb-DOWN-A.F	U: 5' TTTCAAACACCATGACCCAA 3'	59.7
1.5kb-DOWN-A.R	D: 5' ACCGGAGAAGTTACGACCCT 3'	60
1.5kb-DOWN-B.F	U: 5' TTTCAAACACCATGACCCA 3'	59.7
1.5kb-DOWN-B.R	D: 5' TTTCCTTTTGGGGAACACA 3'	59.9
M.screen.1F	U: 5' CGGATTTGCCCAGAGCCCT 3'	66.9
M.screen.1R	D: 5' GCCAACCTTGGAATCCCATAGG 3'	65.8
H.screen.1F	U: 5' CGGATTTGCCCAGAGCCTG 3'	66.3
H.screen.1R	D: 5' TCTCCCAACCTTGAAATCCCATAAA 3'	65.6
M-splice.1F	U: 5' CTGTGAAGATATCCAGTGTGGC 3'	59.4
M-splice.1R	D: 5' GCTATGTCAACACTGAACATTGG 3'	59.3

H-splice.1F	U: 5' CCTGTGAAGATATCCAGTGCAC 3'	59.4
H-splice.1R	D: 5' AGGCTATGTGAACACTGAACACTTA 3'	59.1
LC-primer.1F	U: 5' ACGTGTGAGAACGTGGACT 3'	56.1
LC-primer.1R	D: 5' CTTCCTTCATGGCACACTC 3'	56.3
Human.screen.2F	5' TGTGGTGGACCAGACCAATA 3'	59.8
Human.screen.2R	5' TGACTCCATCATTCCCACAG 3'	59.5
Mouse.screen.2F	5' CCAGACTGTTCCAACATCACC 3'	60.4
Mouse.screen.2R	5' CTAGTTCCGGCTGCTCTTTG 3'	60.2
b-actin.F	5' GCTACAGCTTCACCACCACA 3'	59.9
b-actin.R	5' AAGGAAGGCTGGAAAAGAGC 3'	60
human.FS.2F	5' ACTGCTCACTCACCCACCTC 3'	60.3
human.FS.2R	5' CTGCAAGTTGGGAAGAAGGA 3'	60.3
mouse.FS.2F	5' TGTGCCTCTTTCCAACTCCT 3'	59.8
mouse.FS.2R	5' ATCTATCGCCCTTGGGTCTT 3'	59.9
Foldel.F	5' CGCTGCCAGGTCCTGTATAA 3'	60.9
Foldel.R	5' CTTTACAAGGGATGCAGTTGG 3'	59.4

Appendix IV

Supplementary data

Tables:

Table IV.1 The birth weights of mice from the second step of cross-breeding

Transgenic lines	Number	Mean (gm)	Std. Deviation (gm)	Std. Error (gm)	95% Confidence Interval for Mean (gm)		Minimum (gm)	Maximum (gm)
					Lower Bound	Upper Bound		
fs-ko	19	1.00321	.095115	.021821	.95737	1.04905	.850	1.200
FS^{25}-ko.1	11	1.07882	.096600	.029126	1.01392	1.14371	.900	1.200
FS^{25}-ko.2	10	1.06340	.069872	.022095	1.01342	1.11338	.950	1.150
FS^{95}-ko.1	10	1.15460	.081011	.025618	1.09665	1.21255	1.000	1.260
FS^{95}-ko.2	9	1.08511	.083725	.027908	1.02075	1.14947	.959	1.218
wt	19	1.31332	.075678	.017362	1.27684	1.34979	1.100	1.400

Table IV.2 Multiple comparisons between the birth weights of the rescued mice, knockout mice and wild-type mice

Tukey HSD

Transgenic line (I)	Transgenic line (J)	Mean Difference (I-J)	Std. Error	Sig.	95% Confidence Interval	
					Lower Bound	Upper Bound
fs-ko	FS^{25}-ko.1	-.07561	.032146	.187	-.16973	.01851
	FS^{25}-ko.2	-.06019	.033148	.462	-.15724	.03686
	FS^{95}-ko.1	-.15139 *	.033148	.000	-.24844	-.05434
	FS^{95}-ko.2	-.08190	.034334	.175	-.18242	.01862
	wt	-.31011 *	.027528	.000	-.39070	-.22951
FS^{25}-ko.1	fs-ko	.07561	.032146	.187	-.01851	.16973
	FS^{25}-ko.2	.01542	.037072	.998	-.09312	.12396
	FS^{95}-ko.1	-.07578	.037072	.328	-.18432	.03276
	FS^{95}-ko.2	-.00629	.038136	1.000	-.11795	.10536
	wt	-.23450 *	.032146	.000	-.32862	-.14038
FS^{25}-ko.2	fs-ko	.06019	.033148	.462	-.03686	.15724
	FS^{25}-ko.1	-.01542	.037072	.998	-.12396	.09312
	FS^{95}-ko.1	-.09120	.037945	.169	-.20230	.01990
	FS^{95}-ko.2	-.02171	.038985	.993	-.13585	.09243
	wt	-.24992 *	.033148	.000	-.34697	-.15286
FS^{95}-ko.1	fs-ko	.15139 *	.033148	.000	.05434	.24844
	FS^{25}-ko.1	.07578	.037072	.328	-.03276	.18432
	FS^{25}-ko.2	.09120	.037945	.169	-.01990	.20230
	FS^{95}-ko.2	.06949	.038985	.483	-.04465	.18363
	wt	-.15872 *	.033148	.000	-.25577	-.06166
FS^{95}-ko.2	fs-ko	.08190	.034334	.175	-.01862	.18242
	FS^{25}-ko.1	.00629	.038136	1.000	-.10536	.11795
	FS^{25}-ko.2	.02171	.038985	.993	-.09243	.13585
	FS^{95}-ko.1	-.06949	.038985	.483	-.18363	.04465
	wt	-.22820 *	.034334	.000	-.32873	-.12768
wt	fs-ko	.31011 *	.027528	.000	.22951	.39070
	FS^{25}-ko.1	.23450 *	.032146	.000	.14038	.32862
	FS^{25}-ko.2	.24992 *	.033148	.000	.15286	.34697
	FS^{95}-ko.1	.15872 *	.033148	.000	.06166	.25577
	FS^{95}-ko.2	.22820 *	.034334	.000	.12768	.32873

* The mean difference is significant at the 0.05 level.

Table IV.3 The crown-rump length (CRL) of mice at birth from the second step of cross-breeding

Transgenic lines	Number	Mean (cm)	Std. Deviation (cm)	Std. Error (cm)	95% Confidence Interval for Mean		Minimum (cm)	Maximum (cm)
					Lower Bound	Upper Bound		
fs-ko	19	2.01579	.089834	.020609	1.97249	2.05909	1.900	2.200
FS^{25}-ko.1	11	2.11364	.083937	.025308	2.05725	2.17003	1.900	2.200
FS^{25}-ko.2	10	2.08000	.078881	.024944	2.02357	2.13643	1.900	2.150
FS^{95}-ko.1	10	2.21000	.073786	.023333	2.15722	2.26278	2.100	2.300
FS^{95}-ko.2	9	2.20556	.104416	.034805	2.12529	2.28582	2.100	2.400
wt	19	2.50000	.116667	.026765	2.44377	2.55623	2.300	2.700

Table IV.4 Multiple comparisons between crown-rump lengths (CRL) of the rescued mice, knockout mice and wild-type mice

Tukey HSD

Transgenic line (I)	Transgenic line (J)	Mean Difference (I-J)	Std. Error	Sig.	95% Confidence Interval	
					Lower Bound	Upper Bound
fs-ko	FS^{25}-ko.1	-.09785	.036079	.085	-.20348	.00779
	FS^{25}-ko.2	-.06421	.037204	.520	-.17314	.04472
	FS^{95}-ko.1	-.19421 *	.037204	.000	-.30314	-.08528
	FS^{95}-ko.2	-.18977 *	.038535	.000	-.30259	-.07694
	wt	-.48421 *	.030896	.000	-.57467	-.39375
FS^{25}-ko.1	fs-ko	.09785	.036079	.085	-.00779	.20348
	FS^{25}-ko.2	.03364	.041609	.965	-.08819	.15546
	FS^{95}-ko.1	-.09636	.041609	.201	-.21819	.02546
	FS^{95}-ko.2	-.09192	.042802	.275	-.21724	.03340
	wt	-.38636 *	.036079	.000	-.49200	-.28073
FS^{25}-ko.2	fs-ko	.06421	.037204	.520	-.04472	.17314
	FS^{25}-ko.1	-.03364	.041609	.965	-.15546	.08819
	FS^{95}-ko.1	-.13000 *	.042588	.036	-.25469	-.00531
	FS^{95}-ko.2	-.12556	.043755	.058	-.25366	.00255
	wt	-.42000 *	.037204	.000	-.52893	-.31107
FS^{95}-ko.1	fs-ko	.19421 *	.037204	.000	.08528	.30314
	FS^{25}-ko.1	.09636	.041609	.201	-.02546	.21819
	FS^{25}-ko.2	.13000 *	.042588	.036	.00531	.25469
	FS^{95}-ko.2	.00444	.043755	1.000	-.12366	.13255
	wt	-.29000 *	.037204	.000	-.39893	-.18107
FS^{95}-ko.2	fs-ko	.18977 *	.038535	.000	.07694	.30259
	FS^{25}-ko.1	.09192	.042802	.275	-.03340	.21724
	FS^{25}-ko.2	.12556	.043755	.058	-.00255	.25366
	FS^{95}-ko.1	-.00444	.043755	1.000	-.13255	.12366
	wt	-.29444 *	.038535	.000	-.40727	-.18162
wt	fs-ko	.48421 *	.030896	.000	.39375	.57467
	FS^{25}-ko.1	.38636 *	.036079	.000	.28073	.49200
	FS^{25}-ko.2	.42000 *	.037204	.000	.31107	.52893
	FS^{95}-ko.1	.29000 *	.037204	.000	.18107	.39893
	FS^{95}-ko.2	.29444 *	.038535	.000	.18162	.40727

* The mean difference is significant at the 0.05 level.

Table IV.5 The post-fixation organ weights of the rescued mice, knockout mice and wild-type mice-- Descriptives

		N	Mean (mg)	Std. Deviation	Std. Error	95% Confidence Interval for Mean		Minimum	Maximum
						Lower Bound	Upper Bound		
THYROID	fs-ko	12	6.9917	1.82481	.52678	5.8322	8.1511	2.70	10.10
	FS^{25}-ko.1	5	7.4400	1.83929	.82256	5.1562	9.7238	4.90	10.00
	FS^{25}-ko.2	6	7.2167	2.20673	.90089	4.9008	9.5325	5.00	10.30
	FS^{95}-ko.1	5	7.2800	1.03053	.46087	6.0004	8.5596	5.90	8.50
	FS^{95}-ko.2	3	9.0000	1.80278	1.04083	4.5217	13.4783	7.00	10.50
	wt	6	12.2667	.89815	.36667	11.3241	13.2092	11.00	13.40
HEART	fs-ko	12	7.8333	1.30755	.37746	7.0026	8.6641	5.70	9.60
	FS^{25}-ko.1	5	9.6200	2.15685	.96457	6.9419	12.2981	6.30	12.00
	FS^{25}-ko.2	6	7.9667	2.42707	.99085	5.4196	10.5137	5.10	12.20
	FS^{95}-ko.1	5	9.1400	1.21161	.54185	7.6356	10.6444	8.00	11.20
	FS^{95}-ko.2	3	11.0333	.95044	.54874	8.6723	13.3944	10.10	12.00
	wt	6	10.3833	1.51316	.61775	8.7954	11.9713	8.20	12.70
LUNG	fs-ko	12	26.9658	5.40984	1.56169	23.5286	30.4031	20.60	39.86
	FS^{25}-ko.1	5	32.2800	4.41497	1.97444	26.7981	37.7619	29.00	40.00
	FS^{25}-ko.2	6	28.4667	5.66274	2.31181	22.5240	34.4094	23.90	39.20
	FS^{95}-ko.1	5	37.1200	3.58706	1.60418	32.6661	41.5739	33.70	41.30
	FS^{95}-ko.2	3	42.0667	3.63501	2.09868	33.0368	51.0965	38.00	45.00
	wt	6	47.8333	8.12125	3.31549	39.3106	56.3561	34.40	57.30
SPLEEN	fs-ko	12	.8900	.43830	.12653	.6115	1.1685	.40	1.90
	FS^{25}-ko.1	5	1.0200	.42071	.18815	.4976	1.5424	.40	1.50
	FS^{25}-ko.2	6	1.0133	.41889	.17101	.5737	1.4529	.50	1.60
	FS^{95}-ko.1	5	1.1000	.33912	.15166	.6789	1.5211	.70	1.60
	FS^{95}-ko.2	3	1.1667	.30551	.17638	.4078	1.9256	.90	1.50
	wt	6	1.0833	.24014	.09804	.8313	1.3353	.70	1.30
THYMUS	fs-ko	12	1.6667	.27414	.07914	1.4925	1.8408	1.20	2.00
	FS^{25}-ko.1	5	1.5800	.43243	.19339	1.0431	2.1169	1.00	2.10
	FS^{25}-ko.2	6	1.7500	.30822	.12583	1.4265	2.0735	1.40	2.20
	FS^{95}-ko.1	5	1.8800	.22804	.10198	1.5969	2.1631	1.60	2.10
	FS^{95}-ko.2	3	1.9000	.17321	.10000	1.4697	2.3303	1.80	2.10
	wt	6	1.5433	.49241	.20103	1.0266	2.0601	1.06	2.20
LIVER	fs-ko	12	41.1833	10.91353	3.15046	34.2492	48.1175	20.20	64.20
	FS^{25}-ko.1	5	52.0200	8.96002	4.00704	40.8947	63.1453	37.20	61.40
	FS^{25}-ko.2	6	42.6833	3.74989	1.53089	38.7481	46.6186	36.70	47.70
	FS^{95}-ko.1	5	53.6000	3.54612	1.58588	49.1969	58.0031	50.20	57.40
	FS^{95}-ko.2	3	57.3000	1.66433	.96090	53.1656	61.4344	55.40	58.50
	wt	6	69.4667	11.31612	4.61979	57.5911	81.3422	52.00	86.00
KIDNEY	fs-ko	12	9.7167	1.29111	.37271	8.8963	10.5370	7.10	12.50
	FS^{25}-ko.1	5	10.0200	.81056	.36249	9.0136	11.0264	9.00	10.80
	FS^{25}-ko.2	6	9.0500	1.06911	.43646	7.9280	10.1720	7.30	10.50
	FS^{95}-ko.1	5	9.8600	1.82565	.81646	7.5932	12.1268	7.70	12.50
	FS^{95}-ko.2	3	10.2333	1.07858	.62272	7.5540	12.9127	9.00	11.00
	wt	6	11.3833	2.59570	1.05969	8.6593	14.1074	8.80	14.00
GI	fs-ko	12	48.9833	6.20628	1.79160	45.0401	52.9266	40.30	59.80
	FS^{25}-ko.1	5	52.9600	5.45188	2.43816	46.1906	59.7294	47.10	60.80
	FS^{25}-ko.2	6	54.6667	7.41179	3.02585	46.8885	62.4449	43.60	63.00
	FS^{95}-ko.1	5	56.8080	4.69823	2.10111	50.9744	62.6416	51.20	62.10
	FS^{95}-ko.2	3	57.5333	2.83784	1.63843	50.4837	64.5829	55.00	60.60
	wt	6	78.3333	13.56785	5.53905	64.0947	92.5719	63.10	101.20

Table IV.6 The post-fixation organ weights of the rescued mice, knockout mice and wild-type mice-- Multiple comparisons

Tukey HSD

	transgenic line (I)	transgenic line (J)	Mean (mg) Difference (I-J)	Std. Error	Sig.	95% Confidence Interval	
						Lower Bound	Upper Bound
THYROID	fs-ko	FS^{25}-ko.1	-.4483	.90338	.996	-3.1903	2.2936
		FS^{25}-ko.2	-.2250	.84858	1.000	-2.8006	2.3506
		FS^{95}-ko.1	-.2883	.90338	1.000	-3.0303	2.4536
		FS^{95}-ko.2	-2.0083	1.09551	.460	-5.3334	1.3167
		wt	-5.2750 *	.84858	.000	-7.8506	-2.6994
	FS^{25}-ko.1	fs-ko	.4483	.90338	.996	-2.2936	3.1903
		FS^{25}-ko.2	.2233	1.02768	1.000	-2.8959	3.3425
		FS^{95}-ko.1	.1600	1.07338	1.000	-3.0979	3.4179
		FS^{95}-ko.2	-1.5600	1.23943	.804	-5.3219	2.2019
		wt	-4.8267 *	1.02768	.001	-7.9459	-1.7075
	FS^{25}-ko.2	fs-ko	.2250	.84858	1.000	-2.3506	2.8006
		FS^{25}-ko.1	-.2233	1.02768	1.000	-3.3425	2.8959
		FS^{95}-ko.1	-.0633	1.02768	1.000	-3.1825	3.0559
		FS^{95}-ko.2	-1.7833	1.20007	.675	-5.4258	1.8591
		wt	-5.0500 *	.97986	.000	-8.0240	-2.0760
	FS^{95}-ko.1	fs-ko	.2883	.90338	1.000	-2.4536	3.0303
		FS^{25}-ko.1	-.1600	1.07338	1.000	-3.4179	3.0979
		FS^{25}-ko.2	.0633	1.02768	1.000	-3.0559	3.1825
		FS^{95}-ko.2	-1.7200	1.23943	.734	-5.4819	2.0419
		wt	-4.9867 *	1.02768	.000	-8.1059	-1.8675
	FS^{95}-ko.2	fs-ko	2.0083	1.09551	.460	-1.3167	5.3334
		FS^{25}-ko.1	1.5600	1.23943	.804	-2.2019	5.3219
		FS^{25}-ko.2	1.7833	1.20007	.675	-1.8591	5.4258
		FS^{95}-ko.1	1.7200	1.23943	.734	-2.0419	5.4819
		wt	-3.2667	1.20007	.099	-6.9091	.3758
	wt	fs-ko	5.2750 *	.84858	.000	2.6994	7.8506
		FS^{25}-ko.1	4.8267 *	1.02768	.001	1.7075	7.9459
		FS^{25}-ko.2	5.0500 *	.97986	.000	2.0760	8.0240
		FS^{95}-ko.1	4.9867 *	1.02768	.000	1.8675	8.1059
		FS^{95}-ko.2	3.2667	1.20007	.099	-.3758	6.9091
HEART	fs-ko	FS^{25}-ko.1	-1.7867	.88655	.357	-4.4775	.9042
		FS^{25}-ko.2	-.1333	.83277	1.000	-2.6609	2.3943
		FS^{95}-ko.1	-1.3067	.88655	.683	-3.9975	1.3842
		FS^{95}-ko.2	-3.2000	1.07510	.057	-6.4631	.0631
		wt	-2.5500 *	.83277	.047	-5.0776	-.0224
	FS^{25}-ko.1	fs-ko	1.7867	.88655	.357	-.9042	4.4775
		FS^{25}-ko.2	1.6533	1.00854	.580	-1.4077	4.7144
		FS^{95}-ko.1	.4800	1.05338	.997	-2.7172	3.6772
		FS^{95}-ko.2	-1.4133	1.21634	.851	-5.1051	2.2785
		wt	-.7633	1.00854	.973	-3.8244	2.2977
	FS^{25}-ko.2	fs-ko	.1333	.83277	1.000	-2.3943	2.6609
		FS^{25}-ko.1	-1.6533	1.00854	.580	-4.7144	1.4077
		FS^{95}-ko.1	-1.1733	1.00854	.850	-4.2344	1.8877
		FS^{95}-ko.2	-3.0667	1.17772	.126	-6.6412	.5079
		wt	-2.4167	.96160	.151	-5.3353	.5020
	FS^{95}-ko.1	fs-ko	1.3067	.88655	.683	-1.3842	3.9975
		FS^{25}-ko.1	-.4800	1.05338	.997	-3.6772	2.7172
		FS^{25}-ko.2	1.1733	1.00854	.850	-1.8877	4.2344

		FS^{95}-ko.2	-1.8933	1.21634	.632	-5.5851	1.7985
		wt	-1.2433	1.00854	.817	-4.3044	1.8177
	FS^{95}-ko.2	fs-ko	3.2000	1.07510	.057	-.0631	6.4631
		FS^{25}-ko.1	1.4133	1.21634	.851	-2.2785	5.1051
		FS^{25}-ko.2	3.0667	1.17772	.126	-.5079	6.6412
		FS^{95}-ko.1	1.8933	1.21634	.632	-1.7985	5.5851
		wt	.6500	1.17772	.993	-2.9246	4.2246
	wt	fs-ko	2.5500 *	.83277	.047	.0224	5.0776
		FS^{25}-ko.1	.7633	1.00854	.973	-2.2977	3.8244
		FS^{25}-ko.2	2.4167	.96160	.151	-.5020	5.3353
		FS^{95}-ko.1	1.2433	1.00854	.817	-1.8177	4.3044
		FS^{95}-ko.2	-.6500	1.17772	.993	-4.2246	2.9246
LUNG	fs-ko	FS^{25}-ko.1	-5.3142	2.97429	.488	-14.3416	3.7133
		FS^{25}-ko.2	-1.5008	2.79386	.994	-9.9807	6.9790
		FS^{95}-ko.1	-10.1542 *	2.97429	.020	-19.1816	-1.1267
		FS^{95}-ko.2	-15.1008 *	3.60686	.003	-26.0483	-4.1534
		wt	-20.8675 *	2.79386	.000	-29.3473	-12.3877
	FS^{25}-ko.1	fs-ko	5.3142	2.97429	.488	-3.7133	14.3416
		FS^{25}-ko.2	3.8133	3.38353	.866	-6.4563	14.0829
		FS^{95}-ko.1	-4.8400	3.53398	.744	-15.5662	5.8862
		FS^{95}-ko.2	-9.7867	4.08069	.188	-22.1723	2.5989
		wt	-15.5533 *	3.38353	.001	-25.8229	-5.2837
	FS^{25}-ko.2	fs-ko	1.5008	2.79386	.994	-6.9790	9.9807
		FS^{25}-ko.1	-3.8133	3.38353	.866	-14.0829	6.4563
		FS^{95}-ko.1	-8.6533	3.38353	.139	-18.9229	1.6163
		FS^{95}-ko.2	-13.6000 *	3.95111	.019	-25.5923	-1.6077
		wt	-19.3667 *	3.22607	.000	-29.1583	-9.5750
	FS^{95}-ko.1	fs-ko	10.1542 *	2.97429	.020	1.1267	19.1816
		FS^{25}-ko.1	4.8400	3.53398	.744	-5.8862	15.5662
		FS^{25}-ko.2	8.6533	3.38353	.139	-1.6163	18.9229
		FS^{95}-ko.2	-4.9467	4.08069	.828	-17.3323	7.4389
		wt	-10.7133 *	3.38353	.037	-20.9829	-.4437
	FS^{95}-ko.2	fs-ko	15.1008 *	3.60686	.003	4.1534	26.0483
		FS^{25}-ko.1	9.7867	4.08069	.188	-2.5989	22.1723
		FS^{25}-ko.2	13.6000 *	3.95111	.019	1.6077	25.5923
		FS^{95}-ko.1	4.9467	4.08069	.828	-7.4389	17.3323
		wt	-5.7667	3.95111	.691	-17.7590	6.2256
	wt	fs-ko	20.8675 *	2.79386	.000	12.3877	29.3473
		FS^{25}-ko.1	15.5533 *	3.38353	.001	5.2837	25.8229
		FS^{25}-ko.2	19.3667 *	3.22607	.000	9.5750	29.1583
		FS^{95}-ko.1	10.7133 *	3.38353	.037	.4437	20.9829
		FS^{95}-ko.2	5.7667	3.95111	.691	-6.2256	17.7590
SPLEEN	fs-ko	FS^{25}-ko.1	-.1300	.20579	.988	-.7546	.4946
		FS^{25}-ko.2	-.1233	.19331	.987	-.7100	.4634
		FS^{95}-ko.1	-.2100	.20579	.907	-.8346	.4146
		FS^{95}-ko.2	-.2767	.24956	.874	-1.0341	.4808
		wt	-.1933	.19331	.914	-.7800	.3934
	FS^{25}-ko.1	fs-ko	.1300	.20579	.988	-.4946	.7546
		FS^{25}-ko.2	.0067	.23411	1.000	-.7039	.7172
		FS^{95}-ko.1	-.0800	.24451	.999	-.8221	.6621
		FS^{95}-ko.2	-.1467	.28234	.995	-1.0036	.7103
		wt	-.0633	.23411	1.000	-.7739	.6472
	FS^{25}-ko.2	fs-ko	.1233	.19331	.987	-.4634	.7100
		FS^{25}-ko.1	-.0067	.23411	1.000	-.7172	.7039
		FS^{95}-ko.1	-.0867	.23411	.999	-.7972	.6239
		FS^{95}-ko.2	-.1533	.27338	.993	-.9831	.6764

		wt	-.0700	.22321	1.000	-.7475	.6075
	FS^{95}-ko.1	fs-ko	.2100	.20579	.907	-.4146	.8346
		FS^{25}-ko.1	.0800	.24451	.999	-.6621	.8221
		FS^{25}-ko.2	.0867	.23411	.999	-.6239	.7972
		FS^{95}-ko.2	-.0667	.28234	1.000	-.9236	.7903
		wt	.0167	.23411	1.000	-.6939	.7272
	FS^{95}-ko.2	fs-ko	.2767	.24956	.874	-.4808	1.0341
		FS^{25}-ko.1	.1467	.28234	.995	-.7103	1.0036
		FS^{25}-ko.2	.1533	.27338	.993	-.6764	.9831
		FS^{95}-ko.1	.0667	.28234	1.000	-.7903	.9236
		wt	.0833	.27338	1.000	-.7464	.9131
	wt	fs-ko	.1933	.19331	.914	-.3934	.7800
		FS^{25}-ko.1	.0633	.23411	1.000	-.6472	.7739
		FS^{25}-ko.2	.0700	.22321	1.000	-.6075	.7475
		FS^{95}-ko.1	-.0167	.23411	1.000	-.7272	.6939
		FS^{95}-ko.2	-.0833	.27338	1.000	-.9131	.7464
THYMUS	fs-ko	FS^{25}-ko.1	.0867	.17962	.996	-.4585	.6318
		FS^{25}-ko.2	-.0833	.16872	.996	-.3954	.4288
		FS^{95}-ko.1	-.2133	.17962	.839	-.7585	.3318
		FS^{95}-ko.2	-.2333	.21782	.889	-.8945	.4278
		wt	.1233	.16872	.976	-.3888	.6354
	FS^{25}-ko.1	fs-ko	-.0867	.17962	.996	-.6318	.4585
		FS^{25}-ko.2	-.1700	.20433	.959	-.7902	.4502
		FS^{95}-ko.1	-.3000	.21342	.723	-.9478	.3478
		FS^{95}-ko.2	-.3200	.24644	.784	-1.0680	.4280
		wt	.0367	.20433	1.000	-.5835	.6569
	FS^{25}-ko.2	fs-ko	.0833	.16872	.996	-.4288	.5954
		FS^{25}-ko.1	.1700	.20433	.959	-.4502	.7902
		FS^{95}-ko.1	-.1300	.20433	.987	-.7502	.4902
		FS^{95}-ko.2	-.1500	.23861	.988	-.8742	.5742
		wt	.2067	.19483	.893	-.3847	.7980
	FS^{95}-ko.1	fs-ko	.2133	.17962	.839	-.3318	.7585
		FS^{25}-ko.1	.3000	.21342	.723	-.3478	.9478
		FS^{25}-ko.2	.1300	.20433	.987	-.4902	.7502
		FS^{95}-ko.2	-.0200	.24644	1.000	-.7680	.7280
		wt	.3367	.20433	.575	-.2835	.9569
	FS^{95}-ko.2	fs-ko	.2333	.21782	.889	-.4278	.8945
		FS^{25}-ko.1	.3200	.24644	.784	-.4280	1.0680
		FS^{25}-ko.2	.1500	.23861	.988	-.5742	.8742
		FS^{95}-ko.1	.0200	.24644	1.000	-.7280	.7680
		wt	.3567	.23861	.670	-.3676	1.0809
	wt	fs-ko	-.1233	.16872	.976	-.6354	.3888
		FS^{25}-ko.1	-.0367	.20433	1.000	-.6569	.5835
		FS^{25}-ko.2	-.2067	.19483	.893	-.7980	.3847
		FS^{95}-ko.1	-.3367	.20433	.575	-.9569	.2835
		FS^{95}-ko.2	-.3567	.23861	.670	-1.0809	.3676
LIVER	fs-ko	FS^{25}-ko.1	-10.8367	4.68129	.219	-25.0452	3.3719
		FS^{25}-ko.2	-1.5000	4.39731	.999	-14.8466	11.8466
		FS^{95}-ko.1	-12.4167	4.68129	.115	-26.6252	1.7919
		FS^{95}-ko.2	-16.1167	5.67690	.077	-33.3470	1.1137
		wt	-28.2833 *	4.39731	.000	-41.6299	-14.9367
	FS^{25}-ko.1	fs-ko	10.8367	4.68129	.219	-3.3719	25.0452
		FS^{25}-ko.2	9.3367	5.32541	.509	-6.8269	25.5002
		FS^{95}-ko.1	-1.5800	5.56221	1.000	-18.4622	15.3022
		FS^{95}-ko.2	-5.2800	6.42268	.961	-24.7739	14.2139
		wt	-17.4467 *	5.32541	.028	-33.6102	-1.2831

	FS^{25}-ko.2	fs-ko	1.5000	4.39731	.999	-11.8466	14.8466
		FS^{25}-ko.1	-9.3367	5.32541	.509	-25.5002	6.8269
		FS^{95}-ko.1	-10.9167	5.32541	.339	-27.0802	5.2469
		FS^{95}-ko.2	-14.6167	6.21874	.205	-33.4916	4.2583
		wt	-26.7833 *	5.07758	.000	-42.1946	-11.3720
	FS^{95}-ko.1	fs-ko	12.4167	4.68129	.115	-1.7919	26.6252
		FS^{25}-ko.1	1.5800	5.56221	1.000	-15.3022	18.4622
		FS^{25}-ko.2	10.9167	5.32541	.339	-5.2469	27.0802
		FS^{95}-ko.2	-3.7000	6.42268	.992	-23.1939	15.7939
		wt	-15.8667	5.32541	.057	-32.0302	.2969
	FS^{95}-ko.2	fs-ko	16.1167	5.67690	.077	-1.1137	33.3470
		FS^{25}-ko.1	5.2800	6.42268	.961	-14.2139	24.7739
		FS^{25}-ko.2	14.6167	6.21874	.205	-4.2583	33.4916
		FS^{95}-ko.1	3.7000	6.42268	.992	-15.7939	23.1939
		wt	-12.1667	6.21874	.389	-31.0416	6.7083
	wt	fs-ko	28.2833 *	4.39731	.000	14.9367	41.6299
		FS^{25}-ko.1	17.4467 *	5.32541	.028	1.2831	33.6102
		FS^{25}-ko.2	26.7833 *	5.07758	.000	11.3720	42.1946
		FS^{95}-ko.1	15.8667	5.32541	.057	-.2969	32.0302
		FS^{95}-ko.2	12.1667	6.21874	.389	-6.7083	31.0416
KIDNEY	fs-ko	FS^{25}-ko.1	-.3033	.83359	.999	-2.8334	2.2267
		FS^{25}-ko.2	.6667	.78302	.955	-1.7099	3.0433
		FS^{95}-ko.1	-.1433	.83359	1.000	-2.6734	2.3867
		FS^{95}-ko.2	-.5167	1.01087	.995	-3.5848	2.5515
		wt	-1.6667	.78302	.300	-4.0433	.7099
	FS^{25}-ko.1	fs-ko	.3033	.83359	.999	-2.2267	2.8334
		FS^{25}-ko.2	.9700	.94828	.907	-1.9082	3.8482
		FS^{95}-ko.1	.1600	.99045	1.000	-2.8462	3.1662
		FS^{95}-ko.2	-.2133	1.14367	1.000	-3.6846	3.2579
		wt	-1.3623	.94828	.704	-4.2415	1.5149
	FS^{25}-ko.2	fs-ko	-.6667	.78302	.955	-3.0433	1.7099
		FS^{25}-ko.1	-.9700	.94828	.907	-3.8482	1.9082
		FS^{95}-ko.1	-.8100	.94828	.954	-3.6882	2.0682
		FS^{95}-ko.2	-1.1833	1.10736	.890	-4.5443	2.1777
		wt	-2.3333	.90415	.132	-5.0776	.4109
	FS^{95}-ko.1	fs-ko	.1433	.83359	1.000	-2.3867	2.6734
		FS^{25}-ko.1	-.1600	.99045	1.000	-3.1662	2.8462
		FS^{25}-ko.2	.8100	.94828	.954	-2.0682	3.6882
		FS^{95}-ko.2	-.3733	1.14367	.999	-3.8446	3.0979
		wt	-1.5233	.94828	.601	-4.4015	1.3549
	FS^{95}-ko.2	fs-ko	.5167	1.01087	.995	-2.5515	3.5848
		FS^{25}-ko.1	.2133	1.14367	1.000	-3.2579	3.6846
		FS^{25}-ko.2	1.1833	1.10736	.890	-2.1777	4.5443
		FS^{95}-ko.1	.3733	1.14367	.999	-3.0979	3.8446
		wt	-1.1500	1.10736	.901	-4.5110	2.2110
	wt	fs-ko	1.6667	.78302	.300	-.7099	4.0433
		FS^{25}-ko.1	1.3633	.94828	.704	-1.5149	4.2415
		FS^{25}-ko.2	2.3333	.90415	.132	-.4109	5.0776
		FS^{95}-ko.1	1.5233	.94828	.601	-1.3549	4.4015
		FS^{95}-ko.2	1.1500	1.10736	.901	-2.2110	4.5110
GI	fs-ko	FS^{25}-ko.1	-3.9767	4.10321	.924	-16.4306	8.4773
		FS^{25}-ko.2	-5.6833	3.85430	.682	-17.3818	6.0151
		FS^{95}-ko.1	-7.8247	4.10321	.417	-20.2786	4.6293
		FS^{95}-ko.2	-8.5500	4.97588	.531	-23.6526	6.5526
		wt	-29.3500 *	3.85430	.000	-41.0484	-17.6516
	FS^{25}-ko.1	fs-ko	3.9767	4.10321	.924	-8.4773	16.4306

	FS^{25}-ko.2	-1.7067	4.66779	.999	-15.8742	12.4609
	FS^{95}-ko.1	-3.8480	4.87534	.967	-18.6455	10.9495
	FS^{95}-ko.2	-4.5733	5.62956	.963	-21.6600	12.5133
	wt	-25.3733 *	4.66779	.000	-39.5409	-11.2058
FS^{25}-ko.2	fs-ko	5.6833	3.85430	.682	-6.0151	17.3818
	FS^{25}-ko.1	1.7067	4.66779	.999	-12.4609	15.8742
	FS^{95}-ko.1	-2.1413	4.66779	.997	-16.3089	12.0262
	FS^{95}-ko.2	-2.8667	5.45080	.995	-19.4108	13.6774
	wt	-23.6667 *	4.45056	.000	-37.1749	-10.1585
FS^{95}-ko.1	fs-ko	7.8247	4.10321	.417	-4.6293	20.2786
	FS^{25}-ko.1	3.8480	4.87534	.967	-10.9495	18.6455
	FS^{25}-ko.2	2.1413	4.66779	.997	-12.0262	16.3089
	FS^{95}-ko.2	-.7253	5.62956	1.000	-17.8120	16.3613
	wt	-21.5253 *	4.66779	.001	-35.6929	-7.3578
FS^{95}-ko.2	fs-ko	8.5500	4.97588	.531	-6.5526	23.6526
	FS^{25}-ko.1	4.5733	5.62956	.963	-12.5133	21.6600
	FS^{25}-ko.2	2.8667	5.45080	.995	-13.6774	19.4108
	FS^{95}-ko.1	.7253	5.62956	1.000	-16.3613	17.8120
	wt	-20.8000 *	5.45080	.007	-37.3441	-4.2559
wt	fs-ko	29.3500 *	3.85430	.000	17.6516	41.0484
	FS^{25}-ko.1	25.3733 *	4.66779	.000	11.2058	39.5409
	FS^{25}-ko.2	23.6667 *	4.45056	.000	10.1585	37.1749
	FS^{95}-ko.1	21.5253 *	4.66779	.001	7.3578	35.6929
	FS^{95}-ko.2	20.8000 *	5.45080	.007	4.2559	37.3441

*** The mean difference is significant at the 0.05 level.**

Table IV.7 Follistatin mRNA expression in the organs of the rescued mice and wild-type mice-- Descriptives

		N	Mean	Std. Deviation	Std. Error	95% Confidence Interval for Mean		Minimum	Maximum
						Lower Bound	Upper Bound		
HEART	FS^{25}-ko.1	3	4.305E-03	5.195E-03	2.999E-03	-8.599E-03	1.721E-02	8.9E-04	1.0E-02
	FS^{25}-ko.2	3	4.995E-03	6.777E-03	3.913E-03	-1.184E-02	2.183E-02	8.6E-04	1.3E-02
	FS^{95}-ko.1	3	2.394E-04	3.171E-04	1.830E-04	-5.482E-04	1.027E-03	2.8E-05	6.0E-04
	FS^{95}-ko.2	3	2.251E-04	1.730E-04	9.988E-05	-2.045E-04	6.549E-04	2.7E-05	3.5E-04
	wt	3	5.657E-04	6.159E-05	3.556E-05	4.127E-04	7.187E-04	5.2E-04	6.4E-04
LUNG	FS^{25}-ko.1	3	2.495E-02	3.133E-02	1.808E-02	-5.287E-02	1.0278E-01	5.7E-03	6.1E-02
	FS^{25}-ko.2	3	2.129E-03	7.172E-04	4.141E-04	3.473E-04	3.911E-03	1.4E-03	2.8E-03
	FS^{95}-ko.1	3	1.112E-04	1.065E-04	6.150E-05	-1.534E-04	3.758E-04	3.2E-05	2.3E-04
	FS^{95}-ko.2	3	1.287E-03	1.452E-03	8.387E-04	-2.321E-03	4.896E-03	5.7E-05	2.9E-03
	wt	3	3.369E-03	1.720E-03	9.931E-04	-9.037E-04	7.642E-03	2.2E-03	5.3E-03
LIVER	FS^{25}-ko.1	3	6.173E-01	6.058E-01	3.497E-01	-8.876E-01	2.122E+00	2.8E-02	1.2E+00
	FS^{25}-ko.2	3	6.733E-01	3.080E-01	1.778E-01	-9.176E-02	1.438E+00	3.3E-01	9.3E-01
	FS^{95}-ko.1	3	6.366E-02	5.801E-02	3.349E-02	-8.045E-02	2.077E-01	1.4E-02	1.3E-01
	FS^{95}-ko.2	3	1.913E-02	1.636E-02	9.448E-03	-2.151E-02	5.979E-02	2.8E-03	3.6E-02
	wt	3	7.792E-02	3.741E-03	2.160E-03	6.862E-02	8.721E-02	7.5E-02	8.2E-02
KIDNEY	FS^{25}-ko.1	3	5.312E-03	6.248E-03	3.607E-03	-1.020E-02	2.083E-02	9.6E-04	1.2E-02
	FS^{25}-ko.2	3	1.503E-02	1.562E-02	9.018E-03	-2.376E-02	5.383E-02	1.1E-03	3.2E-02
	FS^{95}-ko.1	3	1.445E-03	1.793E-03	1.035E-03	-3.008E-03	5.900E-03	3.0E-04	3.5E-03
	FS^{95}-ko.2	3	1.473E-02	[illegible]97E-03	5.541E-03	-9.102E-03	3.858E-02	4.0E-03	2.2E-02
	wt	3	5.553E-03	E-03	2.071E-03	-3.359E-03	1.446E-02	2.2E-03	9.3E-03
MUSCLE	FS^{25}-ko.1	3	3.851E-04	2.536E-04	1.464E-04	-2.449E-04	1.015E-03	1.0E-04	5.9E-04
	FS^{25}-ko.2	3	2.548E-03	1.746E-03	1.008E-03	-1.789E-03	6.886E-03	7.0E-04	4.2E-03
	FS^{95}-ko.1	3	7.180E-04	3.529E-04	2.037E-04	-1.586E-04	1.594E-03	3.9E-04	1.1E-03
	FS^{95}-ko.2	3	9.0155E-04	6.346E-04	3.664E-04	-6.750E-04	2.478E-03	1.9E-04	1.4E-03
	wt	3	5.605E-02	6.329E-03	3.654E-03	4.033E-02	7.177E-02	4.9E-02	6.2E-02
SKIN	FS^{25}-ko.1	3	1.829E-04	1.071E-04	6.188E-05	-8.336E-05	4.491E-04	1.2E-04	3.1E-04
	FS^{25}-ko.2	3	1.109E-03	1.507E-03	8.701E-04	-2.635E-03	4.853E-03	1.4E-04	2.8E-03
	FS^{95}-ko.1	3	1.434E-04	4.727E-05	2.729E-05	2.597E-05	2.608E-04	1.1E-04	2.0E-04
	FS^{95}-ko.2	3	6.460E-04	6.212E-04	3.586E-04	-8.971E-04	2.189E-03	1.9E-04	1.4E-03
	wt	3	1.325E-01	3.548E-02	2.0488E-02	4.4431E-02	2.207E-01	9.9E-02	1.7E-01

(The data is presented as computer scientific notation. For example, "4.0E-0.2" means "4.0 x 10^{-2}". The follistatin mRNA levels are the ratios of the copy numbers of human or mouse follistatin mRNA to the copy numbers of mouse β actin mRNA in every single organ to avoid sampling errors.)

Table IV.8 Follistatin mRNA expression in the organs of the rescued mice and wild-type mice– Multiple comparisons

Tukey HSD

	Transgenic line (I)	Transgenic line (J)	Mean Difference (I-J)	Std. Error	Sig.	95% Confidence Interval	
						Lower Bound	Upper Bound
HEART	FS^{25}-ko.1	FS^{25}-ko.2	-6.90E-04	3.12E-03	.999	-1.10E-02	9.58E-03
		FS^{95}-ko.1	4.07E-03	3.12E-03	.696	-6.21E-03	1.43E-02
		FS^{95}-ko.2	4.08E-03	3.12E-03	.693	-6.19E-03	1.44E-02
		wt	3.74E-03	3.12E-03	.753	-6.53E-03	1.40E-02
	FS^{25}-ko.2	FS^{25}-ko.1	6.90E-04	3.12E-03	.999	-9.58E-03	1.10E-02
		FS^{95}-ko.1	4.76E-03	3.12E-03	.571	-5.52E-03	1.50E-02
		FS^{95}-ko.2	4.77E-03	3.12E-03	.569	-5.50E-03	1.50E-02
		wt	4.43E-03	3.12E-03	.630	-5.84E-03	1.47E-02
	FS^{95}-ko.1	FS^{25}-ko.1	-4.07E-03	3.12E-03	.696	-1.43E-02	6.21E-03
		FS^{25}-ko.2	-4.76E-03	3.12E-03	.571	-1.50E-02	5.52E-03
		FS^{95}-ko.2	1.43E-05	3.12E-03	1.000	-1.03E-02	1.03E-02
		wr	-3.26E-04	3.12E-03	1.000	-1.06E-02	9.95E-03
	FS^{95}-ko.2	FS^{25}-ko.1	-4.08E-03	3.12E-03	.693	-1.44E-02	6.19E-03
		FS^{25}-ko.2	-4.77E-03	3.12E-03	.569	-1.50E-02	5.50E-03
		FS^{95}-ko.1	-1.43E-05	3.12E-03	1.000	-1.03E-02	1.03E-02
		wr	-3.41E-04	3.12E-03	1.000	-1.06E-02	9.93E-03
	wt	FS^{25}-ko.1	-3.74E-03	3.12E-03	.753	-1.40E-02	6.53E-03
		FS^{25}-ko.2	-4.43E-03	3.12E-03	.630	-1.47E-02	5.84E-03
		FS^{95}-ko.1	3.26E-04	3.12E-03	1.000	-9.95E-03	1.06E-02
		FS^{95}-ko.2	3.41E-04	3.12E-03	1.000	-9.93E-03	1.06E-02
LUNG	FS^{25}-ko.1	FS^{25}-ko.2	2.28E-02	1.15E-02	.336	-1.49E-02	6.06E-02
		FS^{95}-ko.1	2.48E-02	1.15E-02	.267	-1.29E-02	6.26E-02
		FS^{95}-ko.2	2.37E-02	1.15E-02	.306	-1.41E-02	6.14E-02
		wt	2.16E-02	1.15E-02	.385	-1.62E-02	5.93E-02
	FS^{25}-ko.2	FS^{25}-ko.1	-2.28E-02	1.15E-02	.336	-6.06E-02	1.49E-02
		FS^{95}-ko.1	2.018E-03	1.15E-02	1.000	-3.57E-02	3.98E-02
		FS^{95}-ko.2	8.42E-04	1.15E-02	1.000	-3.69E-02	3.86E-02
		wt	-1.24E-03	1.15E-02	1.000	-3.90E-02	3.65E-02
	FS^{95}-ko.1	FS^{25}-ko.1	-2.48E-02	1.15E-02	.267	-6.26E-02	1.29E-02
		FS^{25}-ko.2	-2.02E-03	1.15E-02	1.000	-3.98E-02	3.57E-02
		FS^{95}-ko.2	-1.18E-03	1.15E-02	1.000	-3.89E-02	3.66E-02
		wr	-3.26E-03	1.15E-02	.998	-4.10E-02	3.45E-02
	FS^{95}-ko.2	FS^{25}-ko.1	-2.37E-02	1.15E-02	.306	-6.14E-02	1.41E-02
		FS^{25}-ko.2	-8.42E-04	1.15E-02	1.000	-3.86E-02	3.69E-02
		FS^{95}-ko.1	1.18E-03	1.15E-02	1.000	-3.66E-02	3.89E-02
		wr	-2.08E-03	1.15E-02	1.000	-3.98E-02	3.57E-02
	wt	FS^{25}-ko.1	-2.16E-02	1.15E-02	.385	-5.93E-02	1.62E-02
		FS^{25}-ko.2	1.24E-03	1.15E-02	1.000	-3.65E-02	3.90E-02
		FS^{95}-ko.1	3.26E-03	1.15E-02	.998	-3.45E-02	4.10E-02
		FS^{95}-ko.2	2.08E-03	1.15E-02	1.000	-3.57E-02	3.98E-02
LIVER	FS^{25}-ko.1	FS^{25}-ko.2	-5.61E-02	2.49E-01	.999	-8.76E-01	7.64E-01
		FS^{95}-ko.1	5.54E-01	2.49E-01	.247	-2.66E-01	1.37E+00

		FS^{95}-ko.2	5.98E-01	2.49E-01	.192	-2.22E-01	1.42E+00
		wt	5.39E-01	2.49E-01	.267	-2.81E-01	1.36E+00
	FS^{25}-ko.2	FS^{25}-ko.1	5.61E-02	2.49E-01	.999	-7.64E-01	8.76E-01
		FS^{95}-ko.1	6.10E-01	2.49E-01	.180	-2.10E-01	1.43E+00
		FS^{95}-ko.2	6.54E-01	2.49E-01	.138	-1.66E-01	1.47E+00
		wt	5.95E-01	2.49E-01	.195	-2.24E-01	1.42E+00
	FS^{95}-ko.1	FS^{25}-ko.1	-5.54E-01	2.49E-01	.247	-1.37E+00	2.66E-01
		FS^{25}-ko.2	-6.10E-01	2.49E-01	.180	-1.43E+00	2.10E-01
		FS^{95}-ko.2	4.45E-02	2.49E-01	1.000	-7.75E-01	8.64E-01
		wr	-1.43E-02	2.49E-01	1.000	-8.34E-01	8.06E-01
	FS^{95}-ko.2	FS^{25}-ko.1	-5.98E-01	2.49E-01	.192	-1.42E+00	2.22E-01
		FS^{25}-ko.2	-6.54E-01	2.49E-01	.138	-1.47E+00	1.66E-01
		FS^{95}-ko.1	-4.45E-02	2.49E-01	1.000	-8.64E-01	7.75E-01
		wr	-5.88E-02	2.49E-01	.999	-8.79E-01	7.61E-01
	wt	FS^{25}-ko.1	-5.39E-01	2.49E-01	.267	-1.36E+00	2.81E-01
		FS^{25}-ko.2	-5.95E-01	2.49E-01	.195	-1.42E+00	2.24E-01
		FS^{95}-ko.1	1.43E-02	2.49E-01	1.000	-8.06E-01	8.34E-01
		FS^{95}-ko.2	5.88E-02	2.49E-01	.999	-7.61E-01	8.79E-01
KIDNEY	FS^{25}-ko.1	FS^{25}-ko.2	-9.72E-03	7.22E-03	.671	-3.35E-02	1.40E-02
		FS^{95}-ko.1	3.87E-03	7.22E-03	.981	-1.99E-02	2.76E-02
		FS^{95}-ko.2	-9.43E-03	7.22E-03	.694	-3.32E-02	1.43E-02
		wt	-2.41E-04	7.22E-03	1.000	-2.40E-02	2.35E-02
	FS^{25}-ko.2	FS^{25}-ko.1	9.72E-03	7.22E-03	.671	-1.40E-02	3.35E-02
		FS^{95}-ko.1	1.36E-02	7.22E-03	.384	-1.02E-02	3.74E-02
		FS^{95}-ko.2	2.97E-04	7.22E-03	1.000	-2.35E-02	2.41E-02
		wt	9.48E-03	7.22E-03	.690	-1.43E-02	3.33E-02
	FS^{95}-ko.1	FS^{25}-ko.1	-3.87E-03	7.22E-03	.981	-2.76E-02	1.99E-02
		FS^{25}-ko.2	-1.36E-02	7.22E-03	.384	-3.74E-02	1.02E-02
		FS^{95}-ko.2	-1.33E-02	7.22E-03	.404	-3.71E-02	1.05E-02
		wr	-4.11E-03	7.22E-03	.977	-2.79E-02	1.97E-02
	FS^{95}-ko.2	FS^{25}-ko.1	9.43E-03	7.22E-03	.694	-1.43E-02	3.32E-02
		FS^{25}-ko.2	-2.97E-04	7.22E-03	1.000	-2.41E-02	2.35E-02
		FS^{95}-ko.1	1.33E-02	7.22E-03	.404	-1.05E-02	3.71E-02
		wr	9.19E-03	7.22E-03	.713	-1.46E-02	3.30E-02
	wt	FS^{25}-ko.1	2.41E-04	7.22E-03	1.000	-2.35E-02	2.40E-02
		FS^{25}-ko.2	-9.48E-03	7.22E-03	.690	-3.33E-02	1.43E-02
		FS^{95}-ko.1	4.11E-03	7.22E-03	.977	-1.97E-02	2.79E-02
		FS^{95}-ko.2	-9.19E-03	7.22E-03	.713	-3.30E-02	1.46E-02
MUSCLE	FS^{25}-ko.1	FS^{25}-ko.2	-2.16E-03	2.41E-03	.892	-1.01E-02	5.78E-03
		FS^{95}-ko.1	-3.33E-04	2.41E-03	1.000	-8.28E-03	7.61E-03
		FS^{95}-ko.2	-5.16E-04	2.41E-03	.999	-8.46E-03	7.43E-03
		wt	-5.57E-02 *	2.41E-03	.000	-6.36E-02	-4.77E-02
	FS^{25}-ko.2	FS^{25}-ko.1	2.16E-03	2.41E-03	.892	-5.78E-03	1.01E-02
		FS^{95}-ko.1	1.83E-03	2.41E-03	.937	-6.11E-03	9.78E-03
		FS^{95}-ko.2	1.65E-03	2.41E-03	.956	-6.30E-03	9.59E-03
		wt	-5.35E-02 *	2.41E-03	.000	-6.15E-02	-4.56E-02
	FS^{95}-ko.1	FS^{25}-ko.1	3.33E-04	2.41E-03	1.000	-7.61E-03	8.28E-03
		FS^{25}-ko.2	-1.83E-03	2.41E-03	.937	-9.78E-03	6.11E-03
		FS^{95}-ko.2	-1.83E-04	2.41E-03	1.000	-8.13E-03	7.76E-03

		wr	-5.53E-02 *	2.41E-03	.000	-6.33E-02	-4.74E-02
	FS^{95}-ko.2	FS^{25}-ko.1	5.16E-04	2.41E-03	.999	-7.43E-03	8.46E-03
		FS^{25}-ko.2	-1.65E-03	2.41E-03	.956	-9.59E-03	6.30E-03
		FS^{95}-ko.1	1.83E-04	2.41E-03	1.000	-7.76E-03	8.13E-03
		wr	-5.52E-02 *	2.41E-03	.000	-6.31E-02	-4.72E-02
	wt	FS^{25}-ko.1	5.57E-02 *	2.41E-03	.000	4.77E-02	6.36E-02
		FS^{25}-ko.2	5.35E-02 *	2.41E-03	.000	4.56E-02	6.15E-02
		FS^{95}-ko.1	5.53E-02 *	2.41E-03	.000	4.74E-02	6.33E-02
		FS^{95}-ko.2	5.52E-02 *	2.41E-03	.000	4.72E-02	6.31E-02
SKIN	FS^{25}-ko.1	FS^{25}-ko.2	-9.26E-04	1.30E-02	1.000	-4.36E-02	4.18E-02
		FS^{95}-ko.1	3.95E-05	1.30E-02	1.000	-4.27E-02	4.27E-02
		FS^{95}-ko.2	-4.63E-04	1.30E-02	1.000	-4.32E-02	4.22E-02
		wt	-1.32E-01 *	1.30E-02	.000	-1.75E-01	-8.97E-02
	FS^{25}-ko.2	FS^{25}-ko.1	9.26E-04	1.30E-02	1.000	-4.18E-02	4.36E-02
		FS^{95}-ko.1	9.66E-04	1.30E-02	1.000	-4.17E-02	4.37E-02
		FS^{95}-ko.2	4.63E-04	1.30E-02	1.000	-4.22E-02	4.32E-02
		wt	-1.31E-01 *	1.30E-02	.000	-1.74E-01	-8.88E-02
	FS^{95}-ko.1	FS^{25}-ko.1	-3.95E-05	1.30E-02	1.000	-4.27E-02	4.27E-02
		FS^{25}-ko.2	-9.66E-04	1.30E-02	1.000	-4.37E-02	4.17E-02
		FS^{95}-ko.2	-5.03E-04	1.30E-02	1.000	-4.32E-02	4.22E-02
		wr	-1.32E-01 *	1.30E-02	.000	-1.75E-01	-8.98E-02
	FS^{95}-ko.2	FS^{25}-ko.1	4.63E-04	1.30E-02	1.000	-4.22E-02	4.32E-02
		FS^{25}-ko.2	-4.63E-04	1.30E-02	1.000	-4.32E-02	4.22E-02
		FS^{95}-ko.1	5.03E-04	1.30E-02	1.000	-4.22E-02	4.32E-02
		wr	-1.32E-01 *	1.30E-02	.000	-1.75E-01	-8.92E-02
	wt	FS^{25}-ko.1	1.32E-01 *	1.30E-02	.000	8.97E-02	1.75E-01
		FS^{25}-ko.2	1.31E-01 *	1.30E-02	.000	8.88E-02	1.74E-01
		FS^{95}-ko.1	1.32E-01 *	1.30E-02	.000	8.98E-02	1.75E-01
		FS^{95}-ko.2	1.32E-01 *	1.30E-02	.000	8.92E-02	1.75E-01

*** The mean difference is significant at the 0.05 level.**

- Reference -

Aaltonen J, Laitinen MP, Vuojolainen K, Jaatinen R, Horelli-Kuitunen N, Seppa L *et al.* (1999) Human growth differentiation factor 9 (GDF-9) and its novel homolog GDF-9B are expressed in oocytes during early folliculogenesis. *Journal of Clinical Endocrinology & Metabolism* **84** 2744-2750

Ackland JF, Schwartz NB, Mayo KE and Dodson RE (1992) Nonsteroidal signals originating in the gonads. *Physiological Reviews* **72** 731-787

Alak BM, Smith GD, Woodruff TK, Stouffer RL and Wolf DP (1996) Enhancement of primate oocyte maturation and fertilization in vitro by inhibin A and activin A. *Fertility & Sterility* **66** 646-653

Alak BM, Coskun S, Friedman CI, Kennard EA, Kim MH and Seifer DB (1998) Activin A stimulates meiotic maturation of human oocytes and modulates granulosa cell steroidogenesis in vitro. *Fertility & Sterility* **70** 1126-1130

Albano RM, Arkell R, Beddington RS and Smith JC (1994) Expression of inhibin subunits and follistatin during postimplantation mouse development: decidual expression of activin and expression of follistatin in primitive streak, somites and hindbrain. *Development* **120** 803-813

Aloi JA, Marshall JC, Yasin M, Gilrain JT, Haisenleder DJ and Dalkin AC (1997) Ovarian activin receptor subtype and follistatin gene expression in rats: reciprocal regulation by gonadotropins. *Biology of Reproduction* **56** 1565-1569

Amthor H, Christ B, Weil M and Patel K (1998) The importance of timing differentiation during limb muscle development. *Current Biology* **8** 642-652

Amthor H, Christ B, Rashid-Doubell F, Kemp CF, Lang E and Patel K (2002) Follistatin regulates bone morphogenetic protein-7 (BMP-7) activity to stimulate embryonic muscle growth. *Developmental Biology* **243** 115-127

Anderson RA, Evans LW, Irvine DS, McIntyre MA, Groome NP and Riley SC (1998) Follistatin and activin A production by the male reproductive tract. *Human Reproduction* **13** 3319-3325

Andersson AM, Muller J and Skakkebaek NE (1998) Different roles of prepubertal and postpubertal germ cells and Sertoli cells in the regulation of serum inhibin B levels. *Journal of Clinical Endocrinology & Metabolism* **83** 4451-4458

Asteria C (2000) Identification of follistatin as a possible trait-causing gene in polycystic ovary syndrome. *European Journal of Endocrinology* **143** 467-469

Attisano L, Carcamo J, Ventura F, Weis FM, Massague J and Wrana JL (1993) Identification of human activin and TGF beta type I receptors that form heteromeric kinase complexes with type II receptors. *Cell* **75** 671-680

Attisano L and Wrana JL (1998) Mads and Smads in TGF-beta signaling. *Current Opinion in Cell Biology* **10** 188-194

Baarends WM, Uilenbroek JT, Kramer P, Hoogerbrugge JW, van Leeuwen EC, Themmen AP *et al.* (1995) Anti-mullerian hormone and anti-mullerian hormone type II receptor messenger ribonucleic acid expression in rat ovaries during postnatal development, the estrous cycle, and gonadotropin-induced follicle growth. *Endocrinology* **136** 4951-4962

Baratta M, West LA, Turzillo AM and Nett TM (2001) Activin modulates differential effects of estradiol on synthesis and secretion of follicle-stimulating hormone in ovine pituitary cells. *Biology of Reproduction* **64** 714-719.

Beck HN, Drahushuk K, Jacoby DB, Higgins D and Lein PJ (2001) Bone morphogenetic protein-5 (BMP-5) promotes dendritic growth in cultured sympathetic neurons. *BMC Neuroscience* **2** 12

Bernard DJ, Chapman SC and Woodruff TK (2001) An emerging role for co-receptors in inhibin signal transduction. *Molecular & Cellular Endocrinology* **180** 55-62

Besecke LM, Guendner MJ, Schneyer AL, Bauer-Dantoin AC, Jameson JL and Weiss J (1996) Gonadotropin-releasing hormone regulates follicle-stimulating hormone-beta gene

expression through an activin/follistatin autocrine or paracrine loop. *Endocrinology* **137** 3667-3673

Besecke LM, Guendner MJ, Sluss PA, Polak AG, Woodruff TK, Jameson JL *et al.* (1997) Pituitary follistatin regulates activin-mediated production of follicle-stimulating hormone during the rat estrous cycle. *Endocrinology* **138** 2841-2848

Bessho K, Konishi Y, Kaihara S, Fujimura K, Okubo Y and Iizuka T (2000) Bone induction by Escherichia coli -derived recombinant human bone morphogenetic protein-2 compared with Chinese hamster ovary cell-derived recombinant human bone morphogenetic protein-2. *British Journal of Oral & Maxillofacial Surgery* **38** 645-649

Bilezikjian LM, Corrigan AZ, Vaughan JM and Vale WM (1993) Activin-A regulates follistatin secretion from cultured rat anterior pituitary cells. *Endocrinology* **133** 2554-2560

Bilezikjian LM, Corrigan AZ, Blount AL and Vale WW (1996) Pituitary follistatin and inhibin subunit messenger ribonucleic acid levels are differentially regulated by local and hormonal factors. *Endocrinology* **137** 4277-4284

Bilezikjian LM, Turnbull AV, Corrigan AZ, Blount AL, Rivier CL and Vale WW (1998) Interleukin-1beta regulates pituitary follistatin and inhibin/activin betaB mRNA levels and attenuates FSH secretion in response to activin-A. *Endocrinology* **139** 3361-3364

Bishop CE and Smith P (1989) Mechanism of chromosomal integration of microinjected DNA. *Molecular Biology and Medicine* **6** 283-298

Bodensteiner KJ, Clay CM, Moeller CL and Sawyer HR (1999) Molecular cloning of the ovine Growth/Differentiation factor-9 gene and expression of growth/differentiation factor-9 in ovine and bovine ovaries. *Biology of Reproduction* **60** 381-386

Bodensteiner KJ, McNatty KP, Clay CM, Moeller CL and Sawyer HR (2000) Expression of growth and differentiation factor-9 in the ovaries of fetal sheep homozygous or heterozygous for the inverdale prolificacy gene (FecX(I)). *Biology of Reproduction* **62** 1479-1485

Bohnsack BL, Szabo M, Kilen SM, Tam DH and Schwartz NB (2000) Follistatin suppresses steroid-enhanced follicle-stimulating hormone release in vitro in rats. *Biology of Reproduction* **62** 636-641

Boitani C, Stefanini M, Fragale A and Morena AR (1995) Activin stimulates Sertoli cell proliferation in a defined period of rat testis development. *Endocrinology* **136** 5438-5444

Böttner M, Krieglstein K and Unsicker K (2000) The transforming growth factor-bs: structure, signaling, and roles in nervous system development and functions. *Journal of Neurochemistry* **75** 2227–2240

Braw-Tal R (1994) Expression of mRNA for follistatin and inhibin/activin subunits during follicular growth and atresia. *Journal of Molecular Endocrinology* **13** 253-264

Braw-Tal R, Tisdall DJ, Hudson NL, Smith P and McNatty KP (1994) Follistatin but not alpha or beta A inhibin subunit mRNA is expressed in ovine fetal ovaries in late gestation. *Journal of Molecular Endocrinology* **13** 1-9

Braw-Tal R, Yossefi S, Zenou A and Bor A (1997) Differential expression pattern of inhibin alpha and betaA subunits in the ovaries of postnatal and prepubertal lambs. *Reproduction, Fertility, & Development* **9** 825-832

Burger HG, Farnworth PG, Findlay JK, Gurusinghe CJ, Healy DL, Mamers P *et al.* (1995) Aspects of current and future inhibin research. *Reproduction, Fertility, & Development* **7** 997-1002

Buzzard JJ, Farnworth PG, De Kretser DM, O'Connor AE, Wreford NG and Morrison JR (2003) Proliferative phase sertoli cells display a developmentally regulated response to activin in vitro. *Endocrinology* **144** 474-483.

Callow MJ, Ferrin LJ and Rubin EM (1994) Single base, site-directed mutagenesis of a 90 kilobase-pair P1 clone. *Nucleic Acids Research* **22** 4348-4349

Calvo RM, Villuendas G, Sancho J, San Millan JL and Escobar-Morreale HF (2001) Role of the follistatin gene in women with polycystic ovary syndrome. *Fertility & Sterility* **75** 1020-1023

Camper SA and Saunders TL. Transgenic rescue of mutant phenotypes using large DNA fragments. in *Genetic manipulation of receptor expression and function* (ed. Accili D) 1-22 (John Wiley, New York., 2000).

Cancilla B, Jarred RA, Wang H, Mellor SL, Cunha GR and Risbridger GP (2001) Regulation of prostate branching morphogenesis by activin A and follistatin. *Developmental Biology* **237** 145-158

Candia AF, Watabe T, Hawley SH, Onichtchouk D, Zhang Y, Derynck R *et al.* (1997) Cellular interpretation of multiple TGF-beta signals: intracellular antagonism between activin/BVg1 and BMP-2/4 signaling mediated by Smads. *Development* **124** 4467-4480

Caniggia I, Lye SJ and Cross JC (1997) Activin is a local regulator of human cytotrophoblast cell differentiation. *Endocrinology* **138** 3976-3986.

Carabatsos MJ, Elvin J, Matzuk MM and Albertini DF (1998) Characterization of oocyte and follicle development in growth differentiation factor-9-deficient mice. *Developmental Biology* **204** 373-384

Carroll RS, Corrigan AZ, Gharib SD, Vale W and Chin WW (1989) Inhibin, activin, and follistatin: regulation of follicle-stimulating hormone messenger ribonucleic acid levels. *Molecular Endocrinology* **3** 1969-1976

Cataldo NA, Rabinovici J, Fujimoto VY and Jaffe RB (1994) Follistatin antagonizes the effects of activin-A on steroidogenesis in human luteinizing granulosa cells. *Journal of Clinical Endocrinology & Metabolism* **79** 272-277

Cavolina JM, Evans GL, Harris SA, Zhang M, Westerlind KC and Turner RT (1997) The effects of orbital spaceflight on bone histomorphometry and messenger ribonucleic acid levels for bone matrix proteins and skeletal signaling peptides in ovariectomized growing rats. *Endocrinology* **138** 1567-1576

Chang H, Brown CW and Matzuk MM (2002) Genetic analysis of the mammalian transforming growth factor-beta superfamily. *Endocrine Reviews* **23** 787-823.

Chapman SC and Woodruff TK (2001) Modulation of activin signal transduction by inhibin B and inhibin-binding protein (INhBP). *Molecular Endocrinology* **15** 668-679

Childs GV (1995) Division of labor among gonadotropes. *Vitamins & Hormones* **50** 215-286

Chomczynski P and Sacchi N (1987) Single-step method of RNA isolation by acid guanidinium thiocyanate-phenol-chloroform extraction. *Analytical Biochemistry* **162** 156-159

Chow RL and Lang RA (2001) Early eye development in vertebrates. *Annual Review of Cell & Developmental Biology* **17** 255-296

Copeland NG, Jenkins NA and Court DL (2001) Recombineering: a powerful new tool for mouse functional genomics. *Nature Reviews Genetics* **2** 769-779

Cuevas P, Ying SY, Ling N, Ueno N, Esch F, Guillemin R *et al.* (1987) Immunohistochemical detection of inhibin in the gonad. [erratum appears in Biochem Biophys Res Commun 1987 Jul 31;146(2):926]. *Biochemical & Biophysical Research Communications* **142** 23-30

Dale L and Wardle FC (1999) A gradient of BMP activity specifies dorsal-ventral fates in early Xenopus embryos. *Seminars in Cell & Developmental Biology* **10** 319-326

Dalkin AC, Haisenleder DJ, Yasin M, Gilrain JT and Marshall JC (1996) Pituitary activin receptor subtypes and follistatin gene expression in female rats: differential regulation by activin and follistatin. *Endocrinology* **137** 548-554

Dalkin AC, Haisenleder DJ, Gilrain JT, Aylor K, Yasin M and Marshall JC (1998) Regulation of pituitary follistatin and inhibin/activin subunit messenger ribonucleic acids (mRNAs) in male and female rats: evidence for inhibin regulation of follistatin mRNA in females. *Endocrinology* **139** 2818-2823

Dalkin AC, Haisenleder DJ, Gilrain JT, Aylor K, Yasin M and Marshall JC (1999) Gonadotropin-releasing hormone regulation of gonadotropin subunit gene expression in female rats: actions on follicle-stimulating hormone beta messenger ribonucleic acid (mRNA) involve differential expression of pituitary activin (beta-B) and follistatin mRNAs. *Endocrinology* **140** 903-908

Daluiski A, Engstrand T, Bahamonde ME, Gamer LW, Agius E, Stevenson SL *et al.* (2001) Bone morphogenetic protein-3 is a negative regulator of bone density. *Nature Genetics* **27** 84-88.

D'Antona D, Reis FM, Benedetto C, Evans LW, Groome NP, de Kretser DM *et al.* (2000) Increased maternal serum activin A but not follistatin levels in pregnant women with hypertensive disorders. *Journal of Endocrinology* **165** 157-162

Daopin S, Piez KA, Ogawa Y and Davies DR (1992) Crystal structure of transforming growth factor-bata 2: An unusual fold for the superfamily. *Science* **257** 369-373

Davis AJ and Johnson PA (1998) Expression pattern of messenger ribonucleic acid for follistatin and the inhibin/activin subunits during follicular and testicular development in gallus domesticus. *Biology of Reproduction* **59** 271-277

de Groot E, Veltmaat J, Caricasole A, Defize L and van den Eijnden-van Raaij A (2000) Cloning and analysis of the mouse follistatin promoter. *Molecular biology reports* **27** 129-139.

De Groot E, Feijen A, Eib D, Zwijsen A, Sugino H, Martens G *et al.* (2000) Expression patterns of follistatin and two follistatin-related proteins during mouse development. *International Journal of Developmental Biology* **44** 327-330.

de Jong FH, Grootenhuis AJ, Klaij IA and Van Beurden WM (1990) Inhibin and related proteins: localization, regulation, and effects. *Advances in Experimental Medicine & Biology* **274** 271-293

de Jong FH (1997) Testicular activin--too hot to handle? *European Journal of Endocrinology* **137** 448-449

de Kretser DM, Foulds LM, Hancock M and Robertson DM (1994) Partial characterization of inhibin, activin, and follistatin in the term human placenta. *Journal of Clinical Endocrinology & Metabolism* **79** 502-507

de Kretser DM and Phillips DJ (1998) Mechanisms of protein feedback on gonadotropin secretion. *Journal of Reproductive Immunology* **39** 1-12

de Kretser DM, Meinhardt A, Meehan T, Phillips DJ, O'Bryan MK and Loveland KA (2000) The roles of inhibin and related peptides in gonadal function. *Molecular & Cellular Endocrinology* **161** 43-46

de Kretser DM, Loveland KL, Meehan T, O'Bryan MK, Phillips DJ and Wreford NG (2001) Inhibins, activins and follistatin: actions on the testis. *Molecular & Cellular Endocrinology* **180** 87-92

de Kretser DM, Hedger MP, Loveland KL and Phillips DJ (2002) Inhibins, activins and follistatin in reproduction. *Human Reproduction Update* **8** 529-541.

de Winter JP, Themmen AP, Hoogerbrugge JW, Klaij IA, Grootegoed JA and de Jong FH (1992) Activin receptor mRNA expression in rat testicular cell types. *Molecular & Cellular Endocrinology* **83** R1-8

de Winter JP, Vanderstichele HM, Verhoeven G, Timmerman MA, Wesseling JG and de Jong FH (1994) Peritubular myoid cells from immature rat testes secrete activin-A and express activin receptor type II in vitro. *Endocrinology* **135** 759-767

de Winter JP, ten Dijke P, de Vries CJ, van Achterberg TA, Sugino H, de Waele P *et al.* (1996) Follistatins neutralize activin bioactivity by inhibition of activin binding to its type II receptors. *Molecular & Cellular Endocrinology* **116** 105-114

Delbaere A, Sidis Y and Schneyer AL (1999) Differential response to exogenous and endogenous activin in a human ovarian teratocarcinoma-derived cell line (PA-1): regulation by cell surface follistatin. *Endocrinology* **140** 2463-2470

DePaolo LV, Shimonaka M, Schwall RH and Ling N (1991a) In vivo comparison of the follicle-stimulating hormone-suppressing activity of follistatin and inhibin in ovariectomized rats. *Endocrinology* **128** 668-674

DePaolo LV, Bicsak TA, Erickson GF, Shimasaki S and Ling N (1991b) Follistatin and activin: a potential intrinsic regulatory system within diverse tissues. [erratum appears in Proc Soc Exp Biol Med 1992 Jul;200(3):447]. *Proceedings of the Society for Experimental Biology & Medicine* **198** 500-512

Depaolo LV, Shimonaka M and Ling N (1992) Regulation of pulsatile gonadotropin secretion by estrogen, inhibin, and follistatin (activin-binding protein) in ovariectomized rats. *Biology of Reproduction* **46** 898-904

DePaolo LV, Mercado M, Guo Y and Ling N (1993) Increased follistatin (activin-binding protein) gene expression in rat anterior pituitary tissue after ovariectomy may be mediated by pituitary activin. *Endocrinology* **132** 2221-2228

DePaolo LV (1997) Inhibins, activins, and follistatins: the saga continues. *Proceedings of the Society for Experimental Biology & Medicine* **214** 328-339

Derynck R, Zhang Y and Feng X-H (1998) Smads: Transcriptional activators of TGF-beta responses. *Cell* **95** 737-740

Dewailly D (1999) Physiopathologie du syndrome des ovaires polymicrokystiques. *Annales d Endocrinologie* **60** 123-130

Di Simone N, Crowley WF, Jr., Wang QF, Sluss PM and Schneyer AL (1996) Characterization of inhibin/activin subunit, follistatin, and activin type II receptors in human ovarian cancer cell lines: a potential role in autocrine growth regulation. *Endocrinology* **137** 486-494

Dobens LL, Peterson JS, Treisman J and Raftery LA (2000) Drosophila bunched integrates opposing DPP and EGF signals to set the operculum boundary. *Development - Supplement* **127** 745-754

Dobie KW, Lee M, Fantes JA, Graham E, Clark AJ, Springbett A *et al.* (1996) Variegated transgene expression in mouse mammary gland is determined by the transgene integration locus. *Proceedings of the National Academy of Sciences of the United States of America* **93** 6659-6664

Dong J, Albertini DF, Nishimori K, Kumar TR, Lu N and Matzuk MM (1996) Growth differentiation factor-9 is required during early ovarian folliculogenesis. *Nature* **383** 531-535

Dooley CA, Attia GR, Rainey WE, Moore DR and Carr BR (2000) Bone morphogenetic protein inhibits ovarian androgen production. *Journal of Clinical Endocrinology & Metabolism* **85** 3331-3337

Dosch R and Niehrs C (2000) Requirement for anti-dorsalizing morphogenetic protein in organizer patterning. *Mechanisms of Development* **90** 195-203

Dube JL, Wang P, Elvin J, Lyons KM, Celeste AJ and Matzuk MM (1998) The bone morphogenetic protein 15 gene is X-linked and expressed in oocytes. *Molecular Endocrinology* **12** 1809-1817

Duleba AJ, Pehlivan T, Carbone R and Spaczynski RZ (2001) Activin stimulates proliferation of rat ovarian thecal-interstitial cells. *Biology of Reproduction* **65** 704-709

Ebner R, Chen RH, Lawler S, Zioncheck T and Derynck R (1993) Determination of type I receptor specificity by the type II receptors for TGF-beta or activin. *Science* **262** 900-902

Elvin JA, Yan C, Wang P, Nishimori K and Matzuk MM (1999a) Molecular characterization of the follicle defects in the growth differentiation factor 9-deficient ovary. *Molecular Endocrinology* **13** 1018-1034

Elvin JA, Clark AT, Wang P, Wolfman NM and Matzuk MM (1999b) Paracrine actions of growth differentiation factor-9 in the mammalian ovary. *Molecular Endocrinology* **13** 1035-1048

Elvin JA, Yan C and Matzuk MM (2000) Oocyte-expressed TGF-beta superfamily members in female fertility. *Molecular & Cellular Endocrinology* **159** 1-5

Eramaa M, Hilden K, Tuuri T and Ritvos O (1995) Regulation of inhibin/activin subunit messenger ribonucleic acids (mRNAs) by activin A and expression of activin receptor mRNAs in cultured human granulosa-luteal cells. *Endocrinology* **136** 4382-4389

Erickson GF, Chung DG, Sit A, DePaolo LV, Shimasaki S and Ling N (1995) Follistatin concentrations in follicular fluid of normal and polycystic ovaries. *Human Reproduction* **10** 2120-2124

Erickson GF and Shimasaki S (2001) The physiology of folliculogenesis: the role of novel growth factors. *Fertility & Sterility* **76** 943-949

Esch FS, Shimasaki S, Mercado M, Cooksey K, Ling N, Ying S *et al.* (1987) Structural characterization of follistatin: a novel follicle-stimulating hormone release-inhibiting polypeptide from the gonad. *Molecular Endocrinology* **1** 849-855

Fainsod A, Deissler K, Yelin R, Marom K, Epstein M, Pillemer G *et al.* (1997) The dorsalizing and neural inducing gene follistatin is an antagonist of BMP-4. *Mechanisms of Development* **63** 39-50

Fang J, Yin W, Smiley E, Wang SQ and Bonadio J (1996) Molecular cloning of the mouse activin beta E subunit gene. *Biochemical & Biophysical Research Communications* **228** 669-674

Feijen A, Goumans MJ and van den Eijnden-van Raaij AJ (1994) Expression of activin subunits, activin receptors and follistatin in postimplantation mouse embryos suggests specific developmental functions for different activins. *Development* **120** 3621-3637

Festenstein R, Tolaini M, Corbella P, Mamalaki C, Parrington J, Fox M *et al.* (1996) Locus control region function and heterochromatin-induced position effect variegation. *Science* **271** 1123-1125

Findlay JK, Sai X and Shukovski L (1990) Role of inhibin-related peptides as intragonadal regulators. *Reproduction, Fertility, & Development* **2** 205-218

Findlay JK (1993) An update on the roles of inhibin, activin, and follistatin as local regulators of folliculogenesis. *Biology of Reproduction* **48** 15-23

Fitzpatrick SL, Sindoni DM, Shughrue PJ, Lane MV, Merchenthaler IJ and Frail DE (1998) Expression of growth differentiation factor-9 messenger ribonucleic acid in ovarian and nonovarian rodent and human tissues. *Endocrinology* **139** 2571-2578

Fleming JS, Tisdall DJ, Greenwood PJ, Hudson NL, Heath DA and McNatty KP (1992) Expression of the genes for alpha inhibin, beta A inhibin and follistatin in the ovaries of Booroola ewes which were homozygotes or non-carriers of the fecundity gene FecB. *Journal of Molecular Endocrinology* **8** 265-273

Fowler PA, Evans LW, Groome NP, Templeton A and Knight PG (1998) A longitudinal study of maternal serum inhibin-A, inhibin-B, activin-A, activin-AB, pro-alphaC and follistatin during pregnancy. *Human Reproduction* **13** 3530-3536

Franks S, Gharani N and McCarthy M (2001) Candidate genes in polycystic ovary syndrome. *Human Reproduction Update* **7** 405-410

Frazer KA, Narla G, Zhang JL and Rubin EM (1995) The apolipoprotein (a) gene is regulated by sex hormones and acute-phase inducers in YAC transgenic mice. *Nature Genetics* **9** 424-431

Fujiwara T, Sidis Y, Welt C, Lambert-Messerlian G, Fox J, Taylor A *et al.* (2001) Dynamics of inhibin subunit and follistatin mRNA during development of normal and polycystic ovary syndrome follicles. *Journal of Clinical Endocrinology & Metabolism* **86** 4206-4215

Fukui A, Shiurba R and Asashima M (1999) Activin incorporation into vitellogenic oocytes of Xenopus laevis. *Cellular & Molecular Biology* **45** 545-554

Fuller PJ, Chu S, Jobling T, Mamers P, Healy DL and Burger HG (1999) Inhibin subunit gene expression in ovarian cancer. *Gynecologic Oncology* **73** 273-279

Funaba M, Ogawa K, Murata T, Fujimura H, Murata E, Abe M *et al.* (1996) Follistatin and activin in bone: expression and localization during endochondral bone development. *Endocrinology* **137** 4250-4259

Galloway SM, McNatty KP, Cambridge LM, Laitinen MP, Juengel JL, Jokiranta TS *et al.* (2000) Mutations in an oocyte-derived growth factor gene (BMP15) cause increased ovulation rate and infertility in a dosage-sensitive manner. *Nature Genetics* **25** 279-283

Garces D, Mariana JC, Blanc MR, Knight PG, Monniaux D, Collet A *et al.* (2000) Anastomosis of the ovarian vein to the hepatic portal vein in sheep induces ovarian hyperstimulation associated with increased LH pulsatility, but only in the absence of the contralateral ovary. *Journal of Endocrinology* **165** 411-423

Garillon C, Chevalier A, Marshall B, Godard C, Colombani H, Callet B *et al.* (1997) Incidence des cancers chez les salariees en activite d'Electricite de France Gaz de France. *Bulletin du Cancer* **84** 1025-1031

Ge W (2000) Roles of the activin regulatory system in fish reproduction. *Canadian Journal of Physiology & Pharmacology* **78** 1077-1085

Geyer PK (1997) The role of insulator elements in defining domains of gene expression. *Current Opinion in Genetics & Development* **7** 242

Gharib SD, Leung PCK, Carroll RS and Chin WW (1990) Androgens positively regulate follicle-stimulating hormone beta subunit mRNA levels in rat pituitary cells. *Molecular Endocrinology* **4** 1620-1626

Giudice LC, Chandrasekher YA and Cataldo NA (1993) The potential roles of intraovarian peptides in normal and abnormal mechanisms of reproductive physiology. *Current Opinion in Obstetrics & Gynecology* **5** 350-359

Gluba W, Sutherland A and Scrable H (2003) Disruption of maternal-fetal communication during pre-implantation embryogenesis in mice over-expressing the short form of p53. *SDB Meeting Abstracts, Developmental Biology* **259** 599

Gordon JW, Scangos GA, Plotkin DJ, Barbosa JA and Ruddle FA (1980) Genetic transformation of mouse embryos by microinjection of purified DNA. *Proceedings of the National Academy of Sciences of the United States of America* **77** 7380-7384

Gospodarowicz D and Lau K (1989) Pituitary follicular cells secrete both vascular endothelial growth factor and follistatin. *Biochemical & Biophysical Research Communications* **165** 292-298

Gossler A, Doetschman T, Korn R, Serfling E and Kemler R (1986) Transgenesis by means of blastocyst-derived embryonic stem cell lines. *Proceedings of the National Academy of Sciences of the United States of America* **83** 9065-9069

Gottgens B, Barton LM, Chapman MA, Sinclair AM, Knudsen B, Grafham D *et al.* (2002) Transcriptional regulation of the stem cell leukemia gene (SCL)--comparative analysis of five vertebrate SCL loci. *Genome Research* **12** 749-759.

Gougeon A (1994a) Inhibine, activine, follistatine et transforming growth factor-beta (TGF-beta): presence dans l'ovaire et role possible dans la regulation de la folliculogenese chez les primates. *Fertilite Contraception Sexualite* **22** 571-576

Gougeon A (1994b) Regulation intragonadique de la folliculogenese humaine: faits et hypotheses. *Annales d Endocrinologie* **55** 63-73

Goumans MJ, Valdimarsdottir G, Itoh S, Rosendahl A, Sideras P and ten Dijke P (2002) Balancing the activation state of the endothelium via two distinct TGF-beta type I receptors. *EMBO Journal* **21** 1743-1753

Graff JM (1997) Embryonic patterning: to BMP or not to BMP, that is the question. *Cell* **89** 171-174

Grosveld F, Dillon N and Higgs D (1993) The regulation of human globin gene expression. *Baillieres Clinical Haematology* **6** 31-55

Grudzinskas JG and Yovich JL (1995) Gametes - the oocyte (The Press Syndicate of the University of Cambridge)

Gu Y, Srivastava RK, Clarke DL, Linzer DI and Gibori G (1996) The decidual prolactin receptor and its regulation by decidua-derived factors. *Endocrinology* **137** 4878-4885

Gu Z, Nomura M, Simpson BB, Lei H, Feijen A, van den Eijnden-van Raaij J *et al.* (1998) The type I activin receptor ActRIB is required for egg cylinder organization and gastrulation in the mouse. *Genes & Development* **12** 844-857

Guo Q, Kumar TR, Woodruff T, Hadsell LA, DeMayo FJ and Matzuk MM (1998) Overexpression of mouse follistatin causes reproductive defects in transgenic mice. *Molecular Endocrinology* **12** 96-106

Gurdon JB and Bourillot PY (2001) Morphogen gradient interpretation. *Nature* **413** 797-803

Hakovirta H, Kaipia A, Soder O and Parvinen M (1993) Effects of activin-A, inhibin-A, and transforming growth factor-beta 1 on stage-specific deoxyribonucleic acid synthesis during rat seminiferous epithelial cycle. *Endocrinology* **133** 1664-1668

Hammes A, Guo JK, Lutsch G, Leheste JR, Landrock D, Ziegler U *et al.* (2001) Two splice variants of the Wilms' tumor 1 gene have distinct functions during sex determination and nephron formation. *Cell* **106** 319-329.

Haraguchi R, Suzuki K, Murakami R, Sakai M, Kamikawa M, Kengaku M *et al.* (2000) Molecular analysis of external genitalia formation: the role of fibroblast growth factor (Fgf) genes during genital tubercle formation. *Development* **127** 2471-2479.

Haraguchi R, Mo R, Hui C, Motoyama J, Makino S, Shiroishi T *et al.* (2001) Unique functions of Sonic hedgehog signaling during external genitalia development. *Development* **128** 4241-4250.

Hardison RC (2000) Conserved noncoding sequences are reliable guides to regulatory elements. *Trends in genetics* **16** 369-372.

Harland R and Gerhart J (1997) Formation and function of Spemann's organizer. *Annual Review of Cell & Developmental Biology* **13** 611-667

Hashimoto O, Nakamura T, Shoji H, Shimasaki S, Hayashi Y and Sugino H (1997) A novel role of follistatin, an activin-binding protein, in the inhibition of activin action in rat pituitary cells. Endocytotic degradation of activin and its acceleration by follistatin associated with cell-surface heparan sulfate. *Journal of Biological Chemistry* **272** 13835-13842

Hashimoto O, Kawasaki N, Tsuchida K, Shimasaki S, Hayakawa T and Sugino H (2000) Difference between follistatin isoforms in the inhibition of activin signalling: activin neutralizing activity of follistatin isoforms is dependent on their affinity for activin. *Cell Signal* **12** 565-571

Hashiramoto M, Kadowaki T, Clark AE, Muraoka A, Momomura K, Sakura H *et al.* (1992) Site-directed mutagenesis of GLUT1 in helix 7 residue 282 results in perturbation of exofacial ligand binding. *Journal of Biological Chemistry* **267** 17502-17507

Hedges SB and Kumar S (2002) Vertebrate genomes compared. *Science* **297** 1283-1285

Heikinheimo K, Begue-Kirn C, Ritvos O, Tuuri T and Ruch JV (1998) Activin and bone morphogenetic protein (BMP) signalling during tooth development. *European Journal of Oral Sciences* **106 Suppl 1** 167-173

Heldin CH, Miyazono K and ten Dijke P (1997) TGF-beta signaling from cell membrane to nucleus through SMAD proteins. *Nature* **390** 465-471

Hemmati-Brivanlou A, Kelly OG and Melton DA (1994) Follistatin, an antagonist of activin, is expressed in the Spemann organizer and displays direct neuralizing activity. *Cell* **77** 283-295

Hennebold JD, Tanaka M, Saito J, Hanson BR and Adashi EY (2000) Ovary-selective genes I: the generation and characterization of an ovary-selective complementary deoxyribonucleic acid library. *Endocrinology* **141** 2725-2734

Hillier SG (1991) Regulatory functions for inhibin and activin in human ovaries. *Journal of Endocrinology* **131** 171-175

Hillier SG and Miro F (1993) Inhibin, activin, and follistatin. Potential roles in ovarian physiology. *Annals of the New York Academy of Sciences* **687** 29-38

Hogan BL (1996) Bone morphogenetic proteins in development. *Current Opinion in Genetics & Development* **6** 432-438

Houde A, Lussier JG, Ethier JF, Gagnon C and Silversides DW (1994) Cloning and tissue expression of bovine follistatin cDNA. *Molecular Reproduction & Development* **37** 391-397

Hsueh AJ, Dahl KD, Vaughan J, Tucker E, Rivier J, Bardin CW *et al.* (1987) Heterodimers and homodimers of inhibin subunits have different paracrine action in the modulation of luteinizing hormone-stimulated androgen biosynthesis. *Proceedings of the National Academy of Sciences of the United States of America* **84** 5082-5086

Hsueh AJ, McGee EA, Hayashi M and Hsu SY (2000) Hormonal regulation of early follicle development in the rat ovary. *Molecular & Cellular Endocrinology* **163** 95-100

Huang HJ, Wu JC, Su P, Zhirnov O and Miller WL (2001) A novel role for bone morphogenetic proteins in the synthesis of follicle-stimulating hormone. *Endocrinology* **142** 2275-2283

Hutchinson LA, Findlay JK, de Vos FL and Robertson DM (1987) Effects of bovine inhibin, transforming growth factor-beta and bovine Activin-A on granulosa cell differentiation. *Biochemical & Biophysical Research Communications* **146** 1405-1412

Iemura S, Yamamoto TS, Takagi C, Uchiyama H, Natsume T, Shimasaki S *et al.* (1998) Direct binding of follistatin to a complex of bone-morphogenetic protein and its receptor inhibits ventral and epidermal cell fates in early Xenopus embryo. *Proceedings of the National Academy of Sciences of the United States of America* **95** 9337-9342

Iemura S, Yamamoto TS, Takagi C, Kobayashi H and Ueno N (1999) Isolation and characterization of bone morphogenetic protein-binding proteins from the early Xenopus embryo. *Journal of Biological Chemistry* **274** 26843-26849

Igarashi M (1992) [Mini review on inhibins and activins]. *Nippon Naibunpi Gakkai Zasshi - Folia Endocrinologica Japonica* **68** 71-80

Ikeda T, Takahashi H, Suzuki A, Ueno N, Yokose S, Yamaguchi A *et al.* (1996) Cloning of rat type I receptor cDNA for bone morphogenetic protein-2 and bone morphogenetic protein-4, and the localization compared with that of the ligands. *Developmental Dynamics* **206** 318-329

Incerti B, Dong J, Borsani G and Matzuk MM (1994) Structure of the mouse growth/differentiation factor 9 gene. *Biochimica et Biophysica Acta* **1222** 125-128

Inouye S, Guo Y, Ling N and Shimasaki S (1991a) Site-specific mutagenesis of human follistatin. *Biochemical & Biophysical Research Communications* **179** 352-358

Inouye S, Guo Y, DePaolo L, Shimonaka M, Ling N and Shimasaki S (1991b) Recombinant expression of human follistatin with 315 and 288 amino acids: chemical and biological comparison with native porcine follistatin. *Endocrinology* **129** 815-822

Inouye S and Tsuji FI (1992) Monitoring gene expression in Chinese hamster ovary cells using secreted apoaequorin. *Analytical Biochemistry* **201** 114-118

Inouye S, Ling N and Shimasaki S (1992) Localization of the heparin binding site of follistatin. *Molecular & Cellular Endocrinology* **90** 1-6

Ishihara K, Hatano N, Furuumi H, Kato R, Iwaki T, Miura K *et al.* (2000) Comparative genomic sequencing identifies novel tissue-specific enhancers and sequence elements for methylation-sensitive factors implicated in Igf2/H19 imprinting. *Genome Research* **10** 664-671.

Israel DI, Nove J, Kerns KM, Moutsatsos IK and Kaufman RJ (1992) Expression and characterization of bone morphogenetic protein-2 in Chinese hamster ovary cells. *Growth Factors* **7** 139-150

Israel DI, Nove J, Kerns KM, Kaufman RJ, Rosen V, Cox KA *et al.* (1996) Heterodimeric bone morphogenetic proteins show enhanced activity in vitro and in vivo. *Growth Factors* **13** 291-300

Jaatinen R, Rosen V, Tuuri T and Ritvos O (1996) Identification of ovarian granulosa cells as a novel site of expression for bone morphogenetic protein-3 (BMP-3/osteogenin) and regulation of BMP-3 messenger ribonucleic acids by chorionic gonadotropin in cultured human granulosa-luteal cells. *Journal of Clinical Endocrinology & Metabolism* **81** 3877-3882

Jaatinen R, Laitinen MP, Vuojolainen K, Aaltonen J, Louhio H, Heikinheimo K *et al.* (1999) Localization of growth differentiation factor-9 (GDF-9) mRNA and protein in rat ovaries and cDNA cloning of rat GDF-9 and its novel homolog GDF-9B. *Molecular & Cellular Endocrinology* **156** 189-193

Jenkin G, McFarlane J and de Kretser DM (1995) Inhibin and activin in embryonic and fetal development in ruminants. *Journal of Reproduction & Fertility - Supplement* **49** 177-186

Johnson L, Suggs LC, Norton YM and Zeh WC (1996) Effect of developmental age or time after transplantation on Sertoli cell number and testicular size in inbred Fischer rats. *Biology of Reproduction* **54** 948-959

Jones CM and Smith JC (1998) Establishment of a BMP-4 morphogen gradient by long-range inhibition. *Developmental Biology* **194** 12-17

Jones RL, Salamonsen LA and Findlay JK (2002) Activin A promotes human endometrial stromal cell decidualization in vitro. *Journal of Clinical Endocrinology and Metabolism* **87** 4001-4004.

Juengel JL, Quirke LD, Tisdall DJ, Smith P, Hudson NL and McNatty KP (2000) Gene expression in abnormal ovarian structures of ewes homozygous for the inverdale prolificacy gene. *Biology of Reproduction* **62** 1467-1478

Kaipia A, Penttila TL, Shimasaki S, Ling N, Parvinen M and Toppari J (1992) Expression of inhibin beta A and beta B, follistatin and activin-A receptor messenger ribonucleic acids in the rat seminiferous epithelium. *Endocrinology* **131** 2703-2710

Kaipia A, Parvinen M and Toppari J (1993) Localization of activin receptor (ActR-IIB2) mRNA in the rat seminiferous epithelium. [see comments]. *Endocrinology* **132** 477-479

Kaipia A, Toppari J, Huhtaniemi I and Paranko J (1994) Sex difference in the action of activin-A on cell proliferation of differentiating rat gonad. *Endocrinology* **134** 2165-2170

Kaiser M, Gibori G and Mayo KE (1990) The rat follistatin gene is highly expressed in decidual tissue. *Endocrinology* **126** 2768-2770

Kaiser UB, Lee BL, Carroll RS, Unabia G, Chin WW and Childs GV (1992) Follistatin gene expression in the pituitary: localization in gonadotropes and folliculostellate cells in diestrous rats. *Endocrinology* **130** 3048-3056

Kaiser UB and Chin WW (1993) Regulation of follistatin messenger ribonucleic acid levels in the rat pituitary. *Journal of Clinical Investigation* **91** 2523-2531

Kaufmann E, Paul H, Friedle H, Metz A, Scheucher M, Clement JH *et al.* (1996) Antagonistic actions of activin A and BMP-2/4 control dorsal lip-specific activation of the early response gene XFD-1' in Xenopus laevis embryos. *EMBO Journal* **15** 6739-6749

Kettel LM, DePaolo LV, Morales AJ, Apter D, Ling N and Yen SS (1996) Circulating levels of follistatin from puberty to menopause. *Fertility & Sterility* **65** 472-476

Khoury RH, Wang QF, Crowley WF, Jr., Hall JE, Schneyer AL, Toth T *et al.* (1995) Serum follistatin levels in women: evidence against an endocrine function of ovarian follistatin. *Journal of Clinical Endocrinology & Metabolism* **80** 1361-1368

Kingsley DM (1994) The TGF beta superfamily: new members, new receptors, and new genetic tests of function in different organisms. *Genes & Development* **8** 133-146

Kiyozuka Y, Nakagawa H, Senzaki H, Uemura Y, Adachi S, Teramoto Y *et al.* (2001) Bone morphogenetic protein-2 and type IV collagen expression in psammoma body forming ovarian cancer. *Anticancer Research* **21** 1723-1730

Klein R, Robertson DM, Shukovski L, Findlay JK and de Kretser DM (1991) The radioimmunoassay of follicle-stimulating hormone (FSH)-suppressing protein (FSP): stimulation of bovine granulosa cell FSP secretion by FSH. *Endocrinology* **128** 1048-1056

Klein R, Findlay JK, Clarke IJ, de Kretser DM and Robertson DM (1993) Radioimmunoassay of FSH-suppressing protein in the ewe: concentrations during the oestrous cycle and following ovariectomy. *Journal of Endocrinology* **137** 433-443

Knight PG (1996) Roles of inhibins, activins, and follistatin in the female reproductive system. *Frontiers in Neuroendocrinology* **17** 476-509

Knight PG and Glister C (2001) Potential local regulatory functions of inhibins, activins and follistatin in the ovary. *Reproduction* **121** 503-512

Kobayashi T, Niimi S, Hashimoto O and Hayakawa T (2000) Expression of inhibin betaA, betaB and follistatin mRNAs in the carbon tetrachloride induced rat liver regeneration model. *Biological & Pharmaceutical Bulletin* **23** 755-757

Kogawa K, Nakamura T, Sugino K, Takio K, Titani K and Sugino H (1991a) Activin-binding protein is present in pituitary. *Endocrinology* **128** 1434-1440

Kogawa K, Ogawa K, Hayashi Y, Nakamura T, Titani K and Sugino H (1991b) Immunohistochemical localization of follistatin in rat tissues. *Endocrinologia Japonica* **38** 383-391

Kogure K, Omata W, Kanzaki M, Zhang YQ, Yasuda H, Mine T *et al.* (1995) A single intraportal administration of follistatin accelerates liver regeneration in partially hepatectomized rats. *Gastroenterology* **108** 1136-1142

Kogure K, Zhang YQ, Shibata H and Kojima I (1998) Immediate onset of DNA synthesis in remnant rat liver after 90% hepatectomy by an administration of follistatin. *Journal of Hepatology* **29** 977-984

Kogure K, Zhang YQ, Maeshima A, Suzuki K, Kuwano H and Kojima I (2000) The role of activin and transforming growth factor-beta in the regulation of organ mass in the rat liver. *Hepatology* **31** 916-921

Kojima I, Maeshima A and Zhang Y (2001) Role of the activin-follistatin system in the morphogenesis and regeneration of the renal tubules. *Molecular Cell Endocrinology* **180** 179-182.

Koster M, Plessow S, Clement JH, Lorenz A, Tiedemann H and Knochel W (1991) Bone morphogenetic protein 4 (BMP-4), a member of the TGF-beta family, in early embryos of Xenopus laevis: analysis of mesoderm inducing activity. *Mechanisms of Development* **33** 191-199

Kozian DH, Ziche M and Augustin HG (1997) The activin-binding protein follistatin regulates autocrine endothelial cell activity and induces angiogenesis. *Laboratory Investigation* **76** 267-276

Krey LC, Padmanabhan V and Beitins IZ (1993) Progesterone modulation of gonadotropin secretion by dispersed rat pituitary cells in culture. IV. Follicle-stimulating hormone synthesis and release. *Molecular & Cellular Endocrinology* **91** 13-20

Lacy DA, Wang ZE, Symula DJ, McArthur CJ, Rubin EM, Frazer KA *et al.* (2000) Faithful expression of the human 5q31 cytokine cluster in transgenic mice. *The journal of immunology* **164** 4569-4574.

Lacy E, Roberts S, Evans EP, Burtenshaw MD and Costantini FD (1983) A foreign beta-globin gene in transgenic mice: integration at abnormal chromosomal positions and expression in inappropriate tissues. *Cell* **34** 343-358

Ladd AN, Yatskievych TA and Antin PB (1998) Regulation of avian cardiac myogenesis by activin/TGFbeta and bone morphogenetic proteins. *Developmental Biology* **204** 407-419

Laird PW, Zijderveld A, Linders K, Rudnicki MA, Jaenisch R and Berns A (1991) Simplified mammalian DNA isolation procedure. *Nucleic Acids Research* **19** 4293

Lambert-Messerlian G, Taylor A, Leykin L, Isaacson K, Toth T, Chang Y *et al.* (1997) Characterization of intrafollicular steroid hormones, inhibin, and follistatin in women with and without polycystic ovarian syndrome following gonadotropin hyperstimulation. *Biology of Reproduction* **57** 1211-1216

Lander ES, Linton LM, Birren B, Nusbaum C, Zody MC, Baldwin J *et al.* (2001) Initial sequencing and analysis of the human genome. *Nature* **409** 860-921

Lawson KA, Dunn NR, Roelen BA, Zeinstra LM, Davis AM, Wright CV *et al.* (1999) Bmp4 is required for the generation of primordial germ cells in the mouse embryo. *Genes & Development* **13** 424-436

Lecerf F, Foggia L, Mulsant P, Bonnet A and Hatey F (2001) A novel method to isolate the common fraction of two DNA samples: hybrid specific amplification (HSA). *Nucleic Acids Research* **29** E87-87

Lee BL, Unabia G and Childs G (1993) Expression of follistatin mRNA by somatotropes and mammotropes early in the rat estrous cycle. *Journal of Histochemistry & Cytochemistry* **41** 955-960

Lee SJ and McPherron AC (2001) Regulation of myostatin activity and muscle growth. *Proceedings of the National Academy of Sciences USA* **98** 9306-9311

Lee W, Mason AJ, Schwall R, Szonyi E and Mather JP (1989) Secretion of activin by interstitial cells in the testis. *Science* **243** 396-398

Lee WS, Otsuka F, Moore RK and Shimasaki S (2001) Effect of bone morphogenetic protein-7 on folliculogenesis and ovulation in the rat. *Biology of Reproduction* **65** 994-999

Li R, Phillips DM and Mather JP (1995) Activin promotes ovarian follicle development in vitro. *Endocrinology* **136** 849-856

Li W, Khorasheh S, Yuen BH, Ling N and Leung PC (1993) Stimulation of progesterone secretion by recombinant follistatin-288 in human granulosa cells. *Endocrinology* **132** 1750-1756

Liao WX, Roy AC and Ng SC (2000) Preliminary investigation of follistatin gene mutations in women with polycystic ovary syndrome. *Molecular Human Reproduction* **6** 587-590

Lin SY, Morrison JR, Phillips DJ and De Kretser DM (2003) Regulation of ovarian function by the TGF-beta superfamily and follistatin. *Reproduction* **126** 133-148.

Lindsell CE, Misra V and Murphy BD (1993) Regulation of follistatin messenger ribonucleic acid in porcine granulosa cells by epidermal growth factor and the protein kinase-C pathway. *Endocrinology* **132** 1630-1636

Lindsell CE, Misra V and Murphy BD (1994) Regulation of follistatin gene expression in the ovary and in primary cultures of porcine granulosa cells. *Journal of Reproduction & Fertility* **100** 591-597

Ling N, Ying SY, Ueno N, Esch F, Denoroy L and Guillemin R (1985) Isolation and partial characterization of a Mr 32,000 protein with inhibin activity from porcine follicular fluid. *Proceedings of the National Academy of Sciences USA* **82** 7217-7221

Ling N, Ying SY, Ueno N, Shimasaki S, Esch F, Hotta M *et al.* (1986) Pituitary FSH is released by a heterodimer of the beta-subunits from the two forms of inhibin. *Nature* **321** 779-782

Ling N, DePaolo LV, Bicsak TA and Shimasaki S (1990) Novel ovarian regulatory peptides: inhibin, activin, and follistatin. *Clinical Obstetrics & Gynecology* **33** 690-702

Link BA and Nishi R (1997) Opposing effects of activin A and follistatin on developing skeletal muscle cells. *Experimental Cell Research* **233** 350-362

Link BA and Nishi R (1998) Development of the avian iris and ciliary body: the role of activin and follistatin in coordination of the smooth-to-striated muscle transition. *Developmental Biology* **199** 226-234

Liu F, Ventura F, Doody J and Massague J (1995) Human type II receptor for bone morphogenic proteins (BMPs): extension of the two-kinase receptor model to the BMPs. *Molecular & Cellular Biology* **15** 3479-3486

Liu X, Andoh K, Yokota H, Kobayashi J, Abe Y, Yamada K *et al.* (1998) Effects of growth hormone, activin, and follistatin on the development of preantral follicle from immature female mice. *Endocrinology* **139** 2342-2347

Lois C, Hong EJ, Pease S, Brown EJ and Baltimore D (2002) Germline transmission and tissue-specific ezpression of transgenes delivered by lentiviral vectors. *Science* **295** 862-872

Loots GG, Locksley RM, Blankespoor CM, Wang ZE, Miller W, Rubin EM *et al.* (2000) Identification of a coordinate regulator of interleukins 4, 13, and 5 by cross-species sequence comparisons. *Science* **288** 136-140.

Lyons K, Graycar JL, Lee A, Hashmi S, Lindquist PB, Chen EY *et al.* (1989) Vgr-1, a mammalian gene related to Xenopus Vg-1, is a member of the transforming growth factor beta gene superfamily. *Proceedings of the National Academy of Sciences USA* **86** 4554-4558

Lyons KM, Pelton RW and Hogan BL (1989) Patterns of expression of murine Vgr-1 and BMP-2a RNA suggest that transforming growth factor-beta-like genes coordinately regulate aspects of embryonic development. *Genes & Development* **3** 1657-1668

Macias-Silva M, Hoodless PA, Tang SJ, Buchwald M and Wrana JL (1998) Specific activation of Smad1 signaling pathways by the BMP7 type I receptor, ALK2. *Journal of Biological Chemistry* **273** 25628-25636

Maeshima A, Shiozaki S, Tajima T, Nakazato Y, Naruse T and Kojima I (2000) Number of glomeruli is increased in the kidney of transgenic mice expressing the truncated type II activin receptor. *Biochemical & Biophysical Research Communications* **268** 445-449

Maeshima A, Nojima Y and Kojima I (2001) The role of the activin-follistatin system in the developmental and regeneration processes of the kidney. *Cytokine Growth Factor Review* **12** 289-298

Majdic G, McNeilly AS, Sharpe RM, Evans LR, Groome NP and Saunders PT (1997) Testicular expression of inhibin and activin subunits and follistatin in the rat and human fetus and neonate and during postnatal development in the rat. *Endocrinology* **138** 2136-2147

Massagué J (1998) TGF-beta signal transduction. *Annual Review of Biochemistry* **67** 753-791

Massagué J and Wotton D (2000) Transcriptional control by the TGF-beta/Smad signaling system. *EMBO Journal* **19** 1745-1754

Mather JP, Attie KM, Woodruff TK, Rice GC and Phillips DM (1990) Activin stimulates spermatogonial proliferation in germ-Sertoli cell cocultures from immature rat testis. *Endocrinology* **127** 3206-3214

Mather JP, Roberts PE and Krummen LA (1993) Follistatin modulates activin activity in a cell- and tissue-specific manner. *Endocrinology* **132** 2732-2734

Mather JP (1996) Follistatins and alpha 2-macroglobulin are soluble binding proteins for inhibin and activin. *Hormone Research* **45** 207-210

Mather JP, Moore A and Li RH (1997) Activins, inhibins, and follistatins: further thoughts on a growing family of regulators. *Proceedings of the Society for Experimental Biology & Medicine* **215** 209-222

Matzuk MM, Finegold MJ, Su JG, Hsueh AJ and Bradley A (1992) Alpha-inhibin is a tumour-suppressor gene with gonadal specificity in mice. *Nature* **360** 313-319

Matzuk MM, Finegold MJ, Mather JP, Krummen L, Lu H and Bradley A (1994) Development of cancer cachexia-like syndrome and adrenal tumors in inhibin-deficient mice. *Proceedings of the National Academy of Sciences USA* **91** 8817-8821

Matzuk MM, Kumar TR and Bradley A (1995a) Different phenotypes for mice deficient in either activins or activin receptor type II. *Nature* **374** 356-360

Matzuk MM, Lu N, Vogel H, Sellheyer K, Roop DR and Bradley A (1995b) Multiple defects and perinatal death in mice deficient in follistatin. *Nature* **374** 360-363

Matzuk MM, Kumar TR, Vassalli A, Bickenbach JR, Roop DR, Jaenisch R *et al.* (1995c) Functional analysis of activins during mammalian development. *Nature* **374** 354-356

Matzuk MM, Kumar TR, Shou W, Coerver KA, Lau AL, Behringer RR *et al.* (1996) Transgenic models to study the roles of inhibins and activins in reproduction, oncogenesis, and development. *Recent Progress in Hormone Research* **51** 123-154

Matzuk MM (2000) Revelations of ovarian follicle biology from gene knockout mice. *Molecular & Cellular Endocrinology* **163** 61-66

McAndrews JM, Ringstrom SJ, Dahl KD and Schwartz NB (1994) Corticosterone in vivo increases pituitary follicle-stimulating hormone beta messenger ribonucleic acid content and serum FSH bioactivity selectively in female rats. *Endocrinology* **134** 158-163

McDowell N and Gurdon JB (1999) Activin as a morphogen in Xenopus mesoderm induction. *Semin Cell Dev Biol* **10** 311-317

McGee E, Spears N, Minami S, Hsu SY, Chun SY, Billig H *et al.* (1997) Preantral ovarian follicles in serum-free culture: suppression of apoptosis after activation of the cyclic guanosine 3',5'-monophosphate pathway and stimulation of growth and differentiation by follicle-stimulating hormone. *Endocrinology* **138** 2417-2424

McGee EA and Hsueh AJ (2000) Initial and cyclic recruitment of ovarian follicles. *Endocrine Reviews* **21** 200-214.

McGrath SA, Esquela AF and Lee SJ (1995) Oocyte-specific expression of growth/differentiation factor-9. *Molecular Endocrinology* **9** 131-136

McPherron AC and Lee SJ (1993) GDF-3 and GDF-9: two new members of the transforming growth factor-beta superfamily containing a novel pattern of cysteines. *Journal of Biological Chemistry* **268** 3444-3449

McPherron AC, Lawler AM and Lee SJ (1997) Regulation of skeletal muscle mass in mice by a new TGF-beta superfamily member. *Nature* **387** 83-90

McPherson SJ, Mellor SL, Wang H, Evans LW, Groome NP and Risbridger GP (1999) Expression of activin A and follistatin core proteins by human prostate tumor cell lines. *Endocrinology* **140** 5303-5309

Meehan T, Schlatt S, O'Bryan MK, de Kretser DM and Loveland KL (2000) Regulation of germ cell and Sertoli cell development by activin, follistatin, and FSH. *Developmental Biology* **220** 225-237

Meinhardt A, O'Bryan MK, McFarlane JR, Loveland KL, Mallidis C, Foulds LM *et al.* (1998) Localization of follistatin in the rat testis. *Journal of Reproduction & Fertility* **112** 233-241

Mellor SL, Cranfield M, Ries R, Pedersen J, Cancilla B, de Kretser D *et al.* (2000) Localization of activin beta(A)-, beta(B)-, and beta(C)-subunits in humanprostate and evidence for formation of new activin heterodimers of beta(C)-subunit. *Journal of Clinical Endocrinology & Metabolism* **85** 4851-4858

Menke DB and Page DC (2002) Sexually dimorphic gene expression in the developing mouse gonad. *Gene Expression Patterns* **2** 359-367.

Mercado M, Shimasaki S, Ling N and DePaolo L (1993) Effects of estrous cycle stage and pregnancy on follistatin gene expression and immunoreactivity in rat reproductive tissues: progesterone is implicated in regulating uterine gene expression. *Endocrinology* **132** 1774-1781

Meriggiola MC, Dahl KD, Mather JP and Bremner WJ (1994) Follistatin decreases activin-stimulated FSH secretion with no effect on GnRH-stimulated FSH secretion in prepubertal male monkeys. *Endocrinology* **134** 1967-1970

Merino R, Macias D, Ganan Y, Rodriguez-Leon J, Economides AN, Rodriguez-Esteban C *et al.* (1999) Control of digit formation by activin signalling. *Development* **126** 2161-2170

Meyer MF, Gerresheim F, Pfeiffer A, Epplen JT and Schatz H (2000) Association of polycystic ovary syndrome with an interstitial deletion of the long arm of chromosome 11. *Experimental & Clinical Endocrinology & Diabetes* **108** 519-523

Michalova K, Bucchini D, Ripoche MA, Pictet R and Jami J (1988) Chromosome localization of the human insulin gene in transgenic mouse lines. *Human Genetics* **80** 247-252

Michel U, Albiston A and Findlay JK (1990) Rat follistatin: gonadal and extragonadal expression and evidence for alternative splicing. *Biochemical & Biophysical Research Communications* **173** 401-407

Michel U, McMaster JW and Findlay JK (1992) Regulation of steady-state follistatin mRNA levels in rat granulosa cells in vitro. *Journal of Molecular Endocrinology* **9** 147-156

Michel U, Esselmann J and Nieschlag E (1993) Expression of follistatin messenger ribonucleic acid in Sertoli cell-enriched cultures: regulation by epidermal growth factor and protein kinase C-dependent pathway but not by follicle-stimulating hormone and protein kinase A-dependent pathway. *Acta Endocrinologica* **129** 525-531

Michel U, Schneider O, Kirchhof C, Meisel S, Smirnov A, Wiltfang J *et al.* (1996) Production of follistatin in porcine endothelial cells: differential regulation by bacterial compounds and the synthetic glucocorticoid RU 28362. *Endocrinology* **137** 4925-4934

Miralles F, Czernichow P and Scharfmann R (1998) Follistatin regulates the relative proportions of endocrine versus exocrine tissue during pancreatic development. *Development* **125** 1017-1024

Miro F, Smyth CD and Hillier SG (1991) Development-related effects of recombinant activin on steroid synthesis in rat granulosa cells. *Endocrinology* **129** 3388-3394

Miro F and Hillier SG (1996) Modulation of granulosa cell deoxyribonucleic acid synthesis and differentiation by activin. *Endocrinology* **137** 464-468

Miyake T, Irahara M, Shitukawa K, Yasui T and Aono T (1993) Interaction of activin A and gonadal steroids on FSH secretion from primary cultured rat anterior pituitary cells. *Biochemical & Biophysical Research Communications* **194** 413-419

Miyanaga K and Shimasaki S (1993) Structural and functional characterization of the rat follistatin (activin-binding protein) gene promoter. *Molecular & Cellular Endocrinology* **92** 99-109

Miyanaga K, Erickson GF, DePaolo LV, Ling N and Shimasaki S (1993) Differential control of activin, inhibin and follistatin proteins in cultured rat granulosa cells. *Biochemical & Biophysical Research Communications* **194** 253-258

Mizunuma H, Liu X, Andoh K, Abe Y, Kobayashi J, Yamada K *et al.* (1999) Activin from secondary follicles causes small preantral follicles to remain dormant at the resting stage. *Endocrinology* **140** 37-42

Modrek B and Lee C (2002) A genomic view of alternative splicing. *Nature Genetics* **30** 13-19

Monroe DG, Jin DF and Sanders MM (2000) Estrogen opposes the apoptotic effects of bone morphogenetic protein 7 on tissue remodeling. *Molecular & Cellular Biology* **20** 4626-4634

Montgomery GW, Galloway SM, Davis GH and McNatty KP (2001) Genes controlling ovulation rate in sheep. *Reproduction* **121** 843-852

Mori H, Hashiramoto M, Clark AE, Yang J, Muraoka A, Tamori Y *et al.* (1994) Substitution of tyrosine 293 of GLUT1 locks the transporter into an outward facing conformation. *Journal of Biological Chemistry* **269** 11578-11583

Morrissey J, Hruska K, Guo G, Wang S, Chen Q and Klahr S (2002) Bone morphogenetic protein-7 improves renal fibrosis and accelerates the return of renal function. *J Am Soc Nephrol* **13 Suppl 1** S14-21

Munz B, Tretter YP, Hertel M, Engelhardt F, Alzheimer C and Werner S (2001) The roles of activins in repair processes of the skin and the brain. *Molecular & Cellular Endocrinology* **180** 169-177

Muraoka A, Hashiramoto M, Clark AE, Edwards LC, Sakura H, Kadowaki T *et al.* (1995) Analysis of the structural features of the C-terminus of GLUT1 that are required for transport catalytic activity. *Biochemical Journal* **311** 699-704

Muttukrishna S, Chamberlain P, Evans LW, Asselin J, Groome NP and Ledger WL (1999) Amniotic fluid concentrations of dimeric inhibins, activin A and follistatin in pregnancy. *European Journal of Endocrinology* **140** 420-424

Nakamura T, Takio K, Eto Y, Shibai H, Titani K and Sugino H (1990) Activin-binding protein from rat ovary is follistatin. *Science* **247** 836-838

Nakatani A, Shimasaki S, Depaolo LV, Erickson GF and Ling N (1991) Cyclic changes in follistatin messenger ribonucleic acid and its protein in the rat ovary during the estrous cycle. *Endocrinology* **129** 603-611

Nishitoh H, Ichijo H, Kimura M, Matsumoto T, Makishima F, Yamaguchi A *et al.* (1996) Identification of type I and type II serine/threonine kinase receptors for growth/differentiation factor-5. *Journal of Biological Chemistry* **271** 21345-21352

Noguchi J, Hikono H, Sato S, Watanabe G, Taya K, Sasamoto S *et al.* (1997) Ontogeny of inhibin secretion in the rat testis: secretion of inhibin-related proteins from fetal Leydig cells and of bioactive inhibin from Sertoli cells. *Journal of Endocrinology* **155** 27-34

Nohno T, Ishikawa T, Saito T, Hosokawa K, Noji S, Wolsing DH *et al.* (1995) Identification of a human type II receptor for bone morphogenetic protein-4 that forms differential heteromeric complexes with bone morphogenetic protein type I receptors. *Journal of Biological Chemistry* **270** 22522-22526

Norman RJ, Milner CR, Groome NP and Robertson DM (2001) Circulating follistatin concentrations are higher and activin concentrations are lower in polycystic ovarian syndrome. *Human Reproduction* **16** 668-672

O'Connor AE, McFarlane JR, Hayward S, Yohkaichiya T, Groome NP and de Kretser DM (1999) Serum activin A and follistatin concentrations during human pregnancy: a cross-sectional and longitudinal study. *Human Reproduction* **14** 827-832

Oda S, Nishimatsu S, Murakami K and Ueno N (1995) Molecular cloning and functional analysis of a new activin beta subunit: a dorsal mesoderm-inducing activity in Xenopus. *Biochemical & Biophysical Research Communications* **210** 581-588

Odunsi K and Kidd KK (1999) A paradigm for finding genes for a complex human trait: polycystic ovary syndrome and follistatin. [letter; comment]. *Proceedings of the National Academy of Sciences USA* **96** 8315-8317

Ogawa K, Kurohmaru M, Sugino H and Hayashi Y (1994) Changes in the immunoreactivity of follistatin within preovulatory follicles after the primary gonadotrophin surge in rats. *Journal of Reproduction & Fertility* **101** 577-581

Ogawa K, Hashimoto O, Kurohmaru M, Mizutani T, Sugino H and Hayashi Y (1997) Follistatin-like immunoreactivity in the cytoplasm and nucleus of spermatogenic cells in the rat. *European Journal of Endocrinology* **137** 523-529

Ogino Y, Suzuki K, Haraguchi R, Satoh Y, Dolle P and Yamada G (2001) External genitalia formation: role of fibroblast growth factor, retinoic acid signaling, and distal urethral epithelium. *Ann N Y Acad Sci* **948** 13-31.

Oh SP and Li E (1997) The signaling pathway mediated by the type IIB activin receptor controls axial patterning and lateral asymmetry in the mouse. *Genes & Development* **11** 1812-1826

Onichtchouk D, Chen YG, Dosch R, Gawantka V, Delius H, Massague J *et al.* (1999) Silencing of TGF-beta signalling by the pseudoreceptor BAMBI. *Nature* **401** 480-485

Otsuka F, Yao Z, Lee T, Yamamoto S, Erickson GF and Shimasaki S (2000) Bone morphogenetic protein-15. Identification of target cells and biological functions. *Journal of Biological Chemistry* **275** 39523-39528

Otsuka F, Moore RK and Shimasaki S (2001a) Biological function and cellular mechanism of bone morphogenetic protein-6 in the ovary. *Journal of Biological Chemistry* **276** 32889-32895

Otsuka F, Yamamoto S, Erickson GF and Shimasaki S (2001b) Bone morphogenetic protein-15 inhibits follicle-stimulating hormone (FSH) action by suppressing FSH receptor expression. *Journal of Biological Chemistry* **276** 11387-11392

Otsuka F, Moore RK, Iemura Si S, Ueno N and Shimasaki S (2001c) Follistatin Inhibits the Function of the Oocyte-Derived Factor BMP-15. *Biochemical & Biophysical Research Communications* **289** 961-966

Ozkaynak E, Jin DF, Jelic M, Vukicevic S and Oppermann H (1997) Osteogenic protein-1 mRNA in the uterine endometrium. *Biochemical & Biophysical Research Communications* **234** 242-246

Pang Y and Ge W (1999) Activin stimulation of zebrafish oocyte maturation in vitro and its potential role in mediating gonadotropin-induced oocyte maturation. *Biology of Reproduction* **61** 987-992

Pang Y and Ge W (2002) Epidermal growth factor and TGFalpha promote zebrafish oocyte maturation in vitro: potential role of the ovarian activin regulatory system. *Endocrinology* **143** 47-54

Paralkar VM, Vail AL, Grasser WA, Brown TA, Xu H, Vukicevic S *et al.* (1998) Cloning and characterization of a novel member of the transforming growth factor-beta/bone morphogenetic protein family. *Journal of Biological Chemistry* **273** 13760-13767

Patel K, Makarenkova H and Jung HS (1999) The role of long range, local and direct signalling molecules during chick feather bud development involving the BMPs, follistatin and the Eph receptor tyrosine kinase Eph-A4. *Mechanisms of Development* **86** 51-62

Patthy L and Nikolics K (1993) Functions of agrin and agrin-related proteins. *Trends in Neurosciences* **16** 76-81

Peng C, Ohno T, Khorasheh S and Leung PC (1996) Activin and follistatin as local regulators in the human ovary. *Biological Signals* **5** 81-89

Perriton CL, Powles N, Chiang C, Maconochie MK and Cohn MJ (2002) Sonic hedgehog signaling from the urethral epithelium controls external genital development. *Developmental Biology* **247** 26-46.

Perry AF, Wakayama T, Kishikawa H, Kasai T, Okabe M, Toyoda Y *et al.* (1999) Mammalian transgenesis by intracytoplasmic sperm injection. *Science* **284** 1180-1183

Petraglia F, Vaughan J and Vale W (1989) Inhibin and activin modulate the release of gonadotropin-releasing hormone, human chorionic gonadotropin, and progesterone from cultured human placental cells. *Proceedings of the National Academy USA* **86** 5114-5117

Petraglia F, Vaughan J and Vale W (1990) Steroid hormones modulate the release of immunoreactive gonadotropin-releasing hormone from cultured human placental cells. *Journal of Clinical Endocrinology & Metabolism* **70** 1173-1178

Petraglia F, Gallinelli A, Grande A, Florio P, Ferrari S, Genazzani AR *et al.* (1994) Local production and action of follistatin in human placenta. *Journal of Clinical Endocrinology & Metabolism* **78** 205-210

Pezzani I, Reis FM, Di Leonardo C, Luisi S, Santuz M, Driul L *et al.* (2000) Influence of non-gonadotrophic hormones on gonadal function. *Molecular & Cellular Endocrinology* **161** 37-42

Phillips DJ, McFarlane JR, Hearn MT and de Kretser DM (1997) Inhibin, activin and follistatin bind preferentially to the transformed species of alpha 2-macroglobulin. *Journal of Endocrinology* **155** 65-71

Phillips DJ and de Kretser DM (1998) Follistatin: a multifunctional regulatory protein. *Frontiers in Neuroendocrinology* **19** 287-322

Phillips DJ, Jones KL, McGaw DJ, Groome NP, Smolich JJ, Parsson H *et al.* (2000) Release of activin and follistatin during cardiovascular procedures is largely due to heparin administration. *Journal of Clinical Endocrinology & Metabolism* **85** 2411-2415

Plessow S, Koster M and Knochel W (1991) cDNA sequence of Xenopus laevis bone morphogenetic protein 2 (BMP-2). *Biochimica et Biophysica Acta* **1089** 280-282

Pusch C, Schmitt H and Blin N (1997) Increased cloning efficiency by cycle restriction ligation. *Elsevier trends journals technical tips online* T40071

Qiu Y, Cavelier L, Chiu S, Yang X, Rubin E and Cheng JF (2001) Human and mouse ABCA1 comparative sequencing and transgenesis studies revealing novel regulatory sequences. *Genomics* **73** 66-76.

Rao VV, Loffler C, Wozney JM and Hansmann I (1992) The gene for bone morphogenetic protein 2A (BMP2A) is localized to human chromosome 20p12 by radioactive and nonradioactive in situ hybridization. *Human Genetics* **90** 299-302

Reynolds SD, Angerer LM, Palis J, Nasir A and Angerer RC (1992) Early mRNAs, spatially restricted along the animal-vegetal axis of sea urchin embryos, include one encoding a protein related to tolloid and BMP-1. *Development* **114** 769-786

Riley SC, Balfour C, Wathen NC, Chard T, Evans LW, Groome NP *et al.* (1998) Follistatin and activin A in extra-embryonic coelomic and amniotic fluids and maternal serum in early pregnancy. *Human Reproduction* **13** 2624-2628

Roberts V, Meunier H, Vaughan J, Rivier J, Rivier C, Vale W *et al.* (1989) Production and regulation of inhibin subunits in pituitary gonadotropes. *Endocrinology* **124** 552-554

Roberts VJ, Barth S, el-Roeiy A and Yen SS (1993) Expression of inhibin/activin subunits and follistatin messenger ribonucleic acids and proteins in ovarian follicles and the corpus luteum during the human menstrual cycle. *Journal of Clinical Endocrinology & Metabolism* **77** 1402-1410

Roberts VJ and Barth SL (1994) Expression of messenger ribonucleic acids encoding the inhibin/activin system during mid- and late-gestation rat embryogenesis. *Endocrinology* **134** 914-923

Roberts VJ, Barth S, el-Roeiy A and Yen SS (1994) Expression of inhibin/activin system messenger ribonucleic acids and proteins in ovarian follicles from women with polycystic ovarian syndrome. *Journal of Clinical Endocrinology & Metabolism* **79** 1434-1439

Roberts VJ (1997) Tissue-specific expression of inhibin/activin subunit and follistatin mRNAs in mid- to late-gestational age human fetal testis and epididymis. *Endocrine* **6** 85-90

Robertson DM, Foulds LM, Leversha L, Morgan FJ, Hearn MT, Burger HG *et al.* (1985) Isolation of inhibin from bovine follicular fluid. *Biochemical & Biophysical Research Communications* **126** 220-226

Robertson DM, Klein R, de Vos FL, McLachlan RI, Wettenhall RE, Hearn MT *et al.* (1987) The isolation of polypeptides with FSH suppressing activity from bovine follicular fluid which are structurally different to inhibin. *Biochemical & Biophysical Research Communications* **149** 744-749

Robertson DM, Farnworth PG, Clarke L, Jacobsen J, Cahir NF, Burger HG *et al.* (1990) Effects of bovine 35 kDa FSH-suppressing protein on FSH and LH in rat pituitary cells in vitro: comparison with bovine 31 kDa inhibin. *Journal of Endocrinology* **124** 417-423

Robertson E, Bradley A, Kuehn M and Evans M (1986) Germ-line transmission of genes introduced into cultured pluripotential cells by retroviral vector. *Nature* **323** 445-448

Rombauts L, Vanmontfort D, Decuypere E and Verhoeven G (1996) Inhibin and activin have antagonistic paracrine effects on gonadal steroidogenesis during the development of the chicken embryo. *Biology of Reproduction* **54** 1229-1237

Rosenzweig BL, Imamura T, Okadome T, Cox GN, Yamashita H, ten Dijke P *et al.* (1995) Cloning and characterization of a human type II receptor for bone morphogenetic proteins. *Proceedings of the National Academy of Sciences USA* **92** 7632-7636

Sadatsuki M, Tsutsumi O, Yamada R, Muramatsu M and Taketani Y (1993a) Local regulatory effects of activin A and follistatin on meiotic maturation of rat oocytes. *Biochemical & Biophysical Research Communications* **196** 388-395

Sadatsuki M, Tsutsumi O, Sakai R, Eto Y, Hayashi N and Taketani Y (1993b) Presence and possible function of activin-like substance in human follicular fluid. *Human Reproduction* **8** 1392-1395

Saito S, Nakamura T, Titani K and Sugino H (1991) Production of activin-binding protein by rat granulosa cells in vitro. *Biochemical & Biophysical Research Communications* **176** 413-422

Sakai R, Shiozaki M, Tabuchi M and Eto Y (1992) The measurement of activin/EDF in mouse serum: evidence for extragonadal production. *Biochemical & Biophysical Research Communications* **188** 921-926

Sambrook J, Russell DW, Irwin N and Janssen KA (2001) Molecular Cloning: A Laboratory Manual. (Cold Spring Harbour, Cold Spring Harbour Laboratory Press)

Sasai Y, Lu B, Steinbeisser H and De Robertis EM (1995) Regulation of neural induction by the Chd and Bmp-4 antagonistic patterning signals in Xenopus *Nature* **376** 333-336

Schlunegger MP and Grutter MG (1992) An unusual feature revealed by the crystal structure at 2.2 Å resolution of human transforming growth factor-beta 2. *Nature* **358** 430-434

Schmitt J, Hotten G, Jenkins NA, Gilbert DJ, Copeland NG, Pohl J *et al.* (1996) Structure, chromosomal localization, and expression analysis of the mouse inhibin/activin beta C (inhbc) gene. *Genomics* **32** 358-366

Schneider O, Nau R and Michel U (2000) Comparative analysis of follistatin-, activin beta A- and activin beta B-mRNA steady-state levels in diverse porcine tissues by multiplex S1 nuclease analysis. *European Journal of Endocrinology* **142** 537-544

Schneyer A, Tortoriello D, Sidis Y, Keutmann H, Matsuzaki T and Holmes W (2001) Follistatin-related protein (FSRP): a new member of the follistatin gene family. *Molecular & Cellular Endocrinology* **180** 33-38

Schneyer AL, Hall HA, Lambert-Messerlian G, Wang QF, Sluss P and Crowley WF, Jr. (1996) Follistatin-activin complexes in human serum and follicular fluid differ immunologically and biochemically. *Endocrinology* **137** 240-247

Schneyer AL, Fujiwara T, Fox J, Welt CK, Adams J, Messerlian GM *et al.* (2000) Dynamic changes in the intrafollicular inhibin/activin/follistatin axis during human follicular development: relationship to circulating hormone concentrations. *Journal of Clinical Endocrinology & Metabolism* **85** 3319-3330

Schrewe H, Gendron-Maguire M, Harbison ML and Gridley T (1994) Mice homozygous for a null mutation of activin beta B are viable and fertile. *Mechanisms of Development* **47** 43-51

Schwall RH, Robbins K, Jardieu P, Chang L, Lai C and Terrell TG (1993) Activin induces cell death in hepatocytes in vivo and in vitro. *Hepatology* **18** 347-356

Schwartz S, Zhang Z, Frazer KA, Smit A, Riemer C, Bouck J *et al.* (2000) PipMaker--a web server for aligning two genomic DNA sequences. *Genome Research* **10** 577-586.

Shaha C, Morris PL, Chen CL, Vale W and Bardin CW (1989) Immunostainable inhibin subunits are in multiple types of testicular cells. *Endocrinology* **125** 1941-1950

Shi LY, Zhang ZW and Li WX (1994) Regulation of human chorionic gonadotropin secretion and messenger ribonucleic acid levels by follistatin in the NUCC-3 choriocarcinoma cell line. *Endocrinology* **134** 2431-2437

Shimasaki S, Koga M, Esch F, Mercado M, Cooksey K, Koba A *et al.* (1988a) Porcine follistatin gene structure supports two forms of mature follistatin produced by alternative splicing. *Biochemical & Biophysical Research Communications* **152** 717-723

Shimasaki S, Koga M, Esch F, Cooksey K, Mercado M, Koba A *et al.* (1988b) Primary structure of the human follistatin precursor and its genomic organization. *Proceedings of the National Academy of Sciences USA* **85** 4218-4222

Shimasaki S, Koga M, Buscaglia ML, Simmons DM, Bicsak TA and Ling N (1989) Follistatin gene expression in the ovary and extragonadal tissues. *Molecular Endocrinology* **3** 651-659

Shimasaki S, Zachow RJ, Li D, Kim H, Iemura S, Ueno N *et al.* (1999) A functional bone morphogenetic protein system in the ovary. *Proceedings of the National Academy of Sciences USA* **96** 7282-7287

Shimizu K, Yoshikawa H, Matsui M, Masuhara K and Takaoka K (1994) Periosteal and intratumorous bone formation in athymic nude mice by Chinese hamster ovary tumors expressing murine bone morphogenetic protein-4. *Clinical Orthopaedics & Related Research* 274-280

Shimizu K, Yoshikawa H and Takaoka K (1995) Local effects of bone morphogenetic protein-4 on skeletal tissues. *Clinical Orthopaedics & Related Research* 243-250

Shimonaka M, Inouye S, Shimasaki S and Ling N (1991) Follistatin binds to both activin and inhibin through the common subunit. *Endocrinology* **128** 3313-3315

Shintani Y, Dyson M, Drummond AE and Findlay JK (1997) Regulation of follistatin production by rat granulosa cells in vitro. *Endocrinology* **138** 2544-2551

Shukovski L and Findlay JK (1990) Activin-A inhibits oxytocin and progesterone production by preovulatory bovine granulosa cells in vitro. *Endocrinology* **126** 2222-2224

Shukovski L, Findlay JK and Robertson DM (1991) The effect of follicle-stimulating hormone-suppressing protein or follistatin on luteinizing bovine granulosa cells in vitro and its antagonistic effect on the action of activin. *Endocrinology* **129** 3395-3402

Shukovski L, Dyson M and Findlay JK (1993) The effects of follistatin, activin and inhibin on steroidogenesis by bovine thecal cells. *Molecular & Cellular Endocrinology* **97** 19-27

Shukovski L, Keren-Tal I, Dantes A and Amsterdam A (1995) Regulation of follistatin messenger ribonucleic acid in steroidogenic rat granulosa cell lines. *Endocrinology* **136** 2889-2895

Sidis Y, Fujiwara T, Leykin L, Isaacson K, Toth T and Schneyer AL (1998) Characterization of inhibin/activin subunit, activin receptor, and follistatin messenger ribonucleic acid in human and mouse oocytes: evidence for activin's paracrine signaling from granulosa cells to oocytes. *Biology of Reproduction* **59** 807-812

Sidis Y, Schneyer AL, Sluss PM, Johnson LN and Keutmann HT (2001) Follistatin: essential role for the N-terminal domain in activin binding and neutralization. *Journal of Biological Chemistry* **276** 17718-17726

Sidis Y, Tortoriello DV, Holmes WE, Pan Y, Keutmann HT and Schneyer AL (2002) Follistatin-related protein and follistatin differentially neutralize endogenous vs. exogenous activin. *Endocrinology* **143** 1613-1624.

Silva CC and Knight PG (1998) Modulatory actions of activin-A and follistatin on the developmental competence of in vitro-matured bovine oocytes. *Biology of Reproduction* **58** 558-565

Slack JM (1994) Inducing factors in Xenopus early embryos. *Current Biology* **4** 116-126

Smitz J, Cortvrindt R, Hu Y and Vanderstichele H (1998) Effects of recombinant activin A on in vitro culture of mouse preantral follicles. *Molecular Reproduction & Development* **50** 294-304

Stemmer WP (1991) A 20-minute ethidium bromide/high-salt extraction protocol for plasmid DNA. *Biotechniques* **10** 726

Strauss JF, 3rd and Steinkampf MP (1995) Pituitary-ovarian interactions during follicular maturation and ovulation. *American Journal of Obstetrics & Gynecology* **172** 726-735

Strauss WM and Jaenisch R (1992) Molecular complementation of a collagen mutation in mammalian cells using yeast artificial chromosomes. *The EMBO Journal* **11** 417-422

Sugawara M, Depaolo L, Nakatani A, DiMarzo SJ and Ling N (1990) Radioimmunoassay of follistatin: application for in vitro fertilization procedures. *Journal of Clinical Endocrinology & Metabolism* **71** 1672-1674

Sugino K, Kurosawa N, Nakamura T, Takio K, Shimasaki S, Ling N *et al.* (1993) Molecular heterogeneity of follistatin, an activin-binding protein. Higher affinity of the carboxyl-terminal truncated forms for heparan sulfate proteoglycans on the ovarian granulosa cell. *Journal of Biological Chemistry* **268** 15579-15587

Sugiyama M, Kodama T, Konishi K, Abe K, Asami S and Oikawa S (2000) Compactin and simvastatin, but not pravastatin, induce bone morphogenetic protein-2 in human osteosarcoma cells. *Biochemical & Biophysical Research Communications* **271** 688-692

Sumitomo S, Inouye S, Liu XJ, Ling N and Shimasaki S (1995) The heparin binding site of follistatin is involved in its interaction with activin. *Biochemical & Biophysical Research Communications* **208** 1-9

Suzuki A, Nishimatsu S, Murakami K and Ueno N (1993a) Differential expression of Xenopus BMPs in early embryos and tissues. *Zoological Science* **10** 175-178

Suzuki A, Nishimatsu S, Shoda A, Takebayashi K, Murakami K and Ueno N (1993b) Biochemical properties of amphibian bone morphogenetic protein-4 expressed in CHO cells. *Biochemical Journal* **291** 413-417

Takao M, Hino J, Takeshita N, Konno Y, Nishizawa T, Matsuo H *et al.* (1996) Identification of rat bone morphogenetic protein-3b (BMP-3b), a new member of BMP-3. *Biochemical & Biophysical Research Communications* **219** 656-662

Takaoka K, Yoshikawa H, Hashimoto J, Ono K, Matsui M and Nakazato H (1994) Transfilter bone induction by Chinese hamster ovary (CHO) cells transfected by DNA encoding bone morphogenetic protein-4. *Clinical Orthopaedics & Related Research* 269-273

Takebayashi K, Takakura K, Wang H, Kimura F, Kasahara K and Noda Y (2000) Mutation analysis of the growth differentiation factor-9 and -9B genes in patients with premature ovarian failure and polycystic ovary syndrome. *Fertility & Sterility* **74** 976-979

Tamori Y, Hashiramoto M, Clark AE, Mori H, Muraoka A, Kadowaki T *et al.* (1994) Substitution at Pro385 of GLUT1 perturbs the glucose transport function by reducing conformational flexibility. *Journal of Biological Chemistry* **269** 2982-2986

Tanimoto Y, Tanimoto K, Sugiyama F, Horiguchi H, Murakami K, Yagami K *et al.* (1999) Male sterility in transgenic mice expressing activin betaA subunit gene in testis. *Biochemical & Biophysical Research Communications* **259** 699-705

Tannetta DS, Feist SA, Bleach EC, Groome NP, Evans LW and Knight PG (1998) Effects of active immunization of sheep against an amino terminal peptide of the inhibin alpha C subunit on intrafollicular levels of activin A, inhibin A and follistatin. *Journal of Endocrinology* **157** 157-168

Tano M, Minegishi T, Nakamura K, Nakamura M, Karino S, Miyamoto K *et al.* (1995) Regulation of follistatin messenger ribonucleic acid in cultured rat granulosa cells. *Molecular & Cellular Endocrinology* **109** 167-174

Tashiro K, Yamada R, Asano M, Hashimoto M, Muramatsu M and Shiokawa K (1991) Expression of mRNA for activin-binding protein (follistatin) during early embryonic development of Xenopus laevis. *Biochemical & Biophysical Research Communications* **174** 1022-1027

Tebar M, de Jong FH and Sanchez-Criado JE (2000) Regulation of inhibin/activin subunits and follistatin mRNA expression in the rat pituitary at early estrus. *Life Sciences* **67** 2549-2562

Thurston RJ and Korn N (2000) Spermiogenesis in commercial poultry species: anatomy and control. *Poultry Science* **79** 1650-1668

Tilbrook AJ, Clarke IJ and de Kretser DM (1995) Human recombinant follistatin-288 suppresses plasma concentrations of follicle-stimulating hormone but is not a significant regulator of luteinizing hormone in castrated rams. *Biology of Reproduction* **53** 1353-1358

Tisdall DJ, Hill DF, Petersen GB and Fleming JS (1992) Ovine follistatin: characterization of cDNA and expression in sheep ovary during the luteal phase of the oestrous cycle. *Journal of Molecular Endocrinology* **8** 259-264

Tisdall DJ, Hudson N, Smith P and McNatty KP (1994) Localization of ovine follistatin and alpha and beta A inhibin mRNA in the sheep ovary during the oestrous cycle. *Journal of Molecular Endocrinology* **12** 181-193

Topol LZ, Modi WS, Koochekpour S and Blair DG (2000) DRM/GREMLIN (CKTSF1B1) maps to human chromosome 15 and is highly expressed in adult and fetal brain. *Cytogenetics & Cell Genetics* **89** 79-84

Torney AH, Robertson DM and de Kretser DM (1992) Characterization of inhibin and related proteins in bovine fetal testicular and ovarian extracts: evidence for the presence of inhibin subunit products and FSH-suppressing protein. *Journal of Endocrinology* **133** 111-120

Tortoriello DV, Sidis Y, Holtzman DA, Holmes WE and Schneyer AL (2001) Human follistatin-related protein: a structural homologue of follistatin with nuclear localization. *Endocrinology* **142** 3426-3434

Tretter YP, Hertel M, Munz B, ten Bruggencate G, Werner S and Alzheimer C (2000) Induction of activin A is essential for the neuroprotective action of basic fibroblast growth factor in vivo. *Nature Medicine* **6** 812-815

Tsang TE, Khoo PL, Jamieson RV, Zhou SX, Ang SL, Behringer R *et al.* (2001) The allocation and differentiation of mouse primordial germ cells. *International Journal of Developmental Biology* **45** 549-555

Tsuchida K, Arai KY, Kuramoto Y, Yamakawa N, Hasegawa Y and Sugino H (2000) Identification and characterization of a novel follistatin-like protein as a binding protein for the TGF-beta family. *Journal of Biological Chemistry* **275** 40788-40796

Tsuchiya M, Minegishi T, Kishi H, Tano M, Kameda T, Hirakawa T *et al.* (1999) Control of the expression of luteinizing hormone receptor by local factors in rat granulosa cells. *Archives of Biochemistry & Biophysics* **367** 185-192

Tucci S, Futterweit W, Concepcion ES, Greenberg DA, Villanueva R, Davies TF *et al.* (2001) Evidence for association of polycystic ovary syndrome in caucasian women with a

marker at the insulin receptor gene locus. *Journal of Clinical Endocrinology & Metabolism* **86** 446-449

Tuuri T, Eramaa M, Hilden K and Ritvos O (1994a) Activin-binding protein follistatin messenger ribonucleic acid and secreted protein levels are induced by chorionic gonadotropin in cultured human granulosa-luteal cells. *Endocrinology* **135** 2196-2203

Tuuri T, Eramaa M, Hilden K and Ritvos O (1994b) The tissue distribution of activin beta A- and beta B-subunit and follistatin messenger ribonucleic acids suggests multiple sites of action for the activin-follistatin system during human development. *Journal of Clinical Endocrinology & Metabolism* **78** 1521-1524

Tuuri T and Ritovs O (1995) Regulation of the activin-binding protein follistatin cultured human luteinizing granulosa cells: characterization of the effects of follicle stimulating hormone, prostaglandin E2, and different growth factors. *Biology of Reproduction* **53** 1508-1516

Tuuri T, Eramaa M, Van Schaik RH and Ritvos O (1996) Differential regulation of inhibin/activin alpha- and beta A-subunit and follistin mRNAs by cyclic AMP and phorbol ester in cultured human granulosa-luteal cells. *Molecular & Cellular Endocrinology* **121** 1-10

Ueno N, Ling N, Ying SY, Esch F, Shimasaki S and Guillemin R (1987) Isolation and partial characterization of follistatin: a single-chain Mr 35,000 monomeric protein that inhibits the release of follicle-stimulating hormone. *Proceedings of the National Academy of Sciences USA* **84** 8282-8286

Urbanek M, Legro RS, Driscoll DA, Azziz R, Ehrmann DA, Norman RJ *et al.* (1999) Thirty-seven candidate genes for polycystic ovary syndrome: strongest evidence for linkage is with follistatin. [see comments]. *Proceedings of the National Academy of Sciences USA* **96** 8573-8578

Urbanek M, Wu X, Vickery KR, Kao LC, Christenson LK, Schneyer A *et al.* (2000) Allelic variants of the follistatin gene in polycystic ovary syndrome. *Journal of Clinical Endocrinology & Metabolism* **85** 4455-4461

Vale W, Rivier J, Vaughan J, McClintock R, Corrigan A, Woo W *et al.* (1986) Purification and characterization of an FSH releasing protein from porcine ovarian follicular fluid. *Nature* **321** 776-779

van de Pavert SA, Boerjan ML, Stroband HW, Taverne MA and Van den Hurk R (2001) Uterine-embryonic interaction in pig: activin, follistatin, and activin receptor II in uterus and embryo during early gestation. *Molecular Reproduction & Development* **59** 390-399

van den Eijnden-van Raaij AJ, Feijen A, Lawson KA and Mummery CL (1992) Differential expression of inhibin subunits and follistatin, but not of activin receptor type II, during early murine embryonic development. *Developmental Biology* **154** 356-365

van Dissel-Emiliani FM, Grootenhuis AJ, de Jong FH and de Rooij DG (1989) Inhibin reduces spermatogonial numbers in testes of adult mice and Chinese hamsters. *Endocrinology* **125** 1899-1903

Vassalli A, Matzuk MM, Gardner HA, Lee KF and Jaenisch R (1994) Activin/inhibin beta B subunit gene disruption leads to defects in eyelid development and female reproduction. *Genes & Development* **8** 414-427

Vejda S, Cranfield M, Peter B, Mellor SL, Groome N, Schulte-Hermann R *et al.* (2002) Expression and dimerization of the rat activin subunits bC and bE: evidence for the formation of novel activin dimers. *Journal of Molecular Endocrinology* **28** 137-148

Vitt UA, Hayashi M, Klein C and Hsueh AJ (2000a) Growth differentiation factor-9 stimulates proliferation but suppresses the follicle-stimulating hormone-induced differentiation of cultured granulosa cells from small antral and preovulatory rat follicles. *Biology of Reproduction* **62** 370-377

Vitt UA, McGee EA, Hayashi M and Hsueh AJ (2000b) In vivo treatment with GDF-9 stimulates primordial and primary follicle progression and theca cell marker CYP17 in ovaries of immature rats. *Endocrinology* **141** 3814-3820

Wada M, Shintani Y, Kosaka M, Sano T, Hizawa K and Saito S (1996) Immunohistochemical localization of activin A and follistatin in human tissues. *Endocrine Journal* **43** 375-385

Wakatsuki M, Shintani Y, Abe M, Liu ZH, Shitsukawa K and Saito S (1996) Immunoradiometric assay for follistatin: serum immunoreactive follistatin levels in normal adults and pregnant women. *Journal of Clinical Endocrinology & Metabolism* **81** 630-634

Wang EY, Draper LB, Lee E, Polak A, Sluss P, Weiss J *et al.* (1999) Identification of naturally occurring follistatin complexes in human biological fluids. *Biology of Reproduction* **60** 8-13

Wang Q, Keutmann HT, Schneyer AL and Sluss PM (2000) Analysis of human follistatin structure: identification of two discontinuous N-terminal sequences coding for activin A binding and structural consequences of activin binding to native proteins. *Endocrinology* **141** 3183-3193

Wang QF, Farnworth PG, Burger HG and Findlay JK (1990a) Acute inhibitory effect of follicle-stimulating hormone-suppressing protein (FSP) on gonadotropin-releasing hormone-stimulated gonadotropin secretion in cultured rat anterior pituitary cells. *Molecular & Cellular Endocrinology* **72** 33-42

Wang QF, Farnworth PG, Findlay JK and Burger HG (1990b) Chronic inhibitory effect of follicle-stimulating hormone (FSH)-suppressing protein (FSP) or follistatin on activin- and gonadotropin-releasing hormone-stimulated FSH synthesis and secretion in cultured rat anterior pituitary cells. *Endocrinology* **127** 1385-1393

Wankell M, Munz B, Hubner G, Hans W, Wolf E, Goppelt A *et al.* (2001) Impaired wound healing in transgenic mice overexpressing the activin antagonist follistatin in the epidermis. *EMBO Journal* **20** 5361-5372

Webb R, Campbell BK, Garverick HA, Gong JG, Gutierrez CG and Armstrong DG (1999) Molecular mechanisms regulating follicular recruitment and selection. *Journal of Reproduction & Fertility - Supplement* **54** 33-48

Welt C, Sidis Y, Keutmann H and Schneyer A (2002) Activins, inhibins, and follistatins: from endocrinology to signaling. A paradigm for the new millennium. *Exp Biol Med* **227** 724-752.

Whitman M (1998) Smads and early developmental signaling by the TGF-beta superfamily. *Genes & Development* **12** 1445-1462

Wilson PA and Hemmati-Brivanlou A (1995) Induction of epidermis and inhibition of neural fate by Bmp-4. *Nature* **376** 331-333

Wilson T, Wu XY, Juengel JL, Ross IK, Lumsden JM, Lord EA *et al.* (2001) Highly prolific Booroola sheep have a mutation in the intracellular kinase domain of bone morphogenetic protein IB receptor (ALK-6) that is expressed in both oocytes and granulosa cells. *Biology of Reproduction* **64** 1225-1235

Winters SJ, Kawakami S, Sahu A and Plant TM (2001) Pituitary follistatin and activin gene expression, and the testicular regulation of FSH in the adult Rhesus monkey (Macaca mulatta). *Endocrinology* **142** 2874-2878.

Wongprasartsuk S, Jenkin G, McFarlane JR, Goodman M and de Kretser DM (1994) Inhibin and follistatin concentrations in fetal tissues and fluids during gestation in sheep: evidence for activin in amniotic fluid. *Journal of Endocrinology* **141** 219-229

Woodruff TK, Lyon RJ, Hansen SE, Rice GC and Mather JP (1990) Inhibin and activin locally regulate rat ovarian folliculogenesis. *Endocrinology* **127** 3196-3205

Woodruff TK, Krummen L, McCray G and Mather JP (1993) In situ ligand binding of recombinant human [125I] activin-A and recombinant human [125I]inhibin-A to the adult rat ovary. *Endocrinology* **133** 2998-3006

Woodruff TK, Sluss P, Wang E, Janssen I and Mersol-Barg MS (1997) Activin A and follistatin are dynamically regulated during human pregnancy. *Journal of Endocrinology* **152** 167-174

Woodruff TK (1998) Regulation of cellular and system function by activin. *Biochemical Pharmacology* **55** 953-963

Wrathall JH and Knight PG (1995) Effects of inhibin-related peptides and oestradiol on androstenedione and progesterone secretion by bovine theca cells in vitro. *Journal of Endocrinology* **145** 491-500

Wu DD, Lai M, Hughes PE, Sirimanne E, Gluckman PD and Williams CE (1999) Expression of the activin axis and neuronal rescue effects of recombinant activin A following hypoxic-ischemic brain injury in the infant rat. *Brain Research* **835** 369-378

Wu T, Patel H, Mukai S, Melino C, Garg R, Ni X *et al.* (2000) Activin, inhibin, and follistatin in zebrafish ovary: expression and role in oocyte maturation. *Biology of Reproduction* **62** 1585-1592

Xiao S, Findlay JK and Robertson DM (1990) The effect of bovine activin and follicle-stimulating hormone (FSH) suppressing protein/follistatin on FSH-induced differentiation of rat granulosa cells in vitro. *Molecular & Cellular Endocrinology* **69** 1-8

Xiao S and Findlay JK (1991) Interactions between activin and follicle-stimulating hormone-suppressing protein and their mechanisms of action on cultured rat granulosa cells. *Molecular & Cellular Endocrinology* **79** 99-107

Xiao S, Robertson DM and Findlay JK (1992) Effects of activin and follicle-stimulating hormone (FSH)-suppressing protein/follistatin on FSH receptors and differentiation of cultured rat granulosa cells. *Endocrinology* **131** 1009-1016

Xie T and Spradling AC (1998) decapentaplegic is essential for the maintenance and division of germline stem cells in the Drosophila ovary. *Cell* **94** 251-260

Yamaguchi M, Endo H, Tasaka K and Miyake A (1995a) Mouse growth hormone-releasing factor secretion is activated by inhibin and inhibited by activin in placenta. *Biology of Reproduction* **53** 368-372

Yamaguchi M, Tasaka K, Ogura K, Sakata M, Mizuki J and Miyake A (1995b) Activin inhibits but inhibin activates mouse placental lactogen-II secretion. *Journal of Endocrinology* **146** 469-474

Yamaguchi TP, Bradley A, McMahon AP and Jones S (1999) Wnt5a pathway underlies outgrowth of multiple structures in the vertebrate embryo. *Development* **126** 1211-1223

Yamane Y, Tohno-oka R, Yamada S, Furuya S, Shiokawa K, Hirabayashi Y *et al.* (1998) Molecular characterization of Xenopus embryo heparan sulfate. Differential structural requirements for the specific binding to basic fibroblast growth factor and follistatin. *Journal of Biological Chemistry* **273** 7375-7381

Yamashita H, ten Dijke P, Huylebroeck D, Sampath TK, Andries M, Smith JC *et al.* (1995) Osteogenic protein-1 binds to activin type II receptors and induces certain activin-like effects. *Journal of Cell Biology* **130** 217-226

Yan C, Wang P, DeMayo J, DeMayo FJ, Elvin JA, Carino C *et al.* (2001) Synergistic roles of bone morphogenetic protein 15 and growth differentiation factor 9 in ovarian function. *Molecular Endocrinology* **15** 854-866

Yi SE, LaPolt PS, Yoon BS, Chen JY, Lu JK and Lyons KM (2001) The type I BMP receptor BmprIB is essential for female reproductive function. *Proceedings of the National Academy of Sciences USA* **98** 7994-7999

Ying SY (1989) Inhibins, activins and follistatins. *Journal of Steroid Biochemistry* **33** 705-713

Ying Y, Liu XM, Marble A, Lawson KA and Zhao GQ (2000) Requirement of Bmp8b for the generation of primordial germ cells in the mouse. *Molecular Endocrinology* **14** 1053-1063

Yokota H, Yamada K, Liu X, Kobayashi J, Abe Y, Mizunuma H *et al.* (1997) Paradoxical action of activin A on folliculogenesis in immature and adult mice. *Endocrinology* **138** 4572-4576

Yokoyama Y, Nakamura T, Nakamura R, Irahara M, Aono T and Sugino H (1995) Identification of activins and follistatin proteins in human follicular fluid and placenta. *Journal of Clinical Endocrinology & Metabolism* **80** 915-921

Yoshikawa H, Shimizu K, Nakase T and Takaoka K (1994) Periosteal sunburst spiculation in osteosarcoma. A possible role for bone morphogenetic protein. *Clinical Orthopaedics & Related Research* 213-219

Yoshiki N and Aso T (1997) [The regulation mechanism of the female menstrual cycle]. *Nippon Rinsho - Japanese Journal of Clinical Medicine* **55** 2840-2848

Yoshioka K, Suzuki C and Iwamura S (1998) Activin A and follistatin regulate developmental competence of In vitro-produced bovine embryos. *Biology of Reproduction* **59** 1017-1022

Yoshioka K, Suzuki C and Iwamura S (2000) Effects of activin A and follistatin on developmental kinetics of bovine embryos: cinematographic analysis in a chemically defined medium. *Journal of Reproduction & Fertility* **118** 119-125

Zhao GQ and Hogan BL (1996) Evidence that mouse Bmp8a (Op2) and Bmp8b are duplicated genes that play a role in spermatogenesis and placental development. *Mechanisms of Development* **57** 159-168

Zhao GQ, Deng K, Labosky PA, Liaw L and Hogan BL (1996) The gene encoding bone morphogenetic protein 8B is required for the initiation and maintenance of spermatogenesis in the mouse. *Genes & Development* **10** 1657-1669

Zhao GQ, Liaw L and Hogan BL (1998) Bone morphogenetic protein 8A plays a role in the maintenance of spermatogenesis and the integrity of the epididymis. *Development* **125** 1103-1112

Zimmerman CM and Padgett RW (2000) Transforming growth factor beta signaling mediators and modulators. *Gene* **249** 17-30